

Copyright

by

Bradley Dean Garner

2005

GEOCHEMICAL EVOLUTION OF GROUND WATER  
IN THE BARTON SPRINGS SEGMENT  
OF THE EDWARDS AQUIFER

by

Bradley Dean Garner, B.S.

THESIS

Presented to the Faculty of the Graduate School  
of The University of Texas at Austin  
in Partial Fulfillment  
of the Requirements  
for the Degree of

MASTER OF SCIENCE IN GEOLOGICAL SCIENCES

The University of Texas at Austin

December, 2005

GEOCHEMICAL EVOLUTION OF GROUND WATER  
IN THE BARTON SPRINGS SEGMENT  
OF THE EDWARDS AQUIFER

APPROVED BY

SUPERVISING COMMITTEE:

Supervisor: \_\_\_\_\_  
Jay L. Banner

\_\_\_\_\_  
Barbara J. Mahler

\_\_\_\_\_  
John M. Sharp, Jr.

*To Dr. Leon E. Long,  
who has inspired generations of geology students  
with his enthusiastic and heartfelt teaching,  
and who changed the course of my life.*

## ACKNOWLEDGEMENTS

This thesis was supported by funding from the Jackson School of Geosciences. Jay Banner (my supervisor) and Barbara Mahler (virtually my co-supervisor), paid attention to my needs and had faith in my abilities, often far more than I did myself. Their help immeasurably improved the quality of this thesis.

Support from the USGS was greatly appreciated, including Peter VanMetre, Mike Dorsey, Mike Canova, Venezia Chavez, Lynne Fahlquist, Milton Sunvison, Marcus Gary, and all of my other co-workers. Special thanks are given to Laura Coplin (USGS), who improved the quality of many of the figures in this thesis. Thanks are also extended to Joe Beery (Barton Springs/Edwards Aquifer Conservation District) and Nico Hauwert (City of Austin) for thoughts and insights into the world of karst aquifers.

Analytical assistance and sound scientific advice were provided by Larry Mack (UT), Libby Stern (UT), and Kurt Ferguson (SMU). This thesis benefited from reviews by John Sharp (UT, committee member), David Johns (City of Austin), Greg Stanton (USGS), Brad Wolaver (UT), Brad Cey (UT), and Chris Braun (USGS).

For moral support, I thank my family: Steve, Ann, Dana, Ashley, and Oatmeal. My friends: Chris Clark, Amber Guilfoyle, James McDonald, Diane Paulson, Shad Scharlach, Richard Thrapp, and so many others. Thanks to Great Sand Dunes National Park for being there. And oh my, thanks to Christy Sands, who has been more supportive and loving than I could have ever imagined possible.

Abstract thanks are given to (a) Don Quixote, for dreaming the impossible dream; (b) Kermit the Frog, for telling all the lovers and dreamers about the Rainbow Connection; (c) Planet Earth, for being such an interesting home; (d) Science, for seeking answers; and (e) Hope, for being “a good thing—maybe the best of things.”

GEOCHEMICAL EVOLUTION OF GROUND WATER  
IN THE BARTON SPRINGS SEGMENT  
OF THE EDWARDS AQUIFER

by

Bradley Dean Garner, M.S. Geo. Sci.

The University of Texas at Austin, 2005

SUPERVISOR: Jay L. Banner

The water quality in a karst (limestone) aquifer changes over time, making the application of traditional hydrogeologic principles difficult or impossible. This research's goal was to advance the understanding of the Barton Springs segment of the Edwards aquifer within and around Austin, Texas. This was accomplished by analyzing time-series water-quality data from long, medium, and short time scales. Analysis provided insights into direction of ground-water flow, sources of spring discharge, and mixing of geochemically distinct waters in the aquifer. The results of this research are of interest because of the aquifer's role as a drinking water supply, its role as a habitat for the endangered Barton Springs salamander (*Eurycea sosorum*), and for its central role in creating the popular Barton Springs Pool.

Twenty-six years of water-quality data were compared against contemporaneous streamflow and spring discharge rates to evaluate ground-water connection to surface-water processes. Fifteen of 26 wells in this dataset showed a correlation between these measurements. Ion ratios of Mg/Ca, SO<sub>4</sub>/Cl, and Na/Ca showed that active ground-water processes included dilution by recently-recharged

surface water, incongruent dissolution, and mixing with water from a saline zone and an underlying aquifer. Four wells were shown to intersect major flowpaths, and five wells were shown to intersect minor flowpaths.

Major ion and Sr isotope data collected over two years from four karst springs (Main, Eliza, Old Mill, and Upper Barton Springs) provided insight into water flow in the aquifer. Main and Eliza were fed by ground water from the same flowpath(s) in the aquifer, as their geochemical compositions were indistinguishable. Old Mill received 4–9 percent of its water from a saline zone, as shown by elevated ion concentrations and a quantitative mixing model. Upper Spring obtained some of its water from an isolated subbasin in the aquifer, as indicated by radiogenic  $^{87}\text{Sr}/^{86}\text{Sr}$  values measured in this subbasin. Oxygen and hydrogen isotope values indicated that ground water was well-mixed over year or longer timescales.

Oxygen isotope samples collected from the springs following a rainfall event showed how stormflow recharge flows to the springs. A hydrograph separation using showed an immediate increase in spring discharge following rainfall but a 12-hour delay before storm water reached the spring. This suggested an advancing front of storm water that expelled pre-storm water from the karst conduits. Discharge of pre-storm ground water was reduced by up to 44 percent after rainfall, suggesting that stormflow pressurized the karst conduit system and reduced gradients between the aquifer matrix and conduits. Specific conductance was also an effective and inexpensive tracer of stormflow, on the basis of its strong correlation ( $r^2=0.96$ ) to oxygen isotope values. Resource managers and scientists may be interested in these findings, as the potential for contamination of this spring system is increased after large rainfall events.

## TABLE OF CONTENTS

	<u>PAGE</u>
<b>Abstract</b> .....	<b>vi</b>
<b>Table of Contents</b> .....	<b>viii</b>
<b>List of Tables</b> .....	<b>xii</b>
<b>List of Figures</b> .....	<b>xiv</b>
<b>1. Overview of Thesis and the Barton Springs segment of the Edwards aquifer</b> .....	<b>1</b>
1.1. Introduction and Thesis purpose .....	1
1.2. Geologic history of the Barton Springs segment .....	3
1.2.1. Cretaceous deposition and uplift .....	3
1.2.2. Post-Cretaceous burial .....	5
1.2.3. Miocene faulting and uplift .....	5
1.2.4. Post-Miocene aquifer evolution .....	7
1.2.5. Origin of the saline zone .....	9
1.3. Physical hydrogeology—Recharge, discharge, and flow .....	11
1.3.1. Recharge—Creekbeds, sinkholes, and soil zone .....	11
1.3.2. Discharge—Springs and wells .....	12
1.3.3. Ground-water flow in the aquifer .....	14
1.3.4. Digital aquifer models .....	16
1.4. Geochemistry of the Barton Springs segment .....	19
1.4.1. Major dissolved ions .....	19
1.4.2. Non-Ca-Mg-HCO <sub>3</sub> waters in the Barton Springs segment .....	22
1.4.3. Ratios of ion concentrations .....	24
1.4.4. Specific conductance .....	25
1.4.5. Thermodynamics and mineral saturation .....	26
1.4.6. Strontium—A notable trace element in karst .....	28
1.4.7. Nitrate—A potential anthropogenic tracer .....	30
1.4.8. The water molecule .....	31
1.5. Motivation for Thesis .....	33
1.5.1. Karst as a scientific frontier .....	33
1.5.2. Local need for high-quality ground water .....	34
1.5.3. General public outreach .....	35
1.6. Organization of Thesis .....	36

1.7. Data sources .....	37
1.7.1. Data from 1978–2003 (Chapter 2) .....	37
1.7.2. Data from 2003–2005 (Chapter 3 and 4) .....	39
<b>2. Investigation of the relationship between surface-water flow and karst ground-water geochemistry in the Barton Springs segment of the Edwards aquifer .....</b>	<b>48</b>
2.1. Abstract .....	48
2.2. Introduction .....	49
2.3. Study area .....	52
2.4. Study approach .....	55
2.5. Methods .....	56
2.5.1. Sample collection .....	56
2.5.2. Laboratory analytical methods .....	58
2.5.3. Statistical analysis of specific conductance and flow data .....	59
2.6. Results .....	62
2.6.1. Specific conductance .....	62
2.6.2. Streamflow and aquifer flow condition .....	62
2.6.3. Statistical test .....	63
2.7. Discussion .....	64
2.7.1. Geochemical variability at the event scale .....	64
2.7.2. The four well groups .....	69
2.7.3. Wells and flowpath intersection .....	87
2.7.4. Saline zone and Trinity aquifer mixing .....	90
2.7.5. Geographic patterns .....	91
2.7.6. Individual well comparisons with other studies .....	93
2.7.7. Value of statistical approach .....	96
2.8. Conclusions .....	98
2.9. Acknowledgements .....	100
<b>3. Variability in aqueous and isotope geochemistry of karst ground water used to infer water sources and hydrogeology of the Barton Springs segment of the Edwards aquifer .....</b>	<b>127</b>
3.1. Abstract .....	127
3.2. Introduction .....	129
3.3. Study area .....	132

3.4. Methods .....	135
3.4.1. Sampling from springs .....	135
3.4.2. Sampling from wells .....	137
3.4.3. Analytical methods .....	137
3.4.4. Real-time parameter monitoring .....	140
3.5. Results .....	141
3.5.1. Real-time parameter monitoring .....	141
3.5.2. Major dissolved ions .....	142
3.5.3. Strontium, oxygen, and hydrogen isotopes .....	144
3.6. Discussion .....	145
3.6.1. Major ion geochemistry .....	145
3.6.2. Residence time and geochemical variability .....	151
3.6.3. Well-mixed ground water during baseflow .....	156
3.6.4. Geochemical evolution of spring water .....	157
3.6.5. Urban infrastructure and Upper Barton Spring .....	161
3.6.6. Saline zone effect on Old Mill Spring .....	163
3.7. Conclusions .....	165
3.8. Acknowledgements .....	167
<b>4. Barton Springs during stormflow conditions—Using oxygen isotopes and real-time monitoring parameters to quantify water mixing in karst spring discharge, Austin, TX .....</b>	<b>192</b>
4.1. Abstract .....	192
4.2. Introduction .....	193
4.3. Study area .....	196
4.4. Methods .....	197
4.4.1. Isotope sample collection .....	197
4.4.2. Real-time parameter monitoring .....	199
4.4.3. Hydrograph separation .....	200
4.5. Results .....	201
4.5.1. Rainfall .....	201
4.5.2. Discharge, turbidity, conductance and dissolved oxygen .....	201
4.5.3. Oxygen and hydrogen isotopes .....	202
4.5.4. Hydrograph separation with oxygen isotopes .....	203
4.6. Discussion .....	204
4.6.1. First arrival of stormflow at springs .....	204
4.6.2. Stormflow flushes karst conduits .....	206

4.6.3. Stormflow suppresses discharge of matrix ground water .....	208
4.6.4. Alternative hydrograph separation variables .....	210
4.6.5. Complex signals in real-time data .....	213
4.7. Conclusions .....	214
4.8. Acknowledgements .....	217
<b>5. Summary .....</b>	<b>229</b>
<b>Appendix A. Analytical results for Chapter 2 .....</b>	<b>233</b>
<b>Appendix B. Analytical results for Chapter 3 .....</b>	<b>268</b>
<b>Appendix C. Analytical results for Chapter 4 .....</b>	<b>275</b>
<b>Appendix D. Quality assurance data .....</b>	<b>278</b>
D.1. Historical ground-water data, 1978–2003 (Chapter 2) .....	278
D.2. Major ions, 2003–2005 (Chapter 3) .....	280
D.3. Strontium isotopes (Chapter 3) .....	282
D.4. Oxygen isotopes (Chapters 3 and 4) .....	285
D.5. Hydrogen isotopes (Chapters 3 and 4) .....	286
<b>Appendix E. Methods for isotopic analysis .....</b>	<b>293</b>
E.1. Isotope sampling equipment cleaning .....	293
E.2. Sample collection .....	293
E.3. Sample storage and data management .....	294
E.4. Holding time considerations .....	295
E.5. Sample analysis .....	297
E.6. Results reporting .....	299
<b>References .....</b>	<b>301</b>
<b>Vita .....</b>	<b>317</b>

## LIST OF TABLES

		<u>PAGE</u>
<b>Table 2-1.</b>	Site information for water wells sampled in the Barton Springs segment of the Edwards aquifer, 1978–2003 .....	123
<b>Table 2-2.</b>	Summary of correlation between ground-water specific conductance, streamflow, and aquifer flow condition, 1978–2003....	124
<b>Table 2-3.</b>	Summary of Chapter 2 findings .....	125
<b>Table 3-1.</b>	Summary of water quality analysis results, 2003–2005 .....	189
<b>Table 3-2.</b>	Summary statistics of water quality data, 2003–2005 .....	190
<b>Table 3-3.</b>	Coefficients of variation for water quality data, 2003–2005 .....	191
<b>Table 4-1.</b>	Summary of stormflow arrival times at springs .....	228
<b>Table A-1.</b>	Specific conductance and associated maximum 10-day creek and spring discharge measurements, 1978–2003 .....	234
<b>Table A-2.</b>	Full results of correlation test from Chapter 2 .....	251
<b>Table A-3.</b>	Analytical results for dissolved major ions, 1978–2003 .....	256
<b>Table B-1.</b>	Site information springs and wells sampled, 2003–2005 .....	269
<b>Table B-2.</b>	Analytical results for dissolved major ions and strontium, oxygen, and hydrogen isotope ratios, 2003–2005 .....	270
<b>Table C-1.</b>	Analytical results for isotope ratios and associated real-time monitoring parameters, Main Barton Springs, October 2004 .....	276
<b>Table C-2.</b>	Analytical results for isotope ratios for Eliza, Old Mill, and Upper Barton Springs, October 2004 .....	277
<b>Table D-1.</b>	Quality assurance data for dissolved major ions, 1978–2003 .....	289

<b>Table D-2.</b>	Analytical results of $^{87}\text{Sr}/^{86}\text{Sr}$ external laboratory NBS 987 standard analyses, 2003–2005 .....	290
<b>Table D-3.</b>	Analytical results of $\delta^{18}\text{O}$ internal laboratory standards analyses, 2003–2005 .....	291
<b>Table D-4.</b>	Analytical results of $\delta^2\text{H}$ replicate analyses, 2003–2005 .....	292

## LIST OF FIGURES

	<u>PAGE</u>
<b>Figure 1-1.</b> Study area map .....	40
<b>Figure 1-2.</b> Geologic formations and hydrostratigraphy in study area .....	41
<b>Figure 1-3.</b> Schematic cross section of aquifer .....	42
<b>Figure 1-4.</b> Schematic diagram showing incongruent dissolution .....	43
<b>Figure 1-5.</b> Photographs of the study area .....	44
<b>Figure 1-6.</b> Schematic diagram showing Barton Springs Pool .....	46
<b>Figure 1-7.</b> Photograph of moldic porosity .....	47
<b>Figure 2-1.</b> Study area map .....	101
<b>Figure 2-2.</b> Schematic cross section of aquifer .....	102
<b>Figure 2-3.</b> Distribution of Onion Creek discharge data .....	103
<b>Figure 2-4.</b> Piper diagram showing representative ground waters .....	104
<b>Figure 2-5.</b> Statistical groupings of wells (C1, C2, P, and N) .....	105
<b>Figure 2-6.</b> High-resolution sampling results of well SVW .....	106
<b>Figure 2-7.</b> Group C1 geochemistry .....	107
<b>Figure 2-8.</b> Example of correlation at well FMW .....	110
<b>Figure 2-9.</b> Correlation between well SVE and Barton Springs discharge .....	111
<b>Figure 2-10.</b> Group C2 geochemistry .....	112
<b>Figure 2-11.</b> Group P geochemistry .....	115

<b>Figure 2-12.</b>	Sulfate in well FOW versus Barton Springs system discharge .....	118
<b>Figure 2-13.</b>	Group N geochemistry .....	119
<b>Figure 2-14.</b>	Number of samples compared to range of specific conductance .....	122
<b>Figure 3-1.</b>	Study area map .....	169
<b>Figure 3-2.</b>	Photographs of sampling locations .....	170
<b>Figure 3-3.</b>	Overview of discharge and conductance during study .....	172
<b>Figure 3-4.</b>	Major ion concentration range plot .....	173
<b>Figure 3-5.</b>	Piper diagram showing all Chapter 3 ground-water samples .....	174
<b>Figure 3-6.</b>	Carbonate geochemistry modeling diagrams .....	175
<b>Figure 3-7.</b>	Na/Cl ratio in study .....	177
<b>Figure 3-8.</b>	Sr/Ca ratio through time at springs .....	178
<b>Figure 3-9.</b>	Correlation tests between Sr/Ca, Mg/Ca, and residence time .....	179
<b>Figure 3-10.</b>	Mg/Ca and Sr/Ca values compared with other studies .....	180
<b>Figure 3-11.</b>	Samples plotted against global meteoric water line .....	181
<b>Figure 3-12.</b>	Sr/Ca— <sup>87</sup> Sr/ <sup>86</sup> Sr variations in the Barton Springs segment .....	182
<b>Figure 3-13.</b>	Potential sources of strontium in the study area .....	184
<b>Figure 3-14.</b>	Map of <sup>87</sup> Sr/ <sup>86</sup> Sr values across study area .....	185
<b>Figure 3-15.</b>	SO <sub>4</sub> /Cl—Sr/Ca variations in the Barton Springs segment .....	187
<b>Figure 3-16.</b>	Hypothetical mixing model between spring MSP and well ALB .....	188
<b>Figure 4-1.</b>	Study area map .....	218

<b>Figure 4-2.</b>	Time series of discharge on creeks .....	219
<b>Figure 4-3.</b>	Time series of real-time parameters at Main Barton Spring .....	220
<b>Figure 4-4.</b>	Samples plotted against the global meteoric water line .....	221
<b>Figure 4-5.</b>	Hydrograph separation using $\delta^{18}\text{O}$ .....	222
<b>Figure 4-6.</b>	Time series showing isotopic changes at all springs .....	223
<b>Figure 4-7.</b>	Schematic diagram of karst conduit pressurization .....	224
<b>Figure 4-8.</b>	Correlation tests between $\delta^{18}\text{O}$ and real-time parameters .....	226
<b>Figure 4-9.</b>	Hydrograph separation using specific conductance .....	227
<b>Figure D-1.</b>	Time series of measured $^{87}\text{Sr}/^{86}\text{Sr}$ standard values .....	288
<b>Figure E-1.</b>	Photograph of equipment used for water sample filtration .....	300

# **1. Overview of Thesis and the Barton Springs segment of the Edwards aquifer**

## **1.1. INTRODUCTION AND THESIS PURPOSE**

The Barton Springs segment of the Edwards aquifer within and around Austin, Texas, is a karst limestone aquifer that has received increased attention from the scientific community over the last 30 years. Karst aquifers are important natural resources; worldwide, one out of every four persons obtains their drinking water from a karst aquifer (Ford and Williams, 1989). However, their complex internal structure has made the application of traditional hydrogeologic principles difficult if not impossible. Basic issues such as direction of ground-water flow, sources of spring discharge, and transport of contaminants often remain poorly understood in even the most well studied karst aquifers. As such, scientists must use innovative methods for understanding these systems.

The Barton Springs segment of the Edwards aquifer (herein referred to as the Barton Springs segment) is a hydrologically isolated portion of the much larger karst Edwards aquifer of central and south Texas. The Edwards aquifer is one of the most permeable and productive aquifers in the United States, and over 1.7 million people rely on it as a source of drinking water (Edwards Aquifer Authority, 2004). Within the Edwards aquifer, the Barton Springs segment extends from Town Lake in Austin

to the south-southwest toward the town of Buda (Figure 1-1). The aquifer is bounded on the south by a ground-water divide, on the north by the regional base level of the Colorado River, on the west by a large fault, and on the east by a zone of low permeability known as the saline zone (Abbott, 1975; Slade et al., 1986; Sharp and Banner, 1997). The aquifer's overall hydrogeology is affected by the Balcones Fault Zone, a zone of *en-echelon* normal faults that trend from the southwest to the northeast across the aquifer. Some of these faults provide pathways for rapid ground-water flow, while others may act as barriers to flow (Slade et al., 1986; Hauwert and Vickers, 1994).

Locally, many stakeholders have an interest in the ground-water quality of the Barton Springs segment. Stakeholders include recreational users of spring discharge, domestic and agricultural users of ground water from wells, and a federally-listed endangered species that uses the aquifer as its habitat (Sharp and Banner, 1997). Because of these stakeholders, a substantial body of scientific research exists for the Barton Springs segment. Previous ground-water quality studies have dealt with major ion geochemistry (Senger and Kreitler, 1984; Slade et al., 1986; Clement, 1989; Oetting et al., 1996; City of Austin, 1997), suspended sediment transport (Mahler et al., 1999; Mahler, 2003), effects from stormwater recharge (Andrews et al., 1984; Mahler and VanMetre, 2000), urbanization (St. Clair, 1979; Garcia-Fresca Grocin, 2004), ground-water levels and flow (Slade et al., 1985; Barrett

and Charbeneau, 1997; Scanlon et al., 2003; Hauwert et al., 2005), and isotope geochemistry (Oetting et al., 1996).

The purpose of this thesis is to advance the understanding of the Barton Springs segment by investigating (a) major ion geochemistry of the ground water and its relation to surface-water processes, (b) temporal changes in major ion and isotope geochemistry as tools for understanding ground-water flow and evolution, and (c) short-term water quality changes at karst springs caused by stormflow from large rain events.

## **1.2. GEOLOGIC HISTORY OF THE BARTON SPRINGS SEGMENT**

### **1.2.1. Cretaceous deposition and uplift**

The geologic history of the Barton Springs segment spans over 110 million years. It begins with rocks deposited during the lower Cretaceous period, about 110 million years ago (Rose, 1972). The Barton Springs segment of the Edwards aquifer is contained within the Edwards Limestone and the Georgetown Limestone (Figure 1-2; herein referred to jointly as the aquifer rocks). South of the Barton Springs segment, Rose (1972) divides the Edwards Limestone into a lower Kainer Formation and an upper Person Formation, with nine distinct members therein. In the Barton Springs segment, these nine members are equivalent to Members 1 through 5 of the Edwards Limestone (Small et al., 1996; Sharp and Banner, 1997).

About 100 million years ago, the recently-deposited Edwards Limestone was uplifted and subaerially exposed (Woodruff and Abbott, 1979; Prezbindowski, 1981; Maclay, 1995; Small et al., 1996). As rainwater (or meteoric water) infiltrated into these high-standing carbonate sediments, some of the carbonate rock dissolved. This dissolution enlarged the void spaces in the rock, in a process known as karstification. This Cretaceous-period karstification was not extensive (Abbott, 1975), as evidence of so-called “paleokarst” (e.g., sediment-filled cavities not associated with more recent karstification) is found only rarely in the aquifer rocks. After this period of Cretaceous erosion and diagenesis, the Georgetown Limestone was deposited disconformably atop the Edwards Limestone.

By the convention of Folk (1974), the Edwards and Georgetown Limestones largely are pure chemical rocks, containing less than 10 percent non-carbonate material. Non-carbonate material, while ubiquitous in limestone, is infrequently studied in detail. In the Barton Springs segment, much of the non-carbonate material is organic matter associated with deposition (Deike, 1987). Additional non-carbonate material within the aquifer rocks includes the clay minerals kaolinite, illite, and illite/smectite (Lynch et al., 2004). This is comparable to other karst systems; for example, kaolinite clay and quartz grains were found in the aquifer rocks of a Missouri karst system (Peterson and Wicks, 2003).

The Del Rio Clay (a smectitic, carbonaceous shale formation) overlies the Georgetown Limestone (Rose, 1972). During later periods of aquifer evolution including the present-day, the Del Rio Clay has served as an upper confining layer for the aquifer. After the Del Rio Clay, additional marine and non-marine sediments were deposited during the Gulfian series of geologic time.

### **1.2.2. Post-Cretaceous burial**

In the early Tertiary, the aquifer rocks and overlying confining layers were covered by thick terrigenous clastic deposits associated with the uplift of the Rocky Mountains and subsequent progradation of the Gulf of Mexico Coastal Plain. Owing to their complete burial during this period of time, there was no freshwater flow system established in the aquifer rocks. As a result, meteoric diagenesis did not occur, as meteoric water could not infiltrate into and flow freely through the void spaces in the Cretaceous aquifer rocks (Abbott, 1975). Therefore, the ground-water present in the aquifer rock pore spaces was essentially stagnant, and was probably in chemical equilibrium with the rock matrix (Abbott, 1975).

### **1.2.3. Miocene faulting and uplift**

In the Miocene epoch, about 15 million years ago, tectonic activity resulted in a zone of *en-echelon* normal faults (Rose, 1972). This zone of normal faults extended

about 545 kilometers, from Del Rio to Waco, Texas. Near Austin, these faults cut through the Edwards and Georgetown Limestones and displaced blocks of these units relative to one another (Figure 1-3). This faulting apparently was associated with subsidence of the Gulf of Mexico sedimentary basin. Weakness in this zone of faulting already existed as a result of mountain-building activity during the Pennsylvanian Ouachita orogeny.

Maximum displacement across the entire fault zone was about 520 meters (Woodruff and Abbott, 1979). The largest single fault, the Mount Bonnell fault, became the western boundary of the Barton Springs segment. Significant movement along this fault juxtaposed the aquifer rock against the relatively impermeable Glen Rose Formation (Figure 1-3).

Following uplift, erosion of the material above the Edwards and Georgetown Limestones (Figure 1-2) by surface streams was enhanced as a result of the increased topographic relief. Regionally, the base level of this downcutting activity was (and is today) controlled by the Colorado River (Woodruff and Abbott, 1979). By the mid or late Miocene, sufficient overlying material had been stripped away to allow infiltration of meteoric water into the Edwards and Georgetown Limestones. Meteoric water entered the recharge zone, flowed through the aquifer, and exited through springs, thus establishing a "through-flow system" (Abbott, 1975; Woodruff

and Abbott, 1979). The subsequent 15 million years saw this through-flow system evolve into the aquifer structure seen today (Slade et al., 1986).

#### **1.2.4. Post-Miocene aquifer evolution**

Ample time has passed since the establishment of the through-flow system for substantial meteoric diagenesis to occur. Meteoric diagenesis is a complex set of chemical processes that alter limestone as a result of the influx of rainwater (James and Choquette, 1984). One process in meteoric diagenesis is dedolomitization, wherein the more highly soluble dolomite is dissolved and calcite is precipitated directly in its place. Dedolomitization is probably the dominant diagenetic process occurring in the present-day Barton Springs segment (Maclay, 1995). Meteoric diagenesis also includes incongruent dissolution, a process similar to dedolomitization. In incongruent dissolution, metastable minerals such as high-magnesium calcite and aragonite are dissolved, and the more chemically stable low-magnesium calcite is co-precipitated (Figure 1-4) (James and Choquette, 1984). High-magnesium calcite is about ten times more soluble than calcite (Moore, 1989).

In some places, almost all of the original aquifer rock's primary porosity (i.e., intergranular pore spaces) has been occluded by calcite that precipitated during meteoric diagenesis. This loss of primary porosity has been offset by the

corresponding development of large secondary porosity such as large void spaces and conduits (Maclay and Small, 1983).

Today, the aquifer rock in the freshwater zone (Figure 1-1) is tan to buff colored, calcitic, recrystallized, dense, and contains large void spaces typical of karst aquifers (Maclay and Small, 1983; Maclay, 1995). Where these large void spaces are interconnected, there exists the potential for significant ground-water movement. Well-connected large void spaces are referred to as karst conduits, and are of great interest in the hydrologic study of karst aquifers. These void spaces are not uniformly distributed in the aquifer rock; for example, the distinct members of the Edwards Limestone (Figure 1-2) have varying lithologies which have undergone variable amounts of meteoric diagenesis (Small et al., 1996).

Once started, the process of karst conduit development tends to be self-sustaining and self-accelerating. As chemical dissolution increases the diameter of a conduit, the conduit can transmit more ground water because of its high hydraulic conductivity and low gradient (Palmer, 1991). This leads to an increased volume of chemically aggressive (i.e., calcite-undersaturated) ground water passing through the conduit, which then leads to further, accelerated dissolution. If a conduit grows to a sufficient size, it may become a "master conduit."

Enlargement of Barton Springs segment conduits may have also occurred via mechanical erosion (Mahler et al., 1999). While flow in karst conduits is typically

turbulent and tranquil (Gale, 1984; Halihan et al., 2000), the flow velocities of 6 to 13 kilometers per day observed along major flow routes in the Barton Springs segment are probably sufficient to internally erode conduits in the aquifer (Hauwert et al., 2005).

Both chemical and physical erosion of conduits in the Barton Springs segment has led to a prominent set of conduits that have developed along the northeast-trending Balcones fault zone (Figure 1-3). These master conduits are now “deeply engrained” into the aquifer (Abbott, 1975). The presence of master conduits has been further confirmed by Senger (1983), who found that changes in water levels at Barton Springs Pool affected ground-water levels in wells several kilometers away within minutes, suggesting that these wells intersect a highly transmissive conduit system that is in direct hydraulic communication with the pool.

#### **1.2.5. Origin of the saline zone**

The presence of master conduits in the aquifer might explain the existence of the saline zone along the eastern boundary of the Barton Springs segment (Figure 1-1). Hydrologically, the saline zone boundary appears to be a “deeply engrained bypass boundary” (Abbott, 1975). As the process of conduit enlargement progressed and accelerated through geologic time in the freshwater zone, progressively more meteoric water flowed through these conduits at the expense of flow through other

areas of the aquifer. Apparently, the saline zone was one such area that master conduits eventually “cut off” from the main flow of through-flowing meteoric water. Thus, the saline zone failed to develop large secondary porosity, and retained much of its original depositional character. Alternatively, Hauwert and Vickers (1994) proposed that faults with large displacements offset the aquifer rocks of the saline zone from the aquifer rocks of the freshwater zone, thus impeding fluid flow into or out of the saline zone.

Regardless of the underlying hydrologic and/or structural reasons for the saline zone’s existence, it is apparent that the saline zone has undergone relatively little meteoric water circulation (Abbott, 1975). Consequently, these rocks have retained much of their original lithologic character and have undergone relatively little diagenesis (dedolomitization, incongruent dissolution, etc.) (Prezbindowski, 1981; Maclay, 1995). Rocks from the saline zone are gray to brown, dolomitic, and pyritic, with occasional gypsum and celestite deposits (Maclay and Small, 1983). Saline zone rocks retain much of their original primary sucrosic porosity—up to 28 percent in one core sample (Deike, 1987). However, this porosity is poorly connected and results in the lower permeability of the saline zone relative to the freshwater zone (Abbott, 1975; Maclay, 1995). Despite the lithologic differences between saline zone and freshwater zone rocks, it has been shown that rocks from

both zones are time-correlative (Deike, 1987). This clearly demonstrates the profound changes that meteoric diagenesis can impart to limestone.

### **1.3. PHYSICAL HYDROGEOLOGY—RECHARGE, DISCHARGE, AND FLOW**

#### **1.3.1. Recharge—Creekbeds, sinkholes, and soil zone**

An estimated 85 percent of aquifer recharge is provided by the five principal surface streams that cross the recharge zone (Figure 1-1) (Slade et al., 1986; Slagle et al., 1986). Recharge water enters the aquifer through sinkholes, swallets, and fractures in the creekbeds (Figure 1-5). These “focused recharge” sources can provide large volumes of recharge water rapidly to the aquifer.

Additional sources of recharge are presumed to be minor in comparison to creek recharge. Infiltration of recharge water through upland sinkholes and soil zones has been difficult to quantify precisely, although there is research ongoing (N. Hauwert, University of Texas, personal comm., 2005; A. Lindley, University of Texas, personal comm., 2005). Urban infrastructure such as leaking municipal water supply pipes and sewer pipes may also contribute to recharge, especially during low flow conditions (St. Clair, 1979; Sharp and Banner, 1997; Garcia-Fresca Grocin, 2004; Christian, in preparation), although this has been difficult to quantify. There may also be cross-formational flow from other hydrostratigraphic units (see Chapter 2), but the quantity is generally expected to be small compared to other recharge

sources (Smith and Hunt, 2004). St Clair (1979) proposed that some aquifer recharge may occur near Tom Miller dam, although now this is viewed as unlikely on the basis of potentiometric surface maps (Senger, 1983).

### **1.3.2. Discharge—Springs and wells**

The main discharge point for the Barton Springs segment is a collection of four springs known as the Barton Springs system (Figures 1-1 and 1-5). These springs discharge water at a long-term average rate of 50 ft<sup>3</sup>/s (1.4 m<sup>3</sup>/s), or about 30 million gallons per day (110,000 m<sup>3</sup>/day) (Slade et al., 1986). Historically, this discharge rate has varied from about 9 to 150 ft<sup>3</sup>/s (0.25 to 4.2 m<sup>3</sup>/s) (Slade et al., 1986). The combined discharge of these four springs accounts for over 90 percent of natural (i.e., not pumped) discharge from the aquifer (Hauwert and Vickers, 1994).

One of these springs (Main Barton Spring) fills Barton Springs Pool, a local recreational resource of significant popularity and attention (Figure 1-6). When Barton Creek is not in flood stage, the water in this pool is about 21 degrees Celsius, and is well-known for its striking blue-green clarity. Over 300,000 people swim in this pool annually (City of Austin, 1997).

The four springs are located within 1 kilometer of each other (Figure 1-1). Main Barton Spring (MSP) is located underwater in Barton Springs Pool, and discharges from a solution-enlarge cave; spring MSP water also discharges at the

surface from a fracture in the rocks, and water samples are collected from here (Figure 1-5). Eliza Spring (ESP) is located on the northwest side of Barton Creek in a concrete amphitheater and near a concession stand. Old Mill Spring (OSP) is located on the southeast side of Barton Creek in a stone enclosure and downstream from Barton Springs Pool. Upper Barton Spring (USP) is located in the creekbed of Barton Creek, 0.5 km upstream of Barton Springs Pool. These springs have United States Geological Survey (USGS) site identifiers (Table B-1), and some have been monitored for many years.

Ground water in the Barton Springs segment also discharges at Cold Springs, located on the banks of the Colorado River about 4 kilometers north of the Barton Springs system. Discharge rates from this spring are generally small, and studies have shown that this spring is not connected to the larger part of the aquifer (Hauwert and Vickers, 1994; Hauwert et al., 2005). Cold Spring has been studied by Andrews et al. (1984), St. Clair (1979), and Good (2000), among others. It is also being presently studied by a graduate student at The University of Texas at Austin (J. Thompson, University of Texas, 2005, personal comm.). Discharge rates and geochemistry of Cold Springs are beyond the scope of this thesis.

Other notable discharge from the Barton Springs segment is from approximately 970 active wells drilled into the aquifer. In 2004, these wells pumped 2.5 billion gallons of water, equivalent to a constant withdrawal rate of about 10 ft<sup>3</sup>/s

(0.3 m<sup>3</sup>/s) (Smith and Hunt, 2004). This is equivalent to about 20 percent of the mean discharge from the Barton Springs system. The geochemistry of ground water in some of these wells is considered in Chapters 2 and 3.

### **1.3.3. Ground-water flow in the aquifer**

Ground-water flow in the Barton Springs segment is generally to the north-northeast, following the trend of the Balcones Fault Zone (Figure 1-1 and 1-3). Over time, direction of flow varies with changes in aquifer flow condition and resulting changes in the potentiometric surface (Slade et al., 1986). Ultimately, the ground water flows to the Barton Springs system. Ground water does not usually flow across the southern ground-water divide (Hauwert et al., 2005), although it has been suggested that it may do so under very high aquifer flow conditions (Maclay, 1995) and/or low aquifer flow conditions (Guyton and Associates, 1958).

While ground-water flow in the Barton Springs segment appears simple on a regional scale, it is complex on a local scale (Sharp and Banner, 1997). The aquifer can be classified as a “double -porosity” medium, with conduits and intergranular porosity having very different hydraulic properties and spatial distribution. In karst systems, conduits account for very little ground-water storage but transmit most of the ground water (Sharp, 1993; Maloszewski et al., 2002). Furthermore, in the Barton Springs segment, the conduits are non-uniformly distributed throughout the aquifer

rock (Small et al., 1996). For example, Member 3 of the Edwards Limestone (Figure 1-2) is a dense argillaceous mudstone that has almost no conduit development (Small et al., 1996), and may act as a semi-confining layer (Smith and Hunt, 2004). Because of double porosity and its non-uniform distribution, traditional hydrogeologic methods have proven difficult in the Barton Springs segment, because common assumptions underlying classic hydrologic equations are often violated in karst aquifers.

Some have suggested that the Barton Springs segment is a triple-porosity medium, with fractures, conduits, and intergranular spaces comprising three distinct media (Sharp, 1993; Halihan et al., 2000; Scanlon et al., 2003). Furthermore, research on a karst system in Missouri revealed that substantial ground water may flow through the void spaces in non-carbonate sediment deposited in karst conduits (Peterson and Wicks, 2003), suggesting that some karst aquifers can even be thought of as quadruple-porosity media.

In the face of this complexity, dye-tracing has proven to be one of the most straightforward and useful techniques for understanding ground-water flow in karst aquifers (Quinlan et al., 1995). Dye-trace studies have been carried out extensively in the Barton Springs segment (Hauwert et al., 2005). Hauwert et al. (2005) found that a major conduit system flows along the eastern boundary of the aquifer, which is consistent with flowpaths inferred from potentiometric surface maps (Slade et al.,

1986). The dye trace studies also measured straight-line ground-water transit times exceeding 10 kilometers per day.

#### **1.3.4. Digital aquifer models**

Despite the inherent complexity and non-ideality of a karst aquifer, several attempts to create a digital computer model of the Barton Springs segment have been attempted, all with some degree of apparent success at predicting spring discharge and/or aquifer ground-water levels.

Slade et al. (1985) created a digital computer model that divided the aquifer into a 21 by 29 two-dimensional grid. This type of approach, which uses a number of finite elements, is known as a distributed parameter model. Within each of 318 active grid cells, physical aquifer properties were either estimated from well data, or were calculated by calibrating the model with known ground-water level data. Essentially, this model conceptualized the Barton Springs segment as a porous medium aquifer (e.g., sandstone). Slade et al. (1985) underscore the fact that their model only has broad, regional-scale predictive abilities—one should not necessarily expect the water level in any one well to match their model.

Barrett (1996) created a lumped parameter model for the aquifer, wherein the aquifer was represented as five cells (or tanks, of a sort) that represent the five creeks that recharge the aquifer. Compared to distributed parameter models, lumped

parameter models are very simple, as they contain little spatial information and require much less calibration data than distributed parameter models. Interestingly, this “parsimonious” approach to modeling the Barton Springs segment predicted spring discharge rates just as well as more complex distributed parameter models. It also is appealing because resource managers are not intimidated by it and are therefore more likely to use it in decision making (Barrett and Charbeneau, 1997).

Scanlon et al. (2003) created a distributed parameter model similar in nature to that of Slade et al. (1985). There was a large increase in the number of active cells in the Scanlon model compared to the Slade model (7043 versus 318 active cells, respectively). The Scanlon model was able to predict both spring discharge rates and ground-water levels, although it required a substantial effort to calibrate properly. In spite of the increased number of cells, the Scanlon model is still only one vertical layer thick. While it is difficult to create multiple vertical layers in models, there is increasing evidence that hydraulic properties of the Barton Springs segment vary significantly in the vertical direction (Barrett and Charbeneau, 1997), possibly because of lithologic differences or differing degrees of karstification (B.J. Mahler, U.S. Geological Survey, personal comm., 2005).

The model of Scanlon et al. (2003) was recalibrated by Smith and Hunt (2004) to focus on the effects of severe drought, by using data from a drought in the 1950s for calibration. Smith and Hunt found that a repeat of this large drought combined

with pumping rates from 2004 might cause the Barton Springs system intermittently to stop flowing, and might negatively impact 19 percent of the wells in the Barton Springs segment.

All of the digital models described here implicitly treat the Barton Springs segment as an equivalent porous medium (e.g., sandstone) aquifer, where the standard rules of hydrogeology (e.g., Darcy's law) apply. All things considered, these models have attained some degree of success in prediction of spring discharge and/or ground-water levels, at least on a regional scale. Clement (1989) suggested that this counterintuitive success of porous medium models at the regional scale may be because "interconnected cavernous porosity and faults distribute pressure changes over large areas."

A recent study for the Edwards aquifer south of the Barton Springs segment has modeled the aquifer as a true double-porosity medium, by incorporating discrete conduits into the model (Lindgren et al., 2005). Aquifer water levels and spring discharge rates were simulated in a finite-difference model after extensive model calibration using known water level and spring discharge rates. Palmer (1991) suggested that double porosity models are unlikely to be successful, because the convoluted, non-uniform, generally non-predictable patterns of fractures and conduits can be mathematically modeled only with great difficulty.

## **1.4. GEOCHEMISTRY OF THE BARTON SPRINGS SEGMENT**

Insight can be gained into the functioning of a karst aquifer by studying the chemical properties of its ground water, including its dissolved constituents. In theory, ground-water composition is affected by (1) mineral availability, (2) mineral purity, (3) the amount of rock surface area in contact with ground water, (4) exposure time between ground water and rock, and many other factors (Hem, 1985). This section describes several geochemical tools that can be used to study ground water in the Barton Springs segment.

### **1.4.1. Major dissolved ions**

Typically, 95 percent or more of the dissolved ions in natural waters are a combination of calcium ( $\text{Ca}^{2+}$ ), magnesium ( $\text{Mg}^{2+}$ ), sodium ( $\text{Na}^+$ ), potassium ( $\text{K}^+$ ), bicarbonate ( $\text{HCO}_3^-$ ), chloride ( $\text{Cl}^-$ ), sulfate ( $\text{SO}_4^{2-}$ ), and nitrate ( $\text{NO}_3^-$ ) (Herczeg and Edmunds, 2000). In karst aquifers, strontium ( $\text{Sr}^{2+}$ ) is also usually considered a major ion.

The major ion geochemical signature of karst ground water reflects the initial geochemical signature of the recharging surface water, over which is imprinted the interaction of the ground water with the rock through which it flows (Kehew, 2001, p. 9). Rain and recharging surface water contain carbonic acid, a weak acid that forms from the interaction of water with carbon dioxide in the atmosphere and soils.

In karst terrane, this slightly acidic water dissolves the carbonate rock matrix, releasing  $\text{Ca}^{2+}$ ,  $\text{Mg}^{2+}$ ,  $\text{Sr}^{2+}$ , and  $\text{HCO}_3^-$  ions into solution until an equilibrium concentration is reached or the water exits the aquifer. This process is not instantaneous; several days or more are required to approach within 90 percent of equilibrium of calcite (White, 1988). Most ground-water in karst aquifers is calcium-bicarbonate ( $\text{Ca-HCO}_3$ ) or calcium-magnesium-bicarbonate ( $\text{Ca-Mg-HCO}_3$ ), reflecting the overwhelming preponderance of calcite and dolomite and the high solubility of these minerals.

Other major ions in karst ground water can come from trace quantities of elements in the limestone (for example,  $\text{Sr}^{2+}$ ) or from other minerals sometimes associated with limestone deposits, such as gypsum ( $\text{CaSO}_4$ ), pyrite ( $\text{FeS}_2$ ), and clay particles with iron or manganese oxide coatings. Surface recharge is an additional source of major ion species, as it contains ions associated with the soil zone through which the water has moved and with which the water has reacted. In agricultural or urbanized areas, anthropogenic contaminants such as fertilizers and wastewater effluent also may be sources of major ion species such as  $\text{Na}^+$ ,  $\text{K}^+$ , and  $\text{NO}_3^-$  (Freeze and Cherry, 1979, p. 413). In the Barton Springs segment, a saline zone to the east of the aquifer and an underlying aquifer (Trinity aquifer) are both potential sources of several ion species, including  $\text{Na}^+$ ,  $\text{Cl}^-$ , and  $\text{SO}_4^{2-}$ . Under some hydrologic conditions,

water from the saline zone and Trinity aquifer may flow into the Barton Springs segment (Slade et al., 1986; City of Austin, 1997; Smith and Hunt, 2004).

The overall geochemical character of a water sample can be represented visually with a Piper diagram, which is a group of two trilinear diagrams (one for cations and one for anions) and a diamond-shaped diagram representing the composition of the water for both major dissolved cations and anions (Piper, 1944; Freeze and Cherry, 1979, p. 249). The triangles and diamond are subdivided into smaller areas that indicate which groups of ions dominate the aqueous geochemistry. The Piper diagram allows classification through visual inspection of the hydrochemical facies corresponding to each water sample (Back, 1961). Piper diagrams have the advantage of allowing comparison of multiple water samples on the same diagram, so that mixing and evolution of ground waters is visually evident. Because Piper diagrams display only relative proportions of ions, they are independent of the effects of dilution.

When considering the major ions dissolved in water, complications may arise as a result of chemical complexities. For example, at 500 mg/L total dissolved solids, the effective concentration (or activity) of divalent cations such as  $\text{Ca}^{2+}$  may be only 70 percent of the actual concentration (Hem, 1985). As another example, when  $\text{SO}_4^{2-}$  concentrations above 1000 mg/L, over 50 percent of dissolved calcium exists as a the

aqueous neutral complex  $\text{CaSO}_4^0$  (Hem, 1985). It is especially important to consider these non-idealities if mineral saturation states are being calculated (see 1.4.5).

#### **1.4.2. Non-Ca-Mg- $\text{HCO}_3$ waters in the Barton Springs segment**

Water in the Barton Springs segment is mostly Ca- $\text{HCO}_3$  or Ca-Mg- $\text{HCO}_3$ . However, there are two important sources of ions (other than  $\text{Ca}^{2+}$ ,  $\text{Mg}^{2+}$ , and  $\text{HCO}_3^-$ ) that interact with the aquifer. These two sources, the saline zone and the Trinity aquifer, both contain high concentrations of dissolved solids, usually above 1000 mg/L. Highly saline ground waters are notoriously complex and varied in their geochemical composition and chemical evolution.

The saline zone borders the Barton Springs segment along its eastern boundary (Figure 1-1). Ground water in the saline zone flows slowly because of low aquifer permeability, and appears to undergo substantial water-rock interaction. The saline zone has at least five distinct hydrochemical facies throughout the regional extent of the Edwards aquifer. Following the terminology of Clement (1989), "facies D" is the zone that borders the eastern edge of the Barton Springs segment. Facies D ground waters generally are classified as sodium-chloride (Na-Cl) saline waters, although there is some variability in their composition (Hauwert and Vickers, 1994). Several processes appear to contribute to the varying geochemical composition of facies D, including gypsum dissolution, dedolomitization, ion

exchange with clays, sulfate reduction, halite dissolution, mixing with brines, and interaction with igneous intrusions (Sharp and Clement, 1988; Oetting et al., 1996).

The oil field brines that are hypothesized to mix with saline zone ground water have a complex history that some have tried to unravel. The Na-Ca-Cl composition of these oil field brines may be the result of conversion of plagioclase and halite into albite at high temperatures and pressures (Land and Prezbindowski, 1981). Mixing of these Na-Ca-Cl brines with dilute meteoric water that slowly circulates into the saline zone may account for the observed salinity levels in the saline zone.

While a regional scale study such as that of Sharp and Clement (1988) suggests that the saline zone in the Barton Springs segment is of relatively uniform composition, geochemical variability has been observed in facies D on a local scale. Hauwert and Vickers (1994) reported that the ground-water chemistry of wells in the saline zone varies with ground-water levels, with periods of high recharge being equated with lower sodium concentrations and higher calcium concentrations. It was suggested that this variability is the result of mixing of different ground-water types, which is consistent with other studies of brines that have shown mixing to be a major factor in their variable composition (e.g., Musgrove and Banner, 1993).

The underlying Trinity aquifer is another source of highly mineralized ground water that may flow into the Barton Springs segment (i.e., cross-formational

flow). While some cross-formational flow undoubtedly does occur between the Trinity aquifer and the Barton Springs segment, it is not clear how much occurs, when or where it occurs, or even which direction of flow the hydraulic gradient allows (Hauwert and Vickers, 1994). An investigation into the vertical hydraulic gradient between these two aquifers found that ground water may flow out of the Barton Springs segment into the Trinity aquifer (Smith and Hunt, 2004, p. 9). The possibility of cross-formational flow from the Trinity aquifer is considered in Chapter 2.

#### **1.4.3. Ratios of ion concentrations**

In a karst aquifer with relatively uniform lithology, Mg/Ca and Sr/Ca molar ratios can be used as indicators of ground-water residence time (Musgrove and Banner, 2004). Recharging water that is undersaturated with respect to calcite ( $\text{CaCO}_3$ ) will dissolve calcite and undergo a rapid increase in  $\text{Ca}^{2+}$  and  $\text{HCO}_3^-$  concentration until calcite saturation is reached (Palmer, 1991). Subsequently, incongruent dissolution will dissolve metastable minerals such as high-magnesium calcite and dolomite ( $\text{CaMg}(\text{CO}_3)_2$ ), while stable minerals such as low-magnesium calcite precipitate (Figure 1-4) (James and Choquette, 1984). This process leads to an increase of  $\text{Mg}^{2+}$  and  $\text{Sr}^{2+}$  concentrations relative to  $\text{Ca}^{2+}$  (i.e., higher Mg/Ca and Sr/Ca

ratios) because  $Mg^{2+}$  and  $Sr^{2+}$  are preferentially excluded from the newly precipitated stable minerals (James and Choquette, 1984; Musgrove and Banner, 2004).

Visual evidence of the dissolution of metastable minerals can be observed by inspecting carbonate rocks that contain void spaces shaped like marine shells (Figure 1-7). These shells, originally secreted as the metastable mineral aragonite, have been dissolved by meteoric water while the surrounding calcite-based carbonate mud has remained and been recrystallized into micrite.

Other ion ratios that may indicate water sources involve the ions  $SO_4^{2-}$ ,  $Na^+$ , and  $Cl^-$ . Temporal changes in concentrations of these ions at a well or spring might signal an influx of recharge water from the surface, water from the saline zone, or water from another source. Ratios of ion concentrations, such as  $Na/Cl$  and  $Cl/SO_4$ , can sometimes be used to infer geochemical process and to further distinguish water types and sources.

#### **1.4.4. Specific conductance**

Specific conductance is a measure of the amount of electrical current water can transmit, and is related to the ionic strength, or total amount of dissolved solids, of a water sample (Hem, 1982). Because of the relative ease of measuring specific conductance, it is a widely used master variable in geochemical studies, and is used throughout this thesis.

Rain has very low specific conductance (Freeze and Cherry, 1979, p. 238; Herczeg and Edmunds, 2000); surface water has a higher specific conductance resulting from chemical reactions with the land surface, soils, and the streambed; ground water typically has a higher specific conductance than surface water resulting from the dissolution of the rock matrix of the aquifer.

Water that has recharged a karst aquifer recently will have a lower specific conductance than ground water that has been in contact with the rock for a longer period of time (Freeze and Cherry, 1979, p. 241). As the ground water interacts with the aquifer rock, its specific conductance increases, indicating increasing residence time.

Specific conductance usually is used interchangeably with “conductivity.” Technically, however, specific conductance is a measurement that has had a correction applied that takes into account the large effect that temperature has on conductivity (Hem, 1985). Specific conductance is normalized to 25 degrees Celsius, whereas conductivity is not (Hem, 1985). This thesis always refers to this measurement by the full name of specific conductance.

#### **1.4.5. Thermodynamics and mineral saturation**

Combining the principles of thermodynamics with ion concentrations, it is possible to calculate the chemical aggressiveness of water, that is, its propensity to

dissolve various minerals. Calcite is the most common mineral in limestone, and the so-called “saturation index with respect to calcite” can be calculated for the water. The calcite saturation index ( $\log SI_{\text{calcite}}$ ) is the logarithm of the ratio of the ion activity product of the sample and the solubility product for calcite, and is an indication of how close a water sample is to being in thermodynamic equilibrium with calcite (Stumm and Morgan, 1995). Negative values indicate that the solubility product exceeds the ion activity product and that the water is undersaturated with respect to calcite, indicating that the water should dissolve limestone. Positive values indicate water that is oversaturated with respect to calcite, indicating that calcite should precipitate from the water. Values between -0.1 and 0.1 are considered to indicate saturation (i.e., in chemical equilibrium with calcite). Typically, ground water flowing slowly through small pore spaces in limestone or calcitic soils will reach calcite saturation after flowing only a few meters (Bishop and Lloyd, 1990; Palmer, 1991).

Saturation indices for carbonate minerals such as calcite are very sensitive to temperature, and a temperature correction should be applied to the calcite solubility product whenever possible (Hem, 1985). Also, effective concentrations (i.e., activities) of ions should be corrected for total ionic strength, particularly divalent cations such as  $\text{Ca}^{2+}$  (Hem, 1985). Failing to apply these corrections can result in

unrealistic saturation index calculations that are not useful or appropriate for interpretation.

#### **1.4.6. Strontium—A notable trace element in karst**

Strontium (Sr) is a trace element that behaves similarly to calcium and magnesium, and is present in trace amounts in limestone. Dissolved strontium (i.e., Sr<sup>2+</sup>) may be present in karst ground water as the result of simple carbonate-mineral dissolution. However, Sr<sup>2+</sup> in karst ground water may also be derived from the process of incongruent dissolution. Thus, Sr<sup>2+</sup> concentration can be an indicator of residence time, similar to Mg<sup>2+</sup> concentration (see section 1.4.3). Strontium is also abundantly present in evaporite deposits such as anhydrite and gypsum, which can occur in trace quantities in karst aquifers (Jacobson and Wasserburg, 2005). Any study that examines the major dissolved ions in karst aquifers should probably also consider Sr.

Strontium has several naturally-occurring isotopes. <sup>87</sup>Sr is the product of the radioactive decay of <sup>87</sup>Rb, and is referred to as a radiogenic isotope (Faure, 1986, p. 118). Normalized against the non-radiogenic <sup>86</sup>Sr isotope, a measurement of <sup>87</sup>Sr/<sup>86</sup>Sr can be made. Values of <sup>87</sup>Sr/<sup>86</sup>Sr can vary widely in different rocks, depending on the age of the rock and its initial Rb/Sr ratio (Faure, 1986, p. 119). Because of the slow

decay rate for  $^{87}\text{Rb}$  to  $^{87}\text{Sr}$  ( $t_{1/2} = 48.8 \text{ Ga}$ ), the  $^{87}\text{Sr}/^{86}\text{Sr}$  ratio is essentially constant for any mineral (McNutt, 2000).

The  $^{87}\text{Sr}/^{86}\text{Sr}$  value of the world's oceans has varied considerably through geologic time (Burke et al., 1982). This ocean isotopic composition, which is uniform at any one moment in time (Capo and DePaolo, 1992), is recorded directly in carbonate minerals that precipitate from seawater. Because oceanic  $\text{Sr}^{2+}$  is obtained from input from all of the world's rivers, it tends to reflect relative continental weathering rates, and has what can be called an "average" value.

$\text{Sr}^{2+}$  obtained exclusively from detrital sediments usually is more radiogenic than Sr obtained from carbonate rocks, which generally originate from the oceans. Thus, a karst ground water sample with an  $^{87}\text{Sr}/^{86}\text{Sr}$  value that is more radiogenic than the aquifer carbonate rock may have derived some of its  $\text{Sr}^{2+}$  from detrital sediments (Stueber et al., 1984). Many studies have shown that  $\text{Sr}^{2+}$  isotopic composition in ground water and surface water often is controlled by the balance between weathering of carbonate material and silicate material (Banner et al., 1994; Banner et al., 1996; Han and Liu, 2004).

$^{87}\text{Sr}/^{86}\text{Sr}$  ratios can provide complementary information to major ion concentration information when studying karst aquifers, and can provide information about ground-water evolution (Banner et al., 1994). In some cases, Sr isotopes can provide insights into ground-water sources that cannot be gained

merely from dissolved ion concentration information alone (Banner et al., 1994; Vallejos et al., 1997; Frost and Toner, 2004). Note that Sr isotopic data, however, should always be paired with major ion geochemical data. Without the benefit of additional data, sources of Sr in the environment are likely to be misidentified (McNutt, 2000).

#### **1.4.7. Nitrate—A potential anthropogenic tracer**

Nitrate ( $\text{NO}_3^-$ ) is an ion that, at elevated concentrations, might indicate an anthropogenic source, and may also indicate the presence of other anthropogenic contaminants. Because nitrate is not present in limestone and dolomite deposits, its presence in ground water results from processes other than calcite/dolomite dissolution. Sources of  $\text{NO}_3^-$  include fertilizers, manure, septic tanks, municipal sewage treatment systems, decaying plant debris, soil zones, and nitrogen oxide emissions (Freeze and Cherry, 1979, p. 413). Nitrate concentrations below 2 mg/L (measured as nitrogen) are generally assumed to come from natural sources such as plants and soils (Mueller and Helsel, 1996; Wisconsin Department of Natural Resources, 2003). Nitrate is very soluble, and once present in aerated water generally can be lowered in concentration only by mixing with more dilute water or through uptake by plants or other organisms. Excess  $\text{NO}_3^-$  in aquatic systems leads to eutrophication and has various adverse health effects on humans; the Maximum

Contaminant Level (MCL) allowed in drinking water is 10 mg/L measured as nitrogen (United States Environmental Protection Agency, 2005).

The majority of measured nitrate concentrations are below 2 mg/L in Barton Springs segment ground water, and nitrate has never been detected above the EPA MCL in Barton Springs segment ground water (City of Austin, 1997). Even though nitrate concentrations from Main Barton Spring discharge (in the Barton Springs system) have always measured below 2 mg/L, statistical analysis of nitrate concentrations from 1937 to 1999 indicates an upward trend through time (Turner, 2000), which may be associated with anthropogenic contamination. Nitrate concentrations above 2 mg/L are found in a few ground water samples from wells, and are considered in Chapter 2.

#### **1.4.8. The water molecule**

The isotopic composition of oxygen and hydrogen that comprise the water molecule ( $\text{H}_2\text{O}$ ) can be analyzed, and the ratios of one isotope to another (namely  $^{18}\text{O}/^{16}\text{O}$  and  $^2\text{H}/^1\text{H}$ ) can be used to study hydrologic processes (Clark and Fritz, 1997, p. 36). Evaporation of seawater from the oceans induces fractionation in these light, stable isotopes, and thereby changes the isotopic composition of atmospheric water vapor and the rainfall later created over continents. This relation between oxygen and hydrogen isotope fractionation from oceans has been well-characterized by

studying the global isotopic composition of rainfall (Craig, 1961). The so-called global meteoric water line (GMWL) derived from these studies serves as a starting point for investigations of ground water flowing through an aquifer.

Individual rainfall events that recharge an aquifer typically have a unique isotopic “fingerprint” that reflects the origin, travel path, and rainout history of the storm. In Chapter 4, the isotopes of oxygen trace the flow of recent rainfall through the Barton Springs segment, following in the mold of studies carried out in other karst aquifers (e.g., Siegenthaler and Schotterer, 1984; Lakey and Krothe, 1996; Desmarais and Rojstaczer, 2002). Oxygen isotopes are used in Chapter 4 to develop a new conceptual model for ground-water flow in the Barton Springs segment.

The isotopic ratios  $^{18}\text{O}/^{16}\text{O}$  and  $^2\text{H}/^1\text{H}$  are usually reported in delta ( $\delta$ ) notation (Coplen, 1994), whereby isotopic composition of a sample is expressed relative to the isotopic composition of a known standard (namely standard mean ocean water, or SMOW). This is mainly because it is difficult to analytically determine absolute ratios for these isotopes (Clark and Fritz, 1997, p. 6), but it is also a convenient format in which to read and compare the ratios (i.e., whole numbers instead of ratios much less than 1).

## 1.5. MOTIVATION FOR THESIS

### 1.5.1. Karst as a scientific frontier

It is difficult to understand karst aquifers. Their double, triple, and perhaps even quadruple porosity makes the application of traditional hydrologic equations (e.g., Darcy's Law) questionable at best. Karst aquifers force scientists to find innovative methods for characterizing their behavior. For example, the geochemistry of ground water in a karst aquifer varies over time, sometimes over very small time scales (Shuster and White, 1971). This behavior is generally not observed in porous medium (e.g., sandstone) aquifers, and presents an opportunity to study a time-domain signal that is not available to investigators of porous medium aquifers.

Karst aquifers are also prone to contamination, and as such deserve special attention. This vulnerability to contamination is because of their ability to transmit ground water quickly and their relative inability to filter and reduce pollutants in ground water (Ford and Williams, 1989). As stated by John Black, "in fractured media, contaminants appear where we don't expect, and appear there faster than we predicted" (J.M. Sharp, University of Texas, written comm., 2003). There have been infamous cases of karst aquifer contamination, such as *E. Coli* bacterial contamination in Walkerton, Ontario, that led to illnesses and deaths (Worthington et al., 2002). Again, this type of rapid change in water quality is not observed as

frequently in porous medium aquifers, and karst hydrologists must find innovative ways to characterize the mobility of contaminants.

### **1.5.2. Local need for high-quality ground water**

Several stakeholders have an interest in the ground-water quality of the Barton Springs segment. First, the Barton Springs system is the only known habitat for a federally protected endangered species of salamander (*Eurycea sosorum*; Figure 1-5). Second, the Barton Springs system supplies water for Barton Springs Pool, a popular swimming pool that is enjoyed by over 300,000 visitors annually and is colloquially referred to as the “crown jewel of Austin.” Finally, one of Austin’s three inlets for municipal water is directly downstream from the Barton Springs system’s discharge into Town Lake. Under drought conditions, up to 90 percent of inflow into Town Lake can be discharge from the Barton Springs system (Slade et al., 1986). Thus, although derived from surface water sources, Austin municipal water contains some indirect discharge from the Barton Springs system.

The Barton Springs segment has been shown to undergo rapid changes in water quality, similar to most karst aquifers. Increases in bacteria concentrations have been observed in wells and springs of the Barton Springs segment after rainfall (Andrews et al., 1984), although there have been no major outbreaks of illness as a result of this phenomenon. Also, increases in anthropogenic pesticides have been

detected in the Barton Springs system after rainfall (Mahler and VanMetre, 2000). Finally, urbanization may be leading to long-term increases in contaminant concentrations (Turner, 2000). Because of the many stakeholders, there is a pressing need for monitoring, quantification, and investigation of these changes in water quality.

### **1.5.3. General public outreach**

As nearly 20 percent of the Earth's land surface is covered by karst terrane (White, 1988), and 20 percent of the United States is underlain by limestone or dolomite (Quinlan, 1989), many areas rely on aquifers in these parent rocks for potable water. Worldwide, one out of every four persons obtains their drinking water from a karst aquifer (Ford and Williams, 1989).

Karst springs present a unique scientific opportunity for the scientific community to connect with the general public. Desmarais and Rojstaczer (2002) point out that the springs usually associated with karst are one of the few signs of the influence of ground-water hydrology visible on the Earth's surface, and often attract public attention to the otherwise largely unseen world of ground water. In Texas, Barton Springs, San Marcos Springs, Comal Springs, San Antonio Springs, and San Solomon Springs all are examples of major karst springs that attract significant attention from the public. Some of these springs have even become

“lightning rods,” of sorts, for political and environmental debates about public policy. The Barton Springs system may be the best example of this lightning rod effect in all of Texas. For example, alleged contamination of the water in Barton Springs Pool in 2003 was the front-page headline in a major Austin newspaper (Austin American-Statesman, 2003).

## **1.6. ORGANIZATION OF THESIS**

This thesis is divided into five chapters. Chapter 1 (this chapter) presents an overview of the Barton Springs segment of the Edwards aquifer. A basic explanation of the aquifer is given, previous scientific studies are reviewed, and basic geochemical concepts used throughout this thesis are explained. Chapter 2 is an analysis of a long-term (26-year) ground water-quality dataset. The data, consisting of specific conductance and major ion analyses from wells and springs, are synthesized and analyzed using statistical methods and traditional geochemical analysis. Chapter 3 is an analysis of two years of sampling of the Barton Springs segment. The isotopes of strontium, oxygen, and hydrogen are used as additional hydrologic tools, and the dataset also is much higher resolution (i.e., more samples collected per unit time) than that of Chapter 2. Chapter 4 is an analysis of two weeks of intense sampling of the Barton Springs segment in order to quantify temporal

changes in ground water-quality that occur on the scale of hours to days. Finally, Chapter 5 is a summary of the findings of this thesis.

Chapters 2 through 4 were written as self-contained journal-style papers, each capable of standing on its own. Nevertheless, the chapters are presented in a progression from the large-scale to the small-scale. Chapter 2 is a 26-year dataset, Chapter 3 is a two-year dataset, and Chapter 4 is a two-week dataset. The Barton Springs segment reveals complexity and useful insight at all three of these time scales.

In the interest of disclosure, note that Garner et al. (in press), a USGS Scientific Investigation Report (SIR), was written by the author of this thesis. This SIR was written with the understanding that some of its contents would eventually be incorporated into this thesis. All of Chapter 2 and sections of all other chapters incorporate portions of the SIR into their contents.

## **1.7. DATA SOURCES**

### **1.7.1. Data from 1978–2003 (Chapter 2)**

The ground water-quality data used in Chapter 2 were collected by the USGS (Slade et al., 1979; United States Geological Survey, 1980; Slade et al., 1981). From 1978 to 1983, ground-water samples from 26 water wells were collected and analyzed several times a year for numerous water quality parameters, including

specific conductance and major ions including nitrate. From 1983 to 2003, approximately 11 of the original 26 wells continued to be sampled periodically. Over the years, some sampling sites and analyses were added while others were dropped. Sampling intervals also changed through time, and occasionally years were skipped altogether.

Surface-water discharge measurements for the five principal creeks in the study area (Figure 1-1) have been recorded by the USGS since 1978. These values were measured at gaging stations along creeks that recharge the aquifer. The discharges are computed from stage-discharge relationships that have been developed for each of the sites and that are updated regularly by manual discharge measurements made with current flow meters (Buchanan and Somers, 1969). There are occasional gaps in the dataset, but overall it represents a fairly continuous record of surface-water flow across the Barton Springs segment.

Discharge data for the Barton Springs system have been recorded since 1978. Discharge rates are determined on the basis of ground-water levels in a nearby well, much as a stage-discharge relation is used. The relation between the water level in the well and the spring discharge is well defined, provided that the water level in Barton Springs Pool remains constant. When the water level in the pool changes, for example if it drops when the gates to the lower dam are opened or rises when the upper dam is overtopped by Barton Creek, the established rating can no longer be

used. The relation is periodically verified and refined through the use of manual stream-gaging measurements.

Summaries of these data have been published (Senger, 1983; Slade et al., 1986), and most of the data are available from published USGS annual data reports. A comprehensive compilation of all data is available in Garner et al. (in press), and a subset of these data is provided in the appendixes of this thesis.

#### **1.7.2. Data from 2003–2005 (Chapters 3 and 4)**

In mid-2003, the USGS began a new sampling program for the Barton Springs segment that was carried out concurrently with existing monitoring programs. Samples were collected every two weeks in August 2003 and September 2003, and every three weeks from June 2004 to June 2005. The major ion data presented in Chapter 3 are the product of this sampling effort.

On each sampling trip, several additional sample bottles were filled for the purpose of isotope ratio analysis. The isotope ratio data presented in Chapters 3 and 4 are the product of this effort, and all isotope ratio analytical results are available in the appendixes of this thesis.

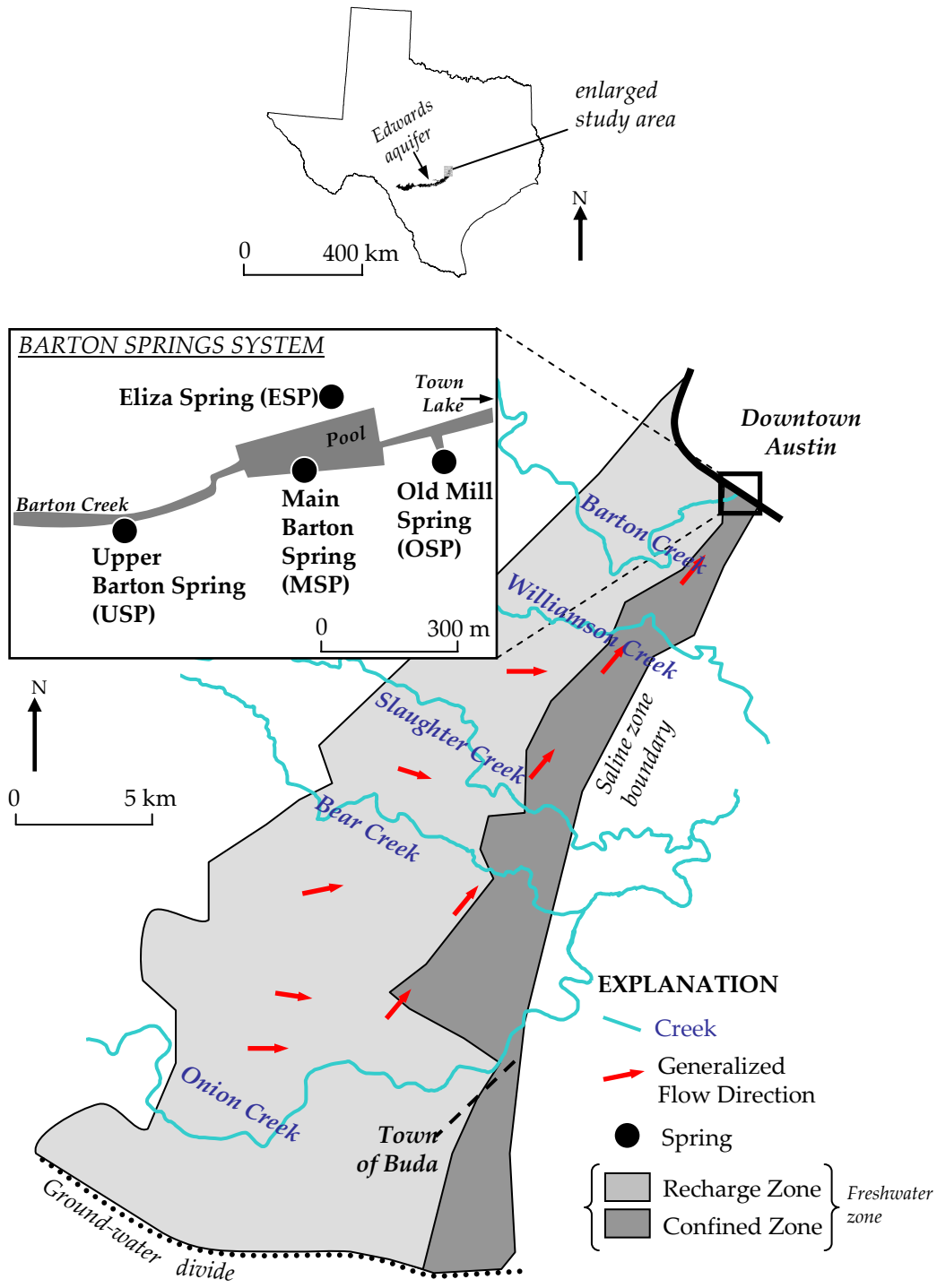
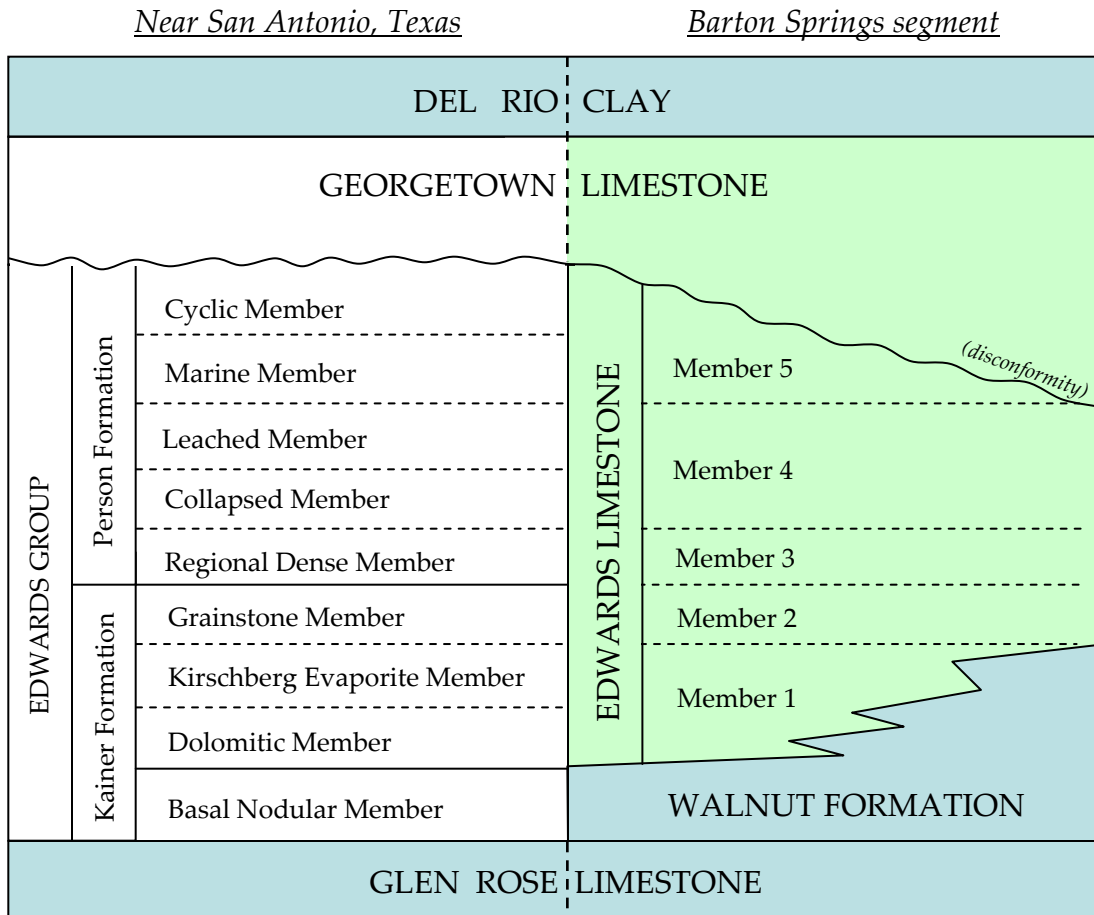


**Figure 1-1.** Map of the Barton Spring segment of the Edwards aquifer (after Slade et al., 1986). For additional spring site information, see Table B-1.



**HYDROSTRATIGRAPHIC EXPLANATION**

- Confining layer
- Barton Springs segment of the Edwards aquifer

**Figure 1-2.** Geologic formations associated with the Barton Springs segment and surrounding regions. Confining units are shaded blue, and the Barton Springs segment is shaded green. Near San Antonio, the nomenclature of Rose (1972) is used (left side of figure). In the Barton Springs segment, the Basal Nodular Member is identified as the Walnut Formation, and serves as a confining layer for the aquifer (right side of figure) (modified from Sharp and Banner, 1997, with data from Small et al., 1996).

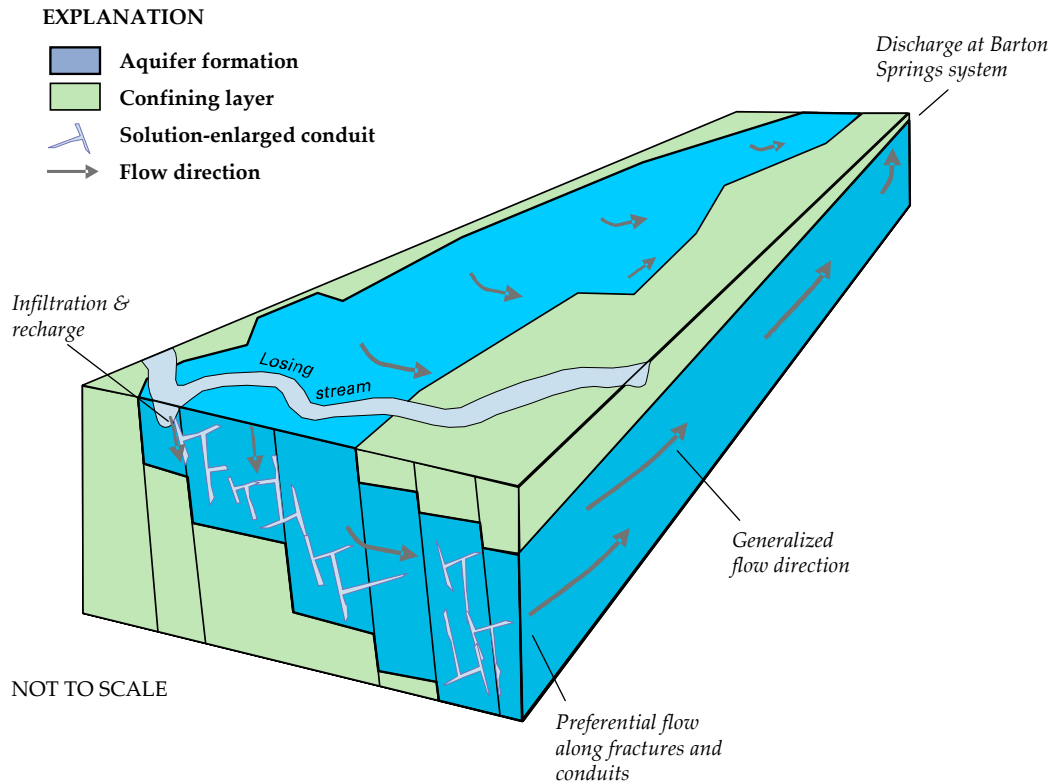


**Figure 1-3.** Schematic diagram of the Barton Springs segment of the Edwards aquifer. Recharge water enters the aquifer through the beds of creeks as they cross the recharge zone. Water in the aquifer flows generally to the north-northeast, generally along solution-enlarged conduits that act at highly preferential flowpaths. The majority of aquifer water eventually discharges at the far northeast corner of the aquifer at the Barton Springs system.

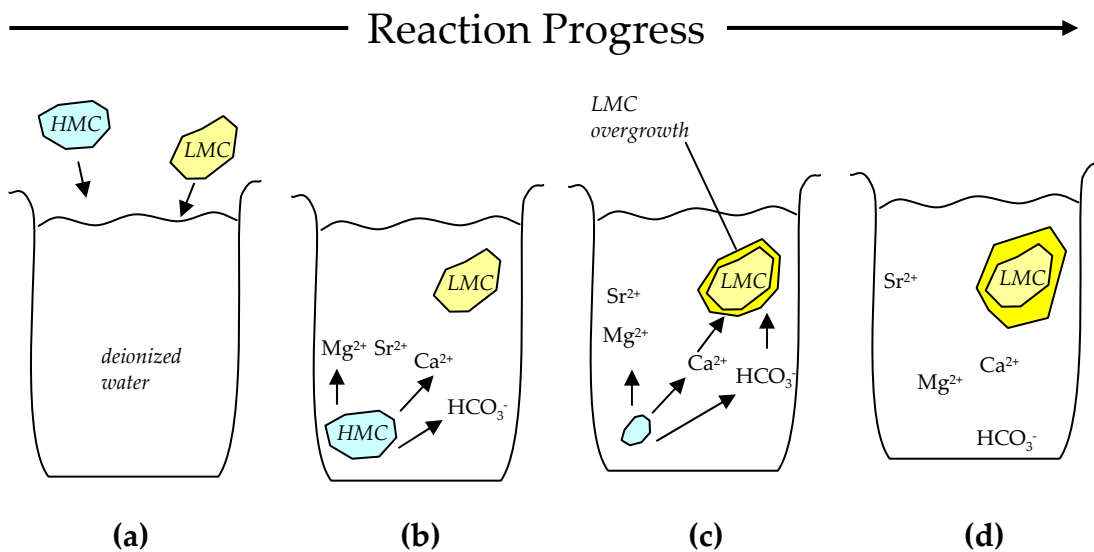


**Figure 1-4.** Schematic diagram showing the principle of incongruent dissolution. (a) High-magnesium calcite and low-magnesium calcite crystals are added to deionized water; (b) The chemically aggressive water begins to dissolve both HMC and LMC, although chemical kinetics cause HMC to dissolve more rapidly than LMC; (c) saturation is reached with LMC, but HMC still continues to dissolve because it is about 10 times more soluble than LMC. Continued dissolution of HMC drives LMC to supersaturation, and a LMC overgrowth begins to form on the original crystal of LMC; (d) reaction has proceeded until all HMC has been dissolved. The LMC overgrowth has grown, and some of the  $Sr^{2+}$  and  $Mg^{2+}$  have been preferentially excluded from the newly precipitated overgrowth and are at elevated levels in the water (modified from James and Choquette, 1984).

**Figure 1-5a.** Onion Creek, immediately upstream of where it crosses onto the Barton Springs segment recharge zone. All of the water seen in this photo entered the Barton Springs segment as recharge within hours after this photograph was taken.

**Figure 1-5b.** Cripple Crawfish sinkhole, a karst feature in the creekbed of Onion Creek. A water vortex indicates rapid infiltration of water into the Barton Springs segment. As of 2005, this sinkhole has been covered by a man-made structure that prevents excessive sediment from entering the cave (K. Thuesen, City of Austin, written comm., 2005). Photograph courtesy of Nico Hauwert (City of Austin).

**Figure 1-5c.** Eastward-looking aerial photo of Barton Springs Pool, which is filled by Main Barton Spring (MSP). Over 300,000 visitors visit this site annually, and it is a centerpiece of local political and environmental dialog. Photograph courtesy of the City of Austin.

**Figure 1-5d.** Old Mill Spring (OSP), one of the four springs in the Barton Spring System. A rock wall was built to contain the spring in the 1930s, but the spring is no longer accessible to the public because of safety issues and its designation as an endangered species habitat.

**Figure 1-5e.** The Barton Springs salamander (*Eurycea sosorum*), a federally-listed endangered species. The salamander's only known habitat is the Barton Springs system (springs MSP, ESP, OSP, and USP). Adults reach about 6 cm in length and retain their gills throughout their entire life cycle. The salamander is very sensitive to changes in water quality (Mahler and Lynch, 1999). Photograph by W. Meinzer (U.S. Fish and Wildlife Service).



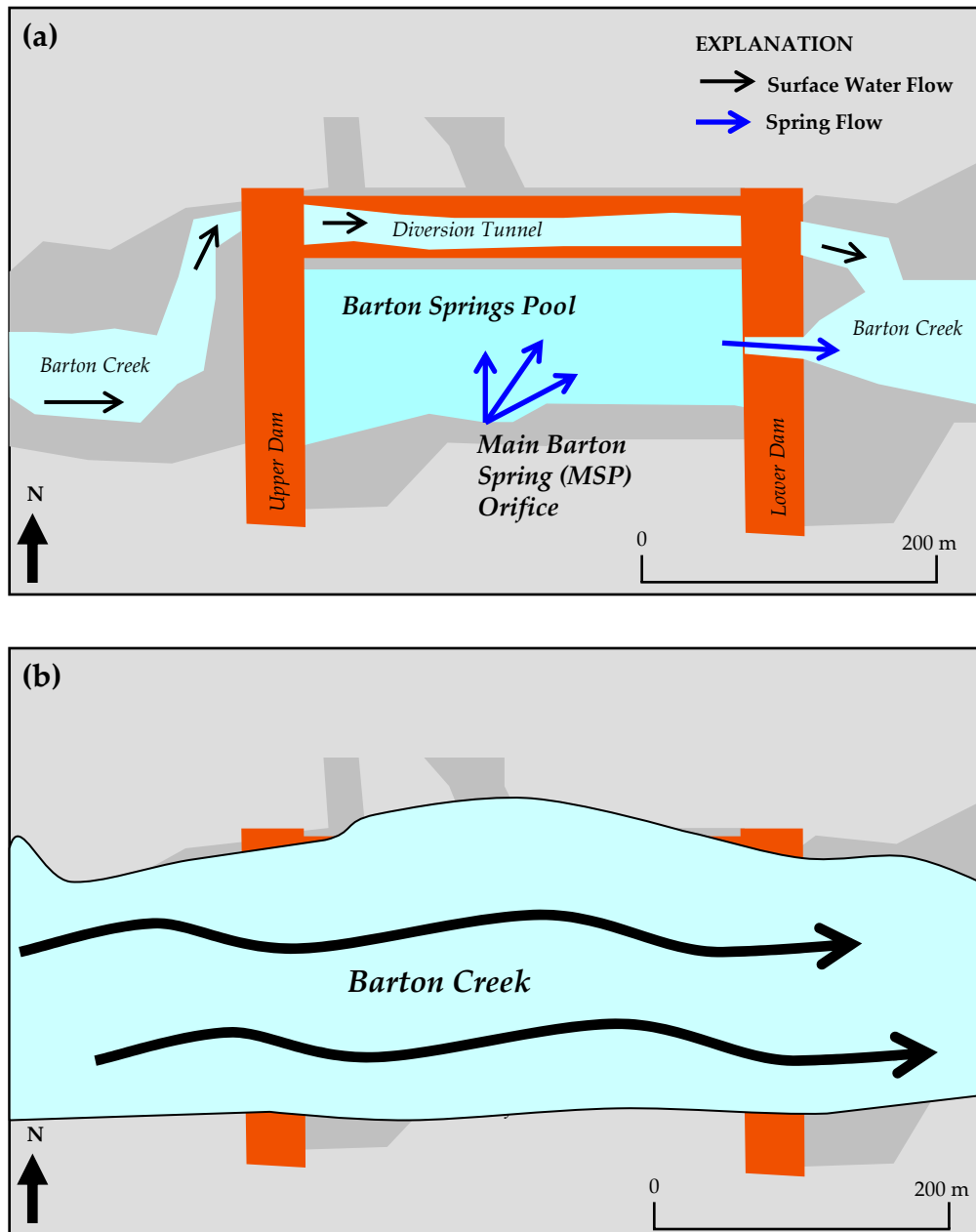


**Figure 1-6.** Schematic diagram showing a plan view of the two modes of operation of Barton Spring Pool with respect to flow in Barton Creek. (a) Under most conditions, the pool is filled solely by discharge from Main Barton Spring, while any surface-water flow in Barton Creek is diverted around the pool by a dam; (b) under very high stormflow conditions, surface-water flow in Barton Creek overtops the upper dam. During these flood conditions, access to Main Barton Spring for water-quality sampling is difficult or impossible.

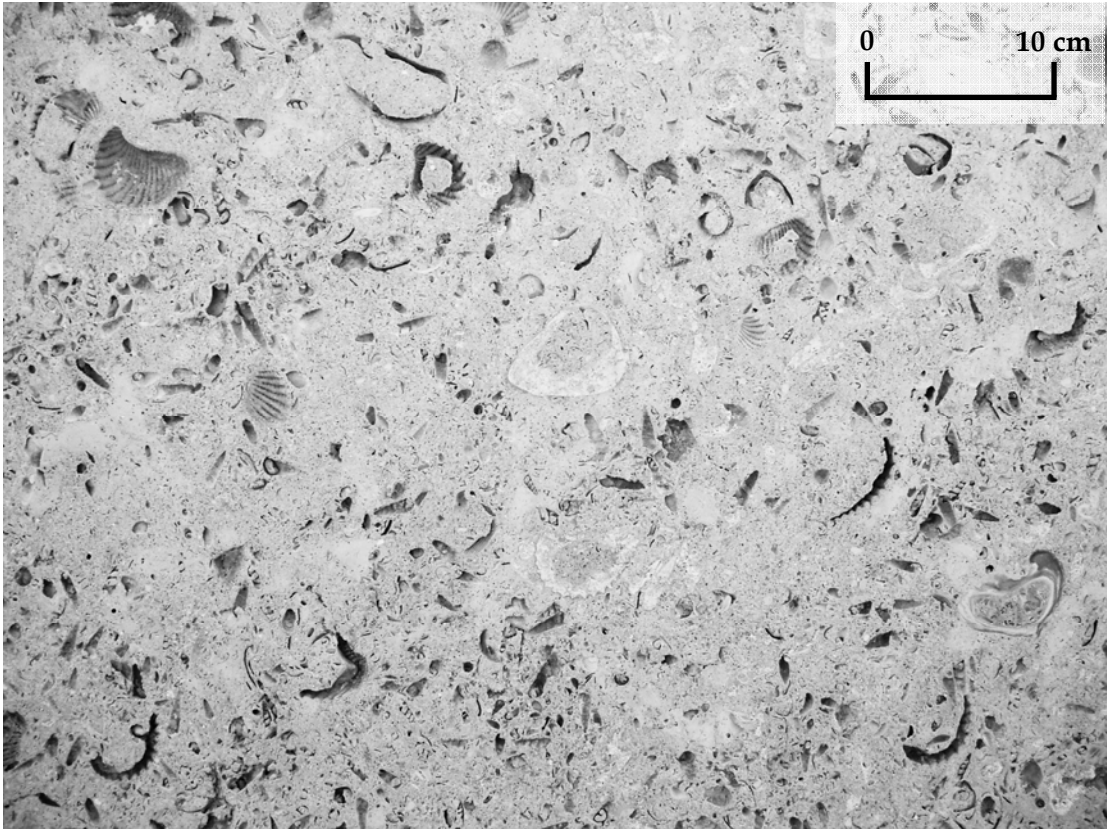


**Figure 1-7.** Polished slab of limestone showing moldic porosity typical of meteoric diagenesis and dissolution of metastable minerals. Some marine pelecypod and gastropod shells are initially deposited as the metastable mineral aragonite, and are subsequently dissolved upon exposure to meteoric water. The surrounding low-magnesium calcitic mud is not dissolved. This process creates a rock with high porosity but low permeability. Permeability may be enhanced by solution enlargement of these original pores, although this is not seen here. Photo is of the Cedar Park Limestone, time-correlative with the upper Walnut Formation and lower Edwards Limestone, as seen on an exterior wall of the University of Texas Geology building.

## **2. Investigation of the relationship between surface-water flow and karst ground-water geochemistry in the Barton Springs segment of the Edwards aquifer**

### **2.1. ABSTRACT**

Historical ground-water geochemistry data from the Barton Springs segment of the Edwards aquifer were analyzed to determine the relation between ground-water geochemistry in 26 wells, flow rates in five creeks that provide recharge to the aquifer, and aquifer flow condition as measured by the discharge rate of a karst spring. Twenty-six years of arbitrarily timed specific conductance measurements in wells were compared to contemporaneous aquifer flow conditions and surface-water discharge rates. Using a non-parametric statistical test, the wells were divided into groups with similar statistical properties. Specific conductance in 9 of the 26 wells exhibited a negative statistical correlation to streamflow or aquifer flow condition. This was interpreted as evidence of an influx of low ionic strength recharge water during periods of high surface flow: four wells were concluded to intersect major aquifer flowpaths, and five were concluded to intersect minor aquifer flowpaths. Six wells had a positive correlation between specific conductance of and aquifer flow condition, which was not interpreted as reflecting intersection of a flowpath, but

rather as the influence of some other process. Of the 17 wells that did not have a negative correlation between specific conductance and streamflow, no conclusions regarding flowpath intersection were drawn. In some cases, data for wells might not have indicated intersection with a flowpath because of small sample sets. Aquifer ground water was generally calcium-bicarbonate to calcium-magnesium-bicarbonate, although some water compositions deviated from this. Multiple geochemical processes were identified that may affect well geochemistry. On the basis on  $\text{SO}_4/\text{Cl}$  and  $\text{Mg}/\text{Na}$  concentration ratios, some wells seemed to receive a portion of their water from the saline zone to the east, which may extend as a saltwater lens under the freshwater portion of the aquifer. Other wells may have received some of their water from the underlying Trinity aquifer, especially when aquifer flow conditions are high. Despite the arbitrary sampling interval of this historic record, use of statistical methods to distinguish between wells controlled by various processes appeared to have value.

## **2.2. INTRODUCTION**

In karst aquifers, surface water can enter the aquifer as focused recharge through fractures, cavities, or sinkholes and move rapidly through the system via solution-enlarged fractures or conduits to discharge from springs or wells. Although ground water is stored throughout the pore spaces in the carbonate rock, the

majority of ground-water transport occurs through these solution-enlarged cavities and conduits (Ford and Williams, 1989; Sharp, 1993; Maloszewski et al., 2002). As a result, recently infiltrated ground water moving through these conduits has little time to equilibrate with the rock matrix, and bears a geochemical signature similar to that of surface water. Because of their high hydraulic conductivity, these conduits also are usually major flowpaths in the aquifer. To understand the way in which a karst aquifer functions, it is desirable to find the locations of these flowpaths. One approach to locating flowpaths is to identify wells that intersect them, and map the geography of these wells and infer flowpaths between them, using their major ion geochemical signatures as verification of the findings.

Several approaches can be used to identify wells that intersect major conduits and flowpaths. Pump tests can identify wells with very high specific capacities, which may be related to intersection of large conduits. Monitoring of physical, chemical, and biological parameters during storm-flow conditions may also identify those wells that intersect flowpaths (Andrews et al., 1984). Dye-trace studies monitoring the arrival or non-arrival of a dye injected at the surface in nearby wells can use this information to map connections between individual recharge locations and wells (Hauwert et al., 2005). In this study, an alternative to these physical approaches is presented—a 26-year record of the aqueous geochemistry of water in wells is used to identify wells that intersect major flowpaths.

Specific conductance is a physical measurement of the amount of electrical current that water can transmit, and a direct reflection of the ionic strength, or total amount of dissolved solids, in the water (Hem, 1982). Rain has very low specific conductance (Herczeg and Edmunds, 2000); surface water has a higher specific conductance resulting from chemical reactions with the land surface, soils, and the streambed; ground water typically has a higher specific conductance than surface water resulting from the dissolution of the rock matrix of the aquifer. Thus, specific conductance can act as a tracer of infiltrated surface water with low specific conductance.

Because of their close connection with the surface-water system, the geochemistry of karst springs can be extremely variable (Shuster and White, 1971). In response to precipitation events, focused recharge moves rapidly through fractures and conduits into the aquifer and springs. As a result, a rapid decrease in total dissolved solids occurs, which gradually increases back to a value more representative of interaction with the rock matrix (e.g., Ryan and Meiman, 1996; Desmarais and Rojstaczer, 2002). In this study, this concept is extended to wells, with the hypothesis that the geochemistry of water in a well that intersects a fracture or conduit along an aquifer flowpath should respond in a similar manner, that is, the specific conductance should decrease in response to the influx of recent recharge.

A high sampling frequency is desirable for investigating the relation between surface water and ground water in a karst aquifer (e.g., Dreiss, 1989; Lakey and Krothe, 1996). However, the dataset for this study generally does not contain high-frequency sampling intervals (hours to days). Nevertheless, it is hypothesized that a large data ensemble even from infrequent and arbitrarily-timed sampling carried out over 26 years contains some of the same information as data from a study with a high sampling frequency.

### **2.3. STUDY AREA**

The Barton Springs segment of the Edwards aquifer (herein referred to as the Barton Springs segment) is a karst aquifer that extends south-southwest of Austin. It is bounded to the north by the Colorado River, to the south by a ground-water divide, to the west by its contact with the Glen Rose Formation, and to the east by a zone of low permeability (Maclay and Land, 1988) containing brackish to saline (> 1000 mg/L total dissolved solids) ground water known as the saline zone (Figure 2-1).

Previous studies have characterized the lithology, structure, and physical and chemical hydrogeology of the Barton Springs segment. The aquifer material is composed principally of Cretaceous limestone that has undergone multiple episodes of karstification (Rose, 1972; Maclay, 1995; Small et al., 1996). In the Miocene epoch,

tectonic activity created a zone of normal faulting, resulting in enhanced karstification and the aquifer structure and behavior seen today (Slade et al., 1986). The aquifer is generally highly transmissive, with some measured straight-line transit times exceeding 10 kilometers per day (Hauwert et al., 2005). The Barton Springs segment resides within the Edwards and Georgetown Limestones, is underlain by the less permeable Walnut and Glen Rose Formations, and is overlain by the less permeable Del Rio Clay (Rose, 1972). In the recharge zone, the aquifer is unconfined, that is, the aquifer rock outcrops on the surface. The confined zone is defined by the area where the Del Rio Clay and younger rocks overlie the Edwards and Georgetown Limestones (Figure 2-2).

The dissolved ion chemistry of Barton Springs segment ground water is generally calcium-bicarbonate ( $\text{Ca-HCO}_3$ ) to calcium-magnesium-bicarbonate ( $\text{Ca-Mg-HCO}_3$ ) containing less than 500 mg/L total dissolved solids, although significant variations in dissolved constituents and molar ratios have been observed (Senger and Kreitler, 1984). Studies such as Andrews et al. (1984) have shown that some geochemical variability is attributable to episodic recharge of meteoric water in response to storms.

About 85 percent of the recharge to the aquifer is estimated to occur through karst features in the creek beds of Barton, Williamson, Slaughter, Bear, and Onion Creeks (Slade et al., 1986). These are ephemeral creeks that cross the recharge zone

from west to east (Figure 2-1). Examples of karst features are fractures, faults, and sinkholes. Additional sources of recharge include upland infiltration through sinkholes and fractures, urban infrastructure, and cross-formational flow from other hydrostratigraphic units (Sharp and Banner, 1997). Flow in the aquifer is generally to the north-northeast, following the trend of the Balcones Fault Zone, although direction of flow varies with changes in aquifer flow condition and resulting changes in the potentiometric surface (Slade et al., 1986).

Discharge from the aquifer is from springs and wells. The primary discharge point is a cluster of springs at the northeastern edge of the aquifer known as the Barton Springs system (Figure 2-1). Combined long-term mean discharge from the three major orifices in the system is about 50 ft<sup>3</sup>/s (Slade et al., 1986). Additional ground water is withdrawn from the aquifer by pumping from domestic, livestock, and public supply wells. In 2004 there were an estimated 970 active wells pumping from the Barton Springs segment, with annual ground-water withdrawals of about 2.5 billion gallons per year (Smith and Hunt, 2004), equivalent to a constant withdrawal rate of about 10 ft<sup>3</sup>/s (0.3 m<sup>3</sup>/s). Since 1978, the United States Geological Survey (USGS) has collected about 600 water quality samples from 26 of these wells (Figure 2-1 and Table 2-1), and these geochemical data are used in this study's analysis.

## 2.4. STUDY APPROACH

The approach taken here was to evaluate historical geochemical data from 26 wells in the Barton Springs segment (Table 2-1) in the context of contemporaneous surface-water flow data and aquifer flow condition data, under the hypothesis that recharging water and variable aquifer flow conditions can result in variations in well geochemistry. The approach was to use statistical correlations between specific conductance in wells, discharge rates in streams, and aquifer flow condition to identify those wells connected to fractures or major flowpaths. Major ion geochemistry data from the wells were used to better understand the geochemical processes affecting the ground water.

Discharge values from gaging stations along Barton, Williamson, Slaughter, Bear, and Onion Creeks were used as measures of streamflow (Figure 2-1). High flow in the creeks was assumed to indicate recent rainfall and associated recharge.

The discharge rate of the Barton Springs system was used as an indicator of aquifer flow condition. High flow rates were assumed to indicate high aquifer flow conditions. Aquifer flow condition thus is represented by a single value that measures the overall state of the Barton Springs segment with respect to ground-water storage and flow velocity. Senger (1983) confirmed that, like most springs, the discharge rate of the Barton Springs system is directly controlled by the amount of water stored in the Barton Springs segment.

Specific conductance was used as an overall measurement of ground-water geochemistry. However, as variations in specific conductance do not indicate which dissolved ion concentrations are changing, the major ion geochemistry of the ground water was interpreted to determine what geochemical processes might be occurring.

## **2.5. METHODS**

### **2.5.1. Sample collection**

Ground-water samples were collected by the USGS from 1978 to 2003, from privately-owned domestic and livestock wells and municipal wells (Table 2-1) in which a variety of construction and plumbing techniques were used. Most wells were completed entirely within the Edwards aquifer (Edwards and Georgetown Limestones), and steel casing was used to seal off formations that are not part of the aquifer (e.g., Del Rio Clay, Buda Limestone, etc.; Figure 2-2). Almost all wells were completed in the aquifer as open hole. Most wells did not penetrate the full thickness of the aquifer; generally, drillers followed a two-step process (Maclay, 1995): (1) drill to the top of the aquifer and install casing, and (2) drill until a cavernous zone is encountered or the bottom of the aquifer is reached. Three wells in the recharge zone (GHW, SLR, and FOW) were drilled partly into the underlying Walnut and Glen Rose Formations and therefore were drilled partly into the Trinity aquifer (N. Houston, U.S. Geological Survey, written comm., 2005). Because of

permeability differences in the aquifer rock, wells may have yielded water that is a mixture of several permeable zones, and variable pumping rates and times may have affected this mixing (Hem, 1985).

Samples were collected from wells at points in the plumbing upstream of pressure tanks or treatment equipment in order to obtain a sample representative of aquifer water. Water was abstracted from the well by either using an electric submersible pump, or by hand-bailing. Samples were collected after purging at least three casing volumes of water from the well and after readings of field parameters (temperature, pH, and specific conductance) had stabilized. Beginning in 2001, USGS National Water Quality Assessment Program sampling protocols and analytical schedules were incorporated into the sampling program (Koterba et al., 1995).

Specific conductance was measured and recorded during all USGS sampling events at wells. The instrument models used to take this measurement changed over the years, but standard procedures were consistently followed (Radtke et al., 1998a). Instruments were calibrated using at least two standard solutions of known specific conductance and documented. Specific conductance measurements were taken after at least three well-volumes of water were purged from wells (United States Geological Survey, 1984; Wilde et al., 1999). The final reported specific conductance

value was typically computed as the median value of five readings taken over a 15-minute period.

Water samples for major ion analysis were collected and filtered through 0.45 µm cellulose filters. Anion samples were dispensed into pre-rinsed polyethylene bottles. Cation samples were placed in pre-rinsed acid-cleaned polyethylene bottles, and the sample was preserved with a strong acid to a pH of less than two. Samples were promptly chilled on ice in dark conditions, and shipped to the USGS National Water Quality Laboratory (NWQL) for analysis.

### **2.5.2. Laboratory analytical methods**

Analytical methods at the NWQL changed over the period of investigation. Major cations were analyzed by atomic absorption spectroscopy (Fishman and Friedman, 1989, p. 137,263,393,425), by atomic emission spectroscopy (Fishman, 1993, p. 101), and most recently by inductively-coupled plasma mass spectrometry. Prior to 1990, chloride concentration was determined using titrimetric or colorimetric methods (Fishman and Friedman, 1989, p. 151-159), and sulfate concentration was measured using turbidimetric analysis by formation of barium sulfate. After 1990, chloride and sulfate were measured using ion chromatography (Fishman, 1993, p. 19). Nitrate ( $\text{NO}_3^-$ ) was analyzed using ion chromatography or cadmium reduction-diazotization colorimetry (Fishman, 1993, p. 157). Based on the findings of

Andrews et al. (1984), concentration of nitrite ( $\text{NO}_2^-$ ) was assumed to be negligible, thus the measured nitrate+nitrite parameter was assumed to solely indicate nitrate concentration. Trace elements such as strontium were assumed to be of negligible concentrations, and ion complexation was assumed to be negligible. Despite variations in collection and analysis methods, this study assumes that methods have been sufficiently consistent to allow side-by-side comparison of major ion concentrations.

Two additional criteria were used to screen analytical results from the large historical record. First, wells with fewer than six specific conductance measurements were excluded, as they did not provide a sufficient record for statistical analysis. Second, water analyses with a charge balance error greater than  $\pm 5$  percent were excluded (Freeze and Cherry, 1979, p. 97), similar to methods employed by other researchers synthesizing large historic datasets (e.g., Uliana and Sharp, 2001)

### **2.5.3. Statistical analysis of specific conductance and flow data**

Data were compared to see if there was a statistical relation between streamflow rates and specific conductance measured in well water, and between aquifer flow condition and specific conductance measured in well water. For each specific conductance value, data for the previous ten days of streamflow in the five creeks were inspected, and the maximum mean daily streamflow rate for each creek

for that 10-day period was recorded (Appendix A, Table A-1). The relations between the specific conductance data and corresponding streamflow measurements were compared using the non-parametric Spearman rho rank test (Helsel and Hirsch, 1995). A non-parametric correlation test such as Spearman's rank correlation was used because the surface-water flow and spring discharge data do not follow a normal distribution (Figure 2-3). For the comparison of specific conductance and aquifer flow condition, the Spearman rho test was used to test the relation between specific conductance and Barton Springs system discharge for the day that the specific conductance measurement was collected. Barton Springs system discharge rates were determined by measuring ground-water levels in a nearby well and using a stage-discharge relationship (rating curve) to compute discharge. This rating curve was periodically refined with manual discharge measurements taken using a current velocity meter (Buchanan and Somers, 1969).

The Spearman rho test measures the strength of association between two variables (Helsel and Hirsch, 1995). The data for each variable are ranked, and the differences between the ranks analyzed as

$$\rho = 1 - 6 \sum \frac{d^2}{n(n^2 - 1)} \quad (\text{Eq. 2-1})$$

where d is the difference in ranks and n is the number of ranks.  $\rho$  varies from -1 to 1; a  $\rho$  of -1 expresses a perfect monotonic negative relation, and an  $\rho$  of 1 expresses a

perfect monotonic positive relation. Spearman's  $\rho$  (rho) is analogous to the Pearson  $r$ , the product-moment correlation coefficient, in that it expresses the proportion of the variability accounted for, but on the basis of ranks.

Basic summary statistics were used to describe properties of water samples in a general way. Minimum, maximum, arithmetic mean, and median are examples of common summary statistics used in this study. Median values for groups of wells were computed using a two-step process. First, the median value for each well was computed. Then, the median of these median values was computed, and this is the number reported. This two-step procedure was necessary to avoid sampling bias arising from variable numbers of samples taken from each well. Without this two-step process, median values would be disproportionately influenced by wells with large sample sets, and wells with small sample sets would have comparatively little effect on the average value.

Coefficients of variation ( $C_v$ ) also were computed for several geochemical parameters.  $C_v$  is defined as the standard deviation divided by the arithmetic mean, and is a quantitative measurement of the degree to which numbers in a set deviate from the mean value.

## **2.6. RESULTS**

### **2.6.1. Specific conductance**

The specific conductance dataset for the 26 wells contains 689 values ranging from 388 to 1530 microsiemens per centimeter ( $\mu\text{S}/\text{cm}$ ) (Appendix A; Table A-1).

Eight wells have only six specific conductance values, the minimum number required for inclusion in this study, and four wells have more than 50 values. The widest range (445 to 1530  $\mu\text{S}/\text{cm}$ ) occurs in water from well SVE, and the narrowest range (480 to 495  $\mu\text{S}/\text{cm}$ ) occurs in water from well ISD. One-half of the wells had water with less than 100  $\mu\text{S}/\text{cm}$  variation. The median  $C_v$  for specific conductance for all well samples is 0.035, with a range of 0.011 to 0.283.

### **2.6.2. Streamflow and aquifer flow condition**

The streamflow dataset consists of approximately 9,000 mean daily streamflow values for each of the five creeks. Williamson and Slaughter Creeks have discharge data available for the entire period from 1978 to 2003, data for Bear and Onion Creeks span 94 percent of this period, and data for Barton Creek span 76 percent of this period. Streamflow data for Barton Creek were unavailable from 1983 to 1988, thus 31 percent of specific conductance samples could not be tested against Barton Creek discharge. These full listing of these data are omitted from this study for brevity, but are available in their entirety in Garner et al. (in press).

### 2.6.3. Statistical test

Results from the non-parametric correlation test between specific conductance, streamflow rates, and aquifer flow condition (Appendix A; Table A-2) were used to divide the 26 wells into distinct populations. Fifteen of the 26 wells exhibit a statistically significant relation between well-water specific conductance and streamflow or aquifer flow condition ( $p < 0.05$  confidence level).

The wells were further divided into four groups (Table 2-2, Figure 2-5). Wells in group C1 exhibit a negative correlation between specific conductance and streamflow, and a negative correlation between specific conductance and aquifer flow condition. Wells in group C2 exhibit a negative correlation between specific conductance and streamflow only. Wells in group P exhibit a positive correlation between specific conductance and aquifer flow condition. Wells in group N do not exhibit a correlation between specific conductance, streamflow, or aquifer flow condition.

The statistical analyses produced some spurious correlations resulting from autocorrelation between the streamflow rates in the different creeks.

Autocorrelation occurs when a widespread rainfall produces proportional changes in flow on all five creeks; the geochemistry in well water may be influenced by flow in only one or two of the creeks, but will be correlated to flow in all five. For

example, the specific conductance of samples from well MCH is correlated with flow in Barton, Williamson, and Slaughter Creeks, but as MCH is far upgradient from (south of) these creeks, it is unlikely that flow in these creeks has an influence on the geochemistry of the well water. Spurious correlations were determined on the basis of location of the wells and creeks and existing information on direction of flow. These determinations were made conservatively and with caution, as direction of flow in karst terrane is often difficult to ascertain and can be temporally variable.

## **2.7. DISCUSSION**

### **2.7.1. Geochemical variability at the event scale**

To provide a frame of reference for considering the long-term relation between surface water and ground water in a karst aquifer, a high-frequency sampling event (hours to days) in this study's dataset is considered in this section. Well SVW exhibits a long-term statistical correlation between the specific conductance of its water and streamflow in all five creeks; the strongest correlation is with Bear Creek (Table 2-2). In October 1994, well SVW was sampled at 6- to 12-hour intervals beginning 2 days after a rain event. The results of this sampling provide an opportunity to investigate how the geochemistry of a well changes in response to rain and resulting flow in a nearby creek at a short time scale.

Flow in all five recharging creeks increased on October 7, 1994. The highest mean daily flow was recorded at Barton Creek (476 ft<sup>3</sup>/s), followed by Slaughter Creek (99 ft<sup>3</sup>/s), Williamson Creek (73 ft<sup>3</sup>/s), Bear Creek (33 ft<sup>3</sup>/s), and Onion Creek (30 ft<sup>3</sup>/s). Fifteen samples were collected at well SVW from October 9 at 7:00 AM to October 15 at 12:30 PM.

Over the sampling period, specific conductance in water from well SVW ranged from 570 to 678  $\mu\text{S}/\text{cm}$ . The lowest specific conductance value was measured in the first sample, collected two days after maximum streamflow. From a comparison of flow in Barton Creek and specific conductance in SVW, it appears that well water responded rapidly to an influx of recharge from one of the nearby creeks (Barton or Williamson) (Figures 2-1 and 2-6a). However, the data indicate that specific conductance had probably already reached the minimum value of 570  $\mu\text{S}/\text{cm}$  and had begun to rise before the first sample was collected. Thus, the lowest specific conductance value and its timing in response to creek flow for this event is unknown. The rapid response to streamflow (less than two days) suggests that the 10-day criteria for response to stream flow for the statistical comparison of specific conductance to peak streamflow is reasonable.

The increase in specific conductance in well SVW water was followed by a subsequent decrease, which indicates that this well may obtain recharge from more than one creek; the first decrease occurred less than 2 days after rainfall, and the

second decrease occurred about 4 days after rainfall (Figure 2-6a). Although Hauwert et al. (2005) suggest that this well is located in a small aquifer subbasin and does not receive recharge from multiple creeks, it is possible that transient flowpaths are activated during high recharge periods. Alternatively, it could have received recharge from two different recharge points in the same creek.

In a plot representing the storm-related samples from well SVW on a Piper diagram (Figure 2-6b), the points representing the 15 samples overlie one another, indicating that the changes in specific conductance largely are attributable to dilution rather than to mixing with another ground-water type. The dilution likely results from infiltration of surface water containing fewer dissolved ions. There is a slight shift along the calcium-magnesium axis, which could simply indicate a change in residence time (Musgrove and Banner, 2004).

Changes in  $\log SI_{\text{calcite}}$  values over time are consistent with the hypothesis of two influxes of recharge water into well SVW (Figure 2-6c).  $\log SI_{\text{calcite}}$  values were low in the first sample, indicating a very recent influx of surface water. As the undersaturated surface water mixed with ground water presumably in equilibrium with calcite, the saturation index increased, before decreasing with the second influx of surface water. The second influx of recharge water was not as undersaturated as the first, indicating that effects from the rainfall had begun to decrease after four days.

During the sampling period, the Mg/Ca molar ratio for water in well SVW increased from 0.35 to 0.47, suggesting that low ionic strength stormflow water began to react with the aquifer and evolve. Alternatively, this behavior could also result as influx of recharging water ceases and is replaced in well SVW by more geochemically evolved ground water that was in the aquifer prior to the recharge event.

Concentrations of other ions in the samples from well SVW varied in response to flow in Barton and Williamson Creeks (Figure 2-6d).  $\text{Na}^+$  and  $\text{Cl}^-$  concentrations were lowest in the first samples collected. Following an increase in  $\text{Na}^+$  and  $\text{Cl}^-$  concentrations that mimicked that of specific conductance, these concentrations decreased again (probably in response to a second influx of recharge water). In the first sample collected, molar concentrations of  $\text{Na}^+$  to  $\text{Cl}^-$  are about 1:1, indicating a potential NaCl (halite) source from surface water, but in the final samples molar concentration ratios of  $\text{Na}^+$  to  $\text{Cl}^-$  are about 0.75:1, suggesting that water in this well under steady-state conditions is more enriched in  $\text{Cl}^-$  than  $\text{Na}^+$ . Sulfate ( $\text{SO}_4^{2-}$ ) concentrations increased in the first few samples, but the lowest concentrations were in the second influx of surface water (Figure 2-6d). This suggests that the two different influxes have different sources or have the same source but follow different flowpaths.

Nitrate ( $\text{NO}_3^-$ ) concentrations were lowest in the first samples collected, suggesting that the influx of surface water has a lower  $\text{NO}_3^-$  concentration than the ground water. Concentrations of  $\text{NO}_3^-$  in streamflow associated with storm events in creeks repeatedly have been observed to be less than those in water discharging from the Barton Springs system (City of Austin, 1997). After the initial recovery from the first influx of surface water,  $\text{NO}_3^-$  concentrations closely track  $\text{Cl}^-$  concentrations (Figure 2-6d).

Overall, this well typifies the geochemical response of a well on a major flowpath, with specific conductance, ion concentrations, and ionic ratios varying on the scale of days following a recharge event (Figures 2-6). The results of this analysis suggest that wells in a karst aquifer can intersect flowpaths that connect to surface-water source areas. Because of this connection, changes in surface-water flow affect the geochemistry of these wells over short time scales. The following section considers this same type of effect, but using a dataset that replaces high-frequency sampling with sampling over a long time period under variable hydrologic conditions.

## 2.7.2. The four well groups

### 2.7.2.1. Group C1 wells

Four wells in Group C1 (FMW, KCH, SLR, and SVE) (Figure 2-7a; Table 2-2) have specific conductance that is negatively correlated to flow in one or more of the five recharging creeks, and also negatively correlated to aquifer flow condition (as measured by discharge from the Barton Springs system). When aquifer flow conditions are high and streamflow rates are high, wells in group C1 are more likely to have water with lower specific conductance values than when aquifer flow conditions are low and streamflow rates are low. This suggests that these wells intersect major flowpaths or conduits that transport recharge from the surface through the aquifer, and that these flowpaths respond to overall aquifer flow conditions, integrating water from a large volume of the aquifer. Examples of the correlations between specific conductance at one of the wells (FMW), flow in Slaughter Creek, and discharge from Barton Springs are shown in Figure 2-8.

The Spearman's  $\rho$  (rank correlation coefficients) for wells in group C1 are among the highest for the wells tested; forty-three percent of all rank correlation coefficients with magnitudes greater than 0.5 are from group C1 (Table 2-2). Of note is a strong correlation ( $\rho=0.63$ ) between specific conductance in well SLR water and flow in Bear Creek. Although the general direction of flow in the aquifer is to the NNE, this well responds to flow in Bear Creek to the north (Figure 2-1), which is

inconsistent with dye traces that have demonstrated this to be an area of eastward flow (Hauwert et al., 2005). One explanation for this behavior could be flowpaths in the vadose zone that only carry water during high streamflow.

Specific conductance in group C1 well water samples ranges from 445 to 1530  $\mu\text{S}/\text{cm}$ , with a median value of 653  $\mu\text{S}/\text{cm}$ . Specific conductance varies more for this group of wells than for the other three groups, with a median  $C_v$  of 0.053. Within group C1, well SVE water has both the minimum and maximum specific conductance values, and has the highest  $C_v$  (0.23) of the four wells.

The hydrochemical facies of group C1 wells range from Ca-HCO<sub>3</sub> to Ca-Mg-HCO<sub>3</sub> (Figure 2-7b). Water samples from wells FMW and SLR, and to a slightly lesser extent well KCH, exhibit few geochemical changes other than dilution. Well SVE water trends toward a more sulfate-type signature.

Mean  $\log\text{SI}_{\text{calcite}}$  values for water from wells in group C1 are about zero (saturated) for wells KCH and SVE, and about 0.2 (oversaturated) for FMW and SLR. During periods of high streamflow and aquifer flow conditions,  $\log\text{SI}_{\text{calcite}}$  values vary less and are typically closer to zero for wells KCH, SVE, and SLR. During periods of no flow in the creeks and low aquifer flow conditions,  $\log\text{SI}_{\text{calcite}}$  values are more variable in both the undersaturated and supersaturated directions. Because group C1 exhibits a correlation with streamflow and aquifer flow condition, it should be the most likely group of wells to exhibit systematic  $\log\text{SI}_{\text{calcite}}$  variability as

a result of recharge, but it is not. The results of  $\log SI_{\text{calcite}}$  analysis for this long-term record are unclear. Although there is a clear relation between  $\log SI_{\text{calcite}}$  values and recent surface water reaching a well on a short time scale (Figure 2-6c), the long-term record does not effectively capture these changes. This may be because long-term samples are collected at somewhat arbitrary intervals, even after large rainfall events. There is also be a seasonal variation in calcite saturation in some recharge water (Banner et al., 2004), making an infrequently and arbitrarily sampled dataset difficult to analyze without a way to account for seasonal variability. Because of the unclear results of  $\log SI_{\text{calcite}}$  analyses, they are not considered in later sections of this study.

The Mg/Ca molar ratio for group C1 wells ranges from 0.3 to 0.9. Median values of Mg/Ca generally increase from southwest to northeast, following the general gradient of flow in the aquifer (Figure 2-2, 2-7b). This is consistent with the chemical process of incongruent dissolution, which creates elevated Mg/Ca ratios as residence time increases (see Chapter 1, section 1.4.3). Thus, water in downgradient wells, on average, has had a longer aquifer residence time than water from upgradient wells. Wells SVE and SLR show a correlation between Mg/Ca ratios and specific conductance when the highest 70 percent of specific conductance values are considered (Figure 2-7b). This correlation suggests that ionic strength is proportional to residence time for wells SVE and SLR, during periods when there is

little recharge (that is, during baseflow conditions). Wells FMW and KCH do not exhibit this relationship.

$\text{SO}_4/\text{Cl}$  and  $\text{Mg}/\text{Na}$  ratios can be used to identify water that is flowing into the Barton Springs segment from the underlying Trinity aquifer or the saline zone. Trinity aquifer water is characterized by a higher  $\text{SO}_4^{2-}$  concentration relative to  $\text{Cl}^-$  and a higher  $\text{Mg}^{2+}$  concentration relative to  $\text{Na}^+$  (Figure 2-4). Conversely, saline zone water is distinguished by a higher  $\text{Cl}^-$  concentration relative to  $\text{SO}_4^{2-}$ , and a higher  $\text{Na}^+$  concentration relative to  $\text{Mg}^{2+}$  (Figure 2-4) (Sharp and Clement, 1988).

Water in some group C1 wells shows evidence of mixing with the saline zone and Trinity aquifer under some conditions, as well as dilution by surface water (Figures 2-7c and 2-7d). Well SVE has the greatest range of  $\text{SO}_4/\text{Cl}$  and  $\text{Mg}/\text{Na}$  ratios in group C1; during periods of low streamflow and aquifer flow conditions, water in well SVE appears to contain some proportion of water from the saline zone.

Although  $\text{SO}_4^{2-}$  concentration in well SVE is not linearly correlated to flow in Slaughter Creek, concentrations above 100 mg/L occur almost exclusively during periods of low (less than 4  $\text{ft}^3/\text{s}$ ) or no flow in Slaughter Creek (Figure 2-9a). Sulfate concentration is inversely proportional to discharge at Barton Springs (Figure 2-9b). This evidence suggests that the source of the  $\text{SO}_4^{2-}$  in well SVE is influx from the saline zone, which is suppressed when aquifer flow conditions and streamflow rates are high. This is supported by the relative increase in  $\text{Na}^+$  concentration with respect

to  $Mg^{2+}$  (Figure 2-7d). Senger (1983) and Slade et al. (1986) have suggested that well SVE might receive some ground water from the saline zone. Well SLR appears to be receiving a small amount of water from the Trinity aquifer, on the basis of slight enrichment in sulfate relative to chloride and magnesium relative to sodium (Figures 2-7c and 2-7d). Drill logs indicate that well SLR is completed in formations that underlie the Barton Springs segment. Samples from wells KCH and FMW have little variability in their  $SO_4/Cl$  and  $Mg/Na$  ratios, suggesting that variations in their geochemical composition is caused primarily by dilution from surface water during periods of high streamflow and aquifer flow conditions.

Nitrate concentrations are consistently below 2 mg/L in wells FMW, SLR, and SVE, but range from 3.8 to 8.6 mg/L in well KCH, with a median concentration of 4.9 mg/L. Nitrate concentrations at all wells are independent of specific conductance, which suggests that there is no relation between  $NO_3^-$  concentrations and recent recharge (Figure 2-7e). Elevated  $NO_3^-$  concentrations appear to be related to localized sources rather than connection to incoming recharge solely, as all the wells in this group have geochemical variations that are affected by recharge but only one has high  $NO_3^-$  concentrations. However, given that well KCH had the highest  $NO_3^-$  concentrations of all 26 wells in this report, the data suggest that a well that is well connected to surface recharge (such as in group C1) might be more vulnerable to localized sources of contamination than one that is not. While the

source of  $\text{NO}_3^-$  in well KCH cannot be determined from the data reported here, historically there was a goat ranch near this well (D. Johns, City of Austin, written comm., 2005), and agricultural runoff is a known source of  $\text{NO}_3^-$  in ground water.

In summary, group C1 wells appear to intersect major aquifer flowpaths. As low ionic strength recharge water from the surface reaches these wells, total dissolved solids concentrations decrease and hydrochemical facies evolve toward more  $\text{Ca-HCO}_3$ . Two wells in this group show evidence of some mixing with water from the saline zone and Trinity aquifer: the hydrochemical facies of water samples from well SVE change in response to low streamflow and low aquifer flow condition, suggesting that water from the saline zone reaches this well under these conditions, and well SLR is well drilled into the Trinity aquifer.

#### **2.7.2.2. Group C2 Wells**

For the five wells in group C2 (BDW, HWD, MCH, SVN, SVW) (Figure 2-10a; Table 2-2), specific conductance is negatively correlated with flow in one or more recharging creeks, but is not correlated with aquifer flow condition. This suggests that these wells intercept recharging surface water from creeks but are not connected to a major aquifer flowpath or conduit.

Specific conductance values in group C2 wells range from 388 to 710  $\mu\text{S}/\text{cm}$ , with a median value for the five wells of 560  $\mu\text{S}/\text{cm}$ . The minimum, maximum, and

median values for this group are the lowest of the four groups, indicating that water in these wells is less mineralized than that in wells in the other groups. The median  $C_v$  for group C2 specific conductance is 0.042, making it the group with the second highest variability after group C1, and underscoring its connection to surface recharge. Well SVN has both the minimum and maximum specific conductance values, encompassing the full range for group C2, and its  $C_v$  for specific conductance is the highest of group C2 wells (0.13). SVN undergoes large changes in stage, occasionally going dry to the bottom of its drilled interval (M. Dorsey, U.S. Geological Survey, personal commun., 2005) and its water level changes rapidly in response to flow in Barton Creek (Slade et al., 1986).

The hydrochemical facies of ground waters in group C2 are Ca-HCO<sub>3</sub> to Ca-Mg-HCO<sub>3</sub> (Figure 2-10a), which are similar to those of group C1 (Figure 2-7a). There is slight evolution in the water in wells SVN and SVW toward a more chloride-sulfate type water, suggesting contribution of ions from a source other than surface water. Generally, group C2 geochemical variability is more tightly constrained than that of group C1, suggesting that fewer processes affect the geochemical composition of group C2 wells.

The wells in group C2 have about the same range of Mg/Ca as wells in group C1, but they vary little for individual wells except BDW (Figure 2-10b). There is no apparent relation between Mg/Ca ratios and geography for group C2 wells,

consistent with the hypothesis that group C2 wells intersect isolated flowpaths, and thus are not influenced by the cumulative effects of large catchment areas in the aquifer. Unlike group C1 there is no apparent relation between Mg/Ca and specific conductance for any wells (Figure 2-10b).

Geochemical variability is more tightly constrained in group C2 than in group C1 (Figure 2-10c and 2-10d; compare to Figures 2-7c and 2-7d). Generally, there is little to no evidence for mixing with waters from the saline zone or Trinity aquifer. Samples from wells BDW and HWD have the smallest variations in  $\text{SO}_4/\text{Cl}$  ratios in this group and some variability in Mg/Na ratios, suggesting that their geochemical composition is affected by dilution from surface water during periods of high streamflow, resulting in lower residence time water and lower  $\text{Mg}^{2+}$  concentrations. Well MCH may contain water with a small amount of mixing from the Trinity aquifer. Well SVW samples are somewhat enriched in  $\text{SO}_4^{2-}$  relative to Cl, but their Mg/Na ratios are relatively constant. This suggests that the source of  $\text{SO}_4^{2-}$  in well SVW water is something other than the Trinity aquifer or the saline zone, for example dissolution of gypsum.

Nitrate concentrations in wells in group C2 are consistently less than 2 mg/L with the exception of well SVW, in which  $\text{NO}_3^-$  concentrations range from 1.5 to 3.0 mg/L. Well SVN has low concentrations of nitrate (< 1 mg/L) over a wide range of specific conductance values, but if the other four wells are viewed together

statistically there is an increase in nitrate concentration with an increase in specific conductance (Figure 2-10e). If specific conductance is interpreted as a measure of the proportion of high residence time ground water in relation to recent recharge water, then the increase in  $\text{NO}_3^-$  coupled with the increase in specific conductance suggests that the ground water has higher ambient concentrations of  $\text{NO}_3^-$  than the surface water. Well SVN has relatively constant  $\text{NO}_3^-$  concentrations, and is the one well in group C2 that has high proportions of  $\text{Cl}^-$  under low recharge conditions, suggesting that SVN may receive some of its water from an unidentified source.

In summary, wells in this group are connected to minor aquifer flowpaths that are well connected to the surface. Flowpaths intersected by group C2 wells probably have smaller catchment areas than those in group C1; to use an analogy from surface water hydrology, these flowpaths are the “tributaries” as opposed to the “trunks.” Similarly to group C1, dilution by low ionic strength surface recharge appears to be a dominant process for some wells in this group. Group C2 wells have constrained hydrochemical facies, and show very little evidence of mixing with the saline zone or Trinity aquifer. This suggests that their geochemical composition is affected dominantly by differing amount of limestone dissolution and variable water residence times. In effect, when there is no streamflow, group C2 wells receive their water from diffuse flow from the nearby and surrounding matrix portion of the

limestone rock. Nitrate concentrations in group C2 wells generally indicate a natural source of nitrate.

### **2.7.2.3. Group P Wells**

For the six wells in group P (FOW, GHW, LWK, ROL, SVS, WGF) (Figure 2-11a; Table 2-2), specific conductance is positively correlated with aquifer flow condition. When aquifer flow conditions are high, water samples from wells in this group are more likely to have higher specific conductance values than when aquifer flow conditions are low. This behavior is the inverse of that seen in groups C1 and C2, in which high aquifer flow conditions or high surface-water flows are correlated with low specific conductance of the ground water. Except for well ROL, specific conductance in group P wells is not correlated with surface-water flow. Wells LWK and WGF had only six specific conductance measurements, the minimum for inclusion in the statistical analysis. The smaller the sample size, the less likely a well is to show a correlation between specific conductance and streamflow or aquifer flow conditions, as the number of samples collected during periods when the ground water in these wells was under surface-water influence might have been insufficient to indicate that influence.

Specific conductance values for group P wells range from 480 to 1160  $\mu\text{S}/\text{cm}$ , with a median value of 603  $\mu\text{S}/\text{cm}$ . The median  $C_v$  for specific conductance for the

six wells in Group P is 0.033, the lowest among groups C1, C2, and P. Four of the wells (GHW, LWK, SVS, WGF) have a specific conductance range of less than 100  $\mu\text{S}/\text{cm}$ . Well ROL has the widest range (480 to 1160  $\mu\text{S}/\text{cm}$ ), representing the full range of variation for this group. The wide range in specific conductance for this well suggests that it may be connected to an aquifer flowpath, despite its lack of a negative correlation with streamflow or aquifer flow conditions.

The wells with the strongest correlation to aquifer flow condition in group P are LWK ( $\rho=0.88$ ) and WGF ( $\rho=0.94$ ) (Table 2-2). Correlations for LWK and WGF are based on the minimum six data points and less than 60  $\mu\text{S}/\text{cm}$  of variation in specific conductance. Wells ROL and FOW are the only wells in any group for which specific conductance is positively correlated to streamflow (Barton and Slaughter Creeks, Table 2-2). ROL is located in a subbasin thought to be hydrologically isolated from Barton Springs and the majority of the aquifer (Hauwert et al., 2005). FOW is located far upgradient of Barton Creek, and specific conductance in this well is not correlated to flow in either Williamson or Slaughter Creek. The positive correlation between specific conductance in these two wells and streamflow likely is the result of autocorrelation between streamflow and aquifer flow condition.

The hydrochemical facies of ground waters in group P vary from  $\text{Ca-HCO}_3$  to  $\text{Ca-Mg-HCO}_3$  to  $\text{Ca-Mg-SO}_4$  (Figure 2-11a). Four of the six wells (GHW, LWK, SVS, and WGF) are  $\text{Ca-HCO}_3$  to  $\text{Ca-Mg-HCO}_3$  waters, similar to the dominant

hydrochemical facies of the other three groups. Most of the variation in relative proportions of major ions is accounted for by  $\text{Ca}^{2+}$  and  $\text{Mg}^{2+}$ . In contrast, wells FOW and ROL trend toward  $\text{SO}_4$  and Cl-type facies, respectively. FOW and ROL also have the greatest  $C_v$  for specific conductance in group P. Drill logs indicate that well GHW is drilled into formations that underlie the Barton Springs segment, but its Ca-Mg- $\text{HCO}_3$  chemistry indicates Edwards Limestone water.

Given the positive correlation between specific conductance and aquifer flow condition in group P, an inverse relation between specific conductance and residence time (Mg/Ca ratio) might be expected for all group P wells. However, Mg/Ca ratios are generally independent of specific conductance for most wells in group P (Figure 2-11b). Well ROL is an exception to this, in that its Mg/Ca ratios (residence time indicators) decrease as specific conductance values increase. The fact that this is only observed for well ROL suggests that some other process is occurring, or that Mg/Ca is not an effective measure of residence time for group P wells. Well ROL is known to have a local source of anthropogenic contamination, which may be the source of its inverse relation between specific conductance and Mg/Ca ratios. Well FOW has a direct relation between Mg/Ca ratios and specific conductance, but this is most likely due to cross-formational flow from the Trinity Aquifer during high aquifer flow conditions.

Some wells in group P show evidence of mixing with the Trinity aquifer, while others have an unclear explanation for their geochemical variability. Wells FOW and SVS are enriched in  $\text{SO}_4^{2-}$  relative to  $\text{Cl}^-$  and  $\text{Mg}^{2+}$  relative to  $\text{Na}^+$  under high flow conditions, which is the geochemical signature of the underlying Trinity aquifer (Figure 2-11c and 2-11d). Sulfate concentrations in well FOW can reach up to about four times the baseline level, but this occurs only when Barton Springs system discharge exceeds about 85  $\text{ft}^3/\text{s}$  (Figure 2-12). Other studies have also suggested that sulfate-rich water from the underlying Trinity aquifer (Figure 2-2) enters well FOW when aquifer flow conditions are high (Hauwert and Vickers, 1994; City of Austin, 1997), and these results are consistent with drill logs indicating that well FOW is partially drilled into the Trinity aquifer (N. Houston, U.S. Geological Survey, written comm., 2005). Similar Trinity aquifer mixing is apparent in well SVS, and is seen in well GHW to a lesser extent. This suggests that cross-formational flow from the Trinity aquifer occurs in the Barton Springs segment, particularly during high aquifer flow conditions. Thus for these wells, the positive correlation between aquifer flow conditions and specific conductance is the result of mixing with high-sulfate Trinity aquifer water. These findings are supported by a quantitative mixing model (e.g., Banner et al., 1989); a hypothetical mixture between an “average” Barton Springs segment groundwater and an average Trinity aquifer water yields a line

along which samples from wells SVS and FOW plot closely (Figures 2-11c and 2-11d).

In contrast, water in well ROL has proportions of  $\text{SO}_4^{2-}$  relative to  $\text{Cl}^-$  and  $\text{Mg}^{2+}$  relative to  $\text{Na}^+$  that are more or less constant (Figure 2-11c), with perhaps a slight enrichment in  $\text{Cl}^-$ . This geochemical signature corresponds to neither the Trinity aquifer nor the saline zone. One explanation for excess  $\text{Cl}^-$  and increased specific conductance with high aquifer flow conditions is contamination from surface water; the use of well ROL was discontinued several years ago because of defective well casing that allowed contaminated surface water to easily reach the water table (City of Austin, 1997). Wells LWK and WGF have small datasets that do not indicate a clear source of geochemical variability.

Nitrate concentrations in this group are generally less than 2 mg/L except for well SVS samples, which have a median  $\text{NO}_3^-$  concentration of 3 mg/L (Figure 2-11e). Although the specific source of elevated  $\text{NO}_3^-$  in SVS is not known, it is located near an urbanized region of the aquifer with numerous potential  $\text{NO}_3^-$  sources such as landscaping, septic systems, and wastewater infrastructure. Well GHW has the lowest average  $\text{NO}_3^-$  concentration in group P, and is located in the southwest quadrant of the aquifer, far upgradient from the more urbanized areas of the watershed.

In summary, the water in the wells in group P has a tendency to become more mineralized during periods when aquifer flow conditions are high. For some wells, this may result from cross-formational flow from the Trinity aquifer during high aquifer flow conditions. Urbanization may be another source of increased mineralization during high aquifer flow conditions. Yet another possible explanation for increased mineralization during high aquifer flow conditions is that conduits may reach a maximum capacity, and ground water may temporarily “back up” into large caves that are typically unsaturated (Halihan et al., 1998). These caves may contain soluble minerals (e.g., gypsum) that are rarely accessed. The specific conductance values have less variation than does that in groups C1 and C2, and four of the wells have a range in specific conductance of less than 100  $\mu\text{S}/\text{cm}$ . On the basis of statistical and geochemical data, all of the group P wells except ROL are interpreted as not intersecting flowpaths.

#### **2.7.2.4. Group N Wells**

The 11 wells in Group N (BCK, BPS, CNE, HND, ISD, JBS, PLS, RAB, SNL, TNR, and WBG; Figure 2-13a; Table 2-2) do not show a statistically significant correlation to streamflow or aquifer flow condition. so none of these wells are interpreted as intersecting a flowpath. However, of the 11 wells in group N, five wells had the minimum number of specific conductance values for testing (six

values), and eight wells had fewer than the median number of specific conductance measurements for this study (23 values). Only three other wells from the other three groups had the minimum number of six conductance values. In effect, many of the wells in group N may be in this group simply because of the number and timing of samples was insufficient to correlate significantly to streamflow or aquifer flow conditions.

Specific conductance values for wells in Group N range from 460 to 1190  $\mu\text{S}/\text{cm}$ , with a median value for the 11 wells of 581  $\mu\text{S}/\text{cm}$ . The median  $C_v$  for specific conductance for group N is 0.029, the lowest value of any group. This group also contains the well with the single highest  $C_v$  among all wells in this study (well RAB,  $C_v = 0.283$ ). Wells BPS, PLS, and TNR have  $C_v$ s of 0.029, 0.025, and 0.026 respectively; these low values are consistent with the hypothesis that they do not intersect flowpaths.

Ground water represented by group N has diverse hydrochemical facies, from  $\text{Ca-HCO}_3$  to  $\text{Na-K-Cl-SO}_4$  (mixed) water types (Figure 2-13a). As this group includes all wells that do not fall into the other three groups, they are not necessarily expected to have similar geochemical compositions or even be controlled by similar geochemical processes; rather, they are in this group by default. Water in most of the wells is a  $\text{Ca-HCO}_3$  to  $\text{Ca-Mg-HCO}_3$  water type, similar to that in most of the other wells in this report. Two wells, CNE and WBG, have geochemical signatures

unlike those of waters from any other wells in this report, which may be a result of their proximity to the saline zone. The geochemical compositions of wells CNE and WBG (Figure 2-13a) approach the geochemical composition of the saline zone well (Figure 2-4), suggesting saline zone influence. Well RAB has variable hydrochemical facies that are similar to variations in well SVE (group C1).

Group N has the largest range of Mg/Ca, from 0.3 to 1.1, of the four groups (Figure 2-13b). Individual wells in group N have smaller individual Mg/Ca ranges than the group as a whole, with the greatest range occurring in well TNR (0.3 – 0.7). The wells with the largest mean values are wells CNE and WBG, further evidence that these wells have a different geochemical signature. Interestingly, the Mg/Ca ratio of well RAB is almost unvarying despite its range in hydrochemical facies.

On the basis of ion ratios (Figures 2-13c and 2-13d), some wells in group N show evidence of mixing with the saline zone. Well CNE is enriched in  $\text{Cl}^-$  relative to  $\text{SO}_4^{2-}$ , and enriched in  $\text{Na}^+$  relative to  $\text{Mg}^{2+}$ , indicating geochemical influence from the saline zone. Well WBG has a cation signature corresponding to saline zone influence (Figure 2-13d), but the anion signature is less conclusive (Figure 2-13c). These findings are supported by a quantitative mixing model (Banner et al., 1989); by progressively mixing an “average” Barton Springs segment water samples with average saline zone water, it is apparent that samples from wells CNE and WBG plot near this line (Figures 2-13c and 2-13d). The samples do not perfectly fall along this

mixing line, but that is probably due to the known spatial variability of the saline zone's geochemical composition (Sharp and Clement, 1988; Hauwert and Vickers, 1994).

The geochemical composition of well RAB is extremely variable (Figures 2-13a and 2-13b). Although the concentration of  $\text{SO}_4^{2-}$  is elevated relative to  $\text{Cl}^-$ , the  $\text{Mg}^{2+}$ - $\text{Na}^+$  relation is not indicative of either a Trinity aquifer or saline zone source, suggesting an alternative source of  $\text{SO}_4^{2-}$ , such as dissolution of gypsum. Well TNR shows evidence of mixing with water from the Trinity aquifer. Well TNR is located only 15 meters away from well BDW, yet the two wells have different geochemical compositions. This is consistent with the spatial heterogeneity observed in karst aquifers (e.g., Sharp, 1993; Malard and Chapuis, 1995; Long and Putnam, 2004, among many others), and is a reminder that geographic patterns in karst aquifers are difficult to generalize.

Nitrate concentrations in all wells in Group N are below 2 mg/L except for one sample in well JBS (Figure 2-13e). Wells CNE and WBG have the lowest  $\text{NO}_3^-$  levels of the 26 wells in this report. These two wells are near the chemically-reducing saline zone (Sharp and Clement, 1988), so the low  $\text{NO}_3^-$  levels may be the result of denitrification, a biological process that converts  $\text{NO}_3^-$  to nitrogen gas under anoxic conditions (Freeze and Cherry, 1979, p. 415). Denitrification has been documented in several karst aquifers, including the Lincolnshire Limestone of

England (Bishop and Lloyd, 1990) and the Illinois sinkhole plain aquifer (Panno et al., 2001).

In summary, few generalizations can be made about wells in group N. Most of the wells in this group have fewer specific conductance measurements than the other groups, which decreases the likelihood that the samples would reflect periods when ground-water chemistry was influenced by recharge through streambeds. In other words, their sample sets were too small to adequately capture the range of geochemical changes that they typically undergo. In other cases, there may be unidentified processes affecting the geochemical composition of well water; for example, well RAB is thought to intersect a highly transmissive conduit system of the aquifer (Senger, 1983), but changes in its geochemical composition are apparently not correlated to streamflow or aquifer flow condition. Ultimately, there is probably no single unifying hydrologic explanation for wells in group N, and it is difficult to make general statements about processes controlling these wells.

### **2.7.3. Wells and flowpath intersection**

This section synthesizes the evidence from the previous four sections, and the results are also summarized in Table 2-3. Some wells appear to intersect major flowpaths, as their geochemical composition is affected by recharging surface water. These wells also appear to integrate water flowing from a large up-gradient part of

the aquifer, as reflected by a negative correlation between specific conductance and aquifer flow condition. Other wells intersect smaller tributary flowpaths that are well connected to the surface, but whose water reflects the geochemistry of a small, localized area when streams are not flowing. These wells have specific conductance that is negatively correlated to streamflow, but not aquifer flow condition. Some wells have no geochemical evidence of intersection of flowpaths, but may be receiving cross-formational flow from the underlying Trinity aquifer under high aquifer flow conditions. Finally, the geochemistry of some wells is influenced by mixing with water from the saline zone under low flow conditions.

Wells in group C1 (FMW, KCH, SLR, SVE) are hypothesized to intersect major aquifer flowpaths that integrate water from a large area of the aquifer, based on their tendency to have less mineralized water when aquifer flow conditions and streamflow are high (Table 2-3). Most group C1 wells have a Ca-HCO<sub>3</sub> water type. The water type changes that do occur are a result of lower Mg/Ca ratios during periods of high recharge (shorter residence time), and dilution of SO<sub>4</sub><sup>2-</sup> during periods of high recharge. Mg/Ca ratios in these wells increase in a downgradient direction, reflecting longer travel times in a downgradient direction, and consistent with the hypothesis that these wells intersect flowpaths that receive water from large sections of the aquifer. Wells that intersect major flowpaths are affected by the quality of recharging surface water, which suggests they may be vulnerable to

localized sources of contamination. High  $\text{NO}_3^-$  levels in well KCH might be evidence of this. Additionally, because these wells are interpreted as receiving water from a large catchment area and a relatively large volume of the aquifer, they are likely to be susceptible to contamination from distant sources.

Wells in group C2 (BDW, HWD, MCH, SVN, SVW) are interpreted as intersecting minor, or tributary, flowpaths in the aquifer (Table 2-3). Group C2 wells generally maintain a Ca- $\text{HCO}_3$  water type. Wells that intersect minor flowpaths are affected by the geochemistry of recharging surface water, which suggests they are vulnerable to contamination from localized sources. However, as these wells do not intersect the main “trunk” of flow in the aquifer, they may be less vulnerable than group C1 wells to contamination outside of the watershed of the stream to which they are connected. Because these wells are affected by surface water recharge only during periods of creek flow, they probably are vulnerable to contamination principally during periods of recharge.

Wells in groups P and N do not display evidence of intersecting aquifer flowpaths. The statistical test used for this report, however, could not distinguish between (a) wells that are not on major flowpaths, (b) wells that are controlled by unknown geochemical processes, and (c) wells placed in this group because of their small sample size. It may be that some of these wells do not intersect flowpaths, and

that others do but were not sampled at times when there was a surface-water influence on ground water.

#### **2.7.4. Saline zone and Trinity aquifer mixing**

Evidence presented here suggests that water flows from the Trinity aquifer into the Barton Springs segment under some hydrologic conditions. In particular, water from three wells in group P (FOW, GHW, and SVS) shows evidence for mixing with the Trinity aquifer during high aquifer flow conditions (Table 2-3). This suggests that the direction of the vertical gradient between the two aquifers is temporally variable, and that the hydraulic heads in the two aquifers are not necessarily comparable or even proportional to one another. Well RAB may also sometimes receive cross-formational flow from the Trinity aquifer, although this hypothesis is made mostly on the basis of one water sample whose geochemical composition is very different from other samples from this well. Well SLR water also shows evidence for mixing with the Trinity aquifer, but this is expected behavior, as drill logs indicate that it was drilled into the upper section of the Trinity aquifer.

Water from the saline zone may mix with water in the Barton Springs segment, and this behavior generally is associated with wells that intersect flowpaths (wells KCH, SVE, and SVW). For these wells, this mixing is associated with low

streamflow and/or low aquifer flow conditions, suggesting that an absence of water recharging the aquifer or lowering of the potentiometric surface associated with low aquifer flow conditions (Slade et al., 1986) allows influx of water from the saline zone. Two other wells (CNE and WBG) also show evidence for saline zone mixing, probably because of their proximity to the saline zone (Figure 2-1).

The saline zone may exist as a saltwater lens that extends under the freshwater part of the aquifer. Three of the deepest wells along the eastern edge of the aquifer (SVE, CNE, and WBG) show evidence of saline zone mixing, while three more shallow wells along the eastern edge (BPS, HND, and PLS) do not show evidence of saline zone mixing. Well SVE is the deepest well in this study but only shows saline zone influence under low aquifer flow conditions, which suggests that the saline zone (or a lower lens thereof) may migrate from east to west as a function of aquifer flow condition. Studies in the San Antonio segment of the Edwards aquifer to the south have demonstrated the existence of a temporally varying saline-zone lens (Groschen, 1994).

#### **2.7.5. Geographic patterns**

One of the most striking characteristics of karst aquifers is their extreme heterogeneity; wells in close proximity may exhibit very different hydrogeologic and geochemical characteristics (Malard and Chapuis, 1995; Long and Putnam, 2004).

The intersection of a fracture or conduit is likely to have a greater effect on well-water geochemistry than the location of the well along the regional gradient. For example, in this report wells TNR and BDW are located within 15 meters of one another, yet have distinct geochemical compositions and were placed in different groups (group N and C2, respectively). However, a few observations concerning geography and geochemistry can be made.

In group C1 wells, Mg/Ca ratios tend to increase in a downgradient direction. This trend is interpreted as reflecting a longer residence time in a downgradient direction, and is consistent with the hypothesis that group C1 wells intersect flowpaths that integrate water from large volumes of the aquifer. Generalized aquifer flow routes were delineated by Hauwert and others (2005), and the conclusion that group C1 wells (FMW, KCH, SLR, SVE) intersect major flowpaths is mostly supported by their findings. This is not observed for the other three groups of wells, which are subject to more localized influences. In karst aquifers, fractures and conduits occupy a very small proportion of the total aquifer volume, and the likelihood of a well intersecting a major conduit is relatively small.

Wells that intersect minor flowpaths are, with one exception, located in the recharge zone (Figure 2-5). This is consistent with the intersection of minor flowpaths. Because there is no direct connection between the land surface and confined zone, any confined zone flowpath must be long enough to reach the

recharge zone. Thus, longer flowpaths are more likely to be major flowpaths, in the same way that stream length in surface water systems is usually proportional to the size of the catchment area.

#### **2.7.6. Individual well comparisons with other studies**

Wells for which data were analyzed in this study have been sampled by other studies whose objective was to assess relation of ground-water geochemistry to surface-water processes. Andrews et al. (1984) and St. Clair (1979) reported high levels of fecal streptococci bacteria in well JBS (up to 44,000 colonies per 100 mL), suggesting a connection to surface-water and/or contamination from wastewater. This study's analysis placed well JBS in group N, and no conclusions were made concerning flowpath intersection. One possibility is that well JBS does intersect a flowpath, but the small specific conductance dataset in (13 values) could not establish this connection. Another possibility is that bacterial contamination of well JBS was caused by a localized source such as a septic tank or leaking wastewater infrastructure. A sewage lift station in nearby Dry Creek historically has experienced numerous accidental sewage releases (Hauwert and Vickers, 1994), and is a probable source for bacterial contamination in well JBS. This is consistent with the data of Andrews et al. (1984), as specific conductance and bacteria levels do not

co-vary in well JBS, as would be expected with low ionic strength surface-water recharge.

Senger and Kreitler (1984) reported a hydrologic connection between wells RAB and SVE and Barton Springs Pool; water level changes in the pool result in nearly-simultaneous water level changes in these two wells. This suggests that these wells intersect transmissive conduits that connect to the Barton Springs system. Similarly, Hauwert and Vickers (1994) suggested that well SVE has “good hydraulic connection to recharge areas” after observing a one-foot rise in water levels following a rainfall event in August, 1994. Hauwert and Vickers (1994) also reported that well RAB contained 2.1 mg/L total petroleum hydrocarbons (TPH) in 1993, suggesting an anthropogenic source of contamination for this well. These findings are consistent with this study’s conclusions for well SVE, and are not contradicted by this study’s inconclusive results for well RAB.

Hauwert and Vickers (1994) reported several instances of sediment filling well holes or discharging with pumped well water, and hypothesize that the presence of sediment in a well or its water may indicate that the well intersects a flowpath with rapidly moving water. Such sediment may originate from the land surface (allochthonous) or from within the aquifer (autochthonous) (Mahler et al., 1999). Hauwert and Vickers (1994) reported that well SVN accumulated over 100 feet (30 m) of sediment accumulation from 1978 to 1993, consistent with this

study's conclusion that it intersects a minor flowpath. Well SVS was reported to contain fine cream-colored sediment in its pumped water, although this study's findings were inconclusive for well SVS. Similarly, well HND was reported to have a small amount of sediment (less than 50 mg/L total suspended solids) in its pumped water, but this study's findings were inconclusive for this well.

Hauwert et al. (2005) reported positive the detection of a dye from a dye-trace in well SVW. The dye had been injected in Williamson creek several days earlier, suggesting that well SVW intersects a flowpath that connects to Williamson Creek. Their finding is consistent with the conclusions of this study.

The City of Austin (1997) conducted an investigation with some of the same major ion data used in this study. They concluded that wells KCH, ROL, SVW, FMW, and BDW may be affected by urbanization, which is consistent with this study's findings that these wells intersect flowpaths. The City of Austin also identified well SVS as potentially being affected by urbanization. Well SVS was placed in this study's group P, and the processes controlling its behavior are not well understood. Finally, wells RAB and TNR were noted as having potential impacts from urbanization (City of Austin, 1997), while this study's findings were inconclusive.

### **2.7.7. Value of statistical approach**

The results of this investigation demonstrate that a long-term geochemical dataset can be of value in characterizing the degree to which wells intersect karst features. Although analysis of multiple samples collected at intervals of hours to days after rainfall remains the most effective way to evaluate the influence of surface water on ground-water geochemistry, this study shows that if a sufficient amount of data exists, historical long-term data can be analyzed statistically to assess surface water-ground water interaction in a karst aquifer. However, there are some limitations to the statistical approach taken here.

In those parts of a karst aquifer where transport occurs, the geochemistry can vary greatly and rapidly. The effects of recharging surface water may be extreme but ephemeral, occurring over only a small proportion of the hydrologic year. If the timing of sampling is random, many water samples may reflect baseflow conditions during which the geochemistry varies little. Thus, either a large number of samples, or random chance, is required to collect samples that reflect the range of geochemical variability that may occur at a site. Five of the 11 wells in the group for which no statistically significant relations were observed (group N) had the minimum number of specific conductance measurements, suggesting that six specific conductance measurements may be too few samples to capture the range of geochemical variability possible in a well (Figure 2-14). Thus, wells with small sample sets and

no statistically-significant negative relation between specific conductance and either streamflow or aquifer flow condition cannot be definitively interpreted as not intersecting a flowpath, but rather as having insufficient evidence for interpretation as intersecting a flowpath.

Four of the wells in this study with the greatest geochemical variability (SVN, FOW, ROL, and SVE) had more than 30 specific conductance measurements (Figure 2-14); all four of these wells had statistically-significant relations and were placed into groups C1, C2, or P. This suggests that a large sample set may be necessary to capture geochemical variability and connection to surface-water processes or flowpath intersection. However, another possible explanation is that wells with the largest sample sets were deliberately selected for extended sampling on the basis of variability in geochemical composition observed early on during the sampling program. In other words, large sample-set size and large geochemical variability may not be independent.

Finally, while 85 percent of aquifer recharge is estimated to derive from the five recharging creeks (Slade et al., 1986), this report was unable to quantitatively consider the estimated remaining 15 percent of recharge (referred to as upland recharge). There is some evidence that upland recharge may rapidly reach some group C1 and C2 wells (particularly the shallow well SLR). The data available for this study cannot be used to determine the degree to which wells are affected by

upland recharge. However, it is likely that periods of upland recharge and stream flow are correlated, and thus the statistical approach taken here may have identified some wells as being affected by stream flow when in fact they are receiving upland recharge. Current ongoing research may address the quantification of upland recharge rates (N. Hauwert, University of Texas, written comm., 2005; A. Lindley, University of Texas, personal comm., 2005).

## 2.8. CONCLUSIONS

Ground-water geochemistry data from the Barton Springs segment of the Edwards aquifer were analyzed to determine the relation between geochemistry in wells, streamflow, and overall aquifer flow condition as measured by Barton Springs system discharge. Twenty-six years of arbitrarily-timed specific conductance measurements were compared to surface-water discharge rates and aquifer flow conditions using a non-parametric statistical test.

From the results of the statistical test, four groups of wells were identified: (1) Group C1—negative correlation with streamflow and aquifer flow condition, (2) Group C2—negative correlation with streamflow only, (3) Group P—positive correlation with aquifer flow condition, and (4) Group N—no correlation to aquifer flow condition or streamflow. On the basis of the statistical test and geochemical evidence, generalizations about aquifer function were made. Four wells (FMW,

KCH, SLR, SVE) intersect major aquifer flowpaths, and five wells (BDW, HWD, MCH, SVN, SVW) intersect minor aquifer flowpaths. For the remaining 17 wells, no conclusions were reached regarding connection to flowpaths.

Analysis of major ion geochemistry indicated that most samples collected from wells belong to the Ca-HCO<sub>3</sub> and Ca-Mg-HCO<sub>3</sub> hydrochemical facies, although some wells contain water with other hydrochemical facies. These variable facies are the result of processes such as incongruent calcite/dolomite dissolution, variable residence time, and dissolution of some non-carbonate minerals such as gypsum. Some wells (KCH, SVE, SVW, CNE, WBG) show evidence of ground-water mixing with water from the eastern saline zone, which may exist as a saltwater lens partially extending under the freshwater zone of the aquifer. This is reflected in elevated levels of Cl<sup>-</sup> relative to SO<sub>4</sub><sup>2-</sup> and of Na<sup>+</sup> relative to Mg<sup>2+</sup>. Some wells show evidence of mixing with water from the underlying Trinity aquifer (wells FOW, GHW, SLR, SVS, BCK, and TNR). This is reflected in elevated levels of SO<sub>4</sub><sup>2-</sup> relative to Cl<sup>-</sup> and of Mg<sup>2+</sup> relative to Na<sup>+</sup>. In some cases (SLR, FOW, GHW) this is because the wells penetrate the Trinity aquifer, but in others (SVS, BCK, TNR) the mixing appears to occur as cross-formational flow from the Trinity when aquifer flow conditions are high.

This long-term historical dataset has proven to be useful for gaining hydrologic insight into flowpaths, water mixing, and geochemical evolution of water

in the Barton Springs segment of the Edwards aquifer. Given the arbitrary nature of the 26-year USGS sampling program for the Barton Springs segment of the Edwards aquifer, it seems noteworthy that the approach taken by this study was useful.

Eagleson (1991) states that long-term data collection programs “provide the basis for understanding hydrologic systems,” and that seems to be true for this study.

## **2.9. ACKNOWLEDGEMENTS**

Data for this study was collected by the USGS, and funded in part by the City of Austin Watershed Protection and Development Review Department. Thanks are extended to David Johns (City of Austin) for providing his insights into the Barton Springs segment and for reviewing this paper. This quality of this manuscript was improved by a review from Greg Stanton (USGS). Additional thanks are given to Barbara Mahler (USGS), Milton Sunvison (USGS), and Peter VanMetre (USGS) for their keen scientific insight. General thanks are extended to the many scientists and technicians who scrupulously collected, analyzed, and archived the 26 years of data used by this study. Finally, thanks are extended to the many landowners and city authorities who allowed access to their wells.

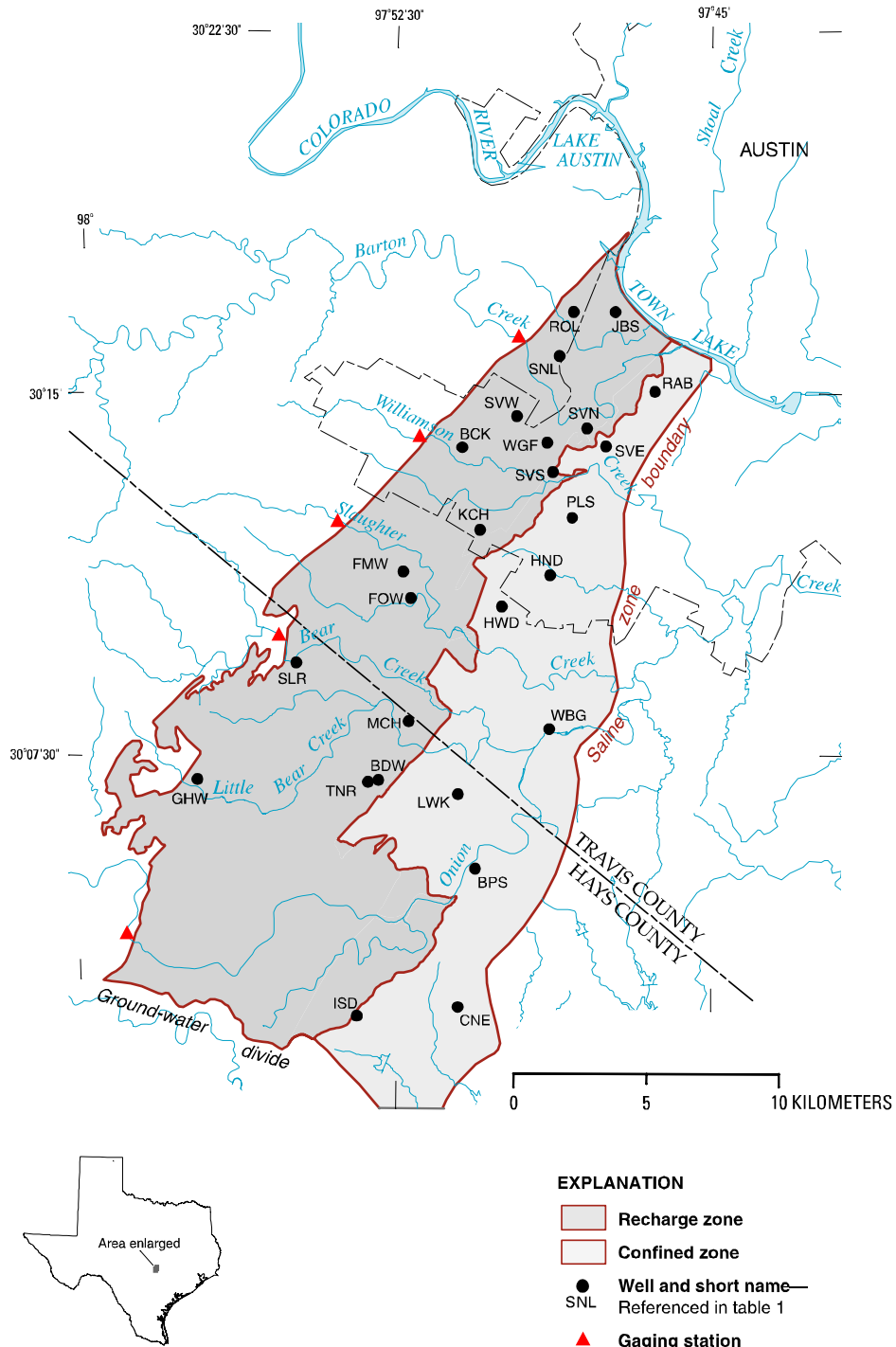


**Figure 2-1.** Location of the Barton Springs segment of the Edwards aquifer in the Austin, Texas area, major creeks, and data-collection sites, 1978–2003.

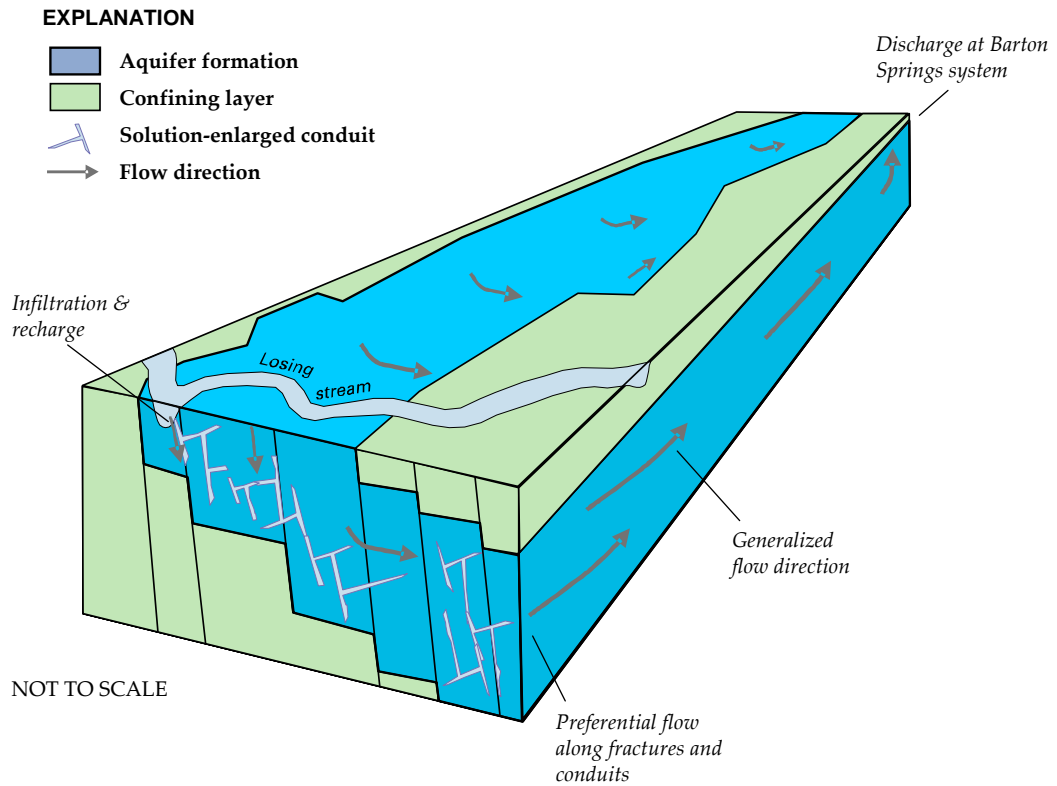


**Figure 2-2.** Schematic diagram of the Barton Springs segment of the Edwards aquifer. Recharge water enters the aquifer through the beds of creeks as they cross the recharge zone. Water in the aquifer flows generally to the north-northeast, generally along solution-enlarged conduits that act at highly preferential flowpaths. The majority of aquifer water eventually discharges at the far northeast corner of the aquifer at the Barton Springs system.

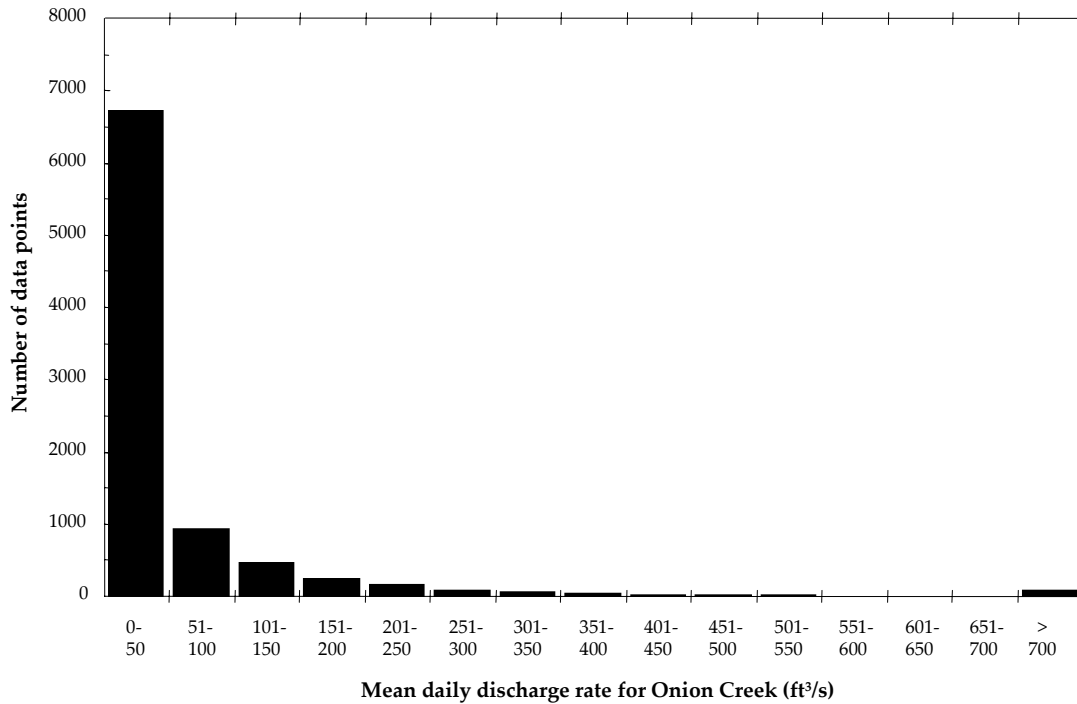


**Figure 2-3.** Histogram showing the non-normal distribution of Onion Creek mean daily discharge data, 1978–2003. The data are skewed to the right, and there are 8 outlier values that are significantly higher than all other values. The other creeks in the study area (Barton, Williamson, Slaughter, and Bear Creeks) show a similar distribution. Therefore, a non-parametric statistical test that does not assume a normal distribution was used when comparing these data against specific conductance of water in wells.

EXPLANATION

- Main Barton Spring, 1987-96
- YD-58-50-840 (Saline zone)
- YD-58-50-301 (Saline zone, CoA)
- YD-58-50-302 (Saline zone, CoA)
- YD-58-50-304 (Saline zone, CoA)
- ▲ YD-58-50-409 (Trinity aquifer)
- ▲ YD-58-49-603 (Trinity aquifer)

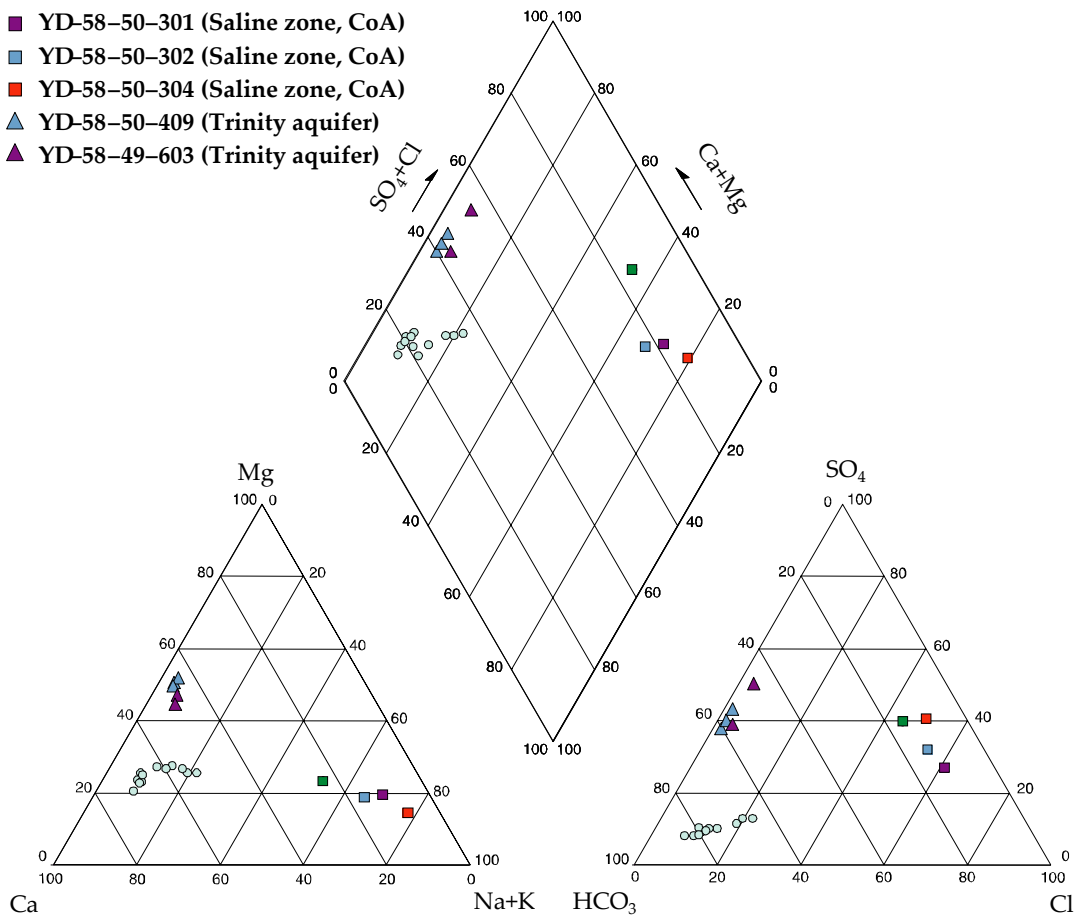


**Figure 2-4.** Piper diagram showing relative proportions of dissolved ions in a visual format. Representative water samples from Main Barton Spring show observed geochemical variability seen at this site through time. Samples from wells in the saline zone (state well numbers YD-58-50-840, YD-58-50-301, YD-58-50-302, and YD-58-50-304) are shown for reference, and selected samples from wells completed in the underlying Trinity aquifer (state well numbers YD-58-50-409 and YD-58-49-603) are shown for reference. Geochemical data for three of the four saline zone wells was provided by the City of Austin (designated as CoA in map explanation).

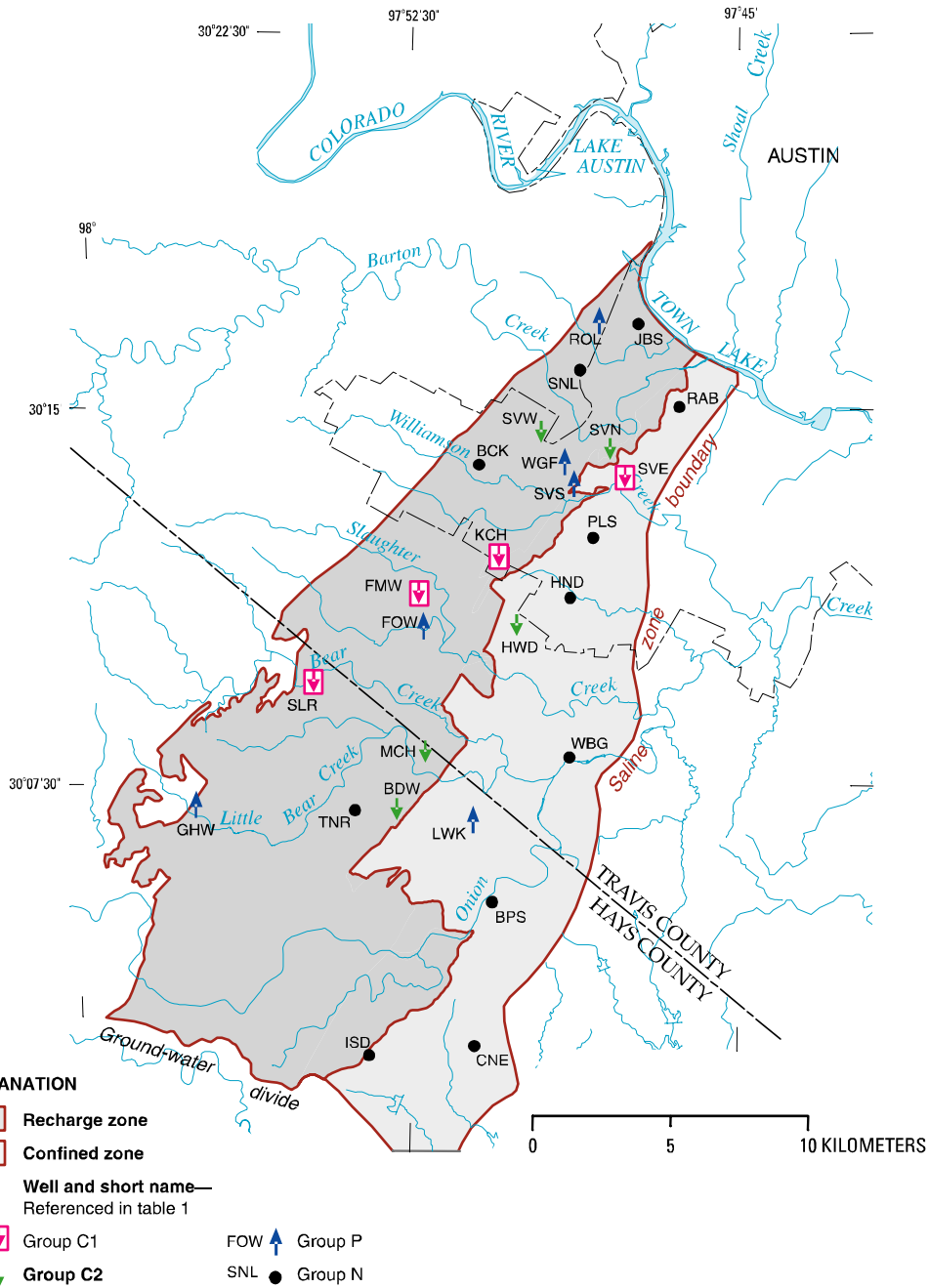


**Figure 2-5.** A nonparametric statistical test between specific conductance in wells, discharge rates of creeks, and aquifer flow condition divides sampled wells into four groups. Group C1 wells are negatively correlated to aquifer flow condition and streamflow. Group C2 wells are negatively correlated to streamflow only. Group P wells are positively correlated with aquifer flow condition, and Group N wells are not correlated to either aquifer flow condition or streamflow.

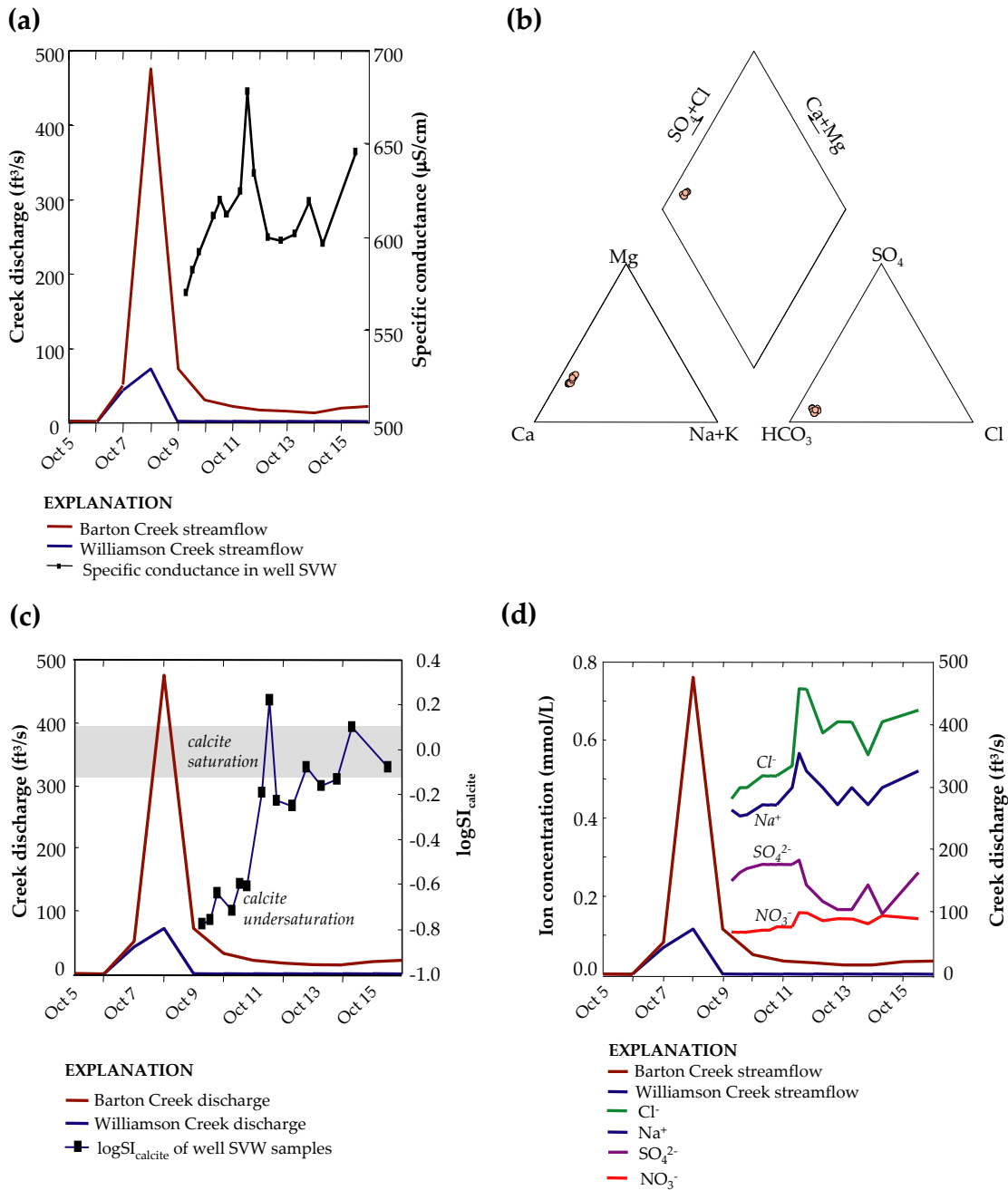


**Figure 2-6.** Results of high-frequency sampling of well SVW, October 9–15, 1995. (a) Specific conductance increases, decreases, and increases again in response to streamflow; (b) Water samples from this event plot in the same region of a Piper diagram, suggesting dilution as a primary process; (c) Calcite saturation indices increase after flow in Barton Creek and/or Williamson Creek probably lowered them to undersaturated values; (d) Concentrations of dissolved ions show a response to streamflow.

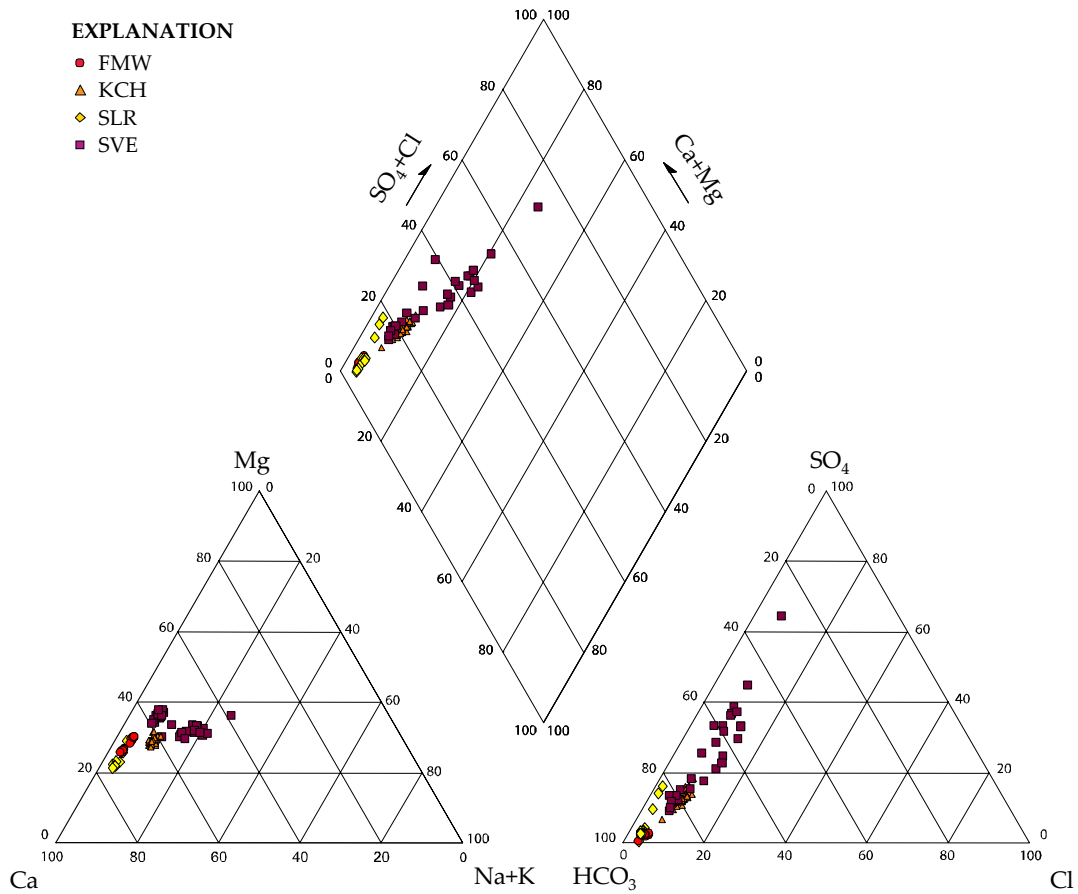


**Figure 2-7a.** Trilinear diagram showing the relations between concentrations of major ions in water sampled from **group C1** wells screened in the Barton Springs segment of the Edwards aquifer, Austin, Texas, 1978–2003.

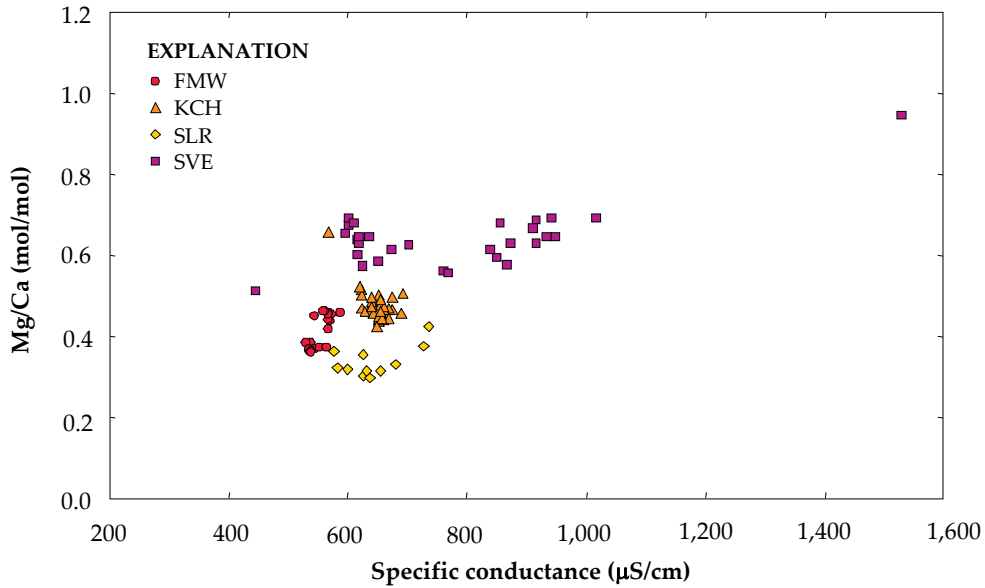


Figure 2-7b. Mg/Ca molar ratios compared against specific conductance of water samples from group C1 wells.

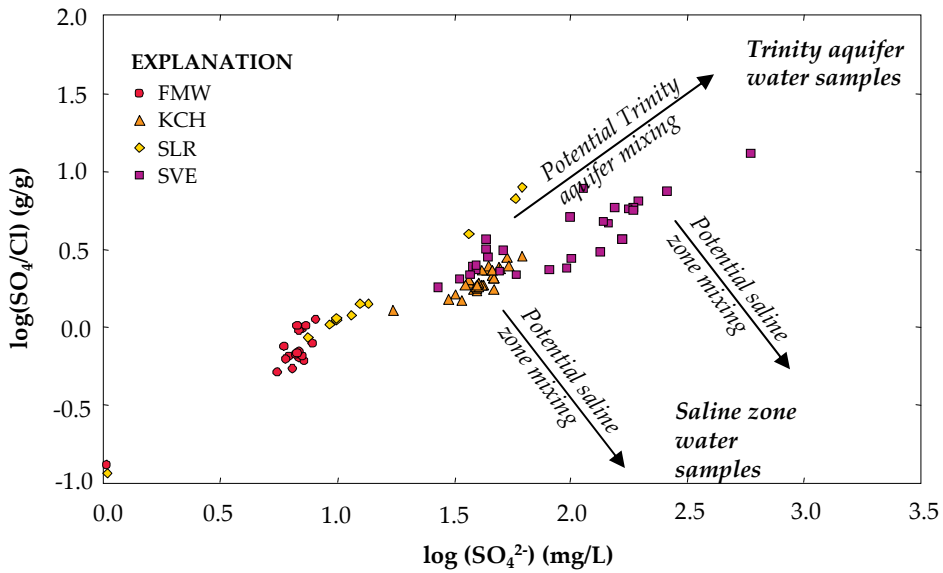
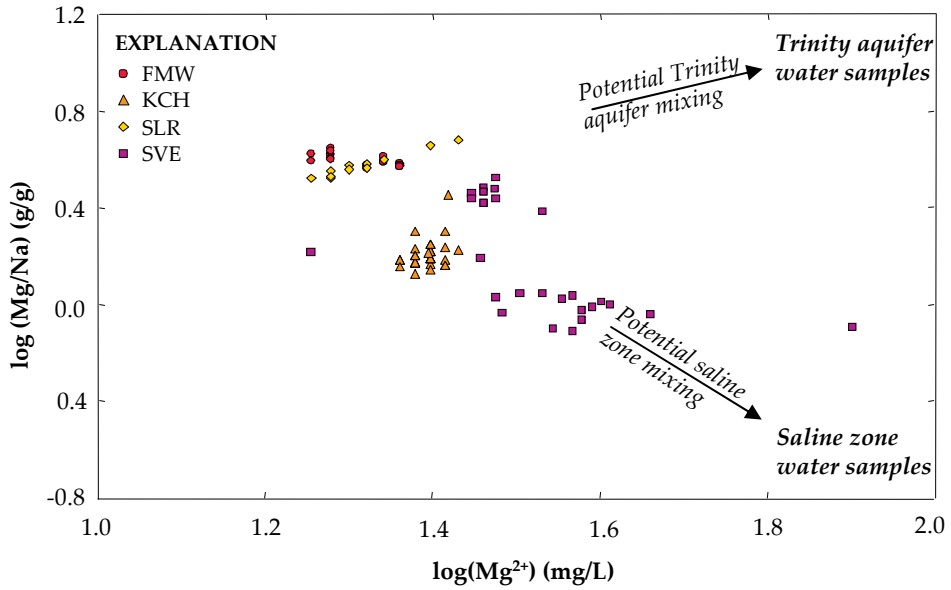
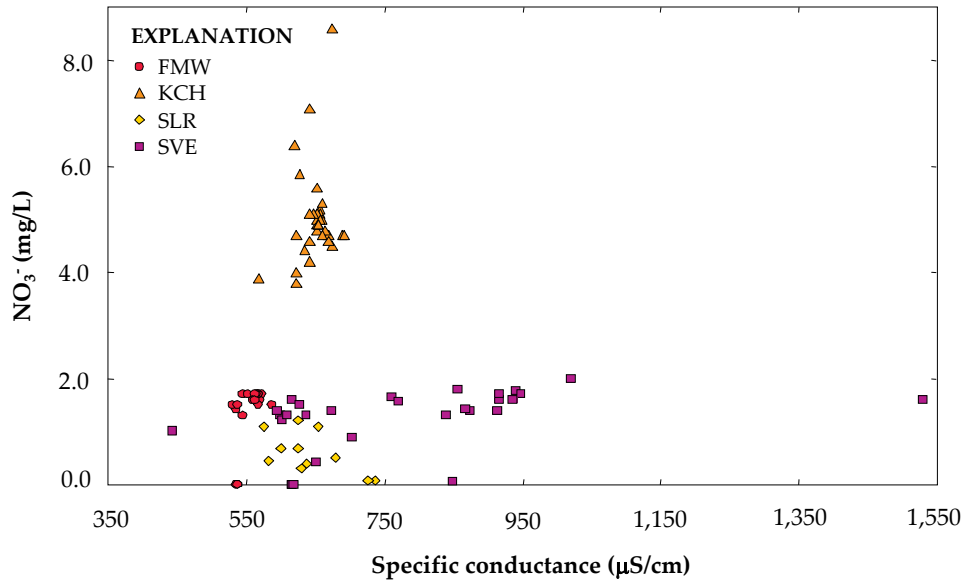


Figure 2-7c.  $\text{SO}_4/\text{Cl}$  ratios compared against  $\text{SO}_4^{2-}$  concentrations of water samples from group C1 wells.

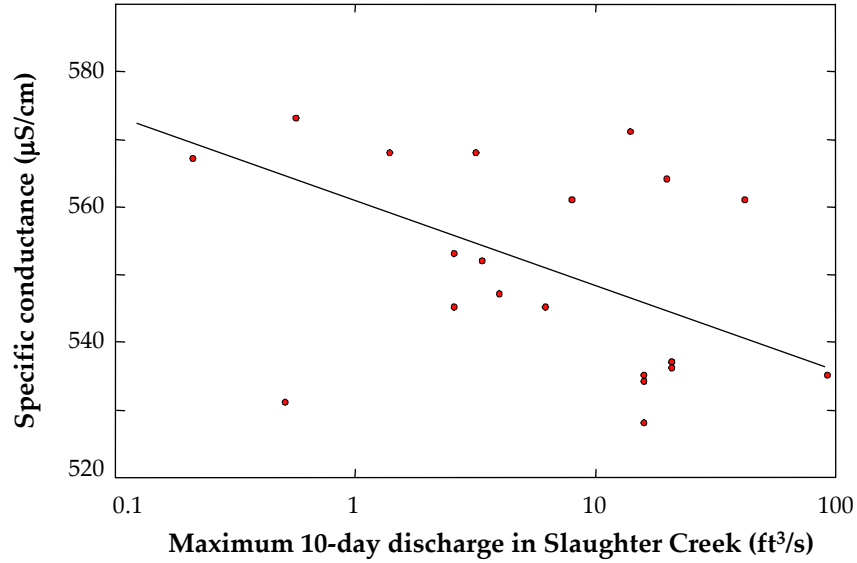


**Figure 2-7d.** Mg/Na ratios compared against Mg<sup>2+</sup> concentrations of water samples from **group C1** wells.



**Figure 2-7e.** NO<sub>3</sub><sup>-</sup> concentrations compared against specific conductance measurements of water samples from **group C1** wells.

(a)



(b)

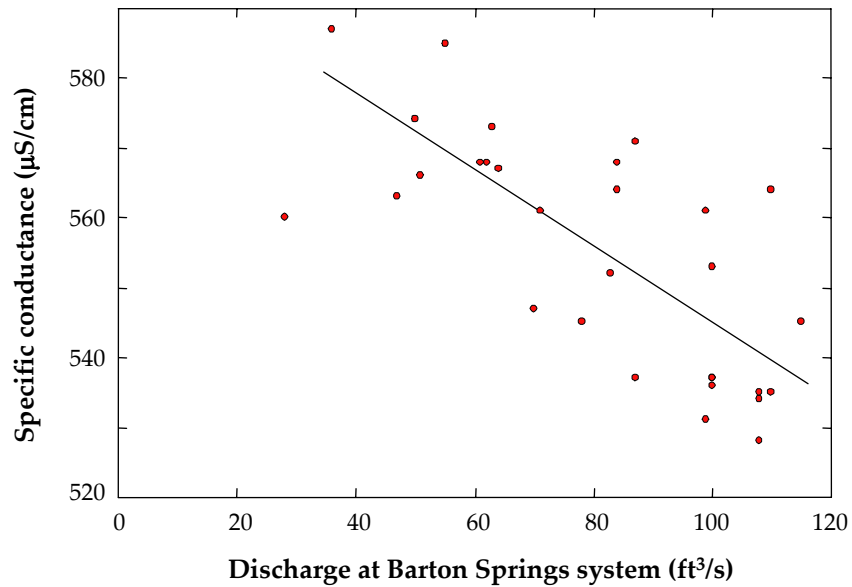


**Figure 2-8.** Specific conductance in well FMW as a function of (a) maximum 10-day discharge of Slaughter Creek; and (b) aquifer flow condition as measured by discharge of the Barton Springs system. In both cases, the compared values are inversely proportional when compared by a nonparametric statistical test. The linear regression line shown on the graphs is calculated using parametric statistics, and is shown for illustrative purposes only.

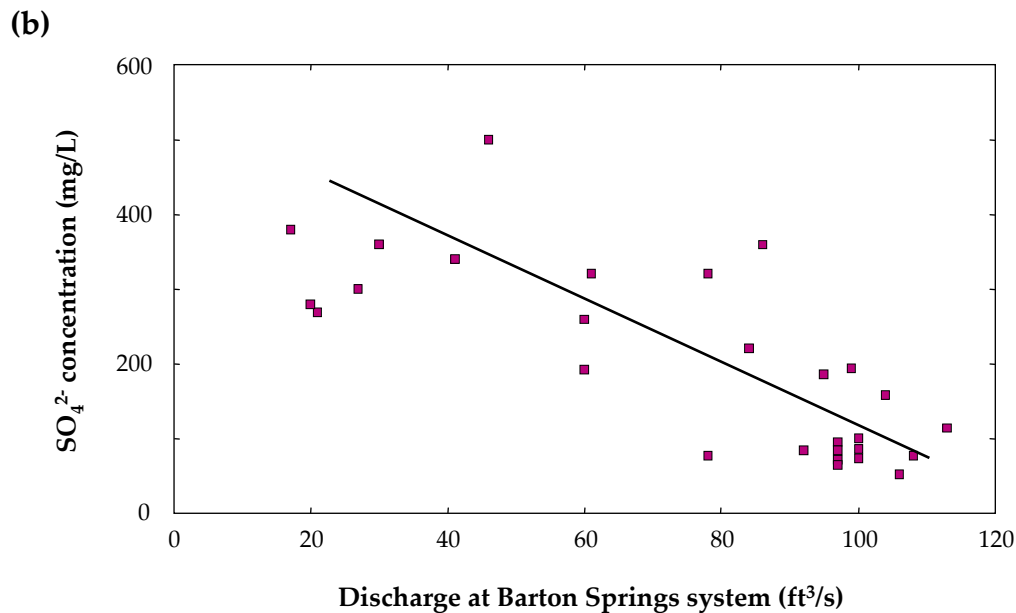
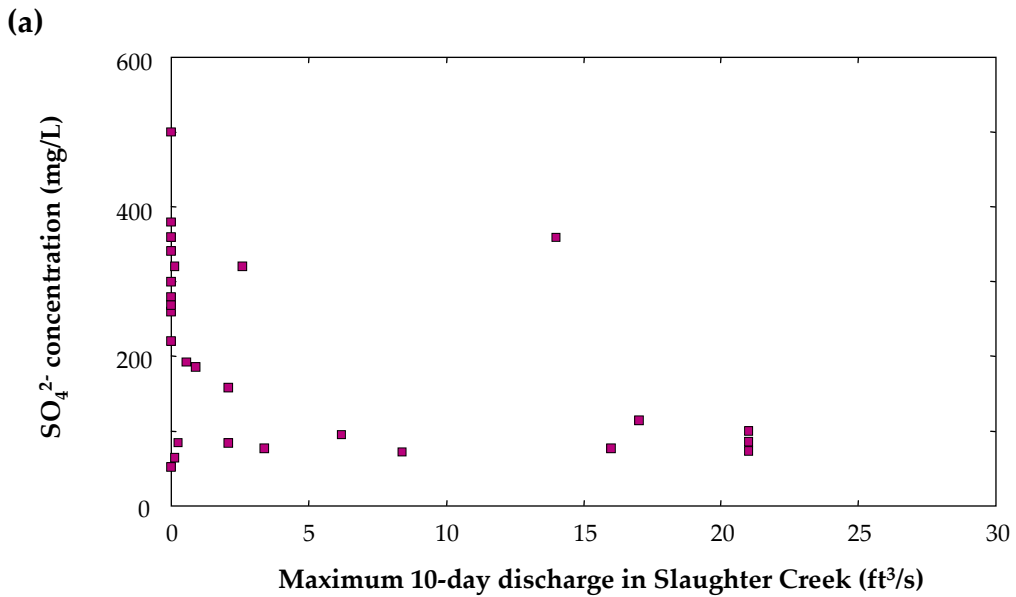


**Figure 2-9.** Sulfate concentration in well SVE, and its variation as a function of (a) maximum 10-day discharge in Slaughter Creek; and (b) aquifer flow condition as measured by Barton Springs system discharge. In both cases, a nonparametric statistical test shows a statistically significant negative correlation between the compared values. The linear regression line shown on graphs (b) is calculated using parametric statistics, and is shown for illustrative purposes only.

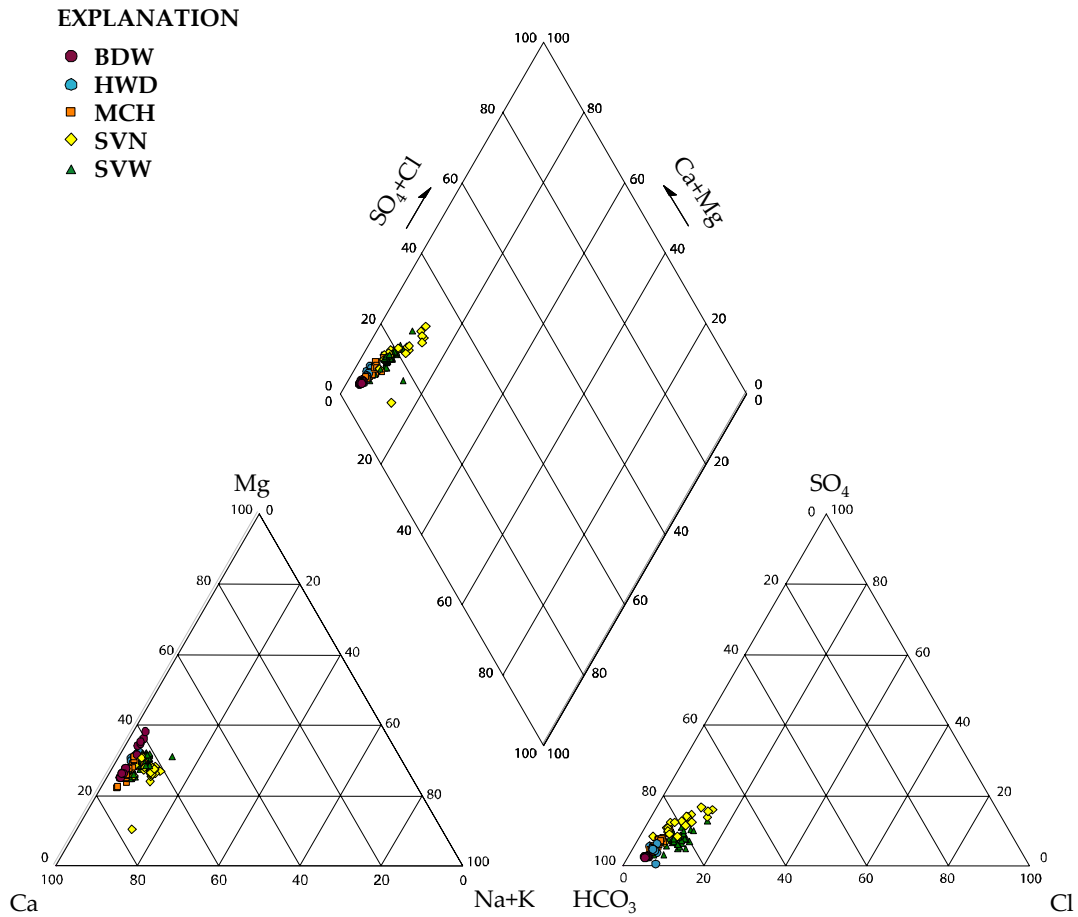


**Figure 2-10a.** Trilinear diagram showing the relations between concentrations of major ions in water sampled from **group C2** wells screened in the Barton Springs segment of the Edwards aquifer, Austin, Texas, 1978–2003.

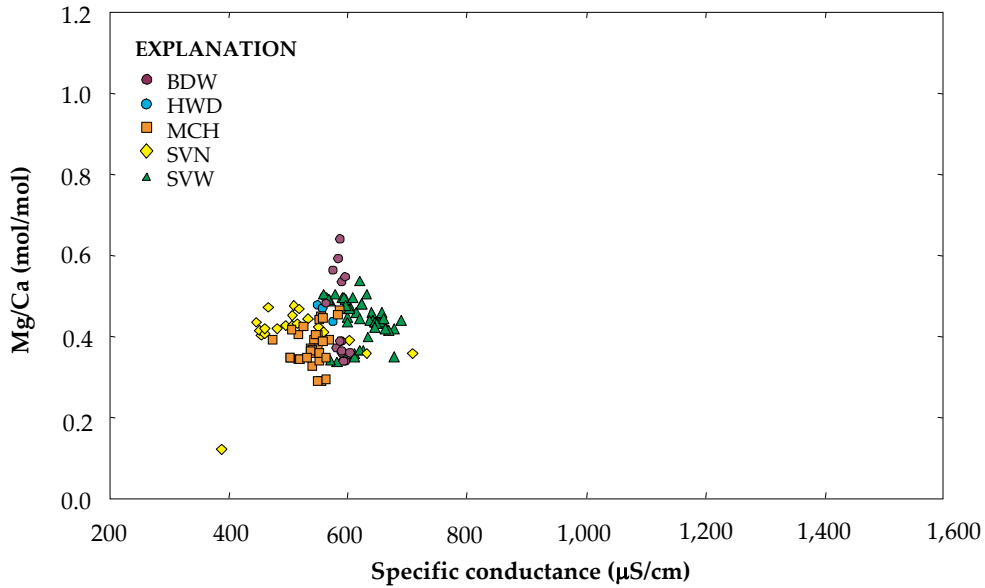


**Figure 2-10b.** Mg/Ca molar ratios compared against specific conductance of water samples from **group C2** wells.

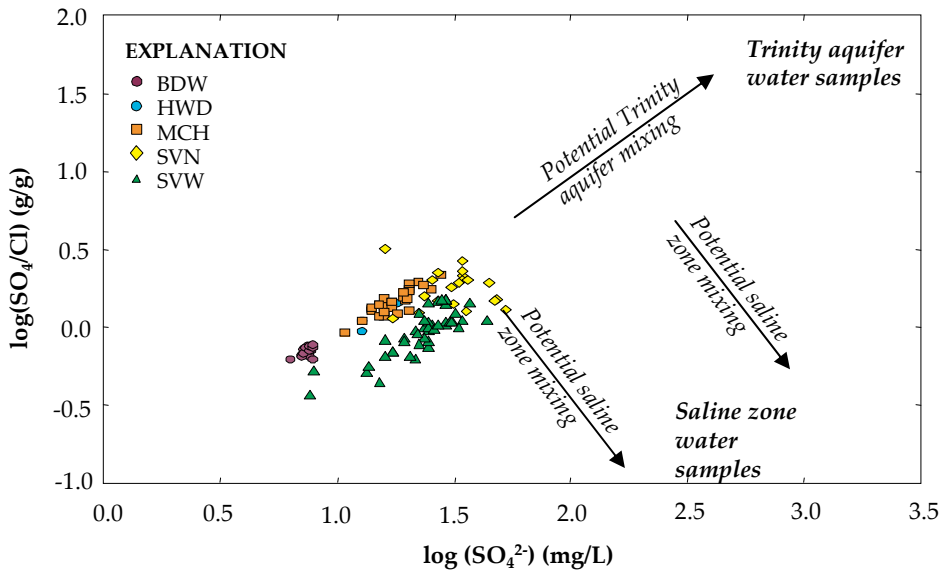


**Figure 2-10c.**  $\text{SO}_4/\text{Cl}$  ratios compared against  $\text{SO}_4^{2-}$  concentrations of water samples from **group C2** wells.

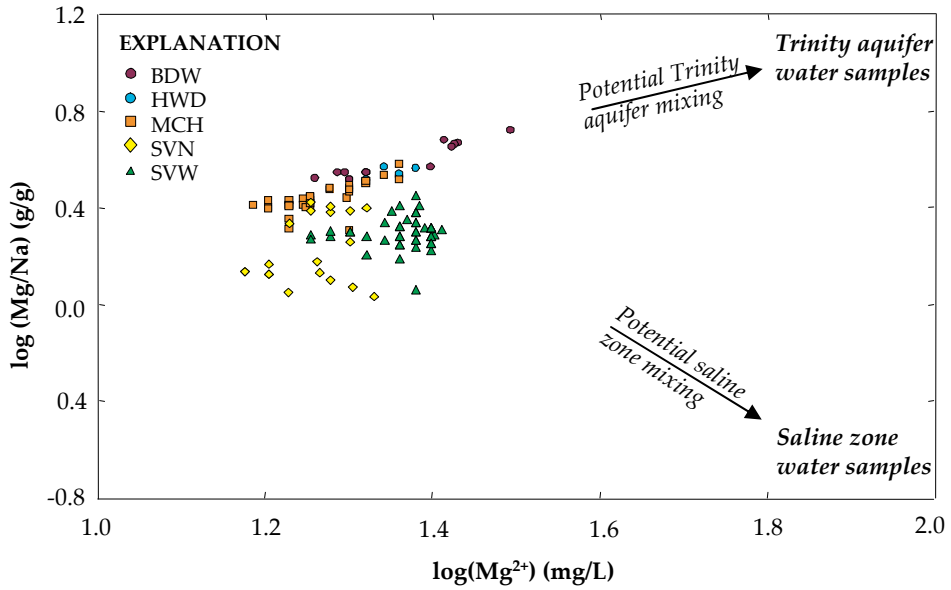


**Figure 2-10d.** Mg/Na ratios compared against Mg<sup>2+</sup> concentrations of water samples from **group C2** wells.

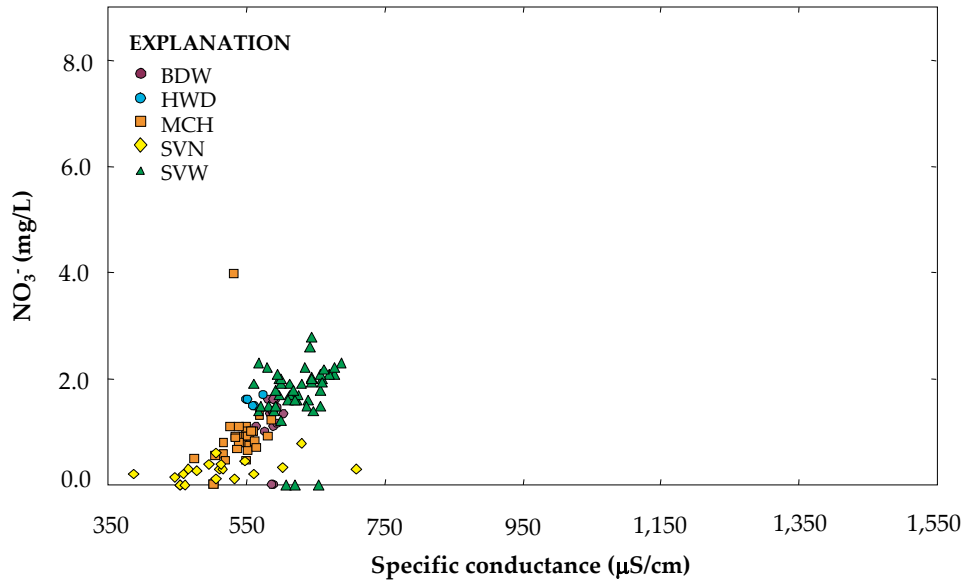


**Figure 2-10e.** NO<sub>3</sub><sup>-</sup> concentrations compared against specific conductance measurements of water samples from **group C2** wells.

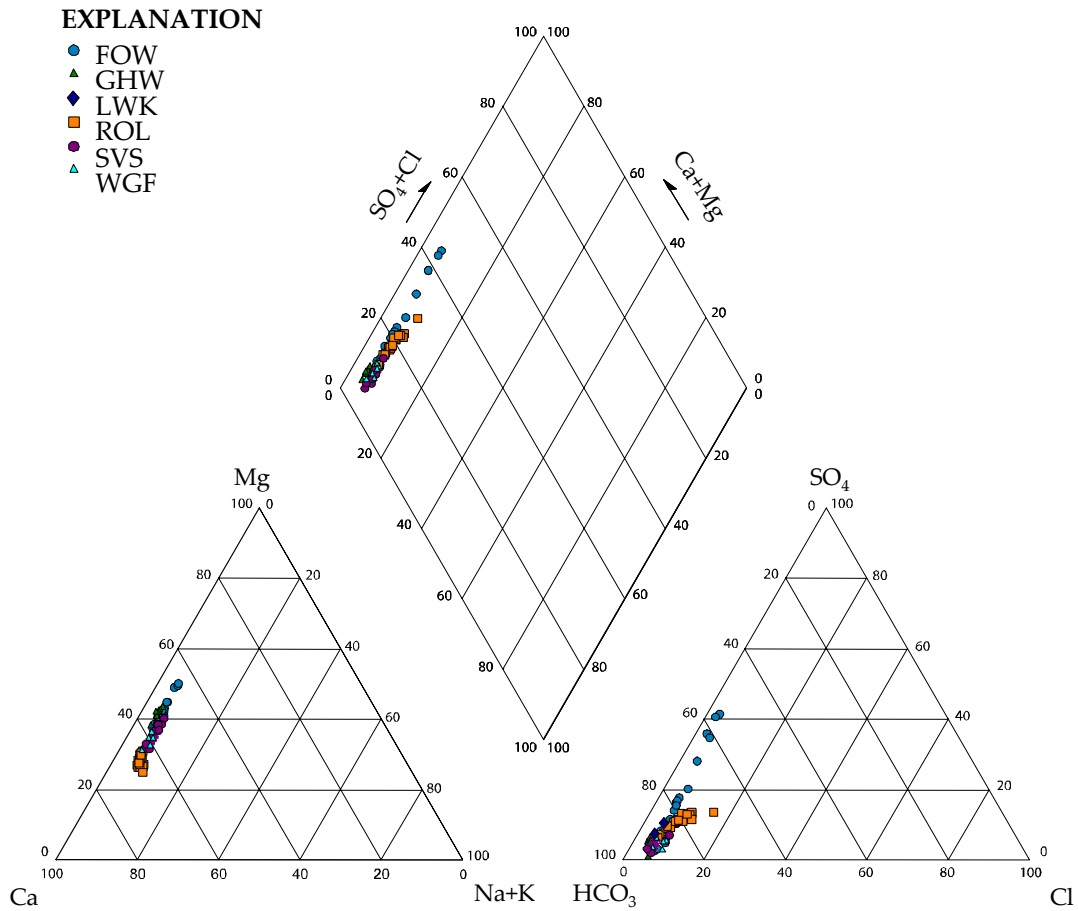


**Figure 2-11a.** Trilinear diagram showing the relations between concentrations of major ions in water sampled from **group P** wells screened in the Barton Springs segment of the Edwards aquifer, Austin, Texas, 1978–2003.

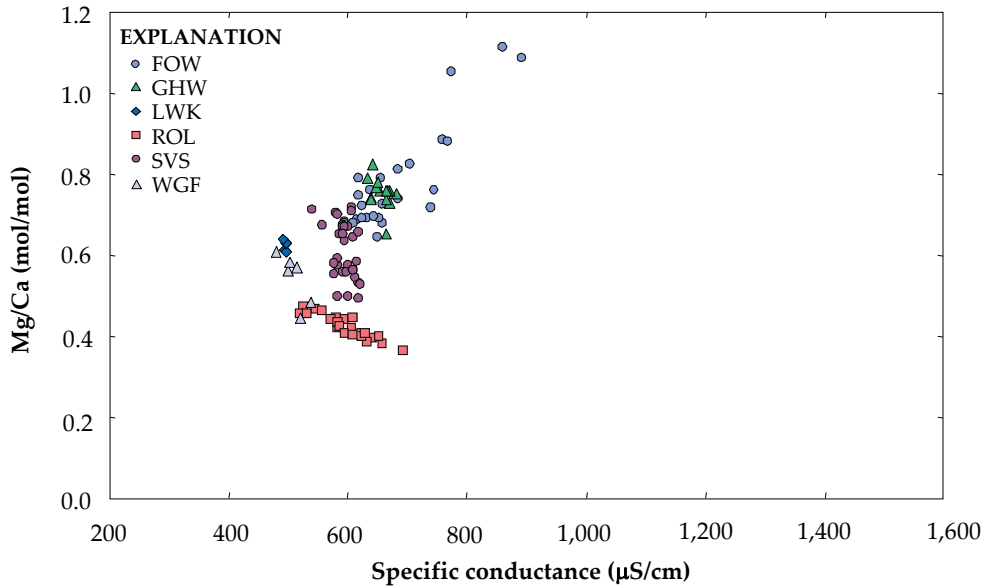


**Figure 2-11b.** Mg/Ca molar ratios compared against specific conductance of water samples from **group P** wells.

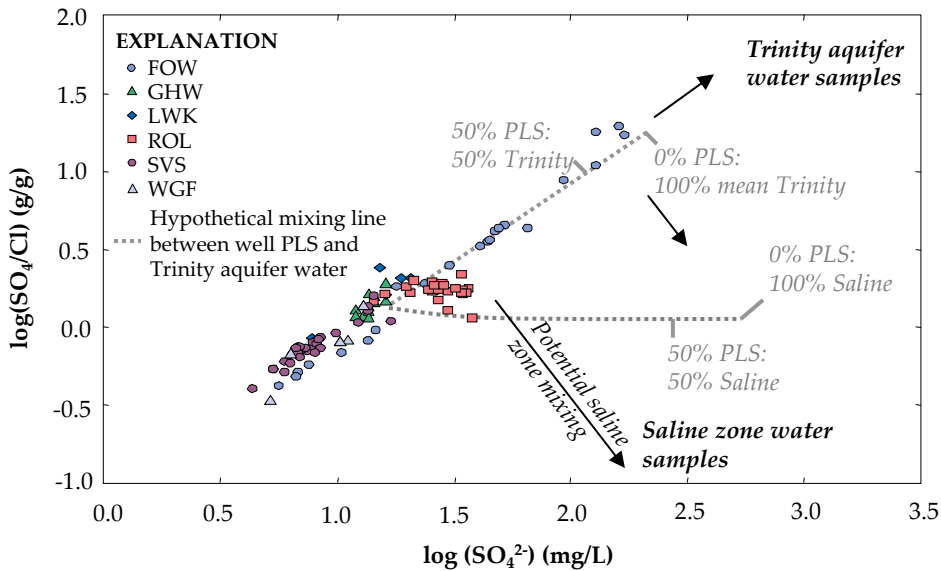


**Figure 2-11c.**  $\text{SO}_4/\text{Cl}$  ratios compared against  $\text{SO}_4^{2-}$  concentrations of water samples from **group P** wells. Samples from wells FOW and SVS plot along a line representing a hypothetical mixture between well PLS and average Trinity water, suggesting that Trinity aquifer water reaches these wells.

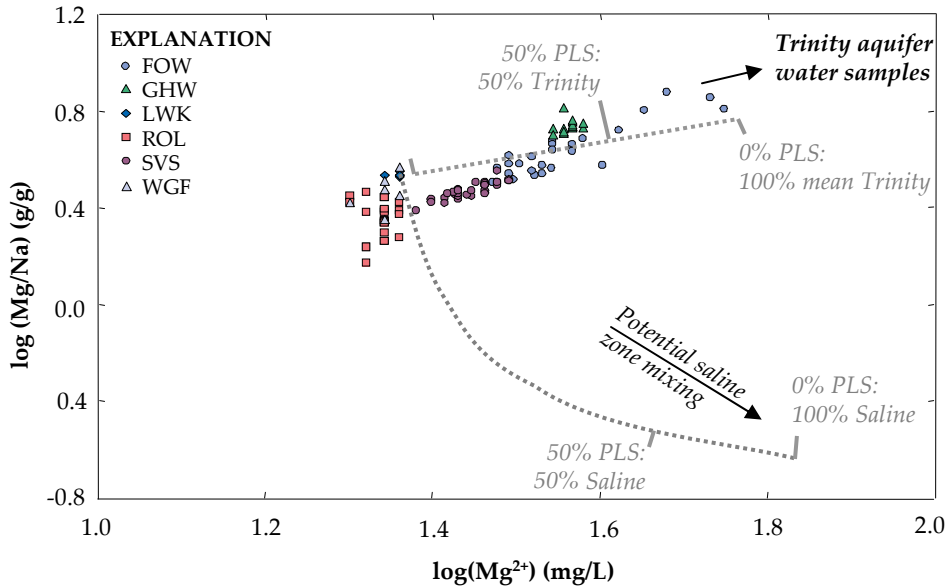


**Figure 2-11d.** Mg/Na ratios compared against  $Mg^{2+}$  concentrations of water samples from **group P** wells. Samples from wells FOW and SVS plot nearly along a line representing a hypothetical mixture between well PLS and average Trinity water, suggesting that Trinity aquifer water reaches these wells.

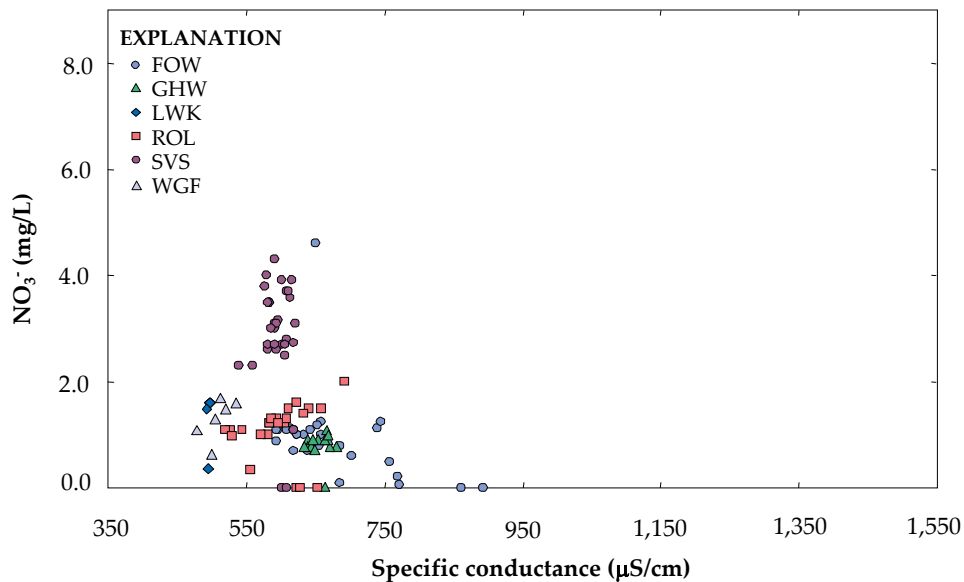


**Figure 2-11e.**  $NO_3^-$  concentrations compared against specific conductance measurements of water samples from **group P** wells.

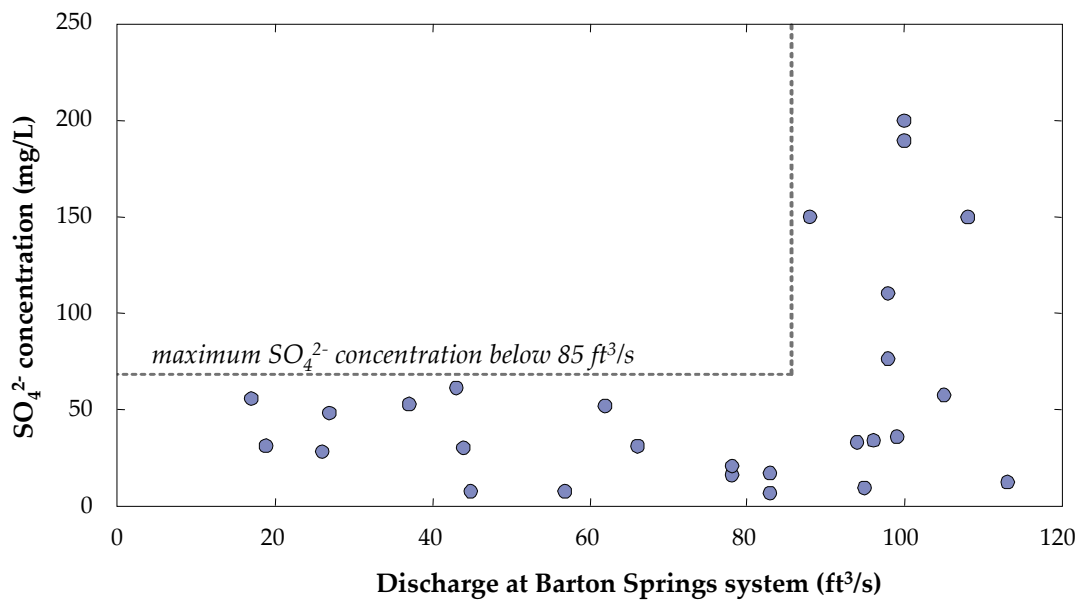


**Figure 2-12.** Sulfate concentration in well FOW as it relates to aquifer flow condition as measured by discharge of the Barton Springs system. Sulfate concentration about 70 mg/L only occur in this well when aquifer flow condition is higher than an amount corresponding to 85 ft<sup>3</sup>/s of Barton Springs system discharge.

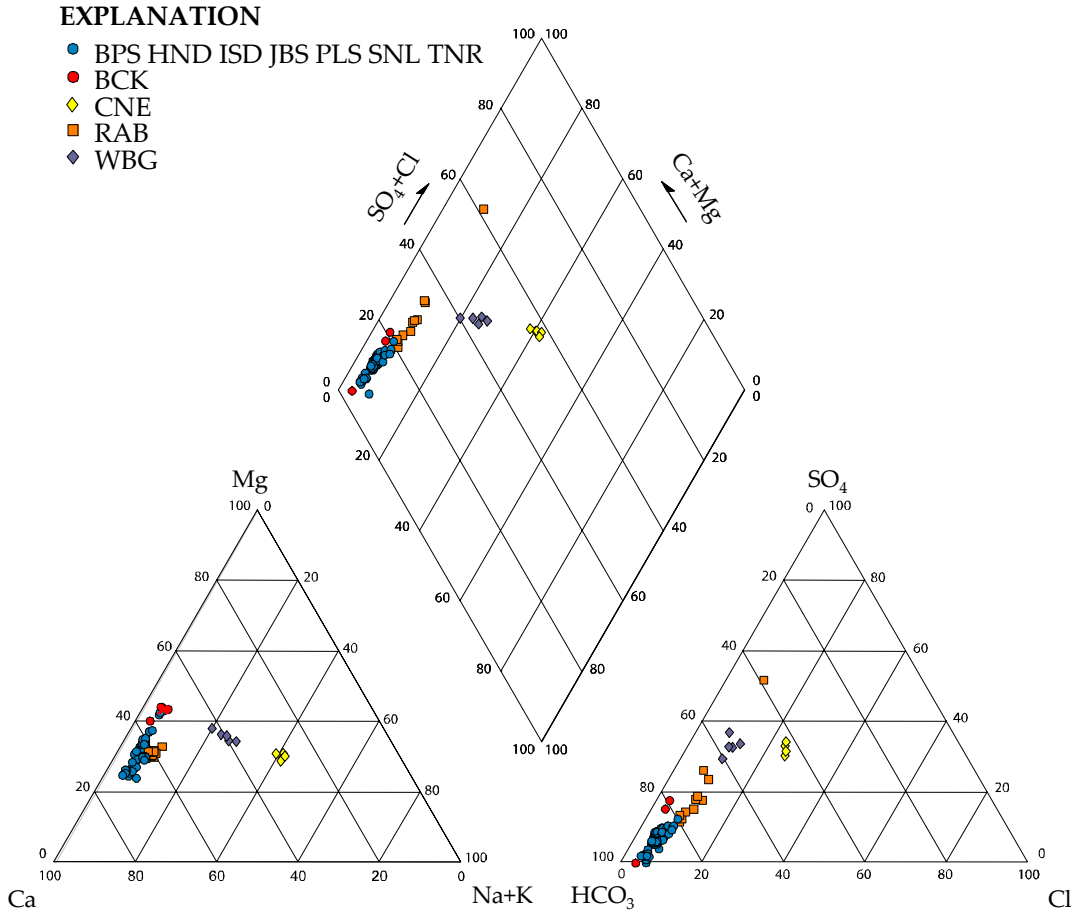


**Figure 2-13a.** Trilinear diagram showing the relations between concentrations of major ions in water sampled from **group N** wells screened in the Barton Springs segment of the Edwards aquifer, Austin, Texas, 1978–2003.

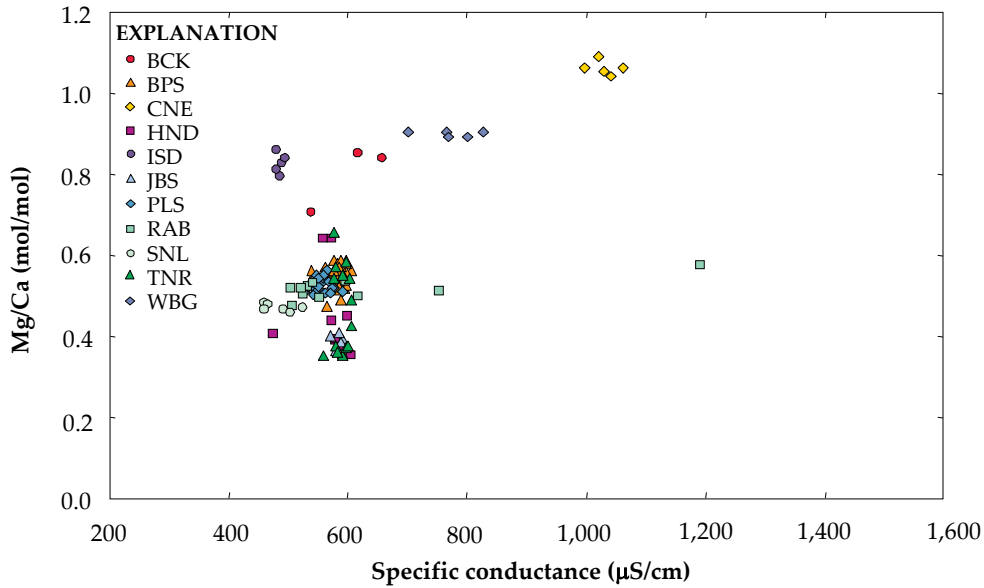


**Figure 2-13b.** Mg/Ca molar ratios compared against specific conductance of water samples from **group N** wells.

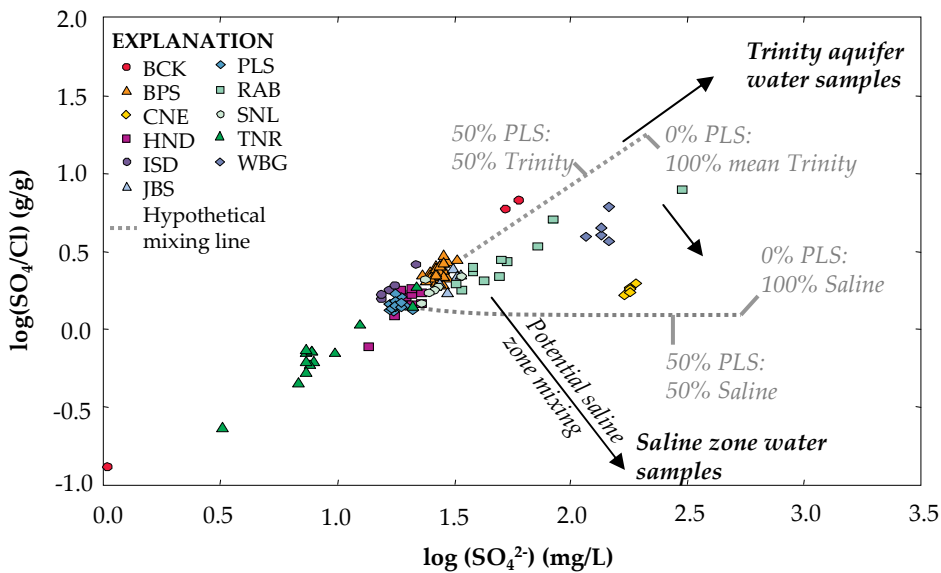


**Figure 2-13c.**  $\text{SO}_4/\text{Cl}$  ratios compared against  $\text{SO}_4^{2-}$  concentrations of water samples from **group N** wells. Variations in well RAB composition cannot be explained simply by simple water mixing between well PLS and the mean composition of Trinity aquifer water used in this study.

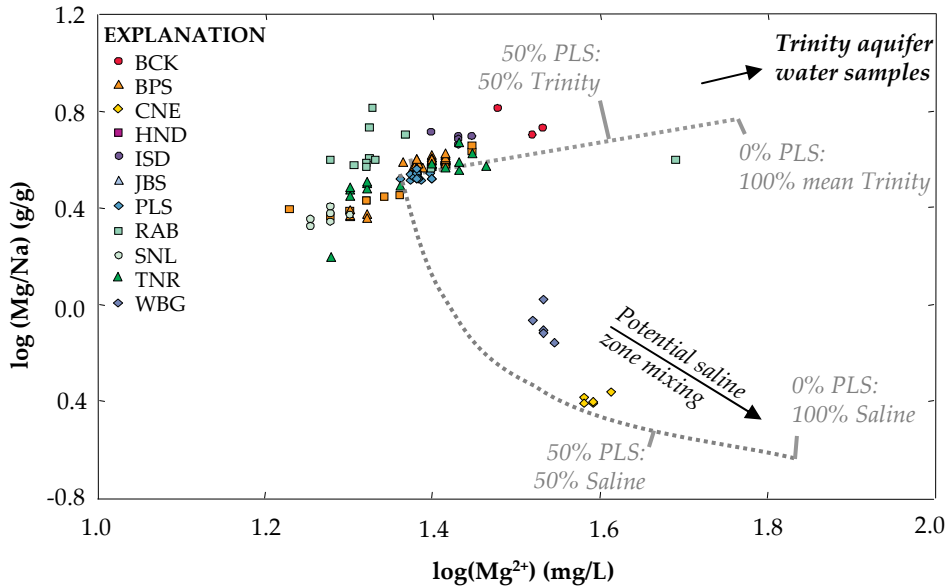


**Figure 2-13d.** Mg/Na ratios compared against  $Mg^{2+}$  concentrations of water samples from **group N** wells. Samples from well RAB do not show evidence of being a mixture between well PLS water and average Trinity aquifer water. Samples from wells CNE and WBG apparently mix with the saline zone.

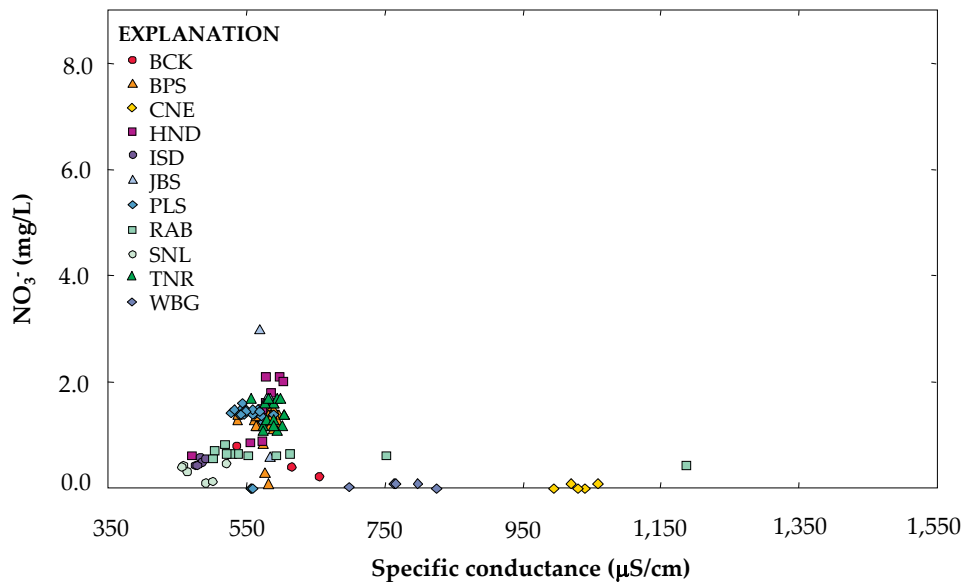


**Figure 2-13e.**  $NO_3^-$  concentrations compared against specific conductance measurements of water samples from **group N** wells.

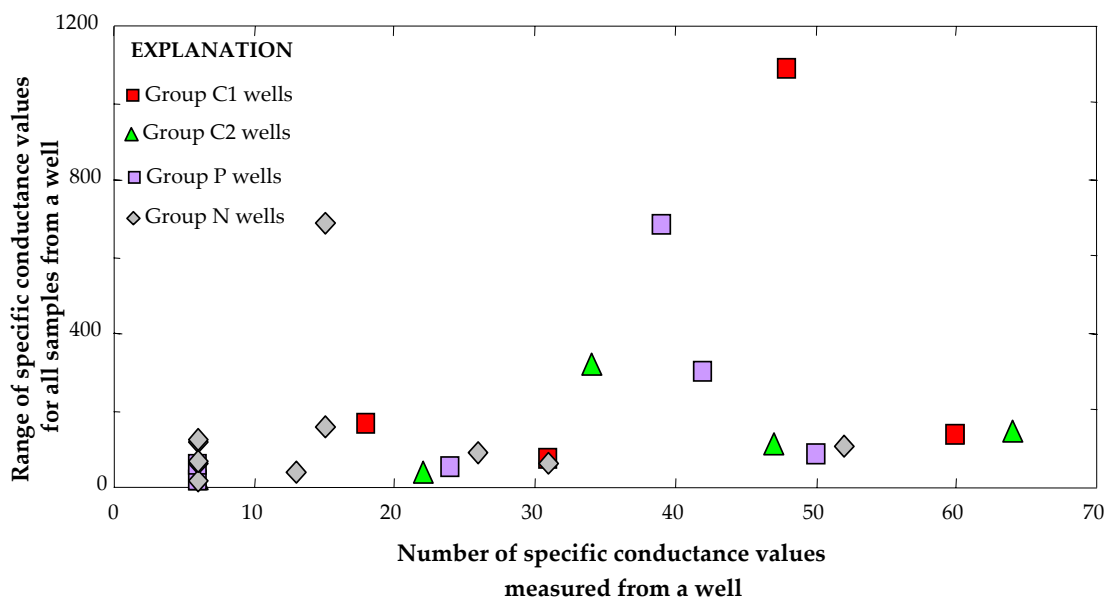


**Figure 2-14.** Comparison between the number of samples collected from a well and the range of measured specific conductance values for that well. Generally, wells with a larger number of values have a larger range of specific conductance values, suggesting that small sample sets may not capture the full range of geochemical variability that is possible within the water of a well.

**Table 2-1.** Wells sampled in Chapter 2, range of sampling dates, and the number of analyses available for each well.

<b>Site ID</b>	<b>State well number<sup>1</sup></b>	<b>USGS site identifier<sup>2</sup></b>	<b>Range of years well was sampled</b>	<b>Number of specific conductance measurements</b>	<b>Number of major ion water analyses</b>
BCK	YD-58-50-101	301317097513801	1978–83	6	3
BDW	LR-58-57-311	300646097533202	1990–03	23	14
BPS	LR-58-58-403	300453097503301	1978–03	53	35
CNE	LR-58-58-704	303138097511501	1978–83	6	5
FMW	YD-58-50-412	301106097520501	1981–94	31	19
FOW	YD-58-50-408	301031097515801	1978–03	43	27
GHW	LR-58-57-202	300639097571001	1978–89	24	14
HND	YD-58-50-502	301113097485401	1978–87	15	9
HWD	YD-58-50-401	301038097500401	1978–83	6	5
ISD	LR-58-57-901	300148097532101	1978–83	6	5
JBS	YD-58-42-926	301634097470001	1978–83	13	5
KCH	YD-58-50-406	301148097503501	1978–99	60	38
LWK	LR-58-58-105	300640097513501	1978–83	6	5
MCH	YD-58-50-704	300813097512101	1978–03	48	31
PLS	YD-58-50-520	301226097480701	1988–03	32	20
RAB	YD-58-42-915	301526097463201	1993–03	16	11
ROL	YD-58-42-813	301628097474001	1978–94	39	23
SLR	LR-58-49-903	300847097545801	1978–89	18	11
SNL	YD-58-42-809	301553097482801	1978–83	6	6
SVE	YD-58-50-216	301356097473301	1978–03	49	29
SVN	YD-58-50-217	301432097480001	1978–03	35	20
SVS	YD-58-50-215	301339097483701	1978–03	51	31
SVW	YD-58-50-211	301423097495901	1978–03	65	46
TNR	LR-58-57-303	300646097533201	1978–92	26	15
WBG	YD-58-50-810	300803097483801	1978–83	6	5
WGF	YD-58-50-206	301414097483601	1978–83	6	6

<sup>1</sup> For locating wells in Texas Water Development Board databases, among others (e.g., <[http://www.twdb.state.tx.us/GwRD/waterwell/well\\_info.asp](http://www.twdb.state.tx.us/GwRD/waterwell/well_info.asp)>).

<sup>2</sup> For locating wells in United States Geological Survey databases (e.g., <<http://waterdata.usgs.gov/>>).

**Table 2-2.** Grouping of wells on the basis of the results of a Spearman rank correlation test between specific conductance, streamflow rates in creeks, and aquifer flow condition as measured by discharge rate of the Barton Springs system.

Site ID	Spearman Rho correlation strengths versus specific conductance <sup>1</sup>					
	Barton Creek	Williamson Creek	Slaughter Creek	Bear Creek	Onion Creek	Aquifer flow condition
<b>Group C1<sup>2</sup></b>						
<i>FMW</i>			-0.55		-0.47	-0.71
<i>KCH</i>			-0.26		-0.47	-0.39
<i>SLR</i>				-0.63		-0.63
<i>SVE</i>	-0.50		-0.44	-0.39	-0.40	-0.69
<b>Group C2<sup>3</sup></b>						
<i>BDW</i>				-0.47		
<i>HWD</i>				-0.90		
<i>MCH</i>	-0.46	-0.42	-0.43	-0.44	-0.42	
<i>SVN</i>	-0.50	-0.63	-0.54	-0.35	-0.41	
<i>SVW</i>	-0.39	-0.28	-0.41	-0.47	-0.31	
<b>Group P<sup>4</sup></b>						
<i>FOW</i>	0.32					0.50
<i>GHW</i>						0.41
<i>LWK</i>						0.88
<i>ROL</i>	0.53		0.33			0.46
<i>SVS</i>						0.29
<i>WGF</i>						0.94
<b>Group N<sup>5</sup></b>						
<i>BCK</i>						
<i>BPS</i>						
<i>CNE</i>						
<i>HND</i>						
<i>ISD</i>						
<i>JBS</i>						
<i>PLS</i>						
<i>RAB</i>						
<i>SNL</i>						
<i>TNR</i>						
<i>WBG</i>						

<sup>1</sup> Numeric values are correlation strengths (rho) for significant correlations (p < 0.05).

<sup>2</sup> Negative correlation between specific conductance and both streamflow and aquifer flow condition.

<sup>3</sup> Negative correlation between specific conductance and streamflow.

<sup>4</sup> Positive correlation between specific conductance and aquifer flow condition.

<sup>5</sup> No correlation between specific conductance and discharge rates.

**Table 2-3.** Summary of Chapter 2 findings.

Site ID	State well number	Saline zone mixing?	Trinity aquifer mixing?	Comments
<b>Wells intersecting major flowpaths</b>				
FMW	YD-58-50-412			<i>Residence time variation is source of geochemical variability.</i>
KCH	YD-58-50-406	<i>small</i>		<i>Saline zone mixing suggested, although not near saline zone. High nitrate concentrations.</i>
SLR	LR-58-49-903		<i>yes</i>	<i>Shallow well drilled into Trinity aquifer along western edge of study area.</i>
SVE	YD-58-50-216	<i>yes</i>	<i>small</i>	<i>Saline zone mixing at low aquifer flow condition and streamflow.</i>
<b>Wells intersecting minor flowpaths</b>				
BDW	LR-58-57-311			<i>Residence time variation is source of geochemical variability.</i>
HWD	YD-58-50-401			
MCH	YD-58-50-704		<i>small</i>	
SVN	YD-58-50-217			<i>Can't be sampled under low aquifer levels. Probably gets water very directly from Barton Creek.</i>
SVW	YD-58-50-211	<i>small</i>		<i>High nitrate concentrations. Identified as a flowpath well by another study.</i>
<b>Unknown / no conclusions</b>				
BCK	YD-58-50-101		<i>yes</i>	<i>Small dataset.</i>
BPS	LR-58-58-403			<i>Large unvarying water quality record. High residence time. No saline zone mixing despite proximity to saline zone.</i>
CNE	LR-58-58-704	<i>yes</i>		<i>Small dataset. Pronounced mixing with nearby saline zone.</i>
FOW	YD-58-50-408		<i>yes</i>	<i>Drilled into Trinity aquifer. Mixing from Trinity aquifer during high aquifer levels.</i>
GHW	LR-58-57-202		<i>yes</i>	<i>Shallow well, small dataset, drilled into Trinity aquifer at western edge of study area.</i>
HND	YD-58-50-502			<i>Small dataset.</i>
ISD	LR-58-57-901			<i>Small dataset.</i>

**Table 2-3. (cont.) Summary of Chapter 2 findings.**

Site ID	State well number	Saline zone mixing?	Trinity aquifer mixing?	Comments
<b>Unknown / no conclusions (cont.)</b>				
JBS	YD-58-42-926			<i>Relatively small dataset. High bacteria and NO<sub>3</sub> levels, suggesting local contamination source.</i>
LWK	LR-58-58-105			<i>Small dataset. Slight Ca<sup>2+</sup> and HCO<sub>3</sub><sup>-</sup> increases during high aquifer flow conditions.</i>
PLS	YD-58-50-520			<i>Large unvarying water quality record.</i>
RAB	YD-58-42-915		<i>maybe</i>	<i>Unusual geochemical behavior controlled by unidentified processes.</i>
ROL	YD-58-42-813			<i>Unusual geochemical behavior. Excess Cl<sup>-</sup> may be anthropogenic. Well was plugged due to bacterial contamination.</i>
SNL	YD-58-42-809			<i>Small dataset.</i>
SVS	YD-58-50-215		<i>yes</i>	<i>Mixing with Trinity aquifer during high aquifer levels.</i>
TNR	LR-58-57-303		<i>yes</i>	<i>Located 50 ft away from well BDW, but different geochemical behavior.</i>
WBG	YD-58-50-810	<i>yes</i>		<i>Small dataset. Pronounced mixing with nearby saline zone.</i>
WGF	YD-58-50-206			<i>Small dataset. Slight Ca<sup>2+</sup> and HCO<sub>3</sub><sup>-</sup> increase during high aquifer levels.</i>

### **3. Variability in aqueous and isotope geochemistry of karst ground water used to infer water sources and hydrogeology of the Barton Springs segment of the Edwards aquifer**

#### **3.1. ABSTRACT**

Mixing of ground water, quantification of residence time, and delineation of flowpaths and catchment areas can be difficult to investigate in karst aquifers. Two years of water-quality sampling from springs and wells in a karst aquifer within and around Austin, Texas, proved to be useful for the investigation of these processes. Ground water in the Barton Springs segment of the Edwards aquifer was generally Ca-HCO<sub>3</sub> to Ca-Mg-HCO<sub>3</sub>, and was near saturation with respect to calcite. Oxygen and hydrogen isotope values indicated that ground water is well-mixed over long periods of time. The Sr/Ca ratio was found to be an effective indicator of ground-water residence time, suggesting that incongruent dissolution was an active process in the aquifer. In addition to carbonate minerals, geochemical modeling indicated that gypsum and/or pyrite may be reacting with ground water. Na/Cl molar ratios for samples were mostly less than 1, and may indicate anthropogenic contamination or ion exchange with clay minerals. <sup>87</sup>Sr/<sup>86</sup>Sr values and major ion concentrations from four hydrologically-connected springs suggested that spring discharge was a

mixture of different waters present in the aquifer, consistent with the expected behavior of karst aquifers. Temporal variation in spring  $^{87}\text{Sr}/^{86}\text{Sr}$  values may have suggested multiple sources of Sr in the study area. Main Barton and Eliza Springs appeared to receive ground water from the same flowpath in the aquifer, as their geochemical compositions were indistinguishable. Old Mill Spring received some water from the saline zone along the eastern boundary of the aquifer, as indicated by elevated  $\text{Na}^+$ ,  $\text{Cl}^-$ , and  $\text{SO}_4^{2-}$  concentrations. Main and Eliza Springs also showed evidence of mixing with the saline zone, but only when spring discharge rates were low. Elevated  $\text{NO}_3^-$  concentrations at Upper Barton Spring suggested anthropogenic contamination, and elevated  $\text{K}^+$  concentrations during high flows suggested that surface water from nearby Williamson Creek reached this spring. Water samples from Upper Barton Spring and four nearby wells had the most radiogenic  $^{87}\text{Sr}/^{86}\text{Sr}$  values in the study area, and are located in an isolated aquifer subbasin. This study's high-resolution geochemical dataset demonstrated that evaluation of temporal and spatial variability in isotopic composition and dissolved ion concentrations of karst ground water can provide insights into the functioning of these complex systems.

### 3.2. INTRODUCTION

It is difficult to understand karst aquifers. Their double, triple, and perhaps even quadruple porosity makes the application of traditional hydrologic equations difficult or impossible (see Chapter 1). To better understand these complex systems, scientists collect water samples from wells and springs, and use variations in dissolved ion concentrations and isotope ratios in the samples to understand how ground water flows and evolves in a karst aquifer. A karst spring is “the mouthpiece of a karst aquifer” (B.J. Mahler, U.S. Geological Survey, personal comm., 2004), that is, karst springs are integrators of water in their aquifers, and are recommended as ideal sites to study aquifer-wide processes (Quinlan, 1989). However, the geochemistry of karst springs varies over time (Shuster and White, 1971), and sampling a karst spring at a single moment in time is unlikely to adequately capture the true nature or scope of the processes affecting the spring’s water. Studying the temporal changes in the aqueous and isotope geochemistry of a karst spring can yield insights into aquifer function.

The major ions dissolved in water ( $\text{Ca}^{2+}$ ,  $\text{Mg}^{2+}$ ,  $\text{Na}^+$ ,  $\text{K}^+$ ,  $\text{HCO}_3^-$ ,  $\text{Cl}^-$ , and  $\text{SO}_4^{2-}$ ) typically comprise more than 95 percent of the dissolved load of natural waters (Herczeg and Edmunds, 2000). Concentrations of these ions can be used as geochemical endmembers to understand regional flowpaths (e.g., Uliana and Sharp, 2001) and mixing of ground water from different aquifer zones (e.g., Musgrove and

Banner, 1993; Swarzenski et al., 2001). For example, in a karst aquifer with relatively uniform lithology, variable dissolved  $Mg^{2+}$  and  $Ca^{2+}$  concentrations can indicate variable ground-water residence times (Musgrove and Banner, 2004).

Strontium (Sr) is an alkaline earth trace metal with a chemical behavior similar to calcium. Despite its low abundance in the Earth's crust, it is present in significant quantities in karst aquifers. Thus, strontium is often analyzed in karst studies. Similar to Mg/Ca ratios, variations in Sr/Ca ratios can be indicators of variable residence time (Musgrove and Banner, 2004).  $Sr^{2+}$  in karst ground water generally represents first-order control of the geology on the strontium concentration (Banner, 2004). That is, strontium concentrations in rainfall and surface water are very low, and what strontium does exist in solution is derived from the soil and rock formations through which the ground water flows (Frost and Toner, 2004).

Strontium has several naturally-occurring isotopes, the ratios of which can be used as identifiers of water sources (Swarzenski et al., 2001), water-rock interaction (Musgrove and Banner, 1993), and water mixing (Banner et al., 1989; Lee and Krothe, 2001). When  $Sr^{2+}$  is dissolved from a mineral, the aqueous solution takes on the  $^{87}Sr/^{86}Sr$  ratio of the mineral (Banner, 2004); if multiple minerals with different  $^{87}Sr/^{86}Sr$  values are dissolved, then the aqueous  $^{87}Sr/^{86}Sr$  ratio will be an intermediate value reflecting the relative mixing of these minerals (Banner and Hanson, 1990).  $Sr^{2+}$  dissolved from silicate material (e.g., many soils) usually is more radiogenic than

$\text{Sr}^{2+}$  dissolved from carbonates (Banner, 2004), and several studies have shown that Sr isotopic composition in ground water and surface water is often controlled by the balance between the weathering of carbonate and silicate minerals (Han and Liu, 2004; Musgrove and Banner, 2004). Strontium isotope ratios complement non-isotopic data well, and can provide insights that cannot be gained merely from dissolved ion concentration data (Banner et al., 1994; Vallejos et al., 1997; Frost and Toner, 2004).

Variations in the abundances of oxygen and hydrogen isotopes in the water molecule ( $\text{H}_2\text{O}$ ) have been studied for over 50 years. Early studies focused on precipitation, the origin of waters, and paleotemperature reconstructions of oceans (e.g., McCrea, 1950; Epstein and Mayeda, 1953; Craig, 1961). Oxygen and hydrogen isotopes also can be used to trace aquifer flowpaths (e.g., Lakey and Krothe, 1996), to estimate evapotranspiration (e.g., Scanlon, 2000), to quantify recharge amounts and timing (e.g., Jones and Banner, 2000), and to estimate elevation of recharge (Yurtsever and Gat, 1981; Ciais and Jouzel, 1994; Kattan, 1997). If temperatures are low and evaporation is not an active process in a system, oxygen and hydrogen isotopes are ideal conservative tracers of water flow, because they are integrated into the water molecule itself (Gat, 1981; Kendall et al., 1995). This is in contrast to solute isotopes (e.g., dissolved  $\text{Sr}^{2+}$ ), whose isotopic compositions are wholly influenced by water-rock interaction (Katz et al., 1998).

Scientists are forced to find innovative methods for characterizing the behavior of karst aquifers. Questions regarding ground-water residence time, flowpaths, and water mixing are difficult to answer, especially when studies fail to account for the temporal variability inherent in karst. In this study, springs were sampled many times over two years, and the results of this sampling showed that water residence time varies, flowpaths to karst springs are numerous, and ground-water is a mixture of several different distinct waters.

### **3.3. STUDY AREA**

The Barton Springs segment of the Edwards aquifer (herein referred to as the Barton Springs segment) is a karst aquifer that extends south-southwest of Austin. It is bounded to the north by the Colorado River, to the south by a ground-water divide, to the west by its contact with the Glen Rose Formation, and to the east by a zone of low permeability (Maclay and Land, 1988) containing brackish to saline (> 1000 mg/L total dissolved solids) ground water known as the saline zone (Figure 3-1).

The aquifer rock is composed principally of limestone and dolomite from the Cretaceous period. The aquifer has undergone multiple episodes of karstification and extensive meteoric diagenesis (Rose, 1972; Maclay, 1995; Small et al., 1996). In the Miocene epoch, tectonic activity created a zone of *en-echelon* normal faults,

resulting in enhanced karstification and the aquifer structure and behavior seen today (Slade et al., 1986). The aquifer is generally highly transmissive, with some measured straight-line transit times exceeding 10 kilometers per day (Hauwert et al., 2005).

An estimated 85 percent of recharge to the aquifer occurs through karst features in the creek beds of Barton, Williamson, Slaughter, Bear, and Onion Creeks (Slade et al., 1986). These are ephemeral creeks that cross the recharge zone from west to east (Figure 3-1). Additional sources of recharge include upland infiltration through sinkholes and fractures, infiltration through soil zones (Musgrove and Banner, 2004), leakage of urban infrastructure (Garcia-Fresca Grocin, 2004), and cross-formational flow from other hydrostratigraphic units (City of Austin, 1997; Sharp and Banner, 1997).

Flow in the aquifer generally is to the north-northeast, following the trend of the Balcones Fault Zone, although the exact direction of flow varies with changes in aquifer flow condition and resulting changes in the potentiometric surface (Slade et al., 1986). As expected in a limestone aquifer, the geochemical composition of ground water in the Barton Springs segment can generally be classified as calcium-bicarbonate (Ca-HCO<sub>3</sub>) to calcium-magnesium-bicarbonate (Ca-Mg-HCO<sub>3</sub>) facies, following the nomenclature of Back (1961). Although most Barton Springs

segment water is Ca-HCO<sub>3</sub> or Ca-Mg-HCO<sub>3</sub>, significant variations in dissolved constituents and molar ratios have been observed (Senger and Kreitler, 1984).

The main discharge point for the aquifer is the Barton Springs system, which is comprised of Main Barton Spring, Eliza Spring, Old Mill Spring, and Upper Barton Spring (herein referred to as MSP, ESP, OSP, and USP, respectively) (Figure 3-2). Combined long-term mean discharge from MSP, ESP and OSP is about 50 ft<sup>3</sup>/s (1.4 m<sup>3</sup>/s) (Slade et al., 1986). MSP is the largest of the four springs by far, generally discharging over five times more water than the other three springs combined (Slade et al., 1986).

Additional ground water is withdrawn from the aquifer by pumping from domestic, livestock, and public supply wells (Figure 3-2e). In 2004 there were an estimated 970 active wells pumping from the Barton Springs segment, with an annual ground-water withdrawal of about 2.5 billion gallons (Smith and Hunt, 2004), equivalent to a constant withdrawal rate of about 10 ft<sup>3</sup>/s (0.3 m<sup>3</sup>/s).

The east side of the aquifer is bounded by the saline zone, which contains concentrations of dissolved ions exceeding 1000 mg/L TDS. The saline zone has many processes that contribute to its unusual chemical and isotopic signatures, including gypsum dissolution, incongruent carbonate dissolution, ion exchange, sulfate reduction, fluid mixing, and interaction with igneous intrusions (Sharp and

Clement, 1988; Oetting et al., 1996). It is generally a minor concern for local resource managers because of its high salinity and low ground-water productivity.

### **3.4. METHODS**

#### **3.4.1. Sampling from springs**

Samples were collected from the four springs that comprise the Barton Springs system (Figure 3-1). All samples except for two were collected by immersing containers 1–2 feet (0.3–0.6 m) below the water surface near the spring orifice, and avoiding contact with the atmosphere and standing surface water (Wilde et al., 1999). Two samples on November 24, 2004 from springs MSP and USP were collected using a peristaltic pump and tubing fed into the springs, as the spring outlets were covered by surface water from record floods in nearby Barton Creek.

Samples were collected in 3-liter Teflon or 1-liter polyethylene containers, placed on ice and returned to the United States Geological Survey (USGS) Austin laboratory for processing. There, sample water was filtered through 0.45  $\mu\text{m}$  cellulose filters, using a peristaltic pump and tygon tubing that had been cleaned (Appendix E; Figure E-1). Filtered water was used to fill two 125-mL polyethylene bottles for major ion analysis. One of the bottles had been pre-cleaned with trace element grade (TEG) HCl, and its contents were preserved with TEG  $\text{HNO}_3$  to a pH < 2. Samples were refrigerated and shipped to the USGS National Water Quality Lab

for analysis. Prior to use, all bottles and sampling equipment had been soaked in Liquinox soap, soaked in TEG HCl, and rinsed with deionized water (DIW) (Horowitz and Sandstrom, 1998).

For Sr isotope analysis, filtered water was dispensed into a 30-mL polyethylene sample bottle that had been pre-cleaned in a clean laboratory using Micro soap solution, 30 percent TEG HNO<sub>3</sub>, and DIW (Appendix E). Sr isotope sample bottles were always the last to be filled by filtered water; this allowed the filtration system to be purged multiple times and minimized Sr isotope sample contamination. Prior to October 23, 2004, Sr isotope samples were collected directly from springs and received no filtration. Another study from the Barton Springs segment found that filtration did not measurably affect the <sup>87</sup>Sr/<sup>86</sup>Sr ratio for samples with low total suspended solids (Christian, in preparation). All unfiltered samples in this study had very low turbidity (< 2 Nephelometric Turbidity Units).

Oxygen and hydrogen isotope samples were collected directly from spring orifices into 7-mL glass vials, ensuring that there was no air in the sample container. Samples caps were wrapped in ParaFilm to minimize evaporation, and were refrigerated pending further analysis.

### **3.4.2. Sampling from wells**

Ground-water samples were collected from 12 wells completed in the Barton Springs segment (Figure 3-1 and 3-2; Table B-1). Ground water was extracted by electric submersible pump. Samples were collected at points in the plumbing upstream of pressure tanks or treatment equipment in order to obtain a sample representative of aquifer water. Samples were collected after at least three well-volumes of water had been purged from the well, and after real-time field parameters (pH, temperature, conductivity) values had stabilized (Wilde et al., 1999).

Sample containers used for well water sampling were the same as those used for spring sampling. Filtration was employed for major ion samples, but not isotope samples. Methods used in this ground-water sampling followed protocols outlined by the USGS National Water Quality Assessment Program (Koterba et al., 1995).

### **3.4.3. Analytical methods**

Major ion samples were analyzed by the USGS National Water Quality Laboratory. Cation concentrations were measured using inductively coupled plasma-mass spectrometry, and anion concentrations were measured using ion-exchange chromatography (Fishman, 1993, p. 19). Samples were analyzed within 180 days of collection, per USGS sampling guidelines. Carbonate species

concentrations were determined in the field using the inflection point titration method with 1.6N sulfuric acid (Radtke et al., 1998b). Based on the findings of Andrews et al. (1984), nitrite ( $\text{NO}_2^-$ ) concentrations were assumed to be negligible in samples, thus the measured nitrate+nitrite parameter was assumed to indicate solely nitrate concentration. Silica concentrations were determined, but are not reported here. Blank and replicate analyses for major ions comprised approximately ten percent of the total analyzed samples (Appendix D).

Strontium isotope samples were analyzed at The University of Texas at Austin in the laboratory of Dr. Jay Banner. Each sample was evaporated and then redissolved in 3N  $\text{HNO}_3$ . This solution was passed through a Sr-spec resin column to selectively sequester dissolved  $\text{Sr}^{2+}$ .  $\text{Sr}^{2+}$  was eluted from the column using 0.1N  $\text{HNO}_3$ . The eluted solution was evaporated, redissolved in 0.01N phosphoric acid, and dispensed onto a tantalum filament. The filament was placed into a Finnigan MAT 261 thermal ionization mass spectrometer. The heated and ionized sample was analyzed in dynamic collection mode. Analyses of the NBS 987 standard (mean=0.710265, n=10) ensured that results were precise. External precision for analyses was estimated to be  $\pm 0.000015$  or better, and a replicate analysis fell within this range of precision. A blank analysis of water dispensed in the laboratory contained less than 10 picograms of Sr, and a blank analysis of water dispensed at the sampling site (and treated as a normal sample) contained about

150 picograms of Sr. These low background concentrations of Sr, which were measured using isotope dilution, are more than three orders of magnitude smaller than the lowest Sr<sup>2+</sup> concentrations measured in water samples (see also Appendix D). All strontium samples except for two were analyzed within 13 months of collection, and the majority were analyzed within five months. Strontium isotope ratios are reported as the ratio of <sup>87</sup>Sr to <sup>86</sup>Sr (<sup>87</sup>Sr/<sup>86</sup>Sr).

Oxygen isotope samples were analyzed at The University of Texas at Austin in the laboratory of Dr. Libby Stern. Samples were dispensed into glass vials filled with carbon dioxide gas, and were allowed to equilibrate with this gas for 8 hours at 40°C. The carbon dioxide gas was fed into a light isotope mass spectrometer alternately with a reference gas of known isotopic composition (Epstein and Mayeda, 1953). Approximately one third of analyzed samples were internal lab standards, and external precision was estimated to be ± 0.1‰ or better. The majority of oxygen isotope samples were analyzed within 5 months of collection.

Hydrogen isotope samples were analyzed at Southern Methodist University. Samples were passed over depleted uranium metal at 800°C (Bigeleisen et al., 1952), which reduced the hydrogen in the water molecule to H<sub>2</sub> gas. The H<sub>2</sub> gas was collected onto activated carbon, and then analyzed by mass spectrometer. Internal laboratory standards were analyzed frequently, but not reported by the lab. The lab reports that standard and duplicate analyses define an analytical precision of ± 1.2‰

or better. Oxygen and hydrogen isotopes are reported using delta notation (Gonfiantini, 1981; Coplen, 1994), and are referenced to standard mean ocean water (SMOW).

#### **3.4.4. Real-time parameter monitoring**

Real-time water quality parameters were monitored by the USGS at spring MSP during the study. A Hydrolab was placed into a submerged solution-enlarged fracture through which the majority of spring MSP discharge flows. Specific conductance and discharge rate were measured and recorded every 15 minutes. Discharge rate was calculated by measuring the ground-water level in a nearby well. The water level in this well has been correlated to spring discharge using a stage-discharge relationship, with periodic discharge measurements made downstream of the spring using a current meter and standard USGS methods (Buchanan and Somers, 1969). Mean daily values were calculated from measured 15-minute values using established USGS methods.

Rainfall data were obtained from the City of Austin Flood Early Warning System, an electronically monitored network of rainfall gauges located throughout the study area. Rainfall is difficult to quantify with high precision and accuracy because of numerous biases introduced by measurement equipment (Groisman and Legates, 1994). However, this study used rainfall data only to identify the general

occurrence of rain, and not to quantify it rigorously. Thus, measurement biases were not considered to be significant.

### **3.5. RESULTS**

#### **3.5.1. Real-time parameter monitoring**

There were 497 mean daily values measured for site MSP from August 6, 2003 to December 23, 2003 and from June 20, 2004 to June 10, 2005. Specific conductance ranged from 520 to 680 microsiemens per centimeter ( $\mu\text{S}/\text{cm}$ ), and discharge ranged from 37 to 130  $\text{ft}^3/\text{s}$  (1.0 to 3.7  $\text{m}^3/\text{s}$ ; Figure 3-3; Appendix E). The maximum discharge rate, recorded in March 2005, may have been underestimated because of changes in the behavior of the stage-discharge relationship at very high discharge rates (Asquith and Gary, 2005).

There was a major rainfall event in June 2004, October 2004, and November 2004 (Figure 3-3). The maximum daily rainfall amount during the study period (about 5 inches, or 120 mm) was measured on November 21, 2004. This rainfall event produced major flooding in the Austin area, and probably substantially altered the geochemistry of the spring samples collected on November 24, 2004.

### 3.5.2. Major dissolved ions

There were 25 sampling events for each of the four springs in the Barton Springs system (Figure 3-3). Generally, major ion analyses were performed on all 25 sets of samples. Major ion analyses were not carried out in September and early October 2004 for springs ESP, OSP, and USP (Table 3-1).

Some analytical results were excluded, or should be interpreted with care. Because of an apparent sample or analysis error, the major ion sample from well SVN sampled in 2005 was excluded from the dataset. In this sample, ion concentrations were approximately half of what the long-term record suggested as a normal analysis for this well, despite the pH and specific conductance values appearing to be correct (V.A. Chavez, U.S. Geological Survey, 2005, personal comm.). On the basis of rainfall data, it was determined that a sample from site USP on October 23, 2004 was affected by intense rainfall 14 hours earlier, and was excluded from this baseline dataset. This late October 2004 storm event is considered separately in Chapter 4. Finally, dissolved ion concentrations from all four springs on November 24, 2004 showed considerable departure from all other measurements during the study period, and were probably affected by flooding associated with an extremely large rainfall event. Because they do not reflect baseline conditions as the other samples in this study, samples from this day are generally excluded from analysis.

Summary statistics for the eight analyzed ions are presented in tabular format (Table 3-2) and graphical format (Figure 3-4). Full results are presented in Appendix B (Table B-2). With one exception, the ranges of ion concentrations observed in springs MSP, ESP, and OSP were smaller than the ranges of values for wells (Figure 3-4). Spring USP had samples with lower concentrations than any wells for  $Mg^{2+}$ ,  $Na^+$ ,  $Cl^-$ , and  $Sr^{2+}$ . All four springs had samples with lower values for  $Mg^{2+}$  than observed in wells. Samples from springs generally contained about 500 mg/L total dissolved solids (TDS), measured as the sum of all ion concentrations.

The coefficient of variation was calculated for each ion for all wells considered together as a group, and for each spring individually (Table 3-3). The coefficient of variation ( $C_v$ ) is calculated as the standard deviation divided by the mean, and quantitatively reflects the variability in a set of numbers. Considered together as a group, water samples from wells had the highest  $C_v$ s for all major ions. Among the four springs, the largest  $C_v$ s were observed in samples from spring USP.

All samples except for one (well ALB) were calcium-bicarbonate ( $Ca-HCO_3$ ) or calcium-magnesium-bicarbonate ( $Ca-Mg-HCO_3$ ) facies (Figure 3-5). Samples from spring OSP plotted closer to  $Na^+$ ,  $K^+$ ,  $Cl^-$ , and  $SO_4^{2-}$  hydrochemical facies than samples from the other three springs. Samples from spring USP plotted closer to a pure  $Ca-HCO_3$  water than any other samples in the study. The sample from well ALB was a sodium-chloride-sulfate ( $Na-Cl-SO_4$ ) water, and the total dissolved solids

concentration was about three times greater than that of any other sample in the study.

### 3.5.3. Strontium, oxygen, and hydrogen isotopes

$^{87}\text{Sr}/^{86}\text{Sr}$  ratios were measured for 45 water samples from wells and springs (Table 3-1; Table B-2). The range of  $^{87}\text{Sr}/^{86}\text{Sr}$  values in the study area was from 0.7076 to 0.7084. The lowest value was measured in well FOW water, a well whose water is known to mix with water from the Trinity aquifer (see Chapter 2). The highest value was measured in well SVS.

Mean values of  $^{87}\text{Sr}/^{86}\text{Sr}$  for the Barton Springs system were 0.70796 (n=13) at spring MSP, 0.70795 (n=7) at spring ESP, 0.70802 (n=7) at spring OSP, and 0.70812 (n=12) at spring USP. At each spring, all measured values were within analytical uncertainty of each other; that is, there was no measurable temporal variability in  $^{87}\text{Sr}/^{86}\text{Sr}$  values at any spring.  $^{87}\text{Sr}/^{86}\text{Sr}$  values from springs MSP and ESP were within analytical uncertainty of each other (i.e., neither spatial nor temporal  $^{87}\text{Sr}/^{86}\text{Sr}$  variation between springs MSP and ESP).  $^{87}\text{Sr}/^{86}\text{Sr}$  ratios from spring OSP samples were more radiogenic than, and did not overlap, samples from MSP and ESP.  $^{87}\text{Sr}/^{86}\text{Sr}$  ratios in samples from spring USP were more radiogenic than those from the other three springs, and never overlapped with samples from the other springs (Figure 3-14a and Table 3-2; considered later in the study).

Results of oxygen and hydrogen isotope analyses were plotted against one another (Figure 3-11) to evaluate their position relative to the global meteoric water line (GMWL) (Craig, 1961). Deviations to the right of this line can indicate evaporation, water mixing, (Clark and Fritz, 1997, p. 36) or water-rock interaction (Faure, 1986, p. 450). Generally, samples should not plot to the left the GMWL as some this study's samples do. These samples probably do in fact, plot on the GMWL, and their apparent deviation from the GMWL probably is related to analytical uncertainty and a small number of samples. There were samples with only oxygen isotope analyses or hydrogen isotope analyses (Table B-2). While these could not be plotted to evaluate their position relative to the GMWL, their values are comparable to those of samples that were plotted against the GMWL.

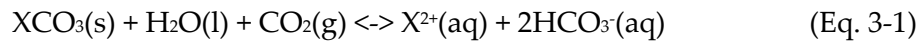
### **3.6. DISCUSSION**

#### **3.6.1. Major ion geochemistry**

The major ion geochemistry of ground water reflects the initial geochemistry of the recharging surface water, over which is imprinted the interaction of the water with the rock through which it flows (Kehew, 2001, p. 9). In karst aquifers, meteoric water enters the aquifer and partially dissolves the carbonate rock matrix (typically calcite,  $\text{CaCO}_3$ ), releasing  $\text{Ca}^{2+}$  and  $\text{HCO}_3^-$  ions into solution until an equilibrium concentration is reached or the water exits the aquifer. Incongruent dissolution of

metastable mineral phases (e.g., aragonite and high-magnesium calcite) can also contribute quantities of  $Mg^{2+}$  and  $Sr^{2+}$  into solution. Because of the overwhelming preponderance of carbonate minerals in the rock, karst ground water is generally expected to be Ca- $HCO_3$  or Ca-Mg- $HCO_3$ . This is the case for all water samples in the Barton Springs segment (Figure 3-5), except for the sample from well ALB, which is located in the saline zone.

In theory, dissolution of calcite and other carbonate minerals proceeds according to the equation:



where X is a group II metal such as Ca, Mg, or Sr. This equation is an oversimplification of the actual dissolution processes—carbonate minerals are rarely pure, and this equation ignores the speciation of  $HCO_3^-$  into  $CO_3^{2-}$  and  $H_2CO_3$  (although this effect is negligible at the pH values of Barton Springs segment ground water). In spite of its oversimplification, this conceptual equation demonstrates that in a system composed of nothing but dissolving carbonate minerals, one mole of dissolved  $Ca^{2+}$ ,  $Mg^{2+}$ , and  $Sr^{2+}$  is produced for every two moles of dissolved  $HCO_3^-$ , a 1:2 ratio. Thus, if the sum of  $Ca^{2+}$ ,  $Mg^{2+}$ , and  $Sr^{2+}$  are plotted against  $HCO_3^-$ , water samples from a pure carbonate aquifer will fall on a line with a slope of 1:2 (Figure 3-6a).

Barton Springs segment waters plot close to, but decidedly above the line that represents the 1:2 slope of pure carbonate dissolution. This suggests a source of “excess” divalent cations ( $\text{Ca}^{2+}$ ,  $\text{Mg}^{2+}$ , and  $\text{Sr}^{2+}$ ) or a process that reduces aqueous  $\text{HCO}_3^-$  concentrations. Two likely sources of excess divalent cations are the evaporite minerals gypsum ( $\text{CaSO}_4 \cdot 2\text{H}_2\text{O}$ ) and anhydrite ( $\text{CaSO}_4$ ) (herein both referred to as gypsum). Using PHREEQC geochemical modeling software (Parkhurst and Appelo, 1999), a second line representing the addition of gypsum to the aquifer can be plotted (Figure 3-6a). This new line is closer to Barton Springs segment water samples, although gypsum dissolution adds dissolved  $\text{SO}_4^{2-}$ , a species which is not represented on Figure 3-6a. By subtracting  $\text{SO}_4^{2-}$  concentration from the total divalent cation concentration, gypsum dissolution no longer affects the graph (Figure 3-6b). Because Barton Springs segment water samples plot closer to the theoretical 1:2 line on Figure 3-6b, this suggests that gypsum may be present and actively dissolving in the aquifer.

The chemical behavior of gypsum in karst ground water is virtually indistinguishable from the chemical behavior of pyrite ( $\text{FeS}_2$ ) (P.C. Bennett, University of Texas, written comm., 2005). Thus, Figure 3-6b may also suggest the presence of pyrite in the aquifer. Both gypsum and pyrite are known to occur in the aquifer rocks (Deike, 1987; Maclay, 1995), and gypsum has been found to be a

significant source of dissolved ions in other karst aquifers (Jacobson and Wasserburg, 2005).

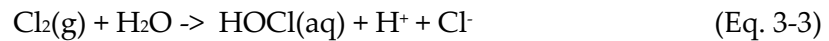
Examination of the other major dissolved ions reveals small but geochemically significant quantities of Na<sup>+</sup> and Cl<sup>-</sup>. These ions can be derived from limestone, in which there are occasional crystals of halite (NaCl) associated with intense evaporation of seawater during deposition. Theoretically, halite dissolution proceeds according to the equation:



which indicates that the Na/Cl molar ratio should equal 1 for a water sample that has dissolved halite. However, all spring samples except for three have Na/Cl values less than 1, and the majority of well water samples also have Na/Cl values less than 1 (Figure 3-7). This suggests that there is a non-halite source for these ions, or that some process adds Cl<sup>-</sup> ions and/or removes Na<sup>+</sup> ions from solution. Furthermore, the Na/Cl ratio does not change appreciably as specific conductance of water samples changes (Figure 3-7), indicating that the Na<sup>+</sup> and Cl<sup>-</sup> sources and/or processes do not change as total dissolved solids vary.

One possible source for Cl<sup>-</sup> may be urban infrastructure (St. Clair, 1979; City of Austin, 1997; Sharp and Banner, 1997; Christian, in preparation) such as leaking sewer pipes, septic tank drain fields, and leaking municipal water supply pipes. For

example, Austin municipal water is treated with chlorine gas, which eventually converts to reduced Cl<sup>-</sup> according to the equation (Droste, 1997):



Further progression of this reaction leads to the breakdown of the HOCl molecule, leading to a further increase in Cl<sup>-</sup> concentration. The net result of this reaction is a reduction in pH and an addition of Cl<sup>-</sup> ions. This reduction in pH can then be offset and masked by the increased dissolution of carbonate minerals that it promotes.

Another explanation for Na/Cl values less than one is ion exchange reactions, in which Na<sup>+</sup> ions are exchanged for divalent cations such as Ca<sup>2+</sup> (e.g., Land and Prezbindowski, 1981). This is commonly associated with clay minerals, which are known to be present in the Barton Springs segment (Mahler et al., 1999). Ion exchange reactions appear to play a role in the geochemistry of other karst aquifers as well, such as the Madison aquifer of South Dakota (Jacobson and Wasserburg, 2005).

Nitrate (NO<sub>3</sub><sup>-</sup>) can be an indicator of anthropogenic contamination, and has been measured in the Barton Springs segment for over 25 years (Chapter 2). The highest concentrations in springs during this study (up to 3 mg/L measured as nitrogen) are found at spring USP. According to dye-trace studies (Hauwert et al., 2005), this spring resides within an isolated subbasin of the Barton Springs segment, and its discharge is derived from a highly urbanized area of the recharge zone.

However, Cl<sup>-</sup> concentrations are another indicator of anthropogenic contamination, and are not unusually high in spring USP. This suggests that there is a source of NO<sub>3</sub><sup>-</sup> that is not high in Cl<sup>-</sup> (e.g., probably not leaking sewer lines). One possible source of elevated NO<sub>3</sub><sup>-</sup> is landscaping fertilizer, the application of which is known to occur throughout the study area (City of Austin, 1997).

Well ALB (Figure 3-1) is located in the saline zone and its water has a hydrochemical facies of Na-Cl-SO<sub>4</sub> (Figure 3-5). This is consistent with the previously-defined hydrochemical facies for the saline zone (Sharp and Clement, 1988), and verifies that the saline zone is indeed a potential source of Na<sup>+</sup>, Cl<sup>-</sup>, and SO<sub>4</sub><sup>2-</sup> ions. These same ions increase in concentration at springs MSP, ESP, and OSP during low discharge rates, suggesting that these springs discharge some water from the saline zone. Hauwert et al. (2005) estimated a maximum saline zone contribution to spring discharge of 3 percent, and Senger (1983) estimated a maximum of 10 percent. The low permeability of the saline zone (Maclay and Land, 1988) suggests that movement of ground water into or out of the saline zone is slow, and will probably never be more than a minor contributor to spring discharge. Spring USP does not have elevated Na<sup>+</sup>, Cl<sup>-</sup>, and SO<sub>4</sub><sup>2-</sup> concentrations, which is consistent with the hypothesis that it receives ground water from an isolated aquifer subbasin that has no contact with the saline zone.

### 3.6.2. Residence time and geochemical variability

For all four springs, the ion with the highest  $C_v$  is  $\text{Sr}^{2+}$ , followed by  $\text{NO}_3^-$  (Table 3-3). This is different than in other karst aquifers, where  $\text{Ca}^{2+}$  and  $\text{HCO}_3^-$  are the ions with the most variable concentrations (Shuster and White, 1971; Dreiss, 1989; Panno et al., 1996). This suggests that, unlike many karst aquifers, overall geochemical variability in Barton Springs system discharge is not dominantly controlled by calcite and dolomite equilibrium. In fact, saturation indices for springs water can be calculated using PHREEQC (Parkhurst and Appelo, 1999), and show that water from springs MSP, ESP, and OSP is nearly saturated with respect to calcite (mean  $\log SI_{\text{calcite}} = -0.13$  for each of MSP, ESP, and OSP), and water from spring USP is only slightly undersaturated with respect to calcite ( $\log SI_{\text{calcite}} = -0.21$ ). In light of this calculation, it is not surprising that ions with the two lowest  $C_v$ s are  $\text{Ca}^{2+}$  and  $\text{HCO}_3^-$  for all springs except spring OSP where the  $C_v$ s for  $\text{Ca}^{2+}$  and  $\text{SO}_4^{2-}$  are lowest (note also Figure 3-4 ranges of  $\text{Ca}^{2+}$  and  $\text{HCO}_3^-$ ).

$\text{Sr}^{2+}$  is the ion with the highest  $C_v$  in all four springs (Table 3-3). Knowing that spring waters are close to saturation with respect to calcite, this suggests that incongruent dissolution is a dominant geochemical process in the Barton Springs segment. In incongruent dissolution, a recharging water that is undersaturated with respect to calcite ( $\text{CaCO}_3$ ) will rapidly dissolve calcite and undergo an increase in  $\text{Ca}^{2+}$  concentration until calcite saturation is reached (Palmer, 1991). Subsequently,

incongruent dissolution of metastable minerals such as high-magnesium calcite and dolomite ( $\text{CaMg}(\text{CO}_3)_2$ ) will result in increased  $\text{Mg}^{2+}$  concentrations, while  $\text{Ca}^{2+}$  concentrations remain essentially constant owing to the simultaneous co-precipitation of more stable minerals such as low-magnesium calcite (James and Choquette, 1984). This behavior has been observed in the Lincolnshire Limestone of England (Edmunds and Walton, 1983), as well as cave dripwaters in the Edwards aquifer (Musgrove and Banner, 2004). Maclay (1995) reported that dedolomitization, a process similar to incongruent dissolution, is active in the present-day phreatic zone of the Edwards aquifer.

The chemical kinetics of incongruent dissolution suggest that  $\text{Sr}^{2+}$  and  $\text{Mg}^{2+}$  concentrations can be used as indicators of ground-water residence time (Musgrove and Banner, 2004). In order to compensate for variable amounts of calcite dissolution,  $\text{Mg}^{2+}$  and  $\text{Sr}^{2+}$  are normalized to  $\text{Ca}^{2+}$ , and we hypothesize that  $\text{Mg}/\text{Ca}$  and  $\text{Sr}/\text{Ca}$  ratios will be indicators of residence time. Residence time is usually not a directly measurable quantity, but we can use the discharge rate from the Barton Springs system (Figure 3-3) as a proxy for residence time. This is probably a valid proxy, as higher discharge rates are associated with higher ground-water levels (Senger, 1983) and faster ground-water flow velocities (Hauwert et al., 2005). Figure 3-8 visually suggests that there is a correlation between Barton Springs discharge and  $\text{Sr}/\text{Ca}$  ratios.

On the basis of a strong linear correlation with spring discharge rates, Mg/Ca and Sr/Ca are effective indicators of residence time for springs MSP, ESP, and OSP (Figure 3-9). The mean  $r^2$  correlation coefficient for Mg/Ca for these three springs is 0.51, and for Sr/Ca is 0.74. This suggests that Sr/Ca is a better indicator of residence time in the Barton Springs segment than Mg/Ca. Note that samples from November 24, 2004 were omitted from these correlation calculations, as these samples were taken during record floods and represent unusual aquifer conditions. Inclusion of these data reduces the correlation coefficients a small amount.

Mg/Ca and Sr/Ca at spring USP do not strongly correlate with Barton Spring system discharge. One possibility is that incongruent dissolution is not a prominent process in the isolated subbasin (Hauwert et al., 2005) that supplies water to springs USP. This basin is small and has shorter residence time than the majority of the Barton Springs segment. Furthermore, shorter residence times suggest that a larger volume of meteoric water has flowed through this subbasin, and that meteoric diagenesis may have already dissolved many of the metastable minerals that bear  $Mg^{2+}$  and  $Sr^{2+}$ . Another possibility for a poor correlation between spring discharge and spring USP Sr/Ca is that spring USP residence time is incorrectly measured by Barton Springs system discharge. Barton Springs system discharge is a measurement of the combined discharge of MSP, ESP, and OSP, and does not

include spring USP (Asquith and Gary, 2005). For example, on December 23, 2003, spring USP was not flowing, while the other three springs were.

Values of Mg/Ca and Sr/Ca from the Barton Springs system are consistent with Mg/Ca and Sr/Ca values reported from cave dripwaters by Musgrove and Banner (2004). While their dripwater sites are not located within the Barton Springs segment, they are in analogous geologic formations and are located within 100 km of the Barton Springs segment. Spring discharge samples (i.e. Barton Springs system samples from this study) have higher average residence times than cave dripwater samples, as dripwaters represent rainfall that has only recently infiltrated through the vadose zone (Figure 3-10).

Concentrations of  $\text{Cl}^-$  and  $\text{Na}^+$  (non-carbonate ions) change in response to discharge rates, much in the same way that  $\text{Mg}^{2+}$  and  $\text{Sr}^{2+}$  change. After  $\text{Sr}^{2+}$  and  $\text{NO}_3^-$ , the ions with the highest  $C_v$  values are  $\text{Cl}^-$  at springs MSP and ESP,  $\text{Na}^+$  at spring OSP, and  $\text{K}^+$  at spring USP (Table 3-3). Elevated levels of  $\text{Na}^+$  and  $\text{Cl}^-$  correspond to periods of low spring discharge at springs MSP, ESP, and OSP (Senger and Kreitler, 1984). This suggests that  $\text{Na}^+$  and  $\text{Cl}^-$  might be indicators of residence time much in the same way as  $\text{Mg}^{2+}$  and  $\text{Sr}^{2+}$ . While this may be true from a statistical point of view, the underlying geochemical explanation probably is not residence time, as  $\text{Na}^+$  and  $\text{Cl}^-$  are associated with very soluble minerals (e.g., halite) that do not undergo incongruent dissolution. Several studies have proposed that the

saline zone on the eastern boundary of the Barton Springs segment is a source of  $\text{Na}^+$ ,  $\text{Cl}^-$ , and  $\text{SO}_4^{2-}$  (Senger and Kreitler, 1984; Slade et al., 1986; City of Austin, 1997), or alternatively that the underlying Trinity aquifer is a source (City of Austin, 1997). Potentiometric surface maps during low ground-water levels indicate that gradients favor movement of ground water from the saline zone into the freshwater zone, while potentiometric surface maps from periods of high ground-water levels indicate little ground water movement out of the saline zone (Slade et al., 1986). Dye trace studies also propose a major aquifer flowpath along the boundary of the freshwater and saline zones (Hauwert et al., 2005).

The high  $C_v$  value for  $\text{K}^+$  at spring USP (Table 3-3) is associated with high aquifer flow levels—the highest  $\text{K}^+$  concentration measured in this study was at spring USP on November 24, 2004, during record floods in the study area.  $\text{K}^+$  is generally not associated with dissolution of limestone rock, and its source may be external to the aquifer. High  $\text{K}^+$  levels have been measured in Williamson Creek (Christian, in preparation), and dye trace studies have shown that Williamson Creek contributes water to spring USP (Hauwert et al., 2005). This suggests that during periods of high ground-water levels and high streamflow rates on Williamson Creek, spring USP may contain a high percentage of recently-recharged surface water from Williamson Creek (see also Chapter 4 and section 3.6.4).

### 3.6.3. Well-mixed ground water during baseflow

Samples with both  $\delta^{18}\text{O}$  and  $\delta^2\text{H}$  values can be plotted against the global meteoric water line (Craig, 1961) to investigate water mixing and evaporation (Figure 3-11) (e.g., Darling and Bath, 1988; Lakey and Krothe, 1996). Studies in other karst aquifers have shown that oxygen and hydrogen isotopes in ground water may show long-term, attenuated, time-delayed variability reflecting seasonal variations in rainfall distribution and/or its isotopic ratios (e.g., Vallejos et al., 1997; Cane and Clark, 1999; Jones and Banner, 2000; Maloszewski et al., 2002). There is no evidence for this behavior in the Barton Springs segment, although the number of samples with both  $\delta^{18}\text{O}$  and  $\delta^2\text{H}$  analyses is small.

$\delta^{18}\text{O}$  and  $\delta^2\text{H}$  values from the Barton Springs segment are similar to long-term mean rainfall isotopic values reported for central Texas (International Atomic Energy Agency, 2005). This suggests that recharge water that enters the Barton Springs segment becomes well-mixed and homogenized, similar to findings in other karst aquifers (e.g., Jones and Banner, 2000). Mixing and homogenization of karst ground-water may be explained by the aquifer conceptual model presented in Chapter 4 (Figure 4-7). This model suggests that ground water flowing through karst conduits can be forced into the diffuse (or matrix) portion of the aquifer under some conditions. This forcing of ground water through the small intergranular pore

spaces may explain the well-mixed ground waters observed in the Barton Springs segment.

It is also possible that Barton Springs segment ground water is not spatially homogeneous, and that spring discharge is a combination of isotopically distinct waters (e.g., Greene, 1997) that mix in some proportion. Two potential recharge sources that can have different isotopic ratios are discrete recharge features in streambeds, and diffuse recharge that has passed through the soil zone. However, water from soil zones presumably would show evidence of evaporation (e.g., Herczeg et al., 1997; Vallejos et al., 1997), which would be detectable as a deviation to the right of the GMWL. As such a deviation is not observed in Barton Springs segment data, this suggests that evaporation effects are minor in the Barton Springs segment, similar to some other karst aquifers (e.g., Jones and Banner, 2000). However, evidence for evaporation (i.e., significant deviation to the right of the GMWL) is observed in the San Antonio segment of the Edwards aquifer to the south (Fahlquist and Ardis, 2004), suggesting that it may occur in the Barton Springs segment as well.

#### **3.6.4. Geochemical evolution of spring water**

To better understand the systematics of Sr isotopes in the Barton Springs segment,  $^{87}\text{Sr}/^{86}\text{Sr}$  ratios are compared to the Sr/Ca residence time indicator (Figure

3-12a). Major ions, in combination with isotopes of strontium ( $^{87}\text{Sr}/^{86}\text{Sr}$ ), are a powerful tool to gain insights into ground-water flow and evolution (McNutt, 2000; Banner, 2004). As ground water flows through an aquifer, it progressively takes on the Sr isotopic composition of the aquifer rock. For example, in the Madison Limestone aquifer of Wyoming, Frost and Toner (2004) found that recharge water entered the aquifer with an  $^{87}\text{Sr}/^{86}\text{Sr}$  value of 0.721, and acquired the Sr isotopic value of the limestone rock (0.709) after only seven days.

Strontium isotope ratios can be used to quantify mixing of waters with unique  $^{87}\text{Sr}/^{86}\text{Sr}$  values. In the Floridan aquifer,  $^{87}\text{Sr}/^{86}\text{Sr}$  variability in ground water is believed to be a result of mixing of ground waters from silicate aquifers with ground waters from carbonate aquifers (Katz et al., 1997). Musgrove and Banner (1993) found evidence of regional-scale mixing of North American mid-continent brines using Sr isotopes. Swarzenski et al. (2001) identified the source of a submarine spring in Florida as the nearby Floridan aquifer using Sr isotopes.

Ultimately, all ground water in an aquifer originates as rainfall. Rainfall has a distinctive geochemical and Sr isotopic signature (Musgrove and Banner, 2004), but the concentrations of  $\text{Sr}^{2+}$  in rainfall are so small that they are unlikely to influence the  $^{87}\text{Sr}/^{86}\text{Sr}$  ratios of karst ground-water (Banner, 2004). As an example, Frost and Toner (2004) measured a  $\text{Sr}^{2+}$  concentration of 0.04 mg/L for recharge water entering the Madison aquifer. After seven days in the aquifer, the  $\text{Sr}^{2+}$  concentration

increased to 0.3 mg/L, and the measured  $^{87}\text{Sr}/^{86}\text{Sr}$  value was comparable to the aquifer rock. In addition to carbonate minerals contributing  $\text{Sr}^{2+}$  to ground water, Jacobson and Wasserburg (2005) noted that Sr is abundant in gypsum deposits, which are known to occur in trace quantities in karst aquifers, including the Barton Springs segment (Deike, 1987).

In the Barton Springs segment, there are numerous potential sources of strontium (Figure 3-13). Musgrove and Banner (2004) reported that  $^{87}\text{Sr}/^{86}\text{Sr}$  ratios in central Texas cave dripwaters are affected by carbonate rock, overlying soils, and trace amounts of clay minerals present in some of the more argillaceous limestone units. Generally, in a karst aquifer the limestone bedrock is expected to be the dominant “first-order” control of the Sr isotopic composition due to its large volume and Sr concentration (Banner, 2004). Other sources of Sr in the study area include saline zone ground water, Trinity aquifer ground water, argillaceous bedrock that has radiogenic  $^{87}\text{Sr}/^{86}\text{Sr}$  values, and anthropogenic sources (Oetting, 1995; Musgrove, 2000; Christian, in preparation). However, most of these sources (excluding possibly soils) are expected to be minor sources of Sr relative to the large amount of Sr available for dissolution in the Edwards and Georgetown Limestones. Soils are potentially a significant source of Sr in the central Texas, and values of  $^{87}\text{Sr}/^{86}\text{Sr}$  derived from these soils have been shown to be significantly higher than those of

Cretaceous carbonate rock (Figure 3-13) (Cooke et al., 2003; Cooke, 2005; Christian, in preparation).

Throughout the Barton Springs segment, there is a wide range of residence times, while there is only a moderate range of  $^{87}\text{Sr}/^{86}\text{Sr}$  values (0.7076 to 0.7084). Compared to ground water from wells in the aquifer, water discharging from the Barton Springs system has a narrow range of residence times and Sr isotopic values (0.7079 to 0.7081; Figure 3-12b). An initial hypothesis might be that Barton Springs system discharge is a weighted average (i.e., a mixture) of ground waters of varying residence times and Sr isotopic compositions, which is consistent with the concept of karst aquifers as heterogeneous, double-porosity systems (Sharp, 1993).

Although  $^{87}\text{Sr}/^{86}\text{Sr}$  values are within analytical uncertainty at each individual spring, there is *apparent* variability within this analytical uncertainty (Figure 3-12b). Under the assumption that this variability (i.e., a hyperbolic shape for springs MSP, ESP, and OSP) is not an artifact of analytical methods, the general trend of this variability can be somewhat accounted for by progressively mixing water from spring USP with water from well BPS. (Figure 3-12b). Well BPS has been shown to have very little geochemical variability in its long term record (Chapter 2), suggesting that its water represents a high-residence time, highly evolved water from the freshwater zone of the Barton Springs segment. Spring USP apparently has small residence time, and its radiogenic  $^{87}\text{Sr}/^{86}\text{Sr}$  values may reflect surface water or

soil processes (see next section, 3.6.5). The fluid mixing line on Figure 3-12 is approximately the same as a water evolution line, if it is assumed that the selected endmember waters (spring USP and well BPS) represent the geochemical composition of one single source of  $\text{Sr}^{2+}$  and  $\text{Ca}^{2+}$ . Deviation from this line, seen in samples from springs MSP, ESP, and OSP, might be the result of spatial and temporal variability of the fully-evolved water sample represented by well BPS, or additional endmembers that are mixing or reacting with ground water.

Mixing between spring USP and well BPS endmembers cannot fully account observed geochemical variability (Figure 3-13b), but that is probably because there are multiple sources of Sr that affect concentrations and isotopic composition in the Barton Springs segment. In the following sections, several additional Sr sources are considered.

### **3.6.5. Urban infrastructure and Upper Barton Spring**

Christian (in preparation) suggests that higher  $^{87}\text{Sr}/^{86}\text{Sr}$  values of surface water in the study area are related to leaking urban infrastructure (water and sewage pipes), although soils are also a potential source. Austin municipal water (i.e., drinking water) is obtained from the Colorado River, a river whose watershed includes a large exposure of Precambrian basement rock (the Llano Uplift). Several minerals in this billion-year-old basement rock have high Rb/Sr ratios (e.g., mica,

potassium-feldspar) (Faure, 1986, p. 136), and water that reacts with these minerals will have radiogenic  $^{87}\text{Sr}/^{86}\text{Sr}$  values (Oetting, 1995; Christian, in preparation). Austin municipal water has  $^{87}\text{Sr}/^{86}\text{Sr}$  values that are more radiogenic than soil or carbonate rock in the study area (Figure 3-13). If leaking urban infrastructure causes this municipal water to recharge the Barton Springs segment, wells and springs with urban infrastructure in their catchment areas may have more radiogenic  $^{87}\text{Sr}/^{86}\text{Sr}$  values for their ground water. Another possibility is that overlying soils are the cause of the radiogenic  $^{87}\text{Sr}/^{86}\text{Sr}$  values in Austin-area surface water and ground water, although Christian (in preparation) considers this unlikely on the basis of an extensive investigation that included surface water major ion concentrations,  $^{87}\text{Sr}/^{86}\text{Sr}$  values obtained from trees along Austin creeks, and several other lines of evidence.

The Cold Springs ground-water basin is highly urbanized (St. Clair, 1979; Hauwert et al., 2005), and more radiogenic  $^{87}\text{Sr}/^{86}\text{Sr}$  ratios are observed in wells and springs that obtain ground water from this area (Figure 3-14). Wells FON, SVS, SVW, and SVN all reside within this subbasin, and contain the most radiogenic  $^{87}\text{Sr}/^{86}\text{Sr}$  values in this study (Figure 3-14). These radiogenic  $^{87}\text{Sr}/^{86}\text{Sr}$  values may result directly from leaking urban infrastructure recharging the aquifer, consistent with the hypothesis of Christian (in preparation). Alternatively, radiogenic Sr may also recharge the aquifer from Williamson Creek, which drains an urbanized watershed and has  $^{87}\text{Sr}/^{86}\text{Sr}$  values ranging from 0.7080 to 0.7087 (Christian, in

preparation). This would be consistent with the findings of dye-trace studies (Hauwert et al., 2005) that show water from Williamson Creek reaching well SVW and other Cold Springs subbasin wells within several days.

The Cold Springs subbasin and the associated Sunset Valley subbasin have been shown to supply a majority of the discharge for spring USP (Hauwert et al., 2005). Spring USP has the highest  $^{87}\text{Sr}/^{86}\text{Sr}$  values of the four springs, which is consistent with some of its water being derived from Williamson Creek or an urbanized area. This also is consistent with geochemical evidence presented elsewhere in this chapter (section 3.6.1).

### **3.6.6. Saline zone effect on Old Mill Spring**

On the basis of  $\text{SO}_4/\text{Cl}$  and  $\text{Sr}/\text{Ca}$  ratios alone, spring MSP water samples appear to be of intermediate composition between spring OSP and USP (Figure 3-15). However, spring MSP geochemical composition cannot be merely explained as a two-endmember mixture between springs USP and OSP, as  $^{87}\text{Sr}/^{86}\text{Sr}$  values for spring MSP samples are not intermediate between those of springs USP and OSP (Figure 3-14). This suggests that more than two endmembers contribute to the geochemical variability of spring MSP, or that spring USP geochemical composition is independent of the other three springs (see previous sections of this chapter).

On the basis of major ion concentrations, samples from spring OSP show evidence of mixing with the saline zone. Spring OSP samples have high Sr/Ca values (i.e., high residence time; Figure 3-15b), which is consistent with the slower and longer flowpath from which some of this spring's discharge derives (Hauwert et al., 2005). Spring OSP samples have low SO<sub>4</sub>/Cl ratios (i.e., elevated Cl<sup>-</sup> concentrations), and Cl<sup>-</sup> is a dominant ion in the saline zone (Sharp and Clement, 1988).

Mean values of <sup>87</sup>Sr/<sup>86</sup>Sr for spring OSP are 0.70802, which is intermediate between the measured saline zone values (0.70806, well ALB), and the mean value for spring MSP discharge (0.70796). This suggests that spring OSP discharges a mixture of water from the primary aquifer flowpath that leads to spring MSP (Hauwert et al., 2005), and from the saline zone. On the basis of a hypothetical mixing model between spring MSP and well ALB, about 4–9 percent of spring OSP discharge may be from the saline zone (Figure 3-16). This range of mixing percentages is comparable to those of Hauwert et al. (2005) (3 percent) and Senger (1983) (maximum of 10 percent). However, the Sr concentrations of spring OSP do not match the mixing model well (Figure 3-16). Furthermore, the saline zone endmember (well ALB) may not represent the geochemical composition of the saline zone accurately, as spatial and temporal geochemical variability exists within the saline zone (Hauwert and Vickers, 1994).

This is the first time that  $^{87}\text{Sr}/^{86}\text{Sr}$  has been measured over such a large space and time scale in the Barton Springs segment. The initial insights into ground-water flow that Sr isotopes provide are first steps toward a much larger picture. Future work, particularly on the origin of the radiogenic  $^{87}\text{Sr}/^{86}\text{Sr}$  values in spring USP and the Cold Springs subbasin, may lead to further insight into aquifer processes.

### 3.7. CONCLUSIONS

During the period of study, spring water in the Barton Springs segment was generally Ca-HCO<sub>3</sub> to Ca-Mg-HCO<sub>3</sub> facies, as predicted for karst aquifers. Unlike some karst systems, however, spring water in the Barton Springs segment generally was close to saturation with respect to calcite. Spring water samples showed evidence of variable residence time and incongruent dissolution, as indicated by increases in Sr/Ca during low spring discharge conditions. Sr/Ca ratios were an effective measure of water residence times for Main Barton, Eliza, and Old Mill Springs. Upper Barton Spring did not show residence time and incongruent dissolution effects as strongly as Main Barton, Eliza, and Old Mill springs.

There were dissolved ions not associated with carbonate minerals (i.e., Na<sup>+</sup>, Cl<sup>-</sup>, SO<sub>4</sub><sup>2-</sup>, and NO<sub>3</sub><sup>-</sup>) present in Barton Springs segment ground water. Na/Cl molar ratios less than 1 suggest a source of excess Cl<sup>-</sup> or a sink for Na<sup>+</sup>. Explanations include an anthropogenic source of Cl<sup>-</sup> and ion exchange with clays. Increases in

Na<sup>+</sup>, Cl<sup>-</sup>, and SO<sub>4</sub><sup>2-</sup> at Main Barton, Eliza, and Old Mill Springs were associated with low discharge rates, and probably represent influx of ground water from the saline zone. On the basis of a two-endmember mixing model, between 4 and 9 percent of the spring OSP discharged appears to have been derived from the saline zone.

Oxygen and hydrogen isotope values indicated that ground water in the aquifer mixes over year or longer time scales. The oxygen and hydrogen data in this study are somewhat sparse, however, and higher-resolution sampling might reveal the variations in isotopic composition observed in other karst aquifers.

<sup>87</sup>Sr/<sup>86</sup>Sr values and dissolved major ion concentrations at the Barton Springs system suggested that spring water was a mixture of different ground waters present in the aquifer. This is consistent with the behavior expected in double porosity systems such as karst aquifers. Apparently variability in <sup>87</sup>Sr/<sup>86</sup>Sr values at each individual spring suggested multiple sources of Sr in the study area, although the limestone aquifer rock is expected to be the dominant source for ground water with high residence time.

Springs MSP and ESP are geochemically indistinguishable from one another, suggesting that they receive ground water from the same aquifer flowpath(s). This is consistent with the findings of Chapter 4. However, this is inconsistent with the findings of Hauwert et al. (2005), who reported the detection of an injected dye-trace at Main Barton Spring but not Eliza Spring. They suggested that Main Barton Spring

obtains some of its water from the “Sunset Valley flow route,” and that this flow route does not reach Eliza Spring.

Samples from Upper Barton Spring and four wells (FON, SVS, SVW, and SVN) had the most radiogenic  $^{87}\text{Sr}/^{86}\text{Sr}$  values in this study. Also, high concentrations of  $\text{K}^+$  occurred at Upper Barton Spring during high aquifer discharge rates. This suggests that Williamson Creek, which also had high  $^{87}\text{Sr}/^{86}\text{Sr}$  values and  $\text{K}^+$  concentrations, contributed to Upper Barton Springs discharge. Elevated concentrations of  $\text{NO}_3^-$  in Upper Barton Spring suggest an anthropogenic source. Radiogenic  $^{87}\text{Sr}/^{86}\text{Sr}$  ratios may be associated with leaking urban infrastructure, the water of which is derived from the Colorado River and the Llano Uplift.

This study presents the most high-resolution geochemical dataset ever collected for the Barton Springs segment. Future research should benefit from the observations made by this study. Additional monitoring, especially high-resolution monitoring of wells, could help to better characterize the geochemical variability in the aquifer.

### **3.8. ACKNOWLEDGEMENTS**

Thanks are extended to the U.S. Geological Survey and the Texas Commission on Environmental Quality for staffing and funding the real-time and major ion data collection program used for this study. Funding for isotopic analyses

was provided by the Jackson School of Geosciences. Thanks are also extended to Jay Banner and Libby Stern for access to analytical facilities, and Larry Mack and Kurt Ferguson for assistance with isotope ratio analysis.

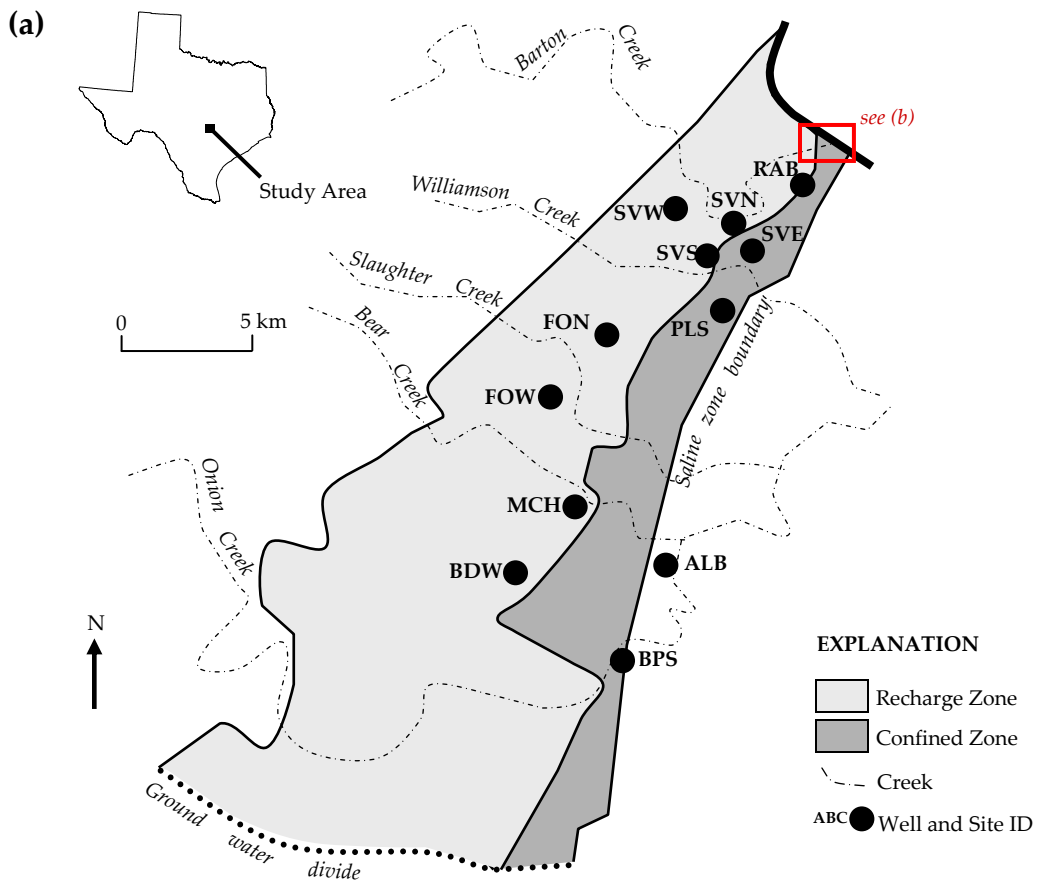


**Figure 3-1a.** Map of the Barton Springs segment of the Edwards Aquifer, showing wells sampled in 2004 and 2005.

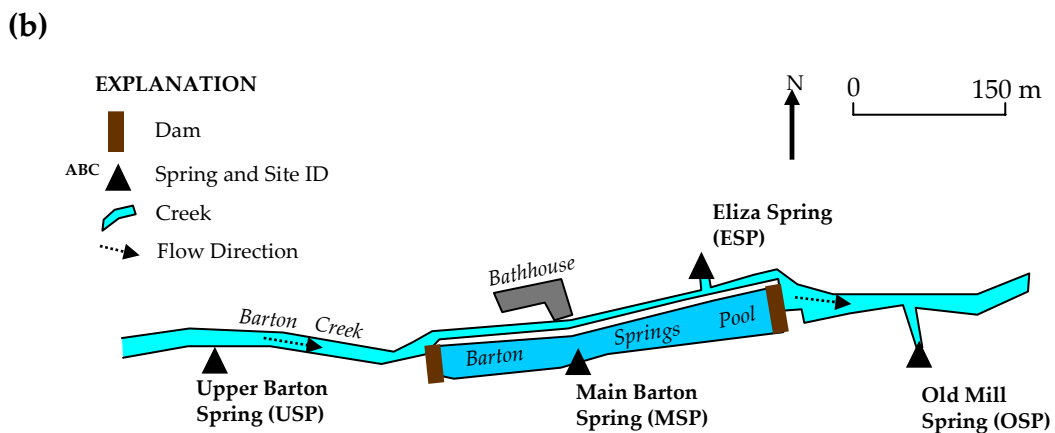


**Figure 3-1b.** Map of the Barton Springs system, and the four springs that were sampled from 2003–2005.

**Figure 3-2a.** Main Barton Spring (MSP). Samples were collected from a fissure near the pool diving board.

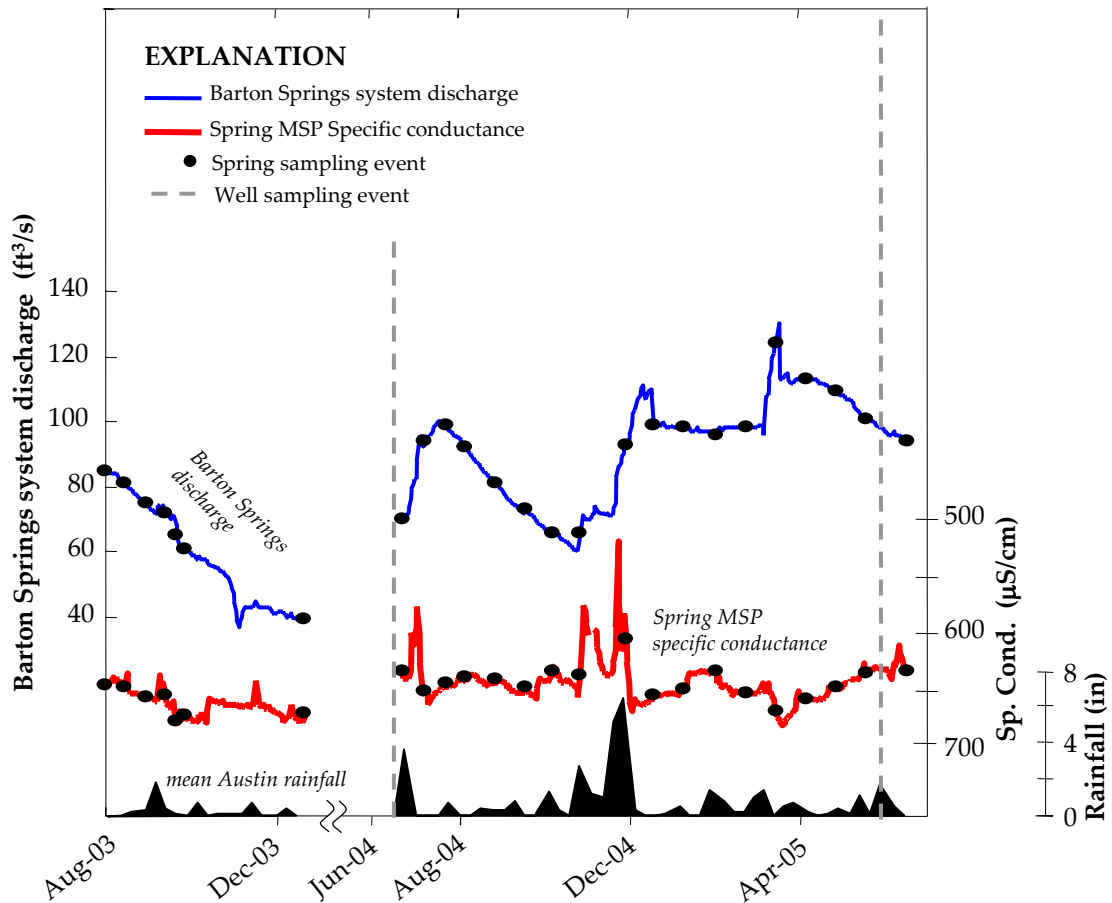
**Figure 3-2b.** Eliza Spring (ESP). Samples were collected from a constructed detention pool.

**Figure 3-2c.** Old Mill Spring (OSP). Samples were collected near the rock wall constructed to contain the spring discharge.

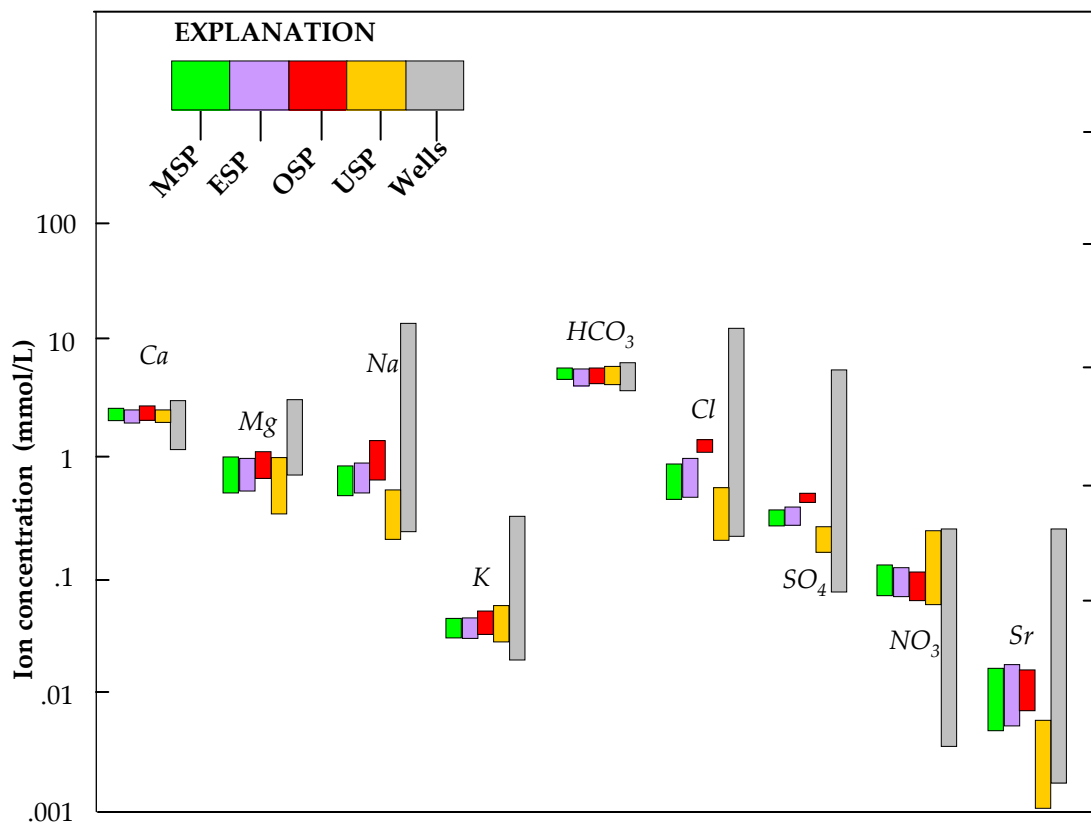
**Figure 3-2d.** Upper Barton Spring (USP). Samples were collected from a prominent orifice in Barton Creek streambed.

**Figure 3-2e.** Sampling point for well MCH, a typical configuration for most domestic well sampling points.

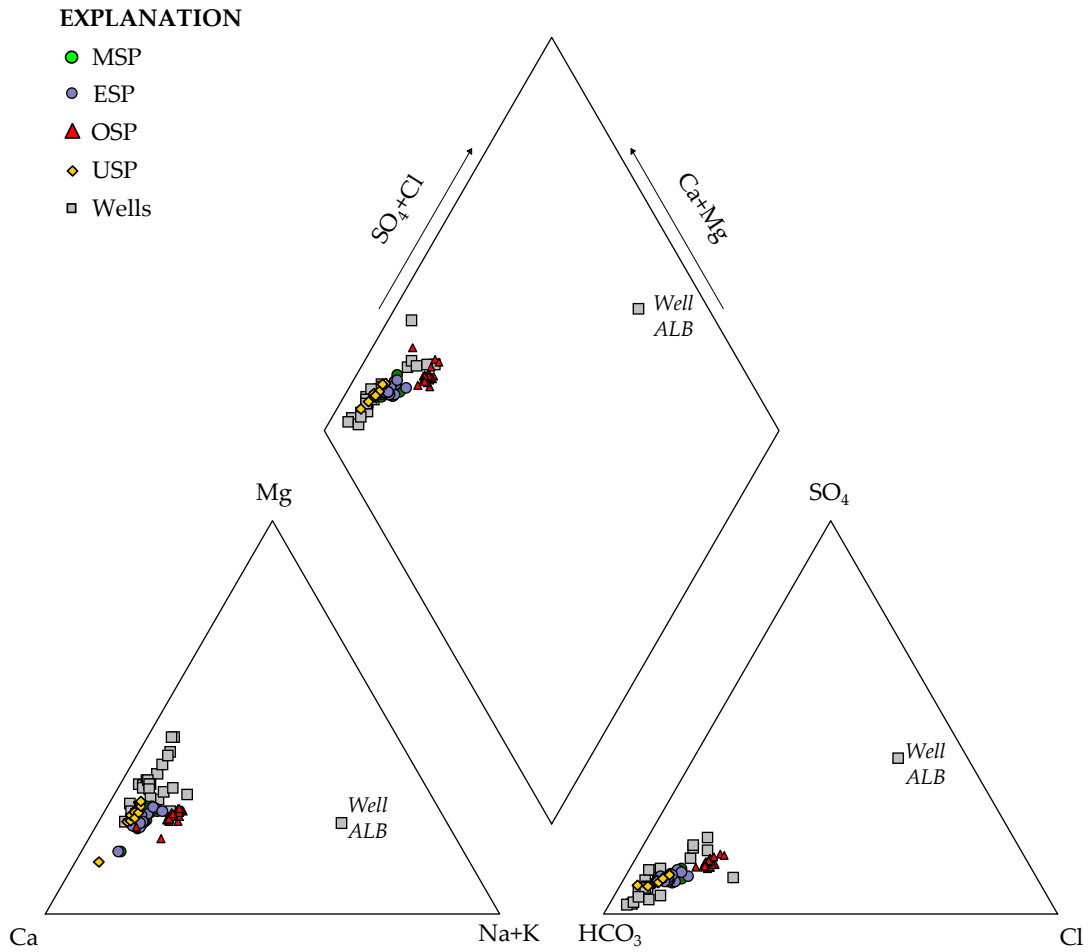




**Figure 3-3.** Time-series graph showing Barton Springs system discharge, spring MSP specific conductance, average area weekly rainfall, sampling events at the Barton Springs system, and sampling events at wells. Specific conductance is plotted with increasing values toward the bottom, in order to highlight its general correlation with spring discharge rates.



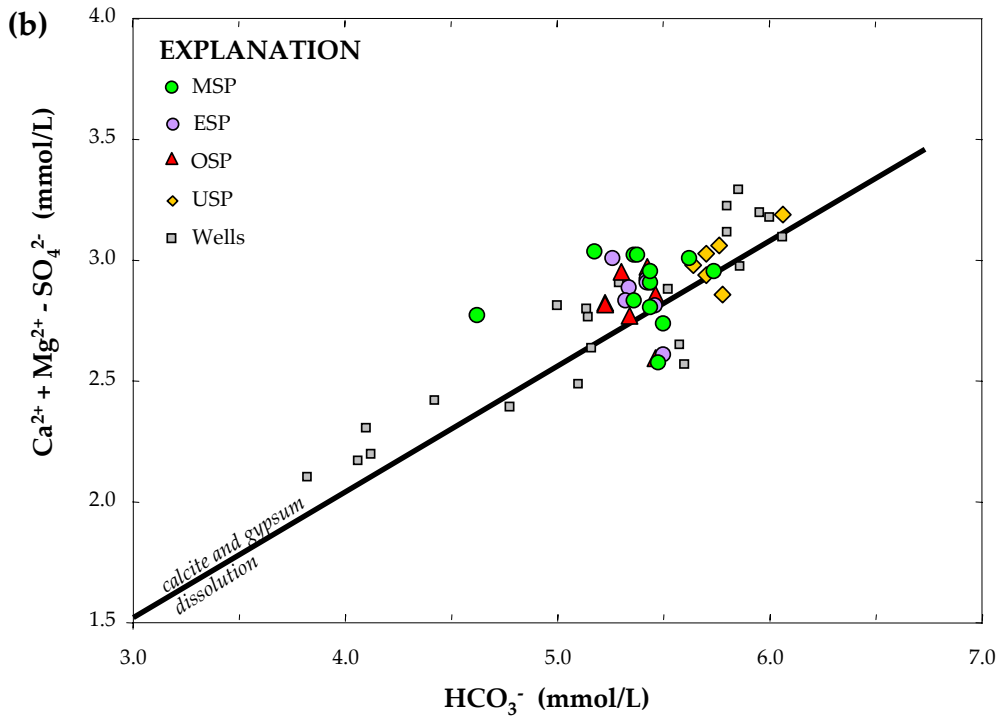
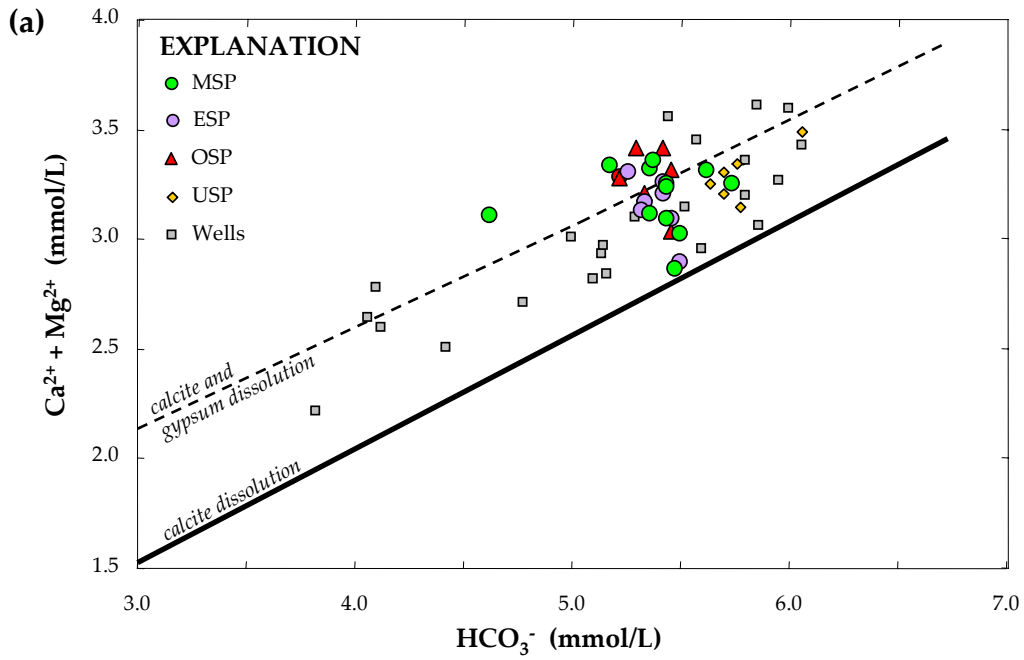
**Figure 3-4.** Ranges of ion concentrations for the Barton Springs segment, 2003–2005. There are no units for the abscissa, and ordinate has a logarithmic scale showing molar concentrations.



**Figure 3-5.** Piper diagram showing major ion water analyses from 2003–2005 from the Barton Springs segment. The one outlier point is well ALB, which receives some of its water from the saline zone (see text section 3.6.1).

**Figure 3-6a.** Comparison of water samples with the theoretical 1:2 calcite dissolution line, which samples would plot along if the only mineral they reacted with was calcite. When gypsum is added as a dissolving mineral (dashed line,  $\log SI_{\text{gypsum}} = -1.5$ ), the theoretical dissolution line shifts up and changes in slope. As all samples in the Barton Springs segment plot above the pure calcite line, this suggests that gypsum or a similar mineral may be present in the aquifer.

**Figure 3-6b.** By subtracting  $\text{SO}_4^{2-}$  from the ordinate, gypsum dissolution no longer distinguishes the two lines of figure (a). The two lines now overlap, and water samples plot closer to the theoretical calcite dissolution line, suggesting that gypsum and/or pyrite is actively dissolving in the aquifer.



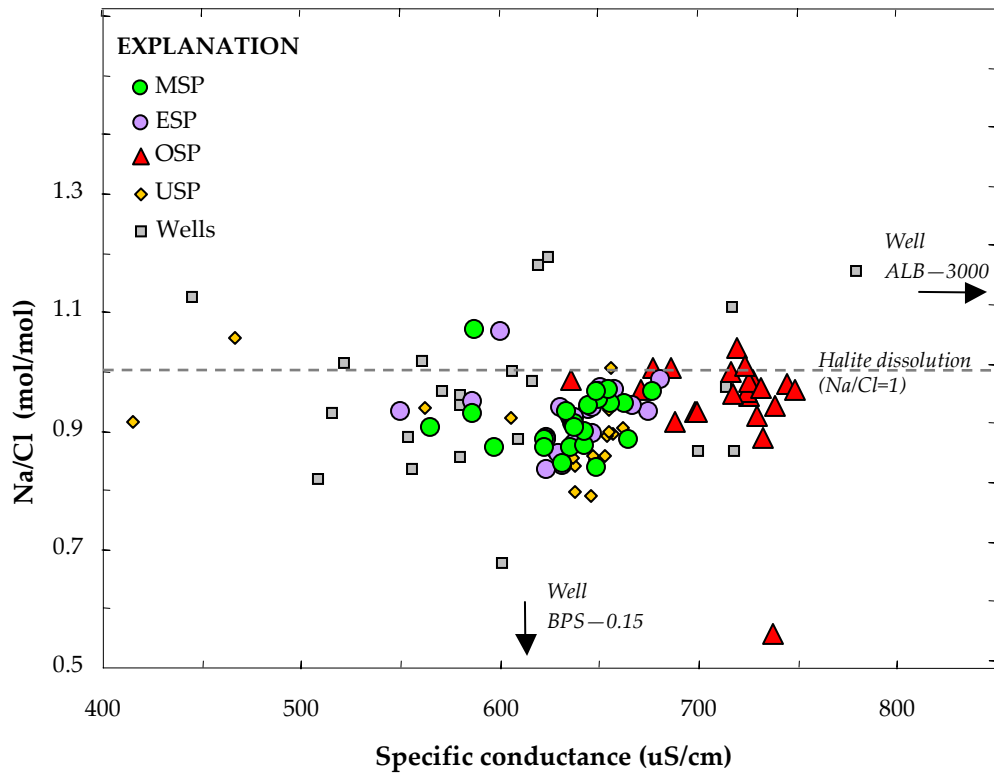


**Figure 3-7.** Na/Cl molar ratios are generally less than 1 in the Barton Springs segment, suggesting a source other than halite source (Na/Cl=1) for these ions. Na/Cl ratios do not vary systematically with specific conductance, suggesting that the source of these ions does not change as specific conductance changes. Well ALB is off-scale with a specific conductance of 3000  $\mu\text{S}/\text{cm}$  and Na/Cl of 1.17, and well BPS is off-scale with a specific conductance of 610  $\mu\text{S}/\text{cm}$  and Na/Cl of 0.15.

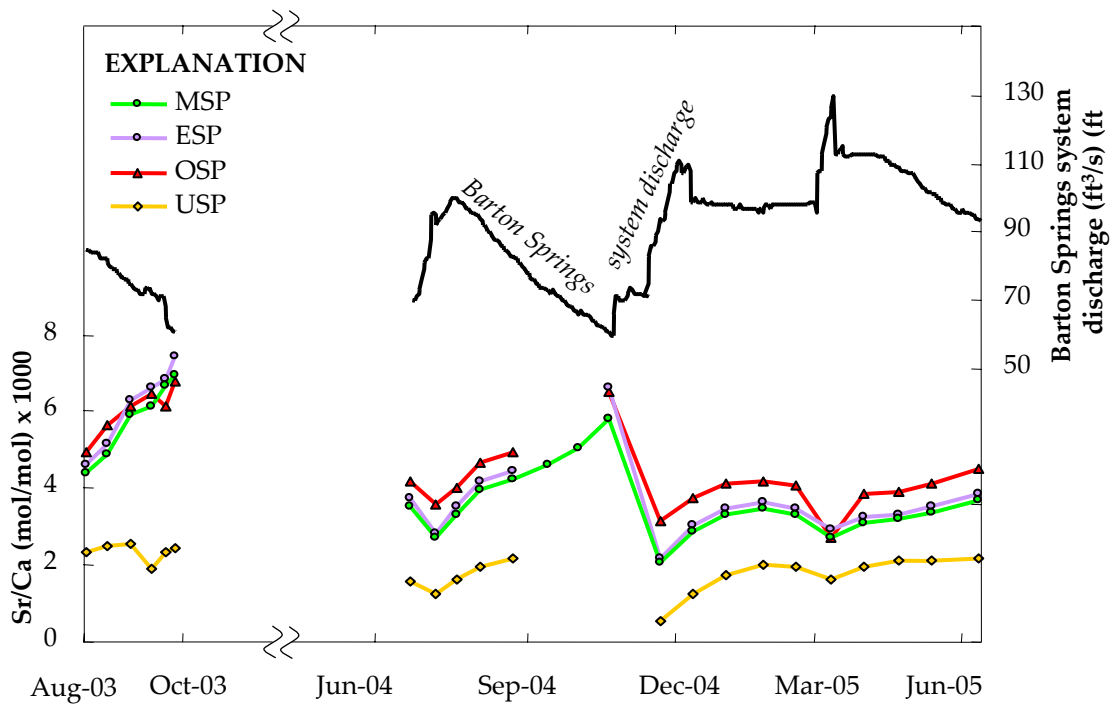


**Figure 3-8.** Time series plot showing systematic variation of Sr/Ca in water samples from springs MSP, ESP, OSP, and USP. Discharge from the Barton Springs system, as measured by real-time monitoring equipment, is shown for comparison.

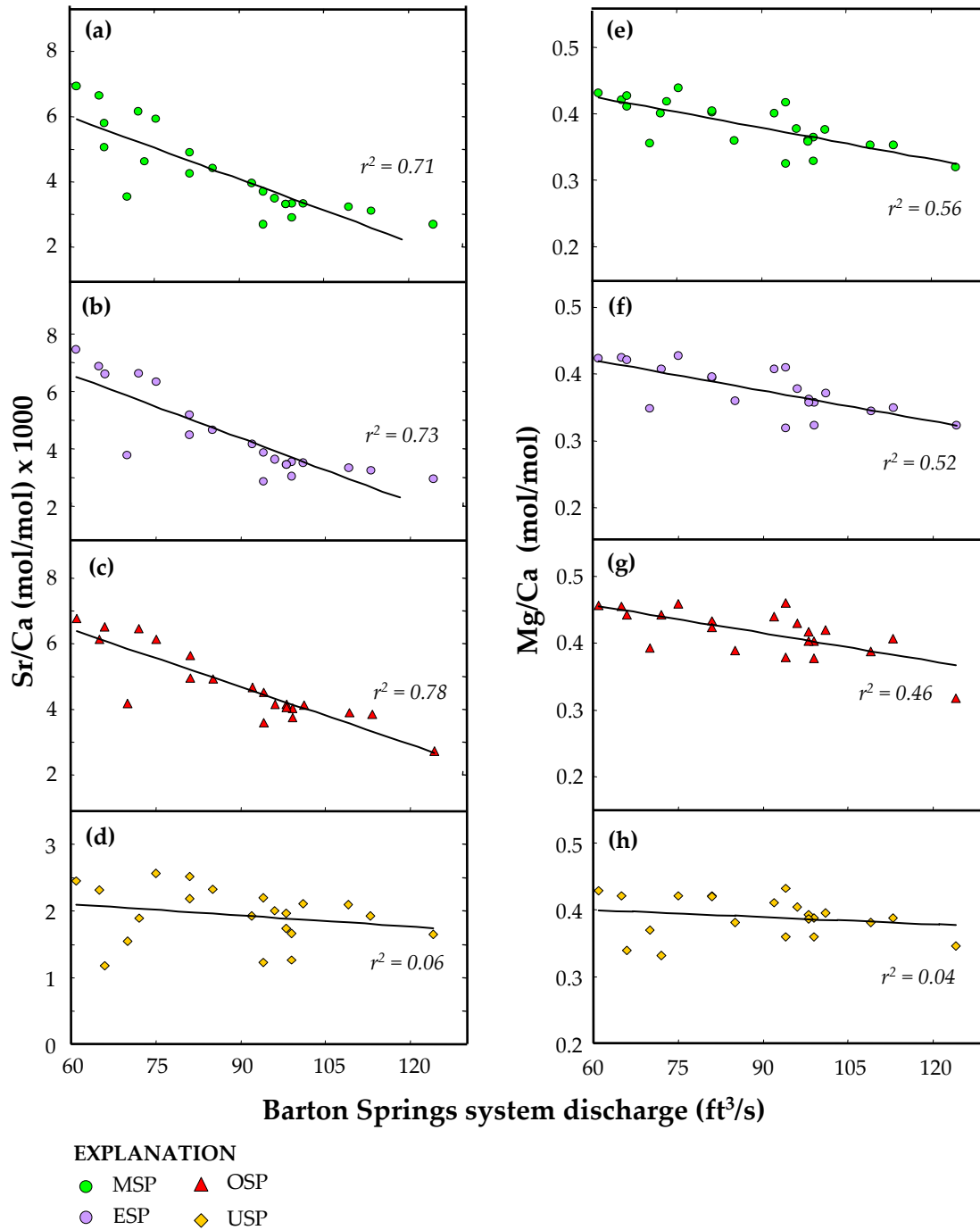


**Figure 3-9.** Comparison of Sr/Ca ratios and Barton Springs system discharge, and comparison of Mg/Ca ratios and Barton Springs system discharge. The linear correlation and corresponding  $r^2$  are shown as well.

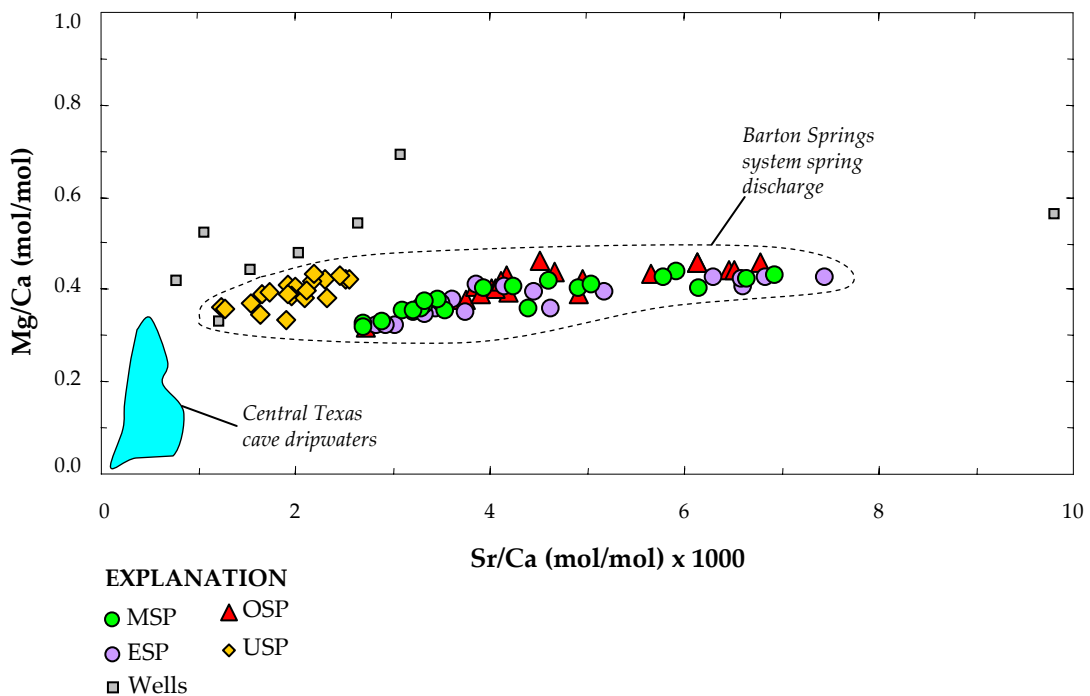
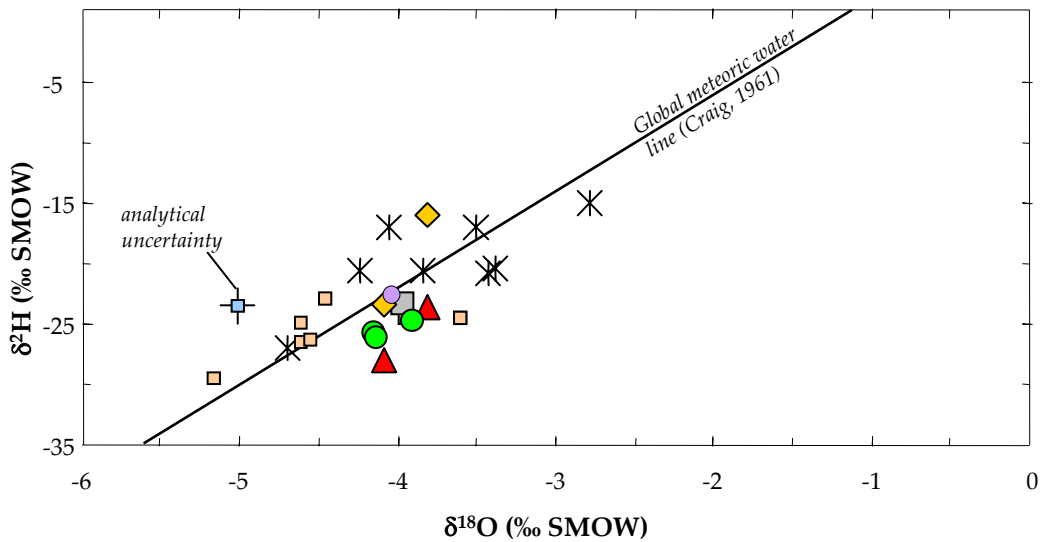


**Figure 3-10.** Comparison of Mg/Ca and Sr/Ca ratios from Barton Springs segment water samples with dripwater samples from central Texas caves (Musgorver and Banner, 2004). Cave dripwater samples are collected from Inner Space Caverns (Georgetown, Texas) and Natural Bridge Caverns (San Antonio, Texas), and represent water infiltrating through the vadose zone and falling into the open space of a cave. Cave dripwaters have lower Sr/Ca and Mg/Ca ratios than any spring samples from the Barton Springs system, which is consistent with the hypothesis that Mg/Ca and Sr/Ca are measurements of ground-water residence time.



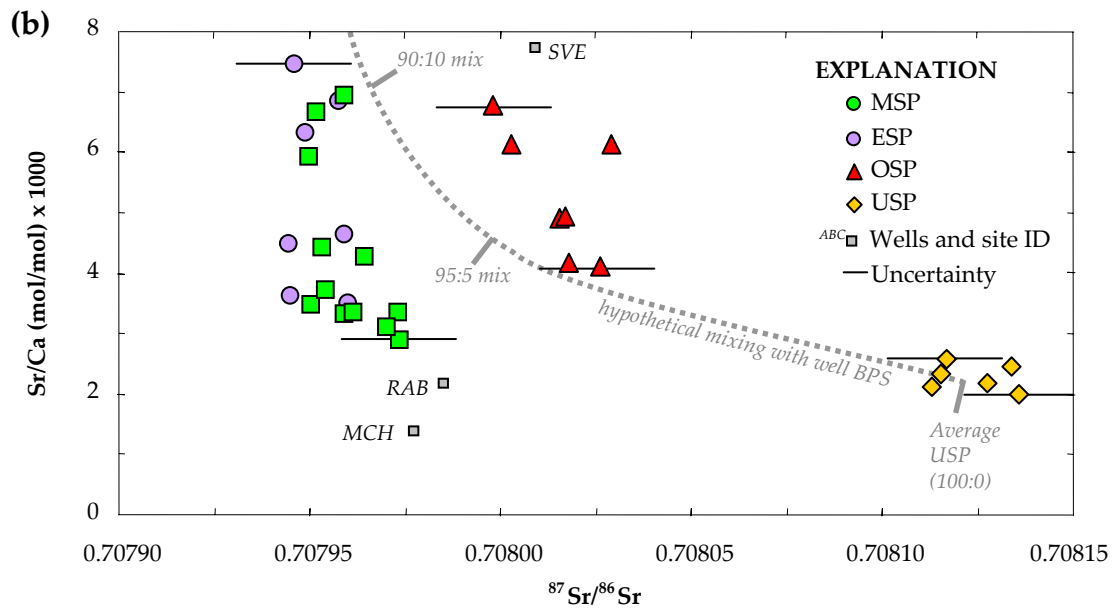
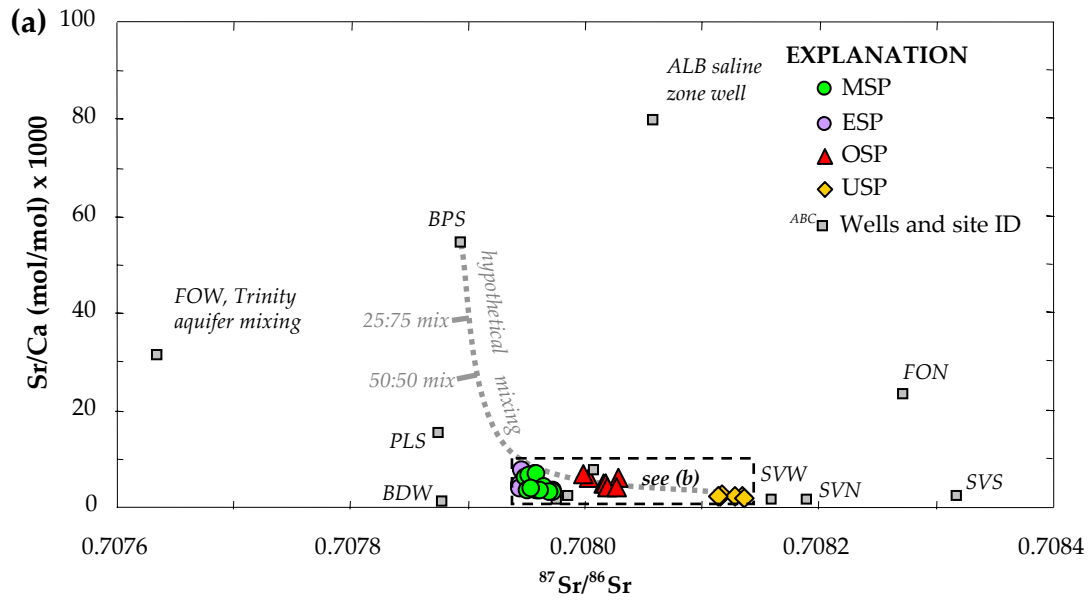
**EXPLANATION**

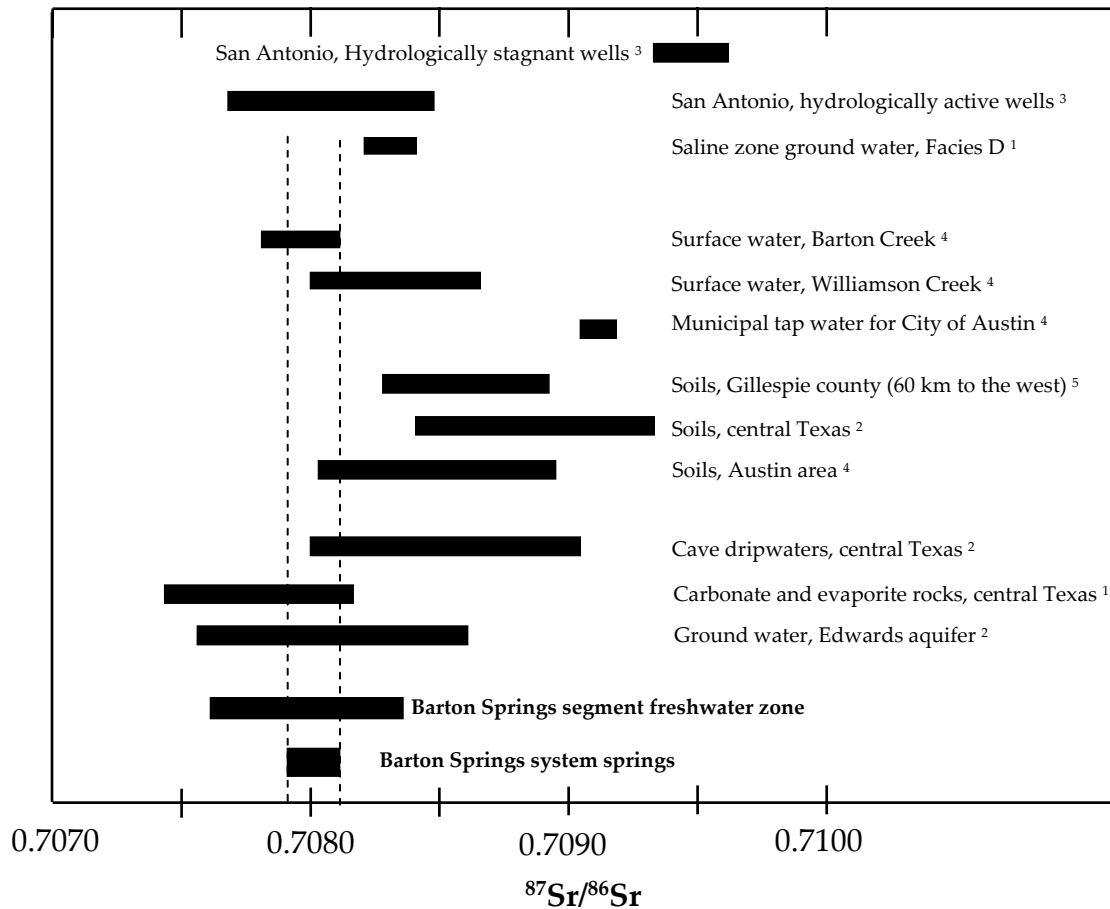
- Spring MSP
- Spring ESP
- ▲ Spring OSP
- ◆ Spring USP
- Well, Saline zone (Oetting et al., 1996)
- Well, Saline zone (ALB)
- ✱ Annual Average Rainfall (Waco, TX; IAEA, 2005)
- Well, San Antonio (Groschen and Buszka, 1997)

**Figure 3-11.** Oxygen and hydrogen isotopic values from the Barton Springs segment, plotted with the global meteoric water line (Craig, 1961) for comparison. The GMWL (Craig, 1961) and data from other studies are shown for comparison. All of the values plot near both the GMWL and each other. Analytical uncertainty is shown for one data point.

**Figure 3-12a.** Sr/Ca— $^{87}\text{Sr}/^{86}\text{Sr}$  variations in the Barton Springs segment. A wide range of residence times and a moderate range of Sr isotope values exist in the study area. A hypothetical mixing line between (1) average spring USP composition (Table 3-2) and well BPS (large historical record showing little geochemical variability; Chapter 2) indicates one potential pathway of water evolution in the Barton Springs segment.

**Figure 3-12b.** Inset of (a). Variation in isotopic composition for springs is within analytical uncertainty, but may suggest an evolution toward less radiogenic values as residence time increases. This could be explained by evolving a low-residence time spring USP sample toward a well BPS sample. Deviation from this line might be the result of spatial and temporal variability in well BPS geochemical composition. Analytical uncertainty is shown for for a few samples.





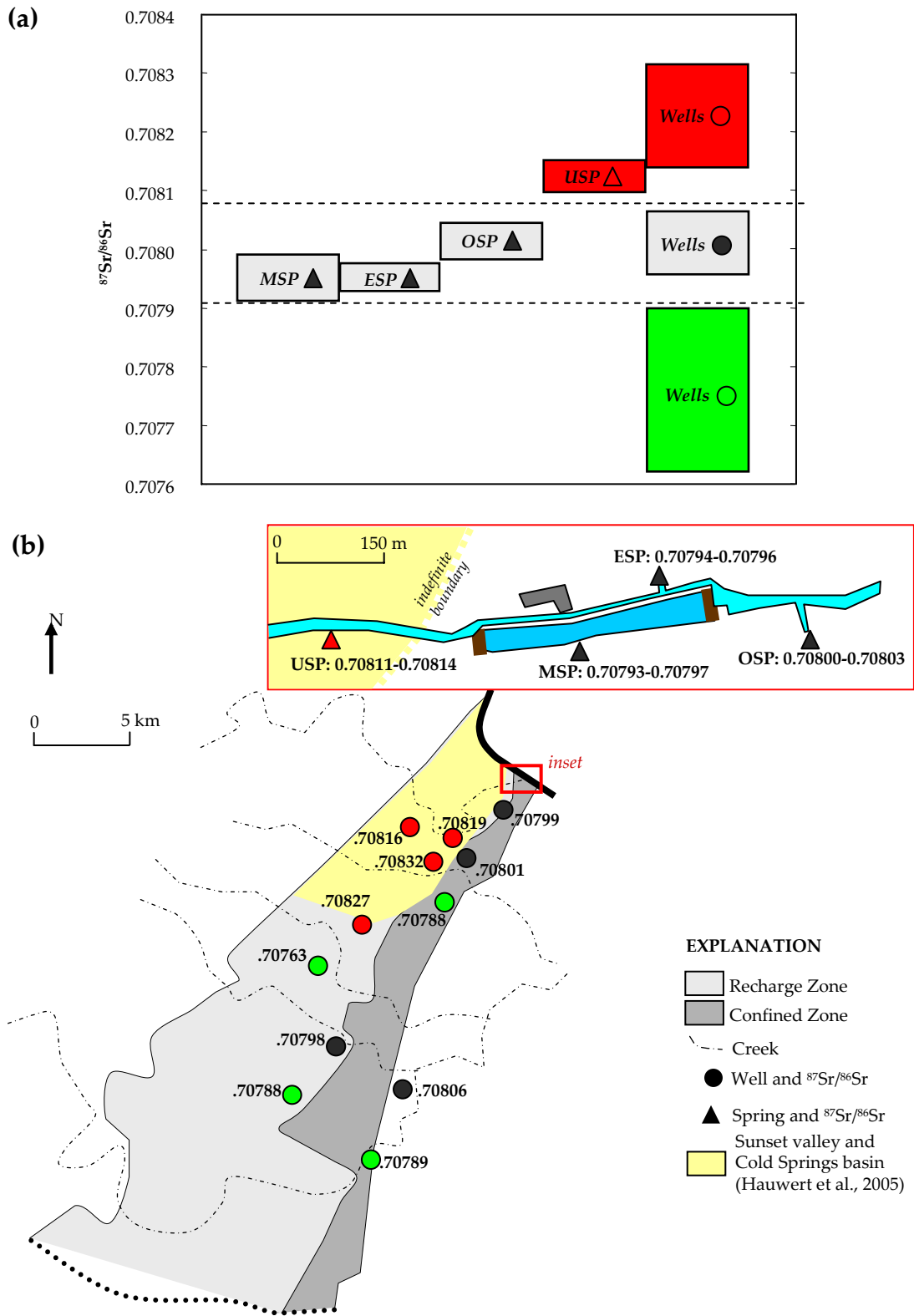
**REFERENCES**

- <sup>1</sup> Oetting (1995)
- <sup>2</sup> Musgrove (2000)
- <sup>3</sup> Groschen and Buzska (1997)
- <sup>4</sup> Christian (in preparation)
- <sup>5</sup> Cooke et al. (2003)

**Figure 3-13.** Potential sources of strontium in the Barton Springs segment, and surrounding areas. Data from this study are shown, as well as data gathered from other studies.

**Figure 3-14a.** Graph showing the range of  $^{87}\text{Sr}/^{86}\text{Sr}$  values for four springs (MSP, ESP, OSP, USP) from August 2003 to June 2005, and the range of  $^{87}\text{Sr}/^{86}\text{Sr}$  values for 12 wells sampled in May and June 2005. Wells are divided into three colors: (1) green wells with  $^{87}\text{Sr}/^{86}\text{Sr}$  less than all spring values; (2) black wells with values within the range of all springs; and (3) red wells with values higher than all springs.

**Figure 3-14b.** Map of study area showing  $^{87}\text{Sr}/^{86}\text{Sr}$  values for wells and springs. Well and spring symbols are shaded according to the designation of (a). A yellow shaded area shows the delineation of the Sunset valley and Cold Springs groundwater basins as mapped by Hauwert et. al (2005). The wells with the most radiogenic  $^{87}\text{Sr}/^{86}\text{Sr}$  values are located in this basin, and radiogenic  $^{87}\text{Sr}/^{86}\text{Sr}$  values at spring USP suggest that it discharges water from this basin.



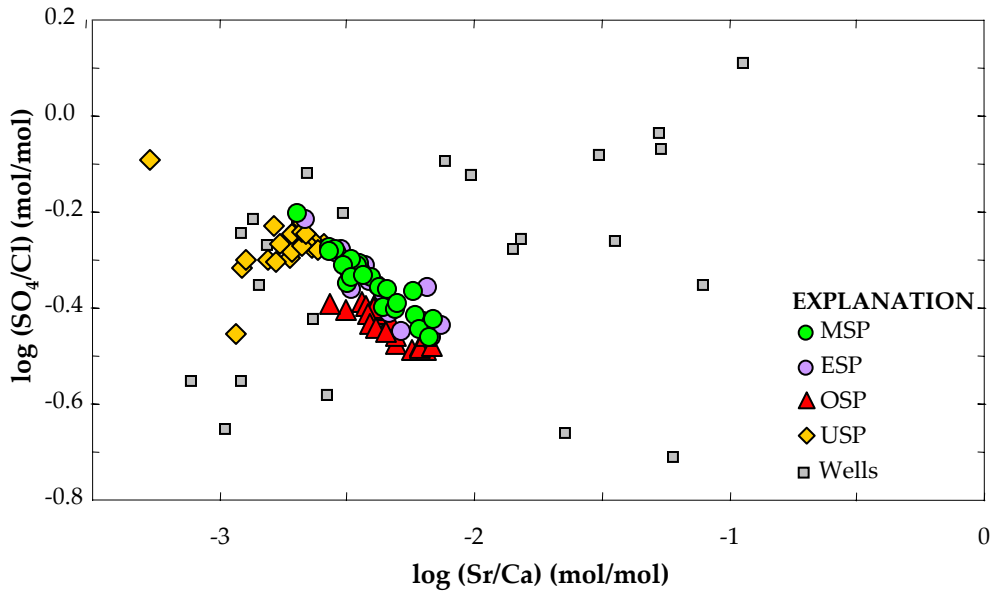


**Figure 3-15a.**  $\text{SO}_4/\text{Cl}$ — $\text{Sr}/\text{Ca}$  variations in wells and springs of the Barton Springs segment. High  $\text{SO}_4/\text{Cl}$  ratios are associated with the Trinity aquifer, while low  $\text{SO}_4/\text{Cl}$  ratios may be associated with the saline zone.  $\text{Sr}/\text{Ca}$  is a measure of water residence time.

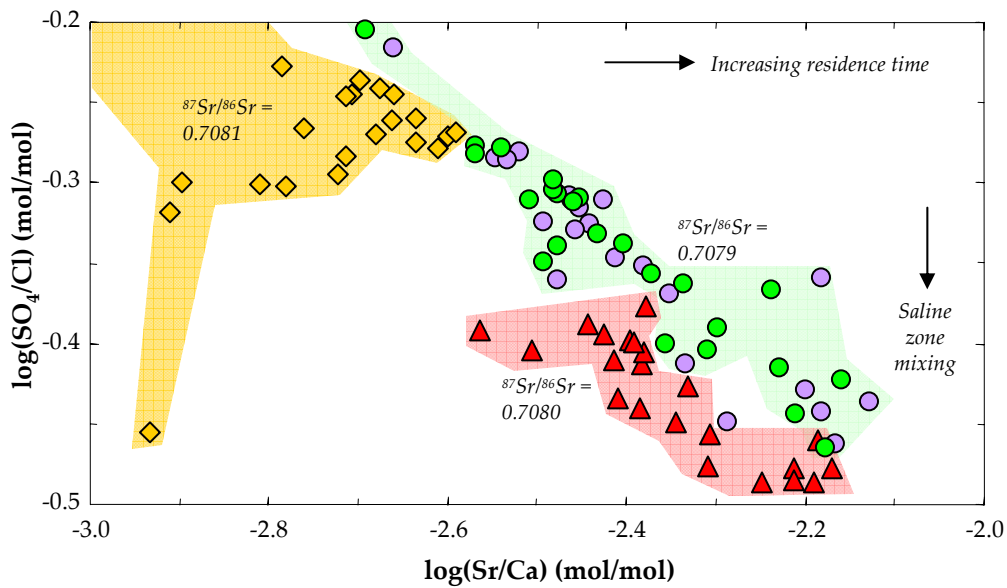


**Figure 3-15b.** Inset of (a), excluding wells, with shaded areas indicating samples with  $^{87}\text{Sr}/^{86}\text{Sr}$  values that are within analytical uncertainty of each other.

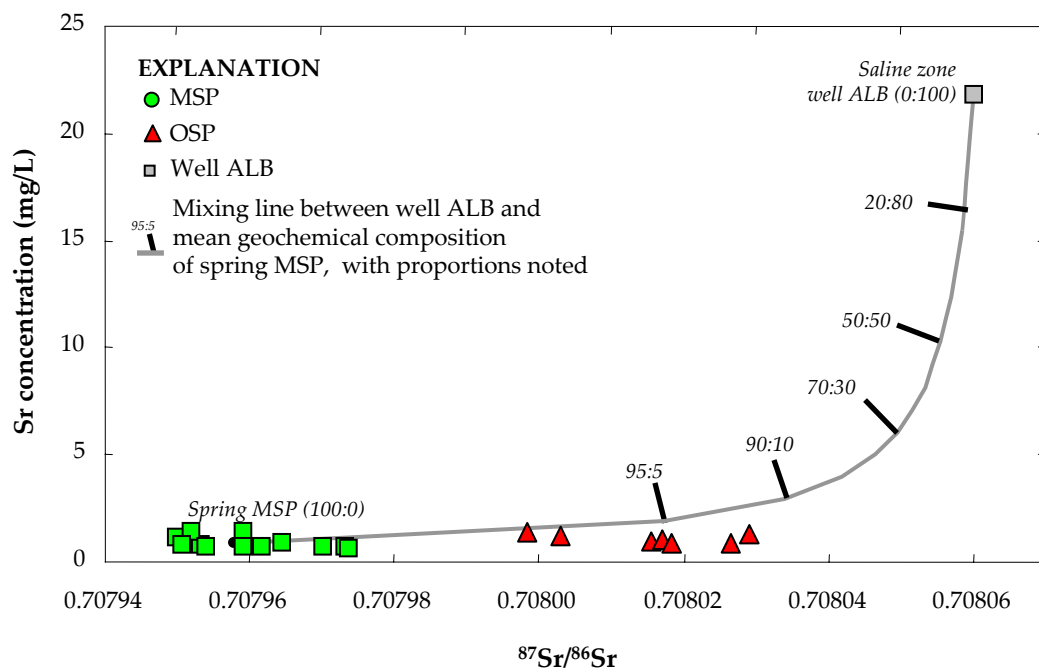


**Figure 3-16.** Sr— $^{87}\text{Sr}/^{86}\text{Sr}$  variations for springs MSP and OSP, and saline zone well ALB. A mixing line between well ALB geochemical composition and the mean geochemical composition for spring MSP is shown, along with tick marks indicating progressive mixing of these two endmembers. On the basis of  $^{87}\text{Sr}/^{86}\text{Sr}$  values, about 4–9 percent of spring OSP discharge may be from the saline zone. However, the Sr concentrations of spring OSP do not fit this mixture well, and the saline zone endmember may not represent a uniform geochemical composition of the saline zone.

**Table 3-1.** Summary of analysis results from Barton Springs segment water-quality sampling, 2003–2005.

Sampling date	Main Barton Spring (MSP)				Eliza Spring (ESP)				Old Mill Spring (OSP)				Upper Barton Spring (USP)				Wells							
	I <sup>1</sup>	Sr	H	O	I	Sr	H	O	I	Sr	H	O	I	Sr	H	O	I	Sr	H	O				
08/06/03	•	•	•		•	•	•		•	•	•		•	•	•									
08/20/03	•				•				•				•											
09/03/03	•	•	•	•	•	•		•	•	•		•	•	•		•								
09/16/03	•				•				•				•											
09/25/03	•	•	•	•	•	•	•	•	•	•	•	•	•		•	•								
09/30/03	•	•	•		•	•			•	•			•	•							• <sup>2</sup>	• <sup>2</sup>		
12/23/03		•																						
06/21/04	•				•				•				•								• <sup>3</sup>			
07/07/04	•				•				•				•											
07/21/04	•	•			•				•				•											
08/04/04	•				•				•				•											
08/25/04	•	•	•	•	•	•	•	•	•	•	•	•	•	•	•	•								
09/15/04	•																							
10/04/04	•																							
10/23/04	•			•	•			•	•			•												
11/24/04	•				•				•				•											
12/14/04	•	•			•				•				•											
01/03/05	•				•				•				•											
01/26/05	•	•	•		•	•	•		•	•	•		•	•	•									
02/16/05	•	•			•				•				•											
03/09/05	•				•				•				•											
03/30/05	•	•			•				•				•											
04/20/05	•				•				•				•											
05/11/05	•	•	•		•	•	•		•	•	•		•	•	•						• <sup>3</sup>	• <sup>3</sup>	• <sup>3</sup>	
06/09/05	•	•			•				•				•											

<sup>1</sup> Abbreviations for analysis types:

I—Dissolved major ion

Sr—Dissolved <sup>87</sup>Sr/<sup>86</sup>Sr analysis

O—δ<sup>18</sup>O analysis

H—δ<sup>2</sup>H analysis

<sup>2</sup> Only well ALB was sampled.

<sup>3</sup> Wells BDW, BPS, FON, FOW, MCH, PLS, RAB, SVE, SVN, SVS, and SVW were sampled.

**Table 3-2.** Summary statistics for ion concentrations and isotope ratios in the Barton Springs system, 2003–2005.

Parameter	Springs				All 12 wells
	MSP	ESP	OSP	USP	
	<i>mean ± std dev</i>				
	<i>range (n)</i>				
<b>pH</b>	7.0 ± 0.1 6.8 - 7.2 (25)	7.0 ± 0.1 6.8-7.2 (25)	7.0 ± 0.1 6.7-7.2 (25)	6.9 ± 0.2 6.6-7.1 (23)	7.1 ± 0.1 6.9-7.4 (25)
<b>Cond (µS/cm)</b>	637 ± 30 565-678 (25)	636 ± 30 550-684 (25)	719 ± 40 636-848 (25)	632 ± 40 466-662 (23)	684 ± 400 445-2600 (25)
<b>Ca (mg/l)</b>	93 ± 5 84-104 (24)	94 ± 6 83-103 (22)	93 ± 5 85-107 (22)	95 ± 5 85-104 (21)	80 ± 15 46-125 (24)
<b>Mg (mg/l)</b>	21 ± 2 12-24 (24)	21 ± 2 13-24 (22)	23 ± 2 17-26 (22)	22 ± 3 8.3-25 (21)	28 ± 11 17-76 (24)
<b>Na (mg/l)</b>	14 ± 2 11-19 (24)	15 ± 2 12-21 (22)	27 ± 3 15-32 (22)	10 ± 1 5-12 (21)	24 ± 64 5-320 (24)
<b>K (mg/l)</b>	1.3 ± 0.1 1.1-1.7 (24)	1.3 ± 0.1 1.2-1.7 (22)	1.6 ± 0.1 1.3-1.9 (22)	1.3 ± 0.2 1.1-2.2 (21)	1.7 ± 2.4 0.7-13 (24)
<b>HCO<sub>3</sub> (mg/l)</b>	325 ± 14 280-350 (24)	322 ± 16 270-340 (22)	316 ± 22 260-250 (22)	337 ± 25 260-370 (21)	315 ± 43 230-370 (24)
<b>Cl (mg/l)</b>	24 ± 3 16-31 (24)	25 ± 3 17-35 (22)	44 ± 3 40-50 (22)	18 ± 3 7-20 (21)	38 ± 88 7-450 (24)
<b>SO<sub>4</sub> (mg/l)</b>	29 ± 3 26-25 (24)	30 ± 3 26-36 (22)	44 ± 2 40-47 (22)	26 ± 3 16-29 (21)	49 ± 105 7-530 (24)
<b>NO<sub>3</sub>-N (mg/l)</b>	1.3 ± 0.2 0.9-1.7 (23)	1.2 ± 0.2 0.9-1.6 (23)	1.2 ± 0.2 0.9-1.5 (23)	2.1 ± 0.4 0.9-3.5 (22)	1.3 ± 0.8 0.05 - 3.0 (21)
<b>Sr (mg/l)</b>	0.83 ± 0.25 0.4-1.4 (24)	0.87 ± 0.28 0.4-1.5 (22)	0.94 ± 0.21 0.64-1.4 (22)	0.40 ± 0.10 0.10-0.52 (21)	3.7 ± 5.5 0.15 - 21 (24)
<b><sup>87</sup>Sr/ <sup>86</sup>Sr</b>	0.70796 0.70728-74 (13)	0.70795 0.70745-96 (7)	0.70802 0.70800-03 (7)	0.70812 0.70811-14 (6)	0.70802 0.70763-832(12)
<b>δ<sup>18</sup>O (‰)</b>	-4.0 ± 0.1 -4.1 - -3.9 (4)	-4.0 ± 0.1 -4.1 - -3.8 (4)	-4.0 ± 0.1 -4.1 - -3.8 (4)	-4.0 ± 0.2 -4.2 - -3.8 (3)	-4.0 ± 0.1 -4.1 - -3.9 (3)
<b>δ<sup>2</sup>H (‰)</b>	-26 ± 1 -28 - -25 (7)	-25 ± 2 -26 - -23 (5)	-25 ± 3 -28 - -21 (5)	-22 ± 4 -26 - -16 (5)	-25 ± 3 -29 - -21 (12)

**Table 3-3.** Coefficients of variation ( $C_v$ ) for major ion concentrations and field parameters in the Barton Springs segment, 2003–2005. Among the four springs, the highest  $C_v$  values are for the  $\text{Sr}^{2+}$  and  $\text{NO}_3^-$  ions.

Site ID	pH	Cond	$\text{Ca}^{2+}$	$\text{HCO}_3^-$	$\text{K}^+$	$\text{Mg}^{2+}$	$\text{Na}^+$	$\text{Cl}^-$	$\text{SO}_4^{2-}$	$\text{NO}_3^-$	$\text{Sr}^{2+}$
<b>MSP</b>	1.7%	4.4%	5.7%	4.4%	8.3%	11%	11%	12%	10%	14%	30%
<b>ESP</b>	2.0%	4.7%	6.2%	4.9%	7.9%	11%	13%	14%	10%	15%	32%
<b>OSP</b>	1.6%	5.2%	5.4%	6.9%	8.0%	9.0%	12%	6.3%	4.3%	15%	23%
<b>USP</b>	2.4%	6.7%	4.9%	7.3%	18%	16%	14%	16%	12%	21%	25%
<b>Wells</b>	2.0%	59%	19%	13%	140%	40%	270%	240%	210%	60%	150%

All units are % coefficient of variation (standard deviation / mean)

#### **4. Barton Springs during stormflow conditions – Using oxygen isotopes and real-time monitoring parameters to quantify water mixing in karst spring discharge, Austin, TX**

##### **4.1. ABSTRACT**

Four hydrologically-connected karst springs in the Barton Springs segment of the Edwards aquifer in Austin, Texas, were monitored for physical, chemical, and isotopic parameters after a three-inch (75 mm) rainfall. Oxygen isotope samples were collected at 12- to 48-hour intervals, and showed an evolution toward more isotopically depleted values after rainfall, suggesting that recent rainfall carried by surface creeks (stormflow) entered the aquifer and reached the springs within 14 hours. Discharge, specific conductance, dissolved oxygen, and turbidity were measured every hour at one spring, and showed substantial changes after rainfall. The maximum discharge of stormflow from springs occurred between 40 and 80 hours after rainfall, and each spring had a unique response to stormflow. A hydrograph separation created for one of the springs using oxygen isotope values showed a rapid increase in discharge at the onset of rainfall, but 14 hours until the first arrival of stormflow. This suggests that that pre-storm water was expelled from the karst conduit system ahead of the advancing front of stormflow. The

hydrograph separation also showed that discharge of pre-storm water (from the aquifer's diffuse matrix) was suppressed by stormflow in the aquifer, suggesting that increased pressure in karst conduits reduced the hydraulic gradients that normally allow matrix water to drain into conduits. Turbidity measurements indicated that a front of turbid water was at the leading edge of stormflow as it passed through aquifer conduits. Dissolved oxygen values generally tracked changes in specific conductance values, but these changes were neither simultaneous nor equal in magnitude, suggesting that another process acted upon dissolved oxygen in the ground water. There was a strong correlation between specific conductance and oxygen isotope values, suggesting that specific conductance may act as an inexpensive and conservative tracer of stormflow. This study showed that high-resolution monitoring of a karst spring can reveal information about aquifer hydrology during stormflow conditions, which may be of use to both resource managers and the scientific community.

## **4.2. INTRODUCTION**

Karst springs are renegades in the world of hydrogeology, especially when there is intense rainfall in their catchment area. In response to rainfall, spring discharge can become turbid, specific conductance can undergo large changes over a few hours (Andrews et al., 1984), and increased concentrations of anthropogenic

contaminants may be detected in the discharge water (Mahler and VanMetre, 2000). Studies of karst springs during these “stormflow conditions” have attributed this behavior to stormflow water recharging the aquifer, traveling rapidly through solution-enlarged conduits, and arriving at springs with very little chance to disperse into the more diffuse (matrix) portion of the aquifer (Siegenthaler and Schotterer, 1984; Hess and White, 1988; Dreiss, 1989; Lakey and Krothe, 1996; Ryan and Meiman, 1996; Desmarais and Rojstaczer, 2002; Liu et al., 2004). This fractured-rock aquifer response to rainfall is difficult to incorporate into a conceptual model; a porous medium aquifer (e.g., sandstone) tends to mix and homogenize recharge water, and hour-scale changes in water quality are rarely observed in porous-medium spring discharge.

The rapid conveyance of stormflow water to karst spring outlets is analogous to surface water systems, in which recent rainfall enters creeks and mixes with older surface water in quantifiable proportions. For many years, studies have successfully traced recent rainfall through surface water catchments using a variety of chemical and isotopic tracers (Fritz et al., 1976; Buttle, 1994).

The stable isotopes of oxygen and hydrogen in the water molecule can be used as conservative tracers (Gat, 1981; Kendall et al., 1995) to trace recharge through a karst aquifer. Under stormflow conditions, oxygen and hydrogen isotopes might potentially vary over a scale of hours to days at karst springs, reflecting the input of

recent rainfall to the system. Individual rainfall events that recharge an aquifer typically have a unique isotopic “fingerprint” that reflects the origin, travel path, and rainout history of the storm (Craig, 1961). Over periods of many years, these individual rainfall fingerprints usually are averaged and mixed together in groundwater systems. As a result, non-stormflow ground water generally reflects the mean isotopic composition of regional rainfall (Darling and Bath, 1988; Lakey and Krothe, 1996), with minor variations (if any) showing an attenuated and time-delayed signal representing seasonal rainfall isotopic variability (Vallejos et al., 1997; Cane and Clark, 1999; Maloszewski et al., 2002). Individual rainfall events, however, typically have widely varying isotopic compositions, and can provide a potential tracer of flow through the aquifer, with “pre-storm” and “stormflow” waters as endmembers in a two-component mixing model.

The isotope geochemistry of a karst spring can be used to (a) detect arrival times of stormflow at springs, (b) separate a hydrograph into its stormflow and pre-storm water components (e.g., Lakey and Krothe, 1996), and (c) evaluate any non-conservative behavior of water isotopes in the system. Each of these is considered in a study carried out on a karst aquifer near Austin, Texas, during October, 2004.

### 4.3. STUDY AREA

The Barton Springs segment of the Edwards aquifer (herein referred to as the Barton Springs segment) is a karst aquifer that extends south-southwest of Austin, Texas (Figure 4-1). It is bounded to the north by the Colorado River, to the south by a ground-water divide, to the west by its contact with relatively impermeable bedrock, and to the east by a zone of low permeability known as the saline zone (Slade et al., 1986; Sharp and Banner, 1997). Aquifer material consists mainly of Cretaceous limestone that has undergone multiple episodes of karstification (Small et al., 1996). In the Miocene epoch, tectonic activity created a zone of normal faulting, resulting in karstification and the aquifer structure and behavior seen today (Slade et al., 1986). The aquifer is generally highly transmissive, with some measured straight-line transit times exceeding 10 km per day (Hauwert et al., 2005).

A major source of recharge to the aquifer is from five ephemeral losing streams that cross the recharge zone (Figure 4-1); these creeks are estimated to provide approximately 85 percent of total recharge to the aquifer. The remaining 15 percent of recharge is derived mostly from precipitation which falls directly on the recharge zone and enters the aquifer (Slade et al., 1986). During large rainfall events (stormflow conditions), the isotopic composition of water in the five recharging creeks is expected to be controlled strongly by the isotopic composition of the rainfall (Fritz et al., 1976; Buttle, 1994).

Ground-water flow in the Barton Springs segment generally is to the north-northeast, following the trend of the Balcones Fault Zone. The water generally discharges from the Barton Springs system, a cluster of four springs that account for over 90 percent of the natural discharge from the aquifer (Figure 4-1) (Hauwert and Vickers, 1994). The quantity and quality of water that discharges from the Barton Springs system varies over time, especially under stormflow conditions, during which stormflow water travels rapidly through solution enlarged conduits and arrives within hours at the Barton Springs system (Andrews et al., 1984; City of Austin, 1997; Mahler and Lynch, 1999; Mahler, 2003).

#### **4.4. METHODS**

##### **4.4.1. Isotope sample collection**

Unfiltered water samples were collected at 12- to 48-hour intervals from the Barton Springs system following a rainfall event on October 23, 2004 from about 12:00 am to 6:00 am. Samples had also been collected from the springs two months earlier (August 25). There had been very little rainfall between these samples and the October rain, thus these “pre-storm” samples were assumed to represent a homogeneous reservoir of water in the aquifer.

Flow-weighted composite samples were collected during the storm from Onion and Bear creeks, which provide recharge to the aquifer. Automated

equipment pumped individual water samples from these creeks into Teflon sample containers at 3-hour intervals. In the laboratory, individual samples were combined using creek hydrographs to create flow-weighted composites, or “average”, water samples (Wilde et al., 1999). Unfiltered water samples were taken from these composites and analyzed for their  $\delta^{18}\text{O}$  and  $\delta^2\text{H}$  values.

Oxygen isotope samples were analyzed at The University of Texas at Austin on a isotope ratio mass spectrometer by equilibrating the sample with  $\text{CO}_2$  gas and subsequently analyzing the  $\text{CO}_2$  isotope ratios (Epstein and Mayeda, 1953). Twenty-two samples of an internal lab standard were used during analysis, and all were within 0.1‰ of the standard value.

Hydrogen isotope samples were analyzed at Southern Methodist University on a Finnigan MAT mass spectrometer. Samples were passed over depleted uranium metal at  $800^\circ\text{C}$  and the liberated hydrogen gas was collected and analyzed (Bigeleisen et al., 1952). A limited number of samples were chosen for analysis of  $\delta^2\text{H}$ , on the basis of oxygen isotope results. Minimum and maximum values of  $\delta^{18}\text{O}$  were assumed to indicate corresponding  $\delta^2\text{H}$  analyses that might be useful for interpretation. Oxygen and hydrogen isotope ratios were expressed in delta notation (Coplen, 1994), and were referenced to standard mean ocean water (SMOW).

#### **4.4.2. Real-time parameter monitoring**

One spring (Main Barton Spring) was monitored with a pressure transducer and Hydrolab equipment. This equipment was placed into a submerged solution-enlarged fracture through which the majority of the spring discharge flows. Values for discharge, specific conductance, turbidity, and temperature were measured and recorded every 15 minutes. Small gaps (one hour or less) in this data arising from equipment malfunction or data transmission errors were filled in by linear interpolation. The 15-minute dataset was converted into an hourly dataset by calculating the mean parameter value using the four measurements taken during the hour.

Surface creeks were monitored for discharge during the study period. Stage levels were correlated to discharge measurements using stage-discharge relationships (Buchanan and Somers, 1969), which had been established for the sites.

Rainfall data were obtained from the City of Austin Flood Early Warning System, an electronically monitored network of rainfall gauges located throughout the study area. The purpose of these data was to identify the occurrence of rainfall, and the results are not used quantitatively.

#### 4.4.3. Hydrograph separation

A “pre-storm/stormflow” two-component mixing model (Fritz et al., 1976; Banner and Hanson, 1990; Kendall et al., 1995; Lakey and Krothe, 1996) was used to perform hydrograph separations on Main Barton Spring. The equations are straightforward derivations of mass balance equations describing discharge and the flux of different endmembers through the system, as expressed by

$$Q_{MIX} = Q_{PRESTORM} + Q_{STORM} \quad (\text{Eq. 4-1})$$

$$Q_{MIX} \delta_{MIX} = Q_{PRESTORM} \delta_{PRESTORM} + Q_{STORM} \delta_{STORM} \quad (\text{Eq. 4-2})$$

and combining (Eq. 4-1) and (Eq. 4-2) yields

$$Q_{STORM} = Q_{MIX} \frac{(\delta_{MIX} - \delta_{PRESTORM})}{(\delta_{STORM} - \delta_{PRESTORM})} \quad (\text{Eq. 4-3})$$

where  $Q_{MIX}$  is the measured discharge of the spring,  $Q_{STORM}$  and  $Q_{PRESTORM}$  are the discharge contributed by stormflow and pre-storm water, and  $\delta_{MIX}$ ,  $\delta_{PRESTORM}$ , and  $\delta_{STORM}$  are measured isotopic values of the reservoirs of mixed and unmixed waters.  $Q_{MIX}$  values were equal to the hourly discharge values measured by real-time monitoring.  $\delta_{MIX}$  values were obtained from 12- to 48- hour sampling of the springs,  $\delta_{PRESTORM}$  values were from samples collected two before rainfall, and  $\delta_{STORM}$  was obtained from the flow-weighted composite samples from two creeks. As there were more discharge readings than isotope results, hourly isotopic values were estimated using linear interpolation.

While this equation makes use of isotopic delta values, any conservative parameter can be used, provided that values for both endmembers are known. With this in mind, we substituted several real-time monitoring parameters into this equation and compared those results with those from oxygen isotopes.

Several assumptions are needed for this hydrograph separation approach (Dreiss, 1989), including that pre-storm water is uniformly distributed throughout the aquifer matrix, and that stormflow water has an isotopic composition sufficiently different from that of pre-storm water (Katz et al., 1998).

## **4.5. RESULTS**

### **4.5.1. Rainfall**

Rainfall lasted from about 12:00 am to 6:00 am on October 23, 2004. Rainfall amounts ranged from 1.9 to 3.8 inches (48–97 mm), with a mean amount of 2.8 inches (71 mm). There was also a small rainfall on October 27 (less than 0.5 inches, or 13 mm), and another rainfall event on November 1 (about 1.5 inches, or 38 mm). Stream discharge rates that resulted from this rainfall are shown in Figure 4-2.

### **4.5.2. Discharge, turbidity, conductance, and dissolved oxygen**

Real-time monitoring of Main Barton Spring beginning at the onset of rainfall resulted in 323 sets of hourly values (Figure 4-3). Discharge ranged from 60 ft<sup>3</sup>/s

(1.7 m<sup>3</sup>/s) on October 23, 2004 at 12:00 am to 76 ft<sup>3</sup>/s (2.2 m<sup>3</sup>/s) on November 5, 2004, the end of the study period. Discharge began to increase within 30 minutes after the onset of rainfall, and reached a maximum of 72 ft<sup>3</sup>/s twenty-four hours later; throughout the remainder of the study period, discharge remained above 70 ft<sup>3</sup>/s. Turbidity increased from zero Nephelometric Turbidity Units (NTU) at the onset of rainfall to a maximum of 17 NTU 16 hours later, and then declined over the next several days. Discharge and turbidity showed relatively simple monotonic increases and decreases, although they did not experience these changes at the same time or in a manner proportional to each other (Figure 4-3).

The initial specific conductance reading of 657 microsiemens per centimeter ( $\mu$ S/cm) began to decrease about 8 hours after the onset of rainfall. Dissolved oxygen values ranged from 6.2 milligrams per liter (mg/L) at the onset of rainfall to a maximum of 6.9 mg/L 36 hours later, and began changing 8 hours after the onset of rainfall. Specific conductance and dissolved oxygen showed complex temporal changes (Figure 4-3), with multiple local maxima and minima, and changes in slope.

#### **4.5.3. Oxygen and hydrogen isotopes**

The twenty-nine  $\delta^{18}\text{O}$  analyses from the four springs yielded values between -5.2‰ and -3.8‰ (Figure 4-3; Tables C-1 and C-2). The most isotopically depleted values were: Main Barton Spring -4.5‰, Upper Barton Spring -5.2‰, Old Mill

Spring -4.4‰, and Eliza Spring -4.4‰. Flow-weighted composite samples from Bear Creek and Onion Creek both had  $\delta^{18}\text{O}$  values of -5.0‰. The pre-storm sample from August 25, 2004 had a  $\delta^{18}\text{O}$  value of -3.8‰, which is similar to the reported long-term mean  $\delta^{18}\text{O}$  composition of rainfall in central Texas (-3.7‰) (International Atomic Energy Agency, 2005). This suggests that the assumption of a well-mixed homogeneous aquifer prior to the storm was reasonable.

Five samples analyzed for  $\delta^2\text{H}$  had values ranging from -38‰ to -16‰. Two samples taken simultaneously on October 25, 2004 had identical  $\delta^2\text{H}$  values of -30‰, suggesting that analytical techniques were carried out appropriately. Comparison of  $\delta^{18}\text{O}$  and  $\delta^2\text{H}$  (Figure 4-4) indicates that these samples plot closely to the global meteoric water line (GMWL) (Craig, 1961).

#### **4.5.4. Hydrograph separation with oxygen isotopes**

The result of a hydrograph separation for Main Barton Spring using  $\delta^{18}\text{O}$  values and (Eq. 4-5) is shown in Figure 4-5. The stormflow endmember was taken to be the value of the creek composite samples, and the pre-storm endmember was taken to be the mean  $\delta^{18}\text{O}$  value measured from the four springs on August 25, 2004. Over long time periods, pre-storm isotopic composition does vary a small amount (from -4.1‰ to -3.9‰; see Chapter 3), but is assumed to have remained constant from August 2004 through October 2004, as little rainfall occurred during this time.

Similarly, the isotopic composition of rainfall probably changes over space and time, but this was assumed to be negligible relative to the effects imparted by stormflow conditions.

It was not possible to create a hydrograph separation for Eliza, Old Mill, and Upper Barton Springs. The discharge rates of these three springs were not measured, and therefore there was no hydrograph available.

## **4.6. DISCUSSION**

### **4.6.1. First arrival of stormflow at springs**

Each spring shows a unique response to stormflow, as measured by changes in oxygen isotope composition. This suggests that stormflow water arrives at the four springs at different times, and/or that each spring discharge stormflow water from different sources. Three of the springs (Main, Eliza, and Old Mill) display comparable behavior, while Upper Barton Spring has a truly unique isotopic response (Figure 4-6; Table 4-1).

At Main Barton Spring, oxygen isotope ratios began to slightly shift toward more isotopically depleted values by 14 hours after the onset of rainfall (i.e., the first collected sample), suggesting that stormflow water reached this spring in about 14 hours (Table 4-1). This is consistent with previous observations of changes in specific conductance and turbidity after rainfall at Main Barton Spring (City of

Austin, 1997; Mahler and Lynch, 1999). These studies reported the arrival of stormflow in about 12 hours, although the arrival time was as short as 5 hours during periods of high spring discharge.

Oxygen isotope ratios at both Main Barton Spring and Eliza Spring reached a minimum value about 60 hours after onset of rainfall (Table 4-1). As in Chapter 3, there are no measurable geochemical differences between Main Barton Spring and Eliza Spring (Chapter 3), and dye trace studies have generally shown these two springs to be very closely connected (Hauwert et al., 2005).

Old Mill Spring isotope ratios reached a minimum value about 80 hours after the onset of rainfall (Table 4-1). Geochemical evidence (Chapter 3) and dye trace studies (Hauwert et al., 2005) suggest that ground water reaches Old Mill Spring by a longer and slower flow path along the far eastern boundary of the aquifer, consistent with the oxygen isotope data in this study.

Upper Barton Spring responds to stormflow conditions more quickly than the other three springs, with large changes in isotopic composition seen in less than 14 hours (i.e., isotopic values had already changed significantly prior to the collection of the first sample). Oxygen isotopes values reached a minimum about 48 hours after the onset of rainfall, 12 hours earlier than at Main Barton and Eliza Springs (Table 4-1). This suggests that either Upper Barton Spring has less pre-storm water available for mixing, or that a large amount of stormflow water was able to

enter shallow conduits rapidly from a nearby creek and discharge from Upper Barton Spring. Upper Barton Spring may have a smaller catchment area, a more shallow flow system, and thus shorter flowpaths; for this type of spring, a fast response to stormflow would be expected (Dreiss, 1989). Independent dye-tracing studies (Hauwert et al., 2005) found that Upper Barton Spring resides within a small and isolated subbasin in the aquifer, which is consistent with these findings. Geochemical evidence is also consistent with these observations (Chapter 3).

#### **4.6.2. Stormflow flushes karst conduits**

Until 14 hours after the onset of rainfall, pre-storm water accounted for over 95 percent of all Main Barton Spring discharge, even as overall discharge rates rose by 15 percent (from 60 to 69 ft<sup>3</sup>/s; Figure 4-5). Thus, during the first 14 hours after the onset of rainfall, pre-storm water was pushed out of the aquifer by the recent influx of recharging stormflow water, a phenomenon known as a pressure pulse.

This flushing behavior has been observed at many karst springs, although the geochemical composition of the flushed ground water can vary. In some cases, specific conductance increases during this flushing event, and is interpreted as mobilization of ground water with a longer residence time (Desmarais and Rojstaczer, 2002). In other cases, as in this study, specific conductance does not change during the flushing (Hess and White, 1988; Lakey and Krothe, 1996; Ryan

and Meiman, 1996), suggesting that ground water already present in the conduits is merely expelled, as opposed to another source of ground water being forced into the conduits.

In theory, only a fully-submerged phreatic conduit can propagate a pressure pulse instantaneously (Ryan and Meiman, 1996). Surprisingly, however, some researchers have observed rapid pressure pulse propagation in unsaturated zone (i.e., perched) karst springs (Siegenthaler and Schotterer, 1984). This may be because once a karst conduit in the unsaturated zone is filled with water, it can effectively propagate a pressure pulse in the same manner as a fully submerged phreatic conduit (B.J. Mahler, U.S. Geological Survey, written comm., 2005).

Following the method of Ashton (1966), we can integrate across these 14 hours to arrive at 3,200,000 ft<sup>3</sup> (91,000 m<sup>3</sup>) of ground water representing the minimum volume of the conduits actively involved in this storm event. This method assumes a single source of recharge and plug-flow conditions. A single conduit 18 cm in width, 25 m tall (an average saturated thickness), and 20 km long (approximate north-south length of the aquifer) has a volume of about 3,200,000 ft<sup>3</sup> (90,000 m<sup>3</sup>). While a conduit of these dimensions approximates the measured conduit volume, it is unlikely that there is one single conduit running the length of the aquifer. It is more likely that the first stormflow water to arrive at Main Barton Spring is from a nearby source such as Barton Creek or Williamson Creek.

#### **4.6.3. Stormflow suppresses discharge of matrix ground water**

Fourteen hours after the onset of rainfall, stormflow water began to arrive at Main Barton Spring (Figure 4-5), but the discharge rate did not increase. Instead, stormflow water progressively became an increasingly larger proportion of spring discharge (up to 56 percent), while pre-storm water discharge was suppressed. One explanation for this behavior is that the reservoir of pre-storm water had been depleted and could no longer contribute discharge to the spring. This is unlikely, as total aquifer volume is large compared to the volume of stormflow water.

Another explanation for suppression of pre-storm water discharge is that stormflow water pressurized the karst conduit system. This would have the effect of reducing gradients between the conduits and the aquifer matrix (Figure 4-7) (Dreiss, 1989). The aquifer matrix, being the major source of pre-storm water in a karst aquifer (Sharp, 1993), was unable to drain water into the karst conduit system as effectively during these stormflow conditions. In fact, over small spatial scales, matrix-to-conduit gradients may have even been reversed, allowing stormflow water to enter the diffuse aquifer matrix.

The reduction of matrix-to-conduit gradients may be analogous to bank storage effects seen in surface-water hydrograph analyses. Pinder and Jones (1969) hypothesized that rivers with permeable alluvial valleys that normally discharge

ground water to streams may have their gradients reversed during floods. This effect temporarily inhibits the discharge of ground water, and actually stores some surface water in the river valley alluvium. This bank storage effect appears to have an analogue in karst caves and conduit systems, where intense flooding can temporarily reverse the typical matrix-to-conduit hydraulic gradient (Palmer, 1991).

Traditionally, resource managers have been more concerned with water quantity than water quality. Thus, because both its volume is small and residence time in the aquifer is short, stormflow water has usually not been considered significant by resource managers (Atkinson, 1977). However, from a water quality perspective, the ability of stormflow water to suppress the discharge of pre-storm water may greatly increase the potential for anthropogenic contaminants to discharge from karst springs. This is because surface water (stormflow water) is generally more contaminated than the ground water (pre-storm water) (Mahler and VanMetre, 2000).

After 72 hours, the suppression of pre-storm water by stormflow water began to decline at Main Barton Spring. This suggests either that there was no longer stormflow water available to enter the aquifer, or that stormflow water was prevented from entering. As most of the five creeks do not have direct contact with the water table, it seems more likely that the observed recession of creek discharge (Figure 4-3) accounted for the decrease in stormflow water discharge. The findings

presented here fit the “flush-dilute-recover” model for a karst spring proposed by Desmaris and Roczaster (2002), although “suppress” is a more appropriate word than “dilute” for this study.

The rapid rise and slow recession of Main Barton Spring discharge (Figure 4-3) is consistent with stormflow response in some karst aquifers (Atkinson, 1977), while it is inconsistent with karst aquifers that undergo both sharp discharge rises and recessions (Lakey and Krothe, 1996). This is probably related to (a) watershed size; (b) nature of the rainfall event; and (c) degree of conduit dominance. Halihan and Wicks (1998) suggested that a pipe flow model can account for this full range of behavior when the correct pipe size is chosen.

#### **4.6.4. Alternative hydrograph separation variables**

Samples from the springs analyzed for both  $\delta^{18}\text{O}$  and  $\delta^2\text{H}$  plot close to the GMWL (Figure 4-4), suggesting that oxygen and hydrogen isotopes were conservative tracers of flow during the period of study. However, it is desirable to find alternative variables for hydrograph separations, as oxygen isotope analysis is time-consuming and expensive relative to other geochemical measurements. Because of budget and time limitations, this study’s sampling interval for oxygen isotopes (12 to 48 hours) was relatively coarse. Thus, this study may have missed subtle but significant temporal variations in pre-storm and stormflow contribution to

spring discharge. In this section, high-resolution real-time monitoring parameters are considered as alternatives hydrograph separation variables, under the assumption that oxygen isotopes created a “correct” hydrograph separation to which comparisons can be made.

Turbidity is not an appropriate hydrograph separation variable, as it did not follow the pattern shown by oxygen isotope ratios. Turbidity reached a maximum value just as the first stormflow water reached Main Barton Spring, and then declined somewhat exponentially during the next four days (Figure 4-3). It is not possible to calibrate a two-endmember mixing model to fit turbidity to the shape of the  $\delta^{18}\text{O}$  hydrograph separation.

Dissolved oxygen concentrations do not produce an effective hydrograph separation, insofar as there is not a high degree of correlation between dissolved oxygen concentrations and oxygen isotope values (Figure 4-8). It is not clear what process/processes caused changes in dissolved oxygen concentrations, but it is apparently was not conservative two-endmember water mixing.

There is a strong linear correlation ( $r^2 = 0.96$ ) between  $\delta^{18}\text{O}$  values and specific conductance values (Figure 4-8), thus specific conductance was tested as an effective and inexpensive hydrograph separation variable. For the pre-storm endmember, the value measured for Main Barton Spring at the onset of rainfall was used (657  $\mu\text{S}/\text{cm}$ , October 23, 2004 at 12:00 am). For stormflow water, a value of 480  $\mu\text{S}/\text{cm}$  was

chosen, such that the specific conductance hydrograph separation (Figure 4-9) approximated the shape and volume of the  $\delta^{18}\text{O}$  hydrograph separation (Figure 4-5). With the aid of 315 additional data points, fine-scale temporal changes not captured with oxygen isotopes are observable. For example, the suppression of pre-storm water between 14 and 72 hours after the onset of rainfall was apparently not a smooth curve, as suggested by the oxygen isotope hydrograph separation.

With the increased resolution of the specific conductance hydrograph separation (Figure 4-9), the effects of a small rainfall event on November 1 can be observed; this rainfall created a response in the spring similar to the larger rainfall on October 23. There is also evidence of a small specific conductance spike on October 28, which is a geochemical response to the lowering of the level of Barton Springs Pool. Main Barton Spring is normally submerged by this pool, and lowering of the pool level leads to geochemical changes in spring discharge (City of Austin, 1997; Mahler, 1997; Mahler and Lynch, 1999) that are not related to stormflow water. During lowered pool levels, specific conductance does not operate correctly as a hydrograph separation variable, as this geochemical change represents a third mixing endmember unaccounted for in this study (B.J. Mahler, U.S. Geological Survey, written comm., 2005).

#### 4.6.5. Complex signals in real-time data

The complex structure of the specific conductance time-series signal at Main Barton Spring (Figure 4-3) is probably the result of individual conduits and catchment areas delivering stormflow water to the spring at different rates and by different routes. This behavior commonly is observed in karst springs (e.g., Siegenthaler and Schotterer, 1984; Hess and White, 1988; Liu et al., 2004).

Turbidity values at Main Barton Spring indicated the passage of a turbid “front” of water located at the leading edge of stormflow water as it flowed toward Main Barton Spring (Figure 4-3). One explanation is that conduits and large void spaces may act as settling basins during non-stormflow conditions (Vineyard, 1960), and this sediment “front” might be the result of turbulent, high-velocity stormflow re-entraining and transporting previously-deposited sediment (Mahler and Lynch, 1999; Massei et al., 2003). Historical observations at Main Barton Spring have noted that maximum turbidity values following rainfall events are lower when there has been another recent rainfall (City of Austin, 1997; Mahler and Lynch, 1999), consistent with a settling basin hypothesis. In addition to settling out of recharge water, aquifer sediment may also originate from the aquifer rock itself (autochthonous), although x-ray diffraction analyses of sediment discharged from Main Barton Spring do not support this hypothesis (Lynch et al., 2004).

Dissolved oxygen concentrations show a complex time-series signal (Figure 4-3). Coarse visual inspection suggests that dissolved oxygen concentrations are inversely correlated with specific conductance values. However, dissolved oxygen does not strongly correlate with specific conductance, as the correlation between  $\delta^{18}\text{O}$  and dissolved oxygen is not as strong as the correlation between  $\delta^{18}\text{O}$  and specific conductance (Figure 4-8). This suggests that some other process affects the concentration of dissolved oxygen in Main Barton Spring discharge. This process is not well understood. One hypothesis, left to future studies to test, is that molecular diffusion of oxygen in water allows it to mix between pre-storm and stormflow water more freely than the bulk water molecules. Another hypothesis is that atmospheric air present in vadose zone conduits at the onset of rainfall becomes trapped by rapidly recharging stormflow water, and is forcefully dissolved into this water (B.J. Mahler, U.S. Geological Survey, written comm., 2005).

#### **4.7. CONCLUSIONS**

Storm water that entered the Barton Springs segment of the Edwards aquifer through losing streams traveled rapidly to the four springs of the Barton Springs system. Analysis of a hydrograph separation for Main Barton Spring showed that pre-storm water was pushed out of major aquifer conduits by an advancing wave of stormflow recharge from creeks. Stormflow water arrived at the Barton Springs

system in less than 14 hours, with different arrival times observed at each of the four springs. Because of karst conduit pressurization, discharge of pre-storm water from the diffuse matrix of the aquifer was suppressed, and a large proportion (up to 56 percent) of Main Barton Spring discharge consisted of recently-recharged stormflow water whose aquifer residence time was only several hours.

On the basis of the Main Barton Spring hydrograph separation, these findings generally fit the “flush-dilute-recover” model for a karst spring proposed by Desmaris and Roczaster (2002). However, instead of “dilute,” the word “suppress” is more fitting. This suppression of longer-residence-time ground water may be of interest to resource managers, as stormflow conditions reduce the already limited mitigation abilities that karst aquifers have for water treatment.

Oxygen isotopes worked well for hydrograph separation purposes, but were sampled too infrequently to capture hour-scale geochemical changes. Specific conductance was well-correlated with  $\delta^{18}\text{O}$  values, and when used for hydrograph separation produced results very similar to those of  $\delta^{18}\text{O}$ , but with higher temporal resolution. Specific conductance is an effective, low-cost, high-resolution measurement relative to oxygen isotopes, although it is not an appropriate hydrograph separation variable when the water level in Barton Springs Pool is actively changing. Presently, it is not possible to construct accurate hydrograph

separations for the other three springs (Eliza, Old Mill, Upper Barton Springs), as their discharge rates are not measured.

Turbidity and dissolved oxygen concentrations in Main Barton Spring discharge showed complex time-series signals that provided different information on aquifer processes. Turbidity values recorded the passage of a wave of turbid water at the leading edge of the stormflow water as it moved through the karst conduit system. This may be the result of remobilization of settled-out sediment, similar to the behavior of a settling basin. The time-series signal for dissolved oxygen generally tracked that of specific conductance, but did not change simultaneously with specific conductance. This suggests that some other process affected the arrival of dissolved oxygen to Main Barton Spring. It may be possible to infer more about aquifer functioning by critical evaluation of the dissolved oxygen time-series signal.

High-resolution monitoring of karst springs revealed substantial information about aquifer processes during stormflow conditions. The findings of this study may be of use to resource managers and future scientific investigations. Strontium isotope ratios could be analyzed to further constrain the sources of stormflow water; for example, strontium isotope ratios should become more radiogenic during stormflow conditions, reflecting the input of surface water that has reacted with soil zones. Major dissolved ion concentrations might also allow discernment of various

water sources. Finally, concentrations of anthropogenic contaminants (pesticides, volatile organic compounds, etc.) might verify the aquifer's sensitivity to contamination predicted by this study.

#### **4.8. ACKNOWLEDGEMENTS**

Funding for this study's isotopic analyses was provided by the University of Texas Jackson School of Geosciences. Funding for USGS real-time monitoring was provided by the Texas Commission on Environmental Quality. Thanks are extended to B. Mahler, L. Mack, M. Gary, and L. Stern for their help in analyzing and interpreting these data. Reviews from B. Wolaver and B. Cey improved the quality of this paper.

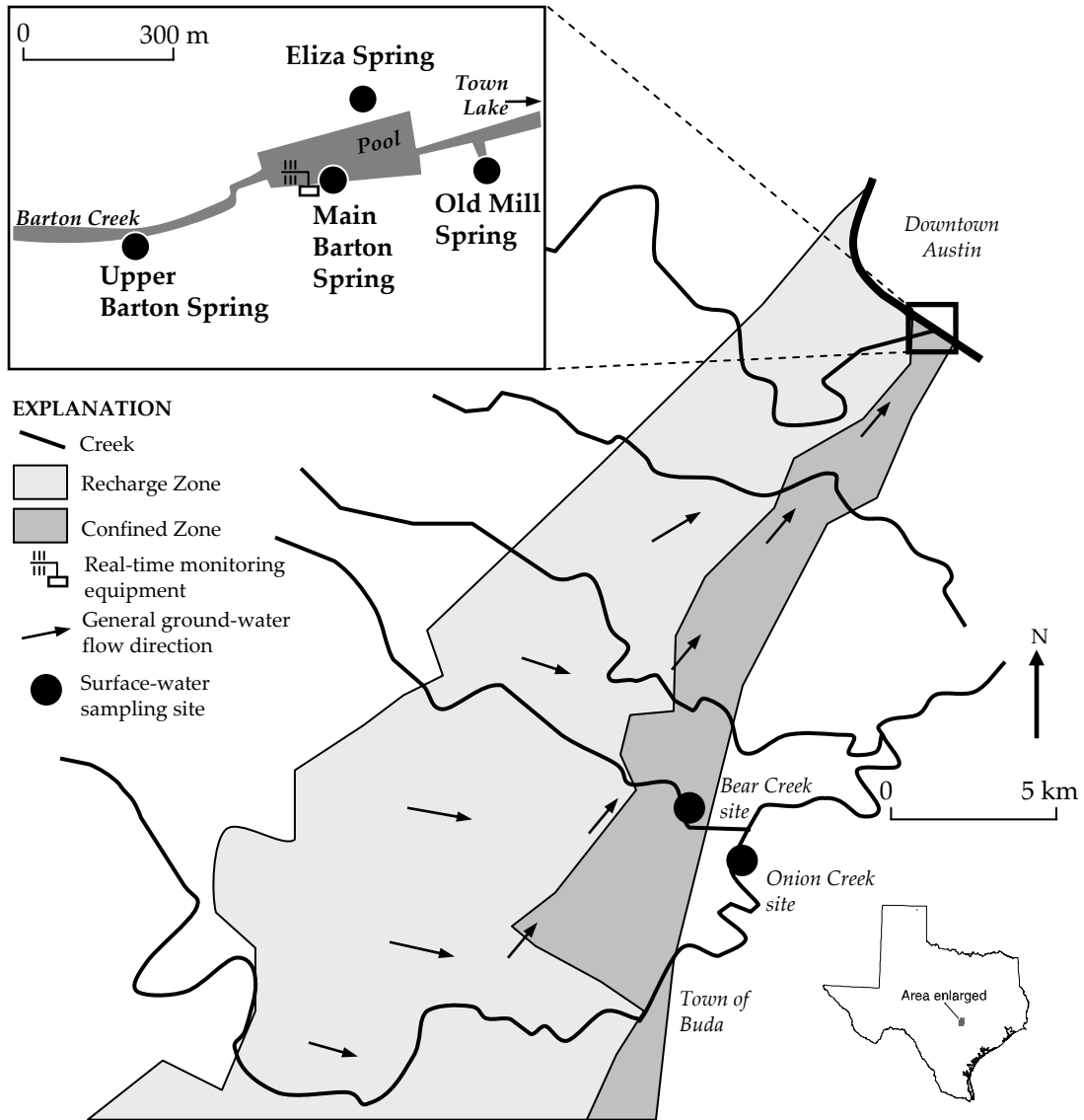


**Figure 4-1.** The Barton Springs segment of the Edwards aquifer. Five creeks cross approximately from west to east, and supply recharge to the aquifer through their streambeds. Water in the aquifer flows generally to the east-northeast, toward the Barton Springs system, which is the main discharge point for the aquifer.

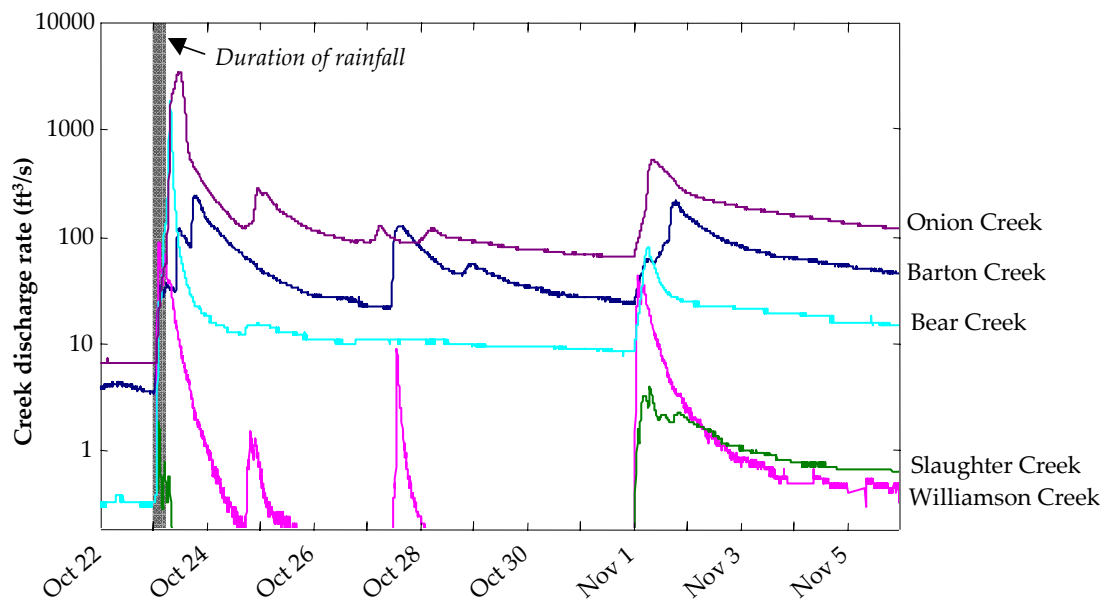


**Figure 4-2.** Discharge rates measured for Barton, Williamson, Slaughter, Bear, and Onion creeks in response to the October 23, 2004 rainfall event. Discharge data were collected by the USGS. Site identifiers for Barton, Williamson, Slaughter, Bear, and Onion creeks are 08155240, 08158920, 08158840, 08158810, and 08158700, respectively.

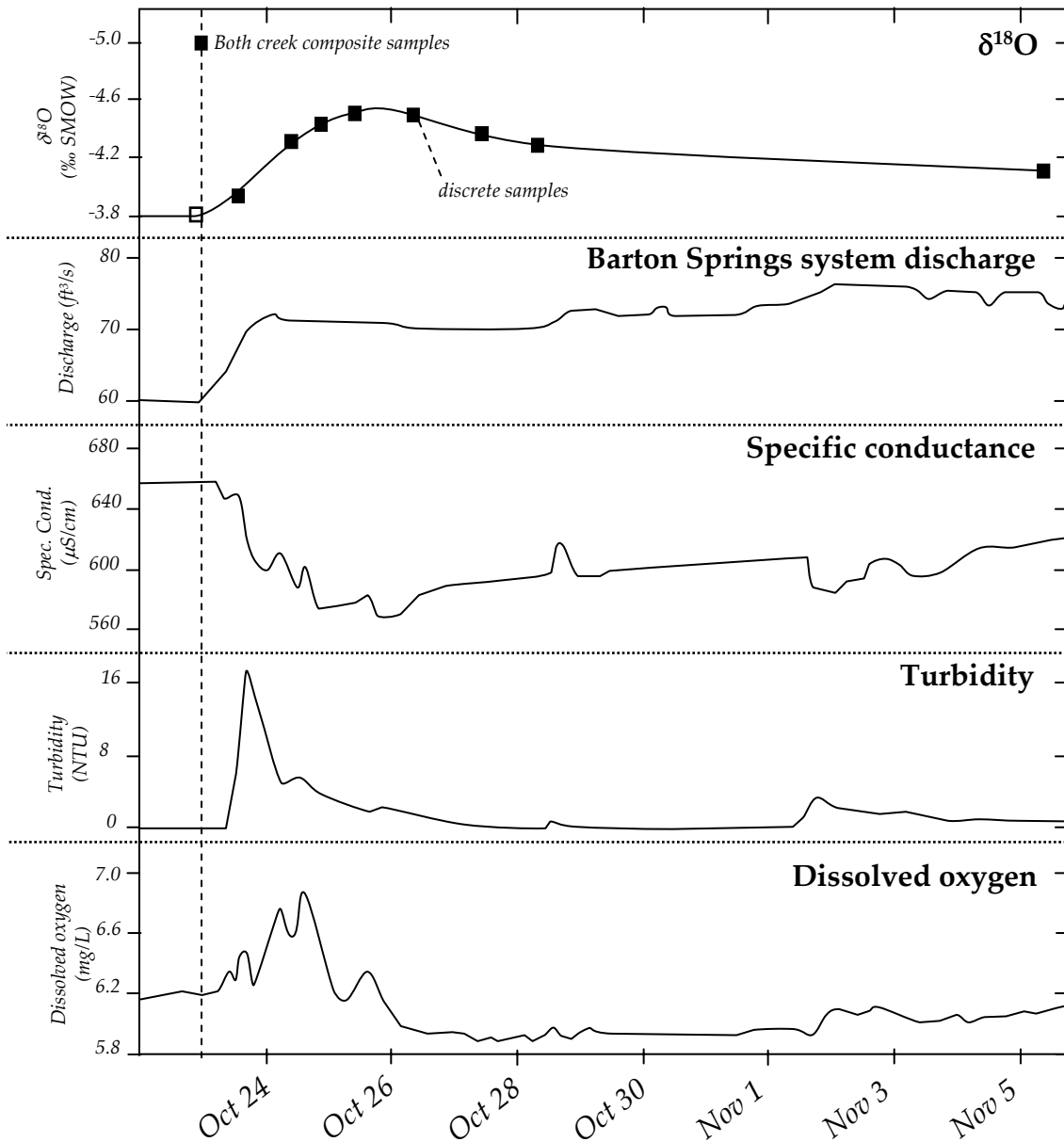


**Figure 4-3.** Multiple physical, chemical, and isotopic values for Main Barton Spring in October and November, 2004. The initial value for  $\delta^{18}\text{O}$  (shown as an open square) is from August 25, 2004, and is assumed to represent the initial pre-storm isotopic composition of the aquifer. The timing of the beginning of the rainfall event is indicated by the vertical dashed line.

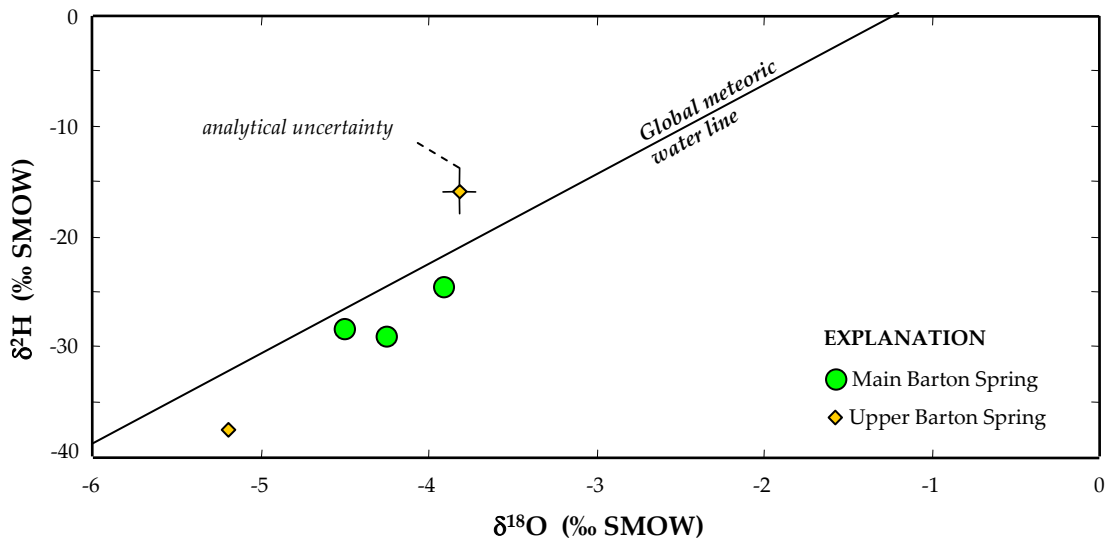


**Figure 4-4.** Samples analyzed for both  $\delta^{18}\text{O}$  and  $\delta^2\text{H}$  plotted with the Global meteoric water line of Craig (1961). Samples plotted close to the line, suggesting that water behaved in a conservative manner during the study period. There is no evidence for evaporation or water-rock interaction.

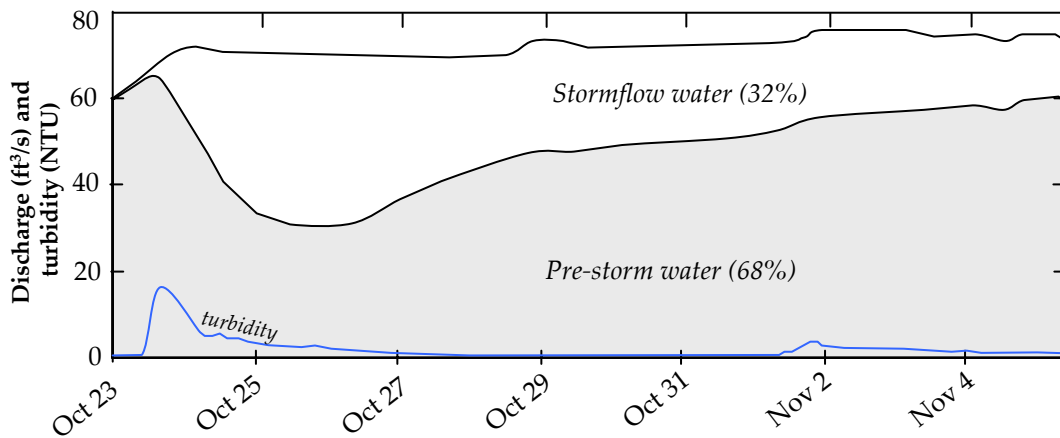


**Figure 4-5.** Hydrograph separation for Main Barton Spring using measured oxygen isotope values. Total volumes of storm and pre-storm water during the period shown (i.e., the areas under the curves) are indicated. Turbidity measurements are shown for reference at the bottom of the graph, and indicate that turbidity values were highest during the first 24 hours after rainfall.

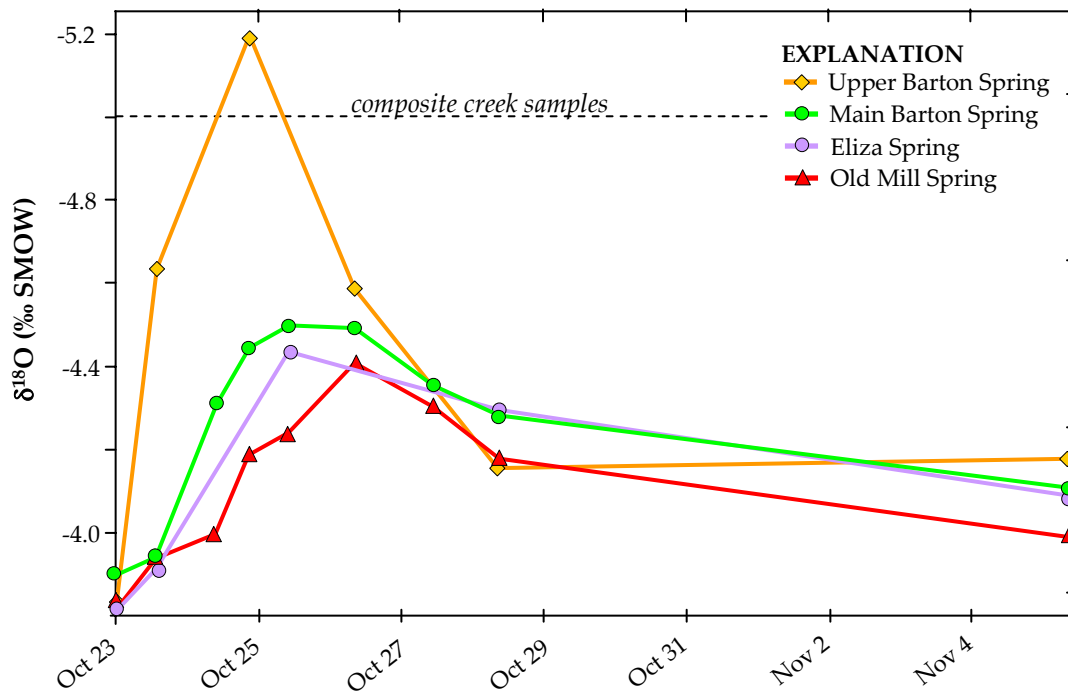
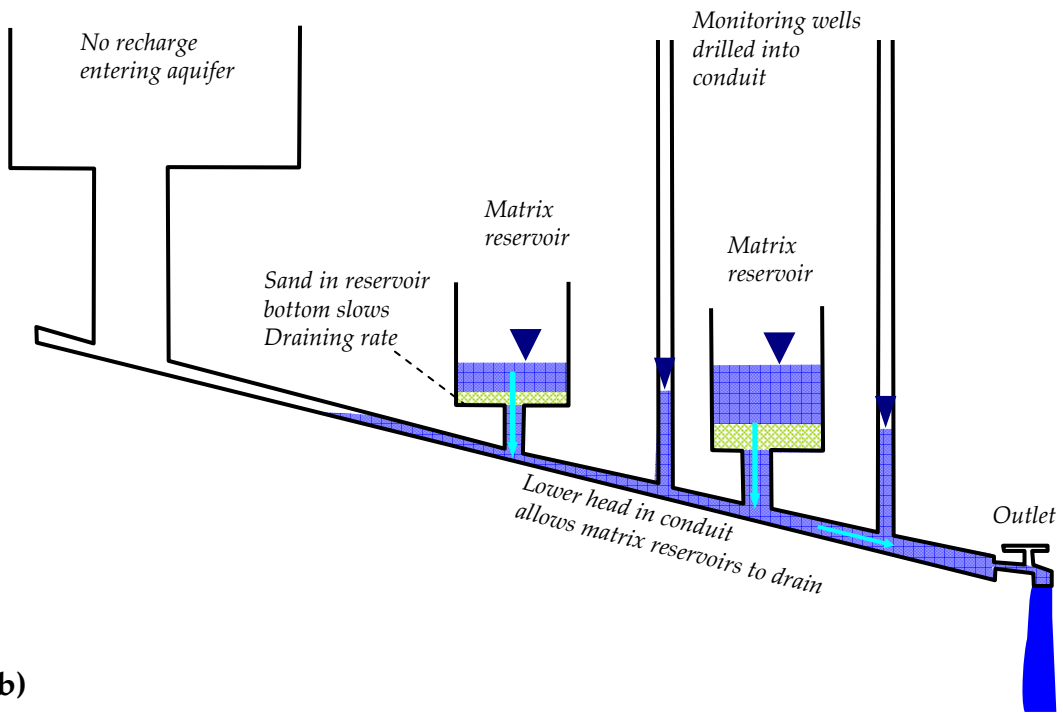


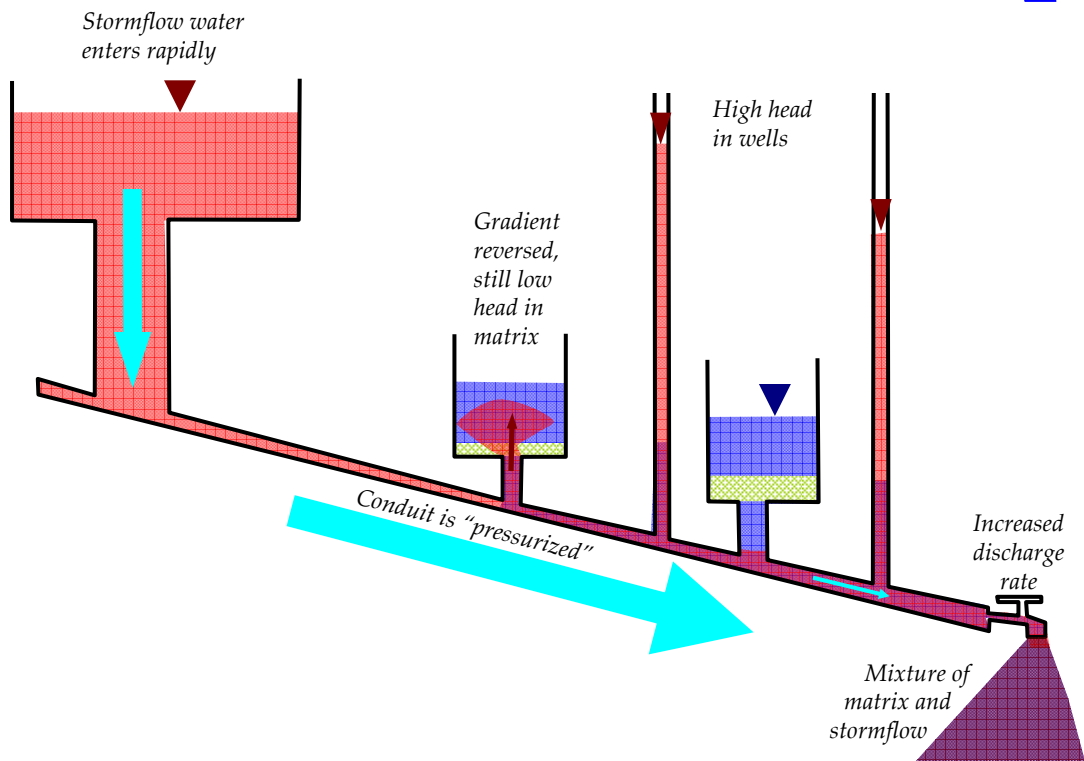
**Figure 4-6.** Oxygen isotope values for the Barton Springs system from October to November, 2004. Two flow-weighted composite creek samples with identical isotopic compositions are shown as a dotted line. During the study period, the isotopic composition of spring discharge evolved toward that of the creek samples before returning to a pre-storm value. One sample from Upper Barton Spring measured a more depleted  $\delta^{18}\text{O}$  value than the composite sample measured.

**Figure 4-7.** Schematic diagram showing the phenomenon of karst conduit pressurization from stormwater. (a) Under non-stormflow conditions, water from the diffuse (or matrix) areas of the aquifer drains into highly-permeable conduits and travels to the spring outlet (shown schematically as a water tap). This draining is relatively slow because of the low hydraulic conductivity of the matrix, shown schematically by beds of sand in the two basins, which represent reservoirs of matrix water; (b) During stormflow conditions, stormflow water (shown in red) enters conduits directly from high-elevation streambeds and travels rapidly to the spring outlet. During this time, pressure (i.e. hydraulic head) in the conduit increases, as indicated by elevated water levels in the two monitoring wells. This decreases the gradient from the matrix into the conduit. In some areas, stormflow water goes into storage in the matrix, to be later discharged when non-stormflow conditions return.

(a)



(b)



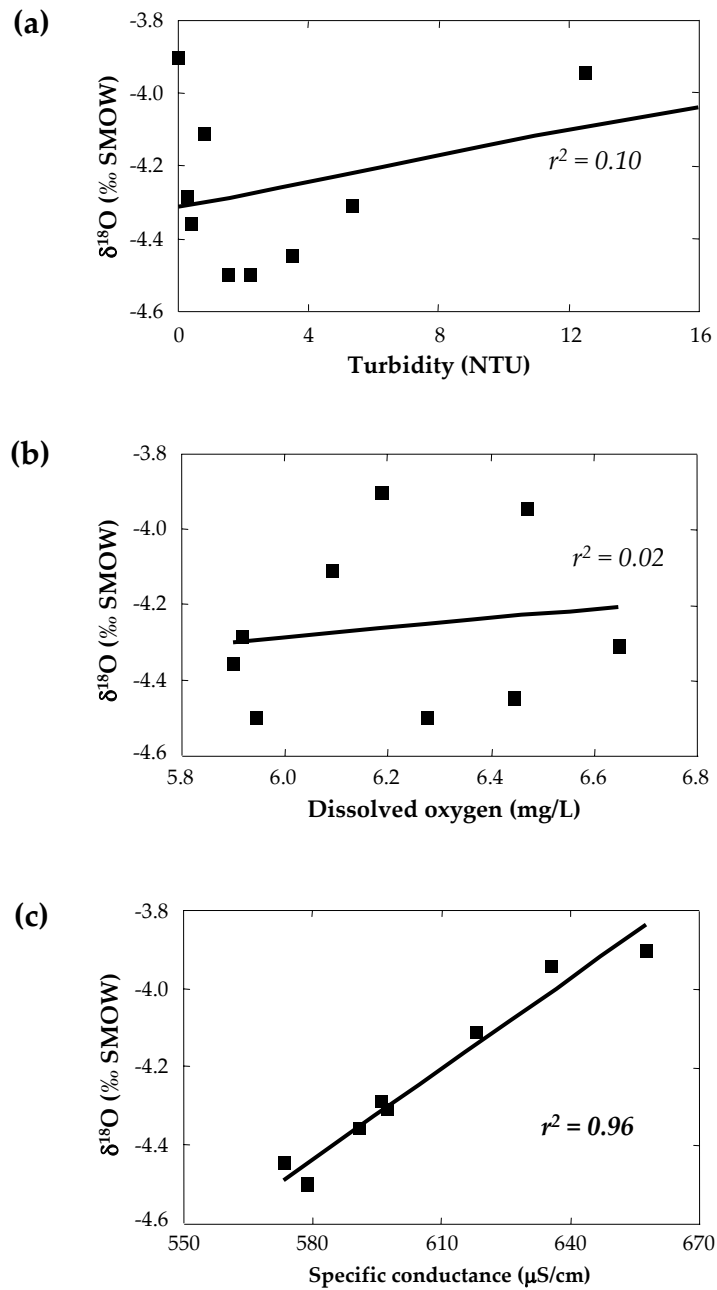


**Figure 4-8.** Comparison of Main Barton Spring  $\delta^{18}\text{O}$  values with real-time water quality parameters collected concurrently by monitoring equipment in Main Barton Spring. (a) Correlation with turbidity is very poor; (b) Correlation with dissolved oxygen is poor; and (c) Correlation is very strong with specific conductance.

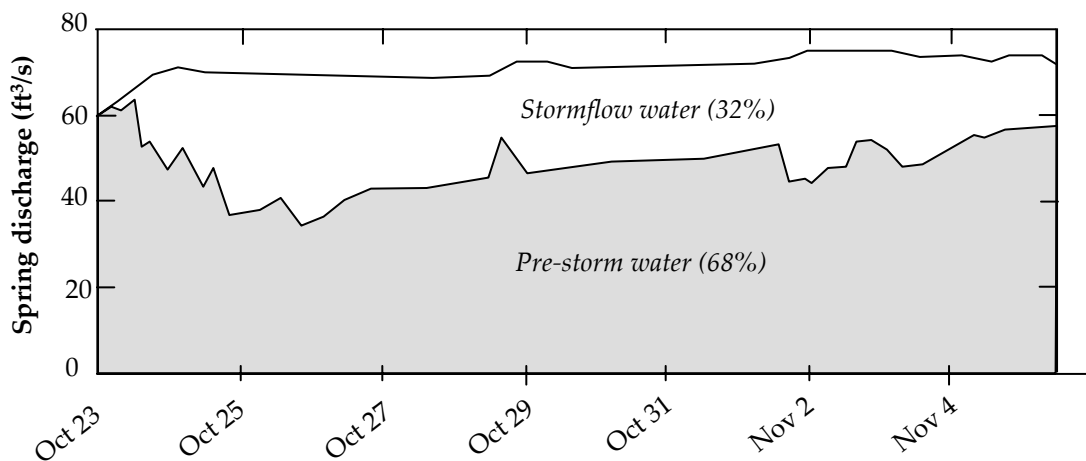


**Figure 4-9.** Hydrograph separation for Main Barton Spring showing discharge of stormflow and pre-storm water. This separation uses a pre-storm specific conductance value of  $657 \mu\text{S}/\text{cm}$ , the value measured at Main Barton Spring at the onset of rainfall. Specific conductance for the stormflow water endmember was calculated by calibrating this separation to the oxygen isotope hydrograph separation, such that the total volumes of water (i.e., areas under the curves) matched.

**Table 4-1.** Summary of stormflow water arrival times for the October, 2004 rainfall event in the Barton Springs segment.

Spring name	First arrival of stormflow water following rainfall	Arrival evidence <sup>2</sup>	Maximum stormflow water discharge following rainfall
Main Barton Spring	about 14 hours <sup>1</sup>	Changes in $\delta^{18}O$ , specific conductance, dissolved oxygen, and turbidity.	about 60 hours
Eliza Spring	over 14 hours, probably no more than 26 hours	Changes in $\delta^{18}O$	about 60 hours
Old Mill Spring	about 14 hours	Changes in $\delta^{18}O$	about 80 hours
Upper Barton Spring	less than 14 hours	Changes in $\delta^{18}O$	about 48 hours

<sup>1</sup> Arrival times of stormflow water also documented in City of Austin (1997), Andrews et al. (1984), and Mahler and Lynch (1999). Minimum historic observed value is 5 hours, when aquifer discharge rates are at very high levels.

<sup>2</sup> Unpublished data shows several other lines of evidence for arrival of stormflow water, including changing dissolved major ion concentrations, and real-time parameters measured at springs other than Main Barton Spring.

## 5. Summary

This research's goal was to advance the study of karst (limestone) aquifers by analyzing time-series water-quality data in the Barton Springs segment of the Edwards aquifer. The water quality in a karst aquifer changes over time, making the application of traditional hydrogeologic principles difficult or impossible. Basic issues such as direction of ground-water flow, sources of spring discharge, and transport of contaminants often remain poorly understood in even the most well studied karst aquifers. As such, scientists must use innovative methods for understanding these systems. This aquifer is of interest because of its central role in creating the popular Barton Springs Pool, its use as a drinking water supply, and its being the only habitat for the endangered Barton Springs salamander (*Eurycea sosorum*).

Water samples collected over 26 years by a long-term USGS monitoring program were analyzed to determine the relation between ground-water geochemistry and rates of aquifer recharge and discharge. On the basis of a non-parametric statistical test, 58 percent of sampled wells showed a correlation between specific conductance and streamflow rates or spring discharge. These correlations resulted from (a) dilution of ground water by recently-recharged surface water, (b) variable residence times of ground water, and (c) mixing between aquifer freshwater and nearby saline waters. These inferences were made on the basis of

changes in specific conductance, Mg/Ca, SO<sub>4</sub>/Cl, and Mg/Na ratios. Four wells (FMW, KCH, SLR, SVE) appeared to intersect major aquifer flowpaths, and five wells (BDW, HWD, MCH, SVN, SVW) intersected minor aquifer flowpaths. For the remaining 17 wells that did not have a negative correlation between specific conductance and streamflow or spring discharge, no conclusions regarding flowpath intersection were drawn. Some wells seemed to receive a portion of their water from the saline zone to the east, which may extend as a saltwater lens under part of the freshwater portion of the aquifer. Other wells may be receiving some of their water from the underlying Trinity aquifer, especially when aquifer flow conditions are high. Given the arbitrary nature of the 26-year USGS sampling program for the Barton Springs segment of the Edwards aquifer, it seems noteworthy that the approach taken by this study had value.

Water-quality data collected over 2 years from the four Barton Springs (Main, Eliza, Old Mill, and Upper Barton Springs) were used to understand water flow in the aquifer. Oxygen and hydrogen isotope values indicated that ground water is well-mixed over long periods of time. Spring water showed evidence of variable residence time and incongruent dissolution, as indicated by increases in Sr/Ca during low spring discharge conditions. Sr/Ca ratios were an effective measure of water residence times for Main, Eliza, and Old Mill Springs. In addition to the limestone aquifer rock, <sup>87</sup>Sr/<sup>86</sup>Sr values indicated that urban infrastructure, soil zones,

and the saline zone are potential sources of dissolved strontium. Main and Eliza Springs apparently received ground water from the same aquifer flowpath(s), as their major ion and isotope compositions were indistinguishable at all times. Upper Barton Spring received some of its water from an isolated subbasin in the aquifer, as indicated by the more radiogenic  $^{87}\text{Sr}/^{86}\text{Sr}$  values measured in this subbasin. There were dissolved ions not associated with carbonate minerals (i.e.,  $\text{Na}^+$ ,  $\text{Cl}^-$ ,  $\text{SO}_4^{2-}$ , and  $\text{NO}_3^-$ ) present in Barton Springs segment ground water. Ratios of  $\text{Na}/\text{Cl}$  less than one suggest an anthropogenic source of  $\text{Cl}^-$  or ion exchange with clays. Increases in  $\text{Na}^+$ ,  $\text{Cl}^-$ , and  $\text{SO}_4^{2-}$  at Main, Eliza, and Old Mill Springs are associated with low discharge rates, and probably represent influx of ground water from the saline zone. Between 4 and 9 percent of the discharge from spring OSP appeared to originate from the saline zone, as determined by a quantitative mixing model.

For 2 weeks after a large rainfall event, water samples were collected to understand how storm-related recharge flows to Main Barton Spring. Storm water that entered the Barton Springs segment of the Edwards aquifer through losing streams traveled rapidly to the Barton Springs system. A hydrograph separation using oxygen isotopes showed an immediate increase in spring discharge following rainfall but a 14-hour delay before storm water first reached the spring. This suggested that an advancing front of storm water expelled pre-storm water from the karst conduits. After arrival of stormflow water at Main Barton Springs, the

discharge of pre-storm water from the diffuse matrix of the aquifer was suppressed, and a majority (up to 56 percent) of spring discharge consisted of recently-recharged stormflow water with an aquifer residence time of only hours. This can be explained by the process of karst conduit pressurization. Oxygen isotopes worked well for hydrograph separation purposes, but were sampled too infrequently to capture hour-scale geochemical changes. Specific conductance measurements were strongly correlated to  $\delta^{18}\text{O}$  values, and when used for hydrograph separation produced results similar to those of  $\delta^{18}\text{O}$ , but with higher temporal resolution. Turbidity and dissolved oxygen at Main Barton Spring showed complex time-series signals that provided different information on aquifer processes. Turbidity values recorded the passage of a wave of turbid water at the leading edge of the stormflow water, which may be the result of remobilization of previously-accumulated sediment. The time-series signal for dissolved oxygen generally tracked that of specific conductance, but did not change simultaneously with specific conductance. This suggests that some other process affected the arrival of dissolved oxygen to the spring.

The results of this research show that karst water quality changes over long, medium, and short time scales. These changes can indicate the potential for contamination, can enable resource managers to make better decisions, and can help scientists better understand the behavior of karst aquifers, the veritable “renegades” of hydrogeology.

## **APPENDIX A. Analytical results for Chapter 2**

This appendix contains most of the analytical results and statistical test results discussed in Chapter 2, including specific conductance data and corresponding streamflow and aquifer flow condition data (Table A-1), results of the statistical test used in the study (Table A-2), and analytical result from dissolved major ion analyses (Table A-3).

Omitted from this appendix are the approximately 9,000 mean daily discharge values for each of the five creeks and the Barton Springs system. Inclusion of these raw data values would add considerably to the bulk of this thesis. For these data, the reader is directed to Garner et al. (in press), which is provided free-of-charge in digital format by the USGS.

**Table A-1.** Specific conductance measurements from wells in the Barton Springs segment, and associated maximum 10-day discharge rates for creeks and the Barton Springs system, 1978–2003.

Site ID	Date	Specific conductance (µS/cm)	Maximum 10-day discharge rates					
			Barton Springs (ft <sup>3</sup> /s)	Barton Creek (ft <sup>3</sup> /s)	Williamson Creek (ft <sup>3</sup> /s)	Slaughter Creek (ft <sup>3</sup> /s)	Bear Creek (ft <sup>3</sup> /s)	Onion Creek (ft <sup>3</sup> /s)
BCK	6/28/1978	630	31	0.7	0.2	0.1		
BCK	7/17/1979	630	100	17	0.9	2.1	2.5	16
BCK	8/28/1980	659	41	0.0	0.0	0.0	0.1	1.1
BCK	8/11/1981	538	99	11	0.0	0.5	2.2	19
BCK	8/10/1982	618	49	1.1	0.0	0.1	0.4	1.2
BCK	7/19/1983	649	84		7.7	1.4	22	90
BDW	6/14/1990	593	49	41	0.5	0.6	1.8	30
BDW	8/22/1990	603	26	0.6	0.5	0.0	0.0	2.2
BDW	3/19/1991	565	85	87	7.6	6.4	11	68
BDW	5/7/1991	584	99	105	10	8.0	20	151
BDW	8/13/1991	600	75	2.5	0.0	0.2	0.4	6.5
BDW	4/30/1992	594	115	94	3.5	4.7	8.5	81
BDW	1/22/1993	590	100	262	16	21	9.0	231
BDW	1/25/1993	589	100	262	16	21	9.0	231
BDW	5/8/1993	584	108	123	1.2	16	10	73
BDW	5/11/1993	593	108	123	1.2	16	10	73
BDW	5/15/1993	589	108	123	0.0	16	10	73
BDW	8/18/1993	594	86	0.5	0.0	0.0	0.1	0.5
BDW	4/15/1994	591	47	6.7	0.0	0.0	0.3	8.4
BDW	6/14/1995	590	104	347	12	108	32	294
BDW	4/25/1996	582	25	0.7	0.0	0.0	0.1	0.9
BDW	7/8/1997	585	113	322	0.9	21	26	510
BDW	4/21/1998	587	98	79	0.0	8.9	7.5	96
BDW	6/11/1999	595	73	21	0.0	1.4	1.4	4.9
BDW	6/2/2000	591	22	2.5	0.0	0.0	0.1	1.2
BDW	6/5/2001	595	103	43	0.0	1.7	3.3	71
BDW	6/5/2002	606	88	7.2	0.0	0.1	0.7	3.8
BDW	5/20/2003	577	102	12	0.0	0.3	1.3	12
BPS	7/12/1978	580	25		0.0	0.0		
BPS	7/24/1978	572	21		0.3	1.1		
BPS	8/24/1979	588	94	9.6	1.8	1.8	4.1	10
BPS	8/1/1980	583	54	0.4	0.0	0.0	0.3	1.3
BPS	8/29/1980	578	40	0.0	0.0	0.0	0.1	1.0
BPS	7/30/1981	583	103	29	1.0	1.4	4.2	50
BPS	8/12/1981	568	98	11	0.0	0.4	2.1	17
BPS	7/19/1982	586	60	4.1	0.0	0.5	1.4	10
BPS	7/22/1983	539	84		7.7	1.4	22	90
BPS	6/27/1984	584	27		0.0	0.0	0.0	4.6
BPS	9/13/1984	590	26		0.0	0.0	0.0	0.2

**Table A-1.** (cont.) Specific conductance and discharge rates, 1978–2003.

Site ID	Date	Specific conduc- tance ( $\mu\text{S}/\text{cm}$ )	Maximum 10-day discharge rates					
			Barton Springs ( $\text{ft}^3/\text{s}$ )	Barton Creek ( $\text{ft}^3/\text{s}$ )	Williamson Creek ( $\text{ft}^3/\text{s}$ )	Slaughter Creek ( $\text{ft}^3/\text{s}$ )	Bear Creek ( $\text{ft}^3/\text{s}$ )	Onion Creek ( $\text{ft}^3/\text{s}$ )
BPS	2/20/1985	586	72		6.3	1.6	8.3	93
BPS	6/19/1985	580	70		2.4	4.0	5.6	145
BPS	8/9/1985	598	64		0.0	0.2	0.9	15
BPS	1/14/1986	579	78		1.5	2.6	5.2	54
BPS	5/3/1986	500	62		59	3.2	6.4	38
BPS	6/24/1986	591	84		13	20	16	216
BPS	6/25/1986	592	84		13	20	16	216
BPS	9/3/1986	589	61		0.0	0.0	0.4	5.8
BPS	2/11/1987	588	80		1.3	3.2	8.9	76
BPS	5/20/1987	595	100		12	2.6	2.8	38
BPS	6/1/1987	591	110		149	93	41	392
BPS	8/19/1987	605	110		0.0	0.0	1.6	33
BPS	2/29/1988	589	61		0.1	0.6	0.9	8.5
BPS	5/3/1988	575	50		1.4	0.1	1.1	7.8
BPS	7/19/1988	572	45		2.0	0.0	0.8	7.5
BPS	8/17/1988	597	45		1.2	0.0	0.0	3.2
BPS	2/27/1989	596	27	1.0	0.3	0.0	0.1	2.4
BPS	5/3/1989	583	33	15	0.2	0.0	3.4	5.4
BPS	7/17/1989	563	55	8.9	2.0	0.2	2.9	12
BPS	8/29/1989	581	33	0.4	0.0	0.0	0.0	2.7
BPS	1/29/1990	585	18	0.6	0.0	0.0	0.0	0.4
BPS	6/5/1990	587	50	41	7.1	1.0	2.5	80
BPS	8/14/1990	566	31	1.6	0.0	0.1	0.0	2.2
BPS	3/22/1991	586	85	87.0	7.6	6.4	11	68
BPS	5/15/1991	569	99	261	68	38	48	218
BPS	8/13/1991	591	75	2.5	0.0	0.2	0.4	6.5
BPS	4/30/1992	589	115	94	3.5	4.7	8.5	81
BPS	8/28/1992	584	125	4.2	0.0	0.0	0.5	9.5
BPS	5/11/1993	584	108	123	1.2	16	10	73
BPS	8/19/1993	539	86	0.4	0.0	0.0	0.0	0.3
BPS	8/20/1993	579	86	0.4	0.0	0.0	0.0	0.3
BPS	4/14/1994	578	47	6.9	0.0	0.0	0.3	9.5
BPS	6/14/1995	585	104	347	12	108	32	294
BPS	5/9/1996	576	25	0.6	0.0	0.0	0.0	0.5
BPS	7/8/1997	575	113	322	0.9	21	26	510
BPS	4/22/1998	565	98	76	0.0	8.4	7.2	93
BPS	6/11/1999	591	73	21	0.0	1.4	1.4	4.9
BPS	6/2/2000	592	22	2.5	0.0	0.0	0.1	1.2
BPS	6/12/2001	593	100	21	0.0	1.0	2.2	41
BPS	6/6/2002	596	88	7.2	0.0	0.1	0.7	3.8
BPS	5/22/2003	591	102	11	0.0	0.3	1.3	12

**Table A-1.** (cont.) Specific conductance and discharge rates, 1978–2003.

Site ID	Date	Specific conductance ( $\mu\text{S}/\text{cm}$ )	Maximum 10-day discharge rates					Onion Creek ( $\text{ft}^3/\text{s}$ )
			Barton Springs ( $\text{ft}^3/\text{s}$ )	Barton Creek ( $\text{ft}^3/\text{s}$ )	Williamson Creek ( $\text{ft}^3/\text{s}$ )	Slaughter Creek ( $\text{ft}^3/\text{s}$ )	Bear Creek ( $\text{ft}^3/\text{s}$ )	
CNE	7/24/1978	1040	21		0.3	1.1		
CNE	7/11/1979	1060	102	27	5.2	4.7	2.6	18
CNE	9/4/1980	1030	38	0.0	0.0	0.0	0.0	0.5
CNE	8/12/1981	996	98	11	0.0	0.4	2.1	17
CNE	8/11/1982	1020	49	1.1	0.0	0.0	0.3	1.5
CNE	7/21/1983	1060	84		7.7	1.4	22	90
FMW	8/11/1981	531	99	11	0.0	0.5	2.2	19
FMW	8/4/1982	566	51	1.1	0.0	0.1	0.5	2.0
FMW	7/19/1983	568	84		7.7	1.4	22	90
FMW	6/19/1985	547	70		2.4	4.0	5.6	145
FMW	8/8/1985	567	64		0.0	0.2	1.0	15
FMW	1/15/1986	545	78		1.5	2.6	5.2	54
FMW	5/3/1986	568	62		59	3.2	6.4	38
FMW	6/25/1986	564	84		13	20	16	216
FMW	9/3/1986	568	61		0.0	0.0	0.4	5.8
FMW	2/9/1987	552	83		1.3	3.4	9.3	81
FMW	5/21/1987	553	100		12	2.6	2.8	38
FMW	6/1/1987	535	110		149	93	41	392
FMW	8/18/1987	564	110		0.0	0.0	1.6	34
FMW	2/25/1988	573	63		0.1	0.6	1.2	8.6
FMW	5/3/1988	574	50		1.4	0.1	1.1	7.8
FMW	2/23/1989	560	28	0.9	0.3	0.0	0.1	1.4
FMW	5/1/1989	600	36	19	0.3	0.0	3.7	7.3
FMW	7/17/1989	585	55	8.9	2.0	0.2	2.9	12
FMW	8/21/1989	587	36	0.6	0.0	0.0	0.0	3.5
FMW	3/5/1991	571	87	106	8.5	14	15	82
FMW	5/7/1991	561	99	105	10	8.0	20	151
FMW	8/19/1991	561	71	467	107	42	11	58
FMW	4/28/1992	545	115	115	4.7	6.2	11	98
FMW	1/21/1993	536	100	262	16	21	9.0	231
FMW	1/24/1993	537	100	262	16	21	9.0	231
FMW	1/28/1993	537	100	262	16	21	9.0	231
FMW	5/8/1993	535	108	123	1.2	16	10	73
FMW	5/11/1993	534	108	123	1.2	16	10	73
FMW	5/15/1993	528	108	123	0.0	16	10	73
FMW	8/16/1993	537	87	0.5	0.0	0.0	0.1	0.5
FMW	4/8/1994	563	47	6.9	0.0	0.0	0.3	9.5

**Table A-1.** (cont.) Specific conductance and discharge rates, 1978–2003.

Site ID	Date	Specific conduc- tance ( $\mu\text{S}/\text{cm}$ )	Maximum 10-day discharge rates					Onion Creek ( $\text{ft}^3/\text{s}$ )
			Barton Springs ( $\text{ft}^3/\text{s}$ )	Barton Creek ( $\text{ft}^3/\text{s}$ )	Williamson Creek ( $\text{ft}^3/\text{s}$ )	Slaughter Creek ( $\text{ft}^3/\text{s}$ )	Bear Creek ( $\text{ft}^3/\text{s}$ )	
FOW	6/28/1978	620	31	0.7	0.2	0.1		
FOW	7/10/1979	620	102	27	5.2	4.7	2.6	18
FOW	8/28/1980	686	41	0.0	0.0	0.0	0.1	1.1
FOW	8/11/1981	595	99	11	0.0	0.5	2.2	19
FOW	8/10/1982	595	49	1.1	0.0	0.1	0.4	1.2
FOW	7/19/1983	597	84		7.7	1.4	22	90
FOW	8/8/1985	641	64		0.0	0.2	1.0	15
FOW	1/14/1986	624	78		1.5	2.6	5.2	54
FOW	5/1/1986	635	62		59	3.2	6.4	26
FOW	6/25/1986	748	84		13	20	16	216
FOW	9/3/1986	610	61		0.0	0.0	0.4	5.8
FOW	2/10/1987	625	83		1.3	3.4	9.3	81
FOW	5/20/1987	647	100		12	2.6	2.8	38
FOW	6/1/1987	630	110		149	93	41	392
FOW	8/26/1987	687	107		0.0	0.0	1.1	21
FOW	5/6/1988	670	50		1.4	0.1	1.1	7.8
FOW	7/18/1988	643	45		2.0	0.0	0.8	7.5
FOW	8/17/1988	705	45		1.2	0.0	0.0	3.2
FOW	2/27/1989	660	27	1.0	0.3	0.0	0.1	2.4
FOW	5/3/1989	647	33	15	0.2	0.0	3.4	5.4
FOW	7/26/1989	602	48	2.5	0.3	0.0	1.6	5.5
FOW	2/9/1990	658	22	4.3	8.6	0.0	0.1	1.5
FOW	6/19/1990	645	47	7.0	0.0	0.4	0.5	16
FOW	8/14/1991	648	75	4.1	12	5.9	1.7	6.5
FOW	5/1/1992	771	115	85	3.4	4.2	8.1	75
FOW	1/21/1993	863	100	262	16	21	9.0	231
FOW	1/24/1993	895	100	262	16	21	9.0	231
FOW	1/28/1993	784	100	262	16	21	9.0	231
FOW	5/7/1993	775	108	123	1.2	16	10	73
FOW	5/14/1993	791	108	123	1.2	16	10	73
FOW	5/27/1993	758	108	42	0.0	5.0	5.2	32
FOW	8/17/1993	697	87	0.5	0.0	0.0	0.1	0.5
FOW	4/18/1994	645	46	4.9	0.0	0.0	0.3	8.2
FOW	6/19/1995	760	102	281	12	108	32	172
FOW	5/7/1996	635	26	0.7	0.0	0.0	0.0	0.5
FOW	7/9/1997	616	113	273	0.0	17	23	455
FOW	4/23/1998	652	98	73	0.0	7.9	6.8	90
FOW	6/11/1999	654	73	21	0.0	1.4	1.4	4.9
FOW	6/1/2000	712	22	2.7	0.0	0.0	0.1	1.4
FOW	6/19/2001	742	97	13	0.0	0.8	1.7	29
FOW	6/5/2002	660	88	7.2	0.0	0.1	0.7	3.8
FOW	5/21/2003	747	102	12	0.0	0.3	1.3	12

**Table A-1.** (cont.) Specific conductance and discharge rates, 1978–2003.

Site ID	Date	Specific conduc- tance ( $\mu\text{S}/\text{cm}$ )	Maximum 10-day discharge rates					
			Barton Springs ( $\text{ft}^3/\text{s}$ )	Barton Creek ( $\text{ft}^3/\text{s}$ )	Williamson Creek ( $\text{ft}^3/\text{s}$ )	Slaughter Creek ( $\text{ft}^3/\text{s}$ )	Bear Creek ( $\text{ft}^3/\text{s}$ )	Onion Creek ( $\text{ft}^3/\text{s}$ )
GHW	7/12/1978	660	25		0.0	0.0		
GHW	7/9/1979	670	103	27	5.2	4.7	2.6	18
GHW	8/29/1980	666	40	0.0	0.0	0.0	0.1	1.0
GHW	8/12/1981	650	98	11	0.0	0.4	2.1	17
GHW	8/16/1982	666	46	1.1	0.0	0.0	0.2	1.9
GHW	7/21/1983	667	84		7.7	1.4	22	90
GHW	6/19/1985	659	70		2.4	4.0	5.6	145
GHW	8/9/1985	648	64		0.0	0.2	0.9	15
GHW	1/13/1986	644	78		1.5	3.0	5.7	61
GHW	5/1/1986	677	62		59	3.2	6.4	26
GHW	6/25/1986	676	84		13	20	16	216
GHW	9/2/1986	671	62		0.0	0.0	0.4	5.8
GHW	2/11/1987	672	80		1.3	3.2	8.9	76
GHW	5/20/1987	685	100		12	2.6	2.8	38
GHW	5/31/1987	656	105		149	93	41	392
GHW	8/19/1987	683	110		0.0	0.0	1.6	33
GHW	2/24/1988	655	63		0.1	0.6	1.2	8.6
GHW	5/9/1988	670	50		0.2	0.1	1.1	7.8
GHW	7/14/1988	670	47		2.0	0.0	0.8	7.5
GHW	8/10/1988	635	43		0.0	0.0	0.0	11
GHW	2/23/1989	640	28	0.9	0.3	0.0	0.1	1.4
GHW	5/3/1989	668	33	15	0.2	0.0	3.4	5.4
GHW	7/26/1989	638	48	2.5	0.3	0.0	1.6	5.5
GHW	8/30/1989	640	32	0.4	0.0	0.0	0.0	2.7
HND	7/5/1978	560	28		0.0	0.0		
HND	7/11/1979	580	102	27	5.2	4.7	2.6	18
HND	9/8/1980	559	38	0.1	8.8	0.0	0.2	29
HND	8/11/1981	589	99	11	0.0	0.5	2.2	19
HND	8/10/1982	575	49	1.1	0.0	0.1	0.4	1.2
HND	7/20/1983	475	84		7.7	1.4	22	90
HND	6/18/1985	516	70		3.4	5.5	6.1	186
HND	8/8/1985	580	64		0.0	0.2	1.0	15
HND	1/13/1986	575	78		1.5	3.0	5.7	61
HND	5/2/1986	559	62		59	3.2	6.4	38
HND	6/23/1986	563	84		13	20	16	216
HND	9/3/1986	600	61		0.0	0.0	0.4	5.8
HND	2/11/1987	607	80		1.3	3.2	8.9	76
HND	5/20/1987	633	100		12	2.6	2.8	38
HND	6/1/1987	564	110		149	93	41	392

**Table A-1.** (cont.) Specific conductance and discharge rates, 1978–2003.

Site ID	Date	Specific conduc- tance ( $\mu\text{S}/\text{cm}$ )	Maximum 10-day discharge rates					
			Barton Springs ( $\text{ft}^3/\text{s}$ )	Barton Creek ( $\text{ft}^3/\text{s}$ )	Williamson Creek ( $\text{ft}^3/\text{s}$ )	Slaughter Creek ( $\text{ft}^3/\text{s}$ )	Bear Creek ( $\text{ft}^3/\text{s}$ )	Onion Creek ( $\text{ft}^3/\text{s}$ )
HWD	6/28/1978	560	31	0.7	0.2	0.1		
HWD	7/9/1979	560	103	27	5.2	4.7	2.6	18
HWD	8/28/1980	575	41	0.0	0.0	0.0	0.1	1.1
HWD	8/18/1981	551	96	16	0.3	0.3	4.3	14
HWD	8/4/1982	563	51	1.1	0.0	0.1	0.5	2.0
HWD	7/22/1983	553	84		7.7	1.4	22	90
ISD	7/12/1978	486	25		0.0	0.0		
ISD	7/11/1979	480	102	27	5.2	4.7	2.6	18
ISD	9/4/1980	487	38	0.0	0.0	0.0	0.0	0.5
ISD	8/12/1981	482	98	11	0.0	0.4	2.1	17
ISD	8/11/1982	495	49	1.1	0.0	0.0	0.3	1.5
ISD	7/22/1983	489	84		7.7	1.4	22	90
JBS	7/17/1978	550	24	0.0	0.0	0.0		
JBS	7/16/1979	580	100	27	0.9	2.2	2.6	18
JBS	8/27/1980	587	41	0.1	0.0	0.0	0.1	1.1
JBS	8/4/1981	570	102	21	1.0	1.4	4.2	38
JBS	4/22/1982	570	46	20	30	7.9	3.2	8.4
JBS	4/23/1982	576	50	31	30	7.9	3.2	14
JBS	4/26/1982	576	51	36	30	9.4	3.2	23
JBS	8/9/1982	592	50	1.1	0.0	0.1	0.4	1.1
JBS	5/21/1983	589	77		39	23	27	265
JBS	5/22/1983	588	79		39	23	27	265
JBS	5/23/1983	586	82		39	23	27	265
JBS	5/25/1983	590	84		39	23	27	265
JBS	7/18/1983	586	84		7.7	1.4	22	90
KCH	7/5/1978	640	28		0.0	0.0		
KCH	7/10/1979	620	102	27	5.2	4.7	2.6	18
KCH	8/28/1980	660	41	0.0	0.0	0.0	0.1	1.1
KCH	8/11/1981	621	99	11	0.0	0.5	2.2	19
KCH	8/10/1982	652	49	1.1	0.0	0.1	0.4	1.2
KCH	7/19/1983	670	84		7.7	1.4	22	90
KCH	6/24/1985	612	72		33	28	8.0	300
KCH	8/7/1985	635	65		0.0	0.2	1.0	16
KCH	5/1/1986	676	62		59	3.2	6.4	26
KCH	6/24/1986	651	84		13	20	16	216
KCH	8/29/1986	674	64		0.0	0.0	0.4	5.8
KCH	2/9/1987	641	83		1.3	3.4	9.3	81
KCH	5/18/1987	660	100		1.0	0.5	2.3	38
KCH	6/1/1987	644	110		149	93	41	392
KCH	8/19/1987	675	110		0.0	0.0	1.6	33
KCH	3/9/1988	655	58		0.2	0.6	1.1	7.8
KCH	5/10/1988	703	50		0.0	0.1	0.7	4.7

**Table A-1.** (cont.) Specific conductance and discharge rates, 1978–2003.

Site ID	Date	Specific conduc- tance ( $\mu\text{S}/\text{cm}$ )	Maximum 10-day discharge rates					
			Barton Springs ( $\text{ft}^3/\text{s}$ )	Barton Creek ( $\text{ft}^3/\text{s}$ )	Williamson Creek ( $\text{ft}^3/\text{s}$ )	Slaughter Creek ( $\text{ft}^3/\text{s}$ )	Bear Creek ( $\text{ft}^3/\text{s}$ )	Onion Creek ( $\text{ft}^3/\text{s}$ )
KCH	7/11/1988	672	47		1.0	0.0	0.1	2.2
KCH	8/11/1988	691	43		1.1	0.0	0.0	11
KCH	2/27/1989	690	27	1.0	0.3	0.0	0.1	2.4
KCH	5/2/1989	693	35	16	0.3	0.0	3.5	5.6
KCH	7/21/1989	676	52	5.8	2.0	0.1	2.1	7.7
KCH	8/29/1989	668	33	0.4	0.0	0.0	0.0	2.7
KCH	2/7/1990	622	22	4.3	8.6	0.0	0.1	1.5
KCH	6/5/1990	665	50	41	7.1	1.0	2.5	80
KCH	8/15/1990	657	30	1.2	0.0	0.0	0.0	2.2
KCH	3/11/1991	642	87	95	6.7	11	14	75
KCH	5/6/1991	636	99	105	10	8.0	20	151
KCH	8/13/1991	650	75	2.5	0.0	0.2	0.4	6.5
KCH	4/29/1992	623	115	104	4.0	5.2	9.8	90
KCH	1/20/1993	652	98	262	16	21	9.0	231
KCH	1/23/1993	650	100	262	16	21	9.0	231
KCH	1/26/1993	652	100	262	16	21	9.0	231
KCH	5/6/1993	641	108	123	1.2	16	10	73
KCH	5/9/1993	639	108	123	1.2	16	10	73
KCH	5/12/1993	641	108	123	1.2	16	10	73
KCH	5/27/1993	644	108	42	0.0	5.0	5.2	32
KCH	8/18/1993	664	86	0.5	0.0	0.0	0.1	0.5
KCH	4/12/1994	652	47	6.9	0.0	0.0	0.3	9.5
KCH	10/10/1994	652	39	476	73	99	33	30
KCH	10/10/1994	660	39	476	73	99	33	30
KCH	10/10/1994	651	39	476	73	99	33	30
KCH	10/11/1994	657	39	476	73	99	33	30
KCH	10/11/1994	654	39	476	73	99	33	30
KCH	10/11/1994	652	39	476	73	99	33	30
KCH	10/12/1994	653	39	476	73	99	33	30
KCH	10/12/1994	653	39	476	73	99	33	30
KCH	10/12/1994	653	39	476	73	99	33	30
KCH	10/12/1994	653	39	476	73	99	33	30
KCH	10/13/1994	655	39	476	73	99	33	30
KCH	10/13/1994	655	39	476	73	99	33	30
KCH	10/14/1994	657	39	476	73	99	33	30
KCH	10/14/1994	657	39	476	73	99	33	30
KCH	10/15/1994	658	39	476	73	99	33	30
KCH	10/15/1994	658	39	476	73	99	33	30
KCH	10/16/1994	660	39	476	73	99	33	30
KCH	6/19/1995	641	102	281	12	108	32	172
KCH	5/6/1996	648	26	0.7	0.0	0.0	0.0	0.5
KCH	7/8/1997	568	113	322	0.9	21	26	510
KCH	4/21/1998	628	98	79	0.0	8.9	7.5	96
KCH	6/9/1999	683	76	35	0.0	1.9	1.6	5.3

**Table A-1.** (cont.) Specific conductance and discharge rates, 1978–2003.

Site ID	Date	Specific conduc- tance ( $\mu\text{S}/\text{cm}$ )	Maximum 10-day discharge rates					Onion Creek ( $\text{ft}^3/\text{s}$ )
			Barton Springs ( $\text{ft}^3/\text{s}$ )	Barton Creek ( $\text{ft}^3/\text{s}$ )	Williamson Creek ( $\text{ft}^3/\text{s}$ )	Slaughter Creek ( $\text{ft}^3/\text{s}$ )	Bear Creek ( $\text{ft}^3/\text{s}$ )	
LWK	8/8/1978	480	24	7.6	14	3.5		
LWK	7/11/1979	499	102	27	5.2	4.7	2.6	18
LWK	8/29/1980	496	40	0.0	0.0	0.0	0.1	1.0
LWK	8/18/1981	499	96	16	0.3	0.3	4.3	14
LWK	8/17/1982	493	46	1.1	0.0	0.0	0.2	1.9
LWK	7/21/1983	499	84		7.7	1.4	22	90
MCH	7/5/1978	540	28		0.0	0.0		
MCH	7/5/1979	540	105	13	0.8	2.9		14
MCH	8/28/1980	570	41	0.0	0.0	0.0	0.1	1.1
MCH	8/11/1981	537	99	11	0.0	0.5	2.2	19
MCH	8/11/1982	528	49	1.1	0.0	0.0	0.3	1.5
MCH	7/20/1983	476	84		7.7	1.4	22	90
MCH	6/19/1985	519	70		2.4	4.0	5.6	145
MCH	8/9/1985	540	64		0.0	0.2	0.9	15
MCH	1/13/1986	537	78		1.5	3.0	5.7	61
MCH	5/1/1986	521	62		59	3.2	6.4	26
MCH	6/24/1986	555	84		13	20	16	216
MCH	9/2/1986	550	62		0.0	0.0	0.4	5.8
MCH	2/10/1987	554	83		1.3	3.4	9.3	81
MCH	5/18/1987	553	100		1.0	0.5	2.3	38
MCH	5/30/1987	512	98		149	93	41	208
MCH	8/17/1987	560	110		0.0	0.0	1.6	34
MCH	2/22/1988	519	64		0.2	0.6	1.2	8.6
MCH	5/3/1988	536	50		1.4	0.1	1.1	7.8
MCH	7/11/1988	557	47		1.0	0.0	0.1	2.2
MCH	8/10/1988	552	43		0.0	0.0	0.0	11
MCH	2/21/1989	584	28	0.9	0.2	0.0	0.1	2.4
MCH	5/2/1989	540	35	16	0.3	0.0	3.5	5.6
MCH	7/24/1989	538	49	3.7	0.0	0.1	1.7	5.0
MCH	8/29/1989	547	33	0.4	0.0	0.0	0.0	2.7
MCH	1/31/1990	587	17	0.7	0.0	0.0	0.0	0.4
MCH	6/12/1990	485	49	41	3.8	0.7	2.5	80
MCH	8/21/1990	542	27	0.9	0.5	0.0	0.0	2.2
MCH	3/13/1991	518	87	74	6.0	8.7	12	65
MCH	5/15/1991	531	99	261	68	38	48	218
MCH	8/13/1991	554	75	2.5	0.0	0.2	0.4	6.5
MCH	4/30/1992	564	115	94	3.5	4.7	8.5	81
MCH	1/22/1993	504	100	262	16	21	9.0	231
MCH	1/25/1993	503	100	262	16	21	9.0	231
MCH	5/8/1993	521	108	123	1.2	16	10	73
MCH	5/11/1993	521	108	123	1.2	16	10	73
MCH	5/15/1993	525	108	123	0.0	16	10	73

**Table A-1.** (cont.) Specific conductance and discharge rates, 1978–2003.

Site ID	Date	Specific conduc- tance ( $\mu\text{S}/\text{cm}$ )	Maximum 10-day discharge rates					Onion Creek ( $\text{ft}^3/\text{s}$ )
			Barton Springs ( $\text{ft}^3/\text{s}$ )	Barton Creek ( $\text{ft}^3/\text{s}$ )	Williamson Creek ( $\text{ft}^3/\text{s}$ )	Slaughter Creek ( $\text{ft}^3/\text{s}$ )	Bear Creek ( $\text{ft}^3/\text{s}$ )	
MCH	8/18/1993	550	86	0.5	0.0	0.0	0.1	0.5
MCH	4/15/1994	506	47	6.7	0.0	0.0	0.3	8.4
MCH	6/14/1995	550	104	347	12	108	32	294
MCH	5/7/1996	555	26	0.7	0.0	0.0	0.0	0.5
MCH	7/8/1997	555	113	322	0.9	21	26	510
MCH	4/22/1998	534	98	76	0.0	8.4	7.2	93
MCH	6/6/1999	545	78	76	0.7	3.4	2.4	7.8
MCH	6/29/2000	538	64	49	0.0	23	5.4	5.2
MCH	6/20/2001	554	96	12	0.0	0.8	1.6	26
MCH	6/4/2002	558	88	7.2	0.0	0.1	0.7	3.8
MCH	5/20/2003	565	102	12	0.0	0.3	1.3	12
PLS	2/26/1988	568	62		0.1	0.6	1.2	8.6
PLS	5/4/1988	574	50		1.4	0.1	1.1	7.8
PLS	7/14/1988	551	47		2.0	0.0	0.8	7.5
PLS	8/11/1988	564	43		1.1	0.0	0.0	11
PLS	2/28/1989	548	27	1.0	0.3	0.0	0.1	2.4
PLS	5/2/1989	582	35	16	0.3	0.0	3.5	5.6
PLS	7/25/1989	572	49	3.1	0.0	0.1	1.6	5.5
PLS	8/30/1989	542	32	0.4	0.0	0.0	0.0	2.7
PLS	2/7/1990	550	22	4.3	8.6	0.0	0.1	1.5
PLS	6/8/1990	559	49	41	3.8	0.8	2.5	80
PLS	8/15/1990	543	30	1.2	0.0	0.0	0.0	2.2
PLS	3/18/1991	533	85	87	7.6	6.4	11	68
PLS	5/15/1991	545	99	261	68	38	48	218
PLS	8/13/1991	558	75	2.5	0.0	0.2	0.4	6.5
PLS	5/1/1992	543	115	85	3.4	4.2	8.1	75
PLS	1/21/1993	560	100	262	16	21	9.0	231
PLS	1/24/1993	559	100	262	16	21	9.0	231
PLS	1/28/1993	559	100	262	16	21	9.0	231
PLS	5/14/1993	555	108	123	1.2	16	10	73
PLS	5/28/1993	559	108	42	0.0	5.0	5.2	32
PLS	8/17/1993	560	87	0.5	0.0	0.0	0.1	0.5
PLS	4/12/1994	546	47	6.9	0.0	0.0	0.3	9.5
PLS	6/19/1995	561	102	281	12	108	32	172
PLS	4/25/1996	544	25	0.7	0.0	0.0	0.1	0.9
PLS	7/8/1997	550	113	322	0.9	21	26	510
PLS	4/21/1998	528	98	79	0.0	8.9	7.5	96
PLS	6/11/1999	564	73	21	0.0	1.4	1.4	4.9
PLS	6/1/2000	573	22	2.7	0.0	0.0	0.1	1.4
PLS	6/8/2001	590	102	26	0.0	1.2	2.7	55
PLS	5/23/2002	570	92	1.9	0.0	0.1	0.4	4.2
PLS	5/21/2003	576	102	12	0.0	0.3	1.3	12

**Table A-1.** (cont.) Specific conductance and discharge rates, 1978–2003.

Site ID	Date	Specific conductance ( $\mu\text{S}/\text{cm}$ )	Maximum 10-day discharge rates					Onion Creek ( $\text{ft}^3/\text{s}$ )
			Barton Springs ( $\text{ft}^3/\text{s}$ )	Barton Creek ( $\text{ft}^3/\text{s}$ )	Williamson Creek ( $\text{ft}^3/\text{s}$ )	Slaughter Creek ( $\text{ft}^3/\text{s}$ )	Bear Creek ( $\text{ft}^3/\text{s}$ )	
RAB	5/6/1993	596	108	123	1.2	16	10	73
RAB	5/9/1993	568	108	123	1.2	16	10	73
RAB	5/12/1993	578	108	123	1.2	16	10	73
RAB	5/27/1993	569	108	42	0.0	5.0	5.2	32
RAB	8/17/1993	570	87	0.5	0.0	0.0	0.1	0.5
RAB	4/15/1994	522	47	6.7	0.0	0.0	0.3	8.4
RAB	6/27/1995	507	98	99	0.0	18	12	96
RAB	5/6/1996	504	26	0.7	0.0	0.0	0.0	0.5
RAB	7/9/1997	542	113	273	0.0	17	23	455
RAB	4/21/1998	525	98	79	0.0	8.9	7.5	96
RAB	6/8/1999	755	77	51	0.0	2.0	2.0	6.8
RAB	5/31/2000	555	23	2.8	0.0	0.0	0.1	1.4
RAB	6/7/2001	532	102	30	0.0	1.3	2.8	58
RAB	6/3/2002	617	88	7.2	0.0	0.1	0.7	3.8
RAB	5/30/2003	1190	98	14	0.0	0.1	0.7	6.1
ROL	6/26/1978	490	32	1.2	0.2	0.1		
ROL	7/10/1979	521	102	27	5.2	4.7	2.6	18
ROL	8/27/1980	559	41	0.1	0.0	0.0	0.1	1.1
ROL	8/4/1981	528	102	21	1.0	1.4	4.2	38
ROL	8/9/1982	532	50	1.1	0.0	0.1	0.4	1.1
ROL	7/18/1983	546	84		7.7	1.4	22	90
ROL	6/20/1985	480	71		1.9	3.2	5.2	116
ROL	8/7/1985	586	65		0.0	0.2	1.0	16
ROL	1/15/1986	610	78		1.5	2.6	5.2	54
ROL	5/2/1986	571	62		59	3.2	6.4	38
ROL	6/23/1986	585	84		13	20	16	216
ROL	9/3/1986	586	61		0.0	0.0	0.4	5.8
ROL	2/9/1987	624	83		1.3	3.4	9.3	81
ROL	5/18/1987	608	100		1.0	0.5	2.3	38
ROL	6/1/1987	598	110		149	93	41	392
ROL	8/17/1987	642	110		0.0	0.0	1.6	34
ROL	2/22/1988	587	64		0.2	0.6	1.2	8.6
ROL	5/6/1988	622	50		1.4	0.1	1.1	7.8
ROL	7/18/1988	585	45		2.0	0.0	0.8	7.5
ROL	8/16/1988	596	45		1.2	0.0	0.0	3.2
ROL	2/27/1989	583	27	1.0	0.3	0.0	0.1	2.4
ROL	5/1/1989	579	36	19	0.3	0.0	3.7	7.3
ROL	7/17/1989	615	55	8.9	2.0	0.2	2.9	12
ROL	8/25/1989	607	34	0.5	0.0	0.0	0.0	3.5
ROL	1/30/1990	572	17	0.6	0.0	0.0	0.0	0.4
ROL	6/12/1990	596	49	41	3.8	0.7	2.5	80
ROL	8/14/1990	608	31	1.6	0.0	0.1	0.0	2.2

**Table A-1.** (cont.) Specific conductance and discharge rates, 1978–2003.

Site ID	Date	Specific conduc- tance ( $\mu\text{S}/\text{cm}$ )	Maximum 10-day discharge rates					Onion Creek ( $\text{ft}^3/\text{s}$ )
			Barton Springs ( $\text{ft}^3/\text{s}$ )	Barton Creek ( $\text{ft}^3/\text{s}$ )	Williamson Creek ( $\text{ft}^3/\text{s}$ )	Slaughter Creek ( $\text{ft}^3/\text{s}$ )	Bear Creek ( $\text{ft}^3/\text{s}$ )	
ROL	3/13/1991	612	87	74	6.0	8.7	12	65
ROL	5/6/1991	585	99	105	10	8.0	20	151
ROL	8/19/1991	638	71	467	107	42	11	58
ROL	4/29/1992	694	115	104	4.0	5.2	9.8	90
ROL	6/23/1992	1160	100	242	7.8	17	20	241
ROL	1/20/1993	654	98	262	16	21	9.0	231
ROL	1/23/1993	630	100	262	16	21	9.0	231
ROL	1/26/1993	625	100	262	16	21	9.0	231
ROL	5/6/1993	635	108	123	1.2	16	10	73
ROL	6/1/1993	642	108	42	0.0	5.0	5.2	32
ROL	8/13/1993	660	88	0.5	0.0	0.0	0.1	0.5
ROL	4/12/1994	597	47	6.9	0.0	0.0	0.3	9.5
SLR	7/11/1978	700	25		0.0	0.0		
SLR	7/5/1979	630	105	13	0.8	2.9		14
SLR	9/4/1980	680	38	0.0	0.0	0.0	0.0	0.5
SLR	8/18/1981	583	96	16	0.3	0.3	4.3	14
SLR	8/17/1982	625	46	1.1	0.0	0.0	0.2	1.9
SLR	7/20/1983	600	84		7.7	1.4	22	90
SLR	5/1/1986	656	62		59	3.2	6.4	26
SLR	6/24/1986	640	84		13	20	16	216
SLR	9/2/1986	655	62		0.0	0.0	0.4	5.8
SLR	2/10/1987	624	83		1.3	3.4	9.3	81
SLR	5/19/1987	642	100		12	2.6	2.8	38
SLR	5/30/1987	635	98		149	93	41	208
SLR	8/18/1987	636	110		0.0	0.0	1.6	34
SLR	2/22/1988	575	64		0.2	0.6	1.2	8.6
SLR	5/3/1988	707	50		1.4	0.1	1.1	7.8
SLR	7/11/1988	721	47		1.0	0.0	0.1	2.2
SLR	8/9/1988	727	43		0.0	0.0	0.0	11
SLR	2/21/1989	736	28	0.9	0.2	0.0	0.1	2.4
SNL	6/26/1978	460	32	1.2	0.2	0.1		
SNL	7/10/1979	525	102	27	5.2	4.7	2.6	18
SNL	8/27/1980	503	41	0.1	0.0	0.0	0.1	1.1
SNL	8/4/1981	462	102	21	1.0	1.4	4.2	38
SNL	8/9/1982	468	50	1.1	0.0	0.1	0.4	1.1
SNL	7/18/1983	494	84		7.7	1.4	22	90
SVE	10/12/1978	820	24	0.4	0.0	0.3		
SVE	7/18/1979	445	100	17	0.9	2.1	2.4	14
SVE	9/8/1980	807	38	0.1	8.8	0.0	0.2	29
SVE	8/19/1981	638	96	35	0.3	0.3	4.3	39
SVE	8/30/1982	1530	43	0.2	0.0	0.0	0.1	2.1
SVE	6/24/1985	838	72		33	28	8.0	300

**Table A-1.** (cont.) Specific conductance and discharge rates, 1978–2003.

Site ID	Date	Specific conduc- tance ( $\mu\text{S}/\text{cm}$ )	Maximum 10-day discharge rates					
			Barton Springs ( $\text{ft}^3/\text{s}$ )	Barton Creek ( $\text{ft}^3/\text{s}$ )	Williamson Creek ( $\text{ft}^3/\text{s}$ )	Slaughter Creek ( $\text{ft}^3/\text{s}$ )	Bear Creek ( $\text{ft}^3/\text{s}$ )	Onion Creek ( $\text{ft}^3/\text{s}$ )
SVE	8/12/1985	936	63		0.0	0.1	0.8	11
SVE	1/15/1986	913	78		1.5	2.6	5.2	54
SVE	5/2/1986	897	62		59	3.2	6.4	38
SVE	6/24/1986	1010	84		13	20	16	216
SVE	8/29/1986	874	64		0.0	0.0	0.4	5.8
SVE	2/10/1987	610	83		1.3	3.4	9.3	81
SVE	5/19/1987	614	100		12	2.6	2.8	38
SVE	5/31/1987	602	105		149	93	41	392
SVE	8/19/1987	603	110		0.0	0.0	1.6	33
SVE	2/24/1988	704	63		0.1	0.6	1.2	8.6
SVE	5/3/1988	833	50		1.4	0.1	1.1	7.8
SVE	7/11/1988	910	47		1.0	0.0	0.1	2.2
SVE	8/9/1988	917	43		0.0	0.0	0.0	11
SVE	2/21/1989	857	28	0.9	0.2	0.0	0.1	2.4
SVE	5/2/1989	897	35	16	0.3	0.0	3.5	5.6
SVE	7/21/1989	975	52	5.8	2.0	0.1	2.1	7.7
SVE	8/25/1989	949	34	0.5	0.0	0.0	0.0	3.5
SVE	1/30/1990	942	17	0.6	0.0	0.0	0.0	0.4
SVE	6/6/1990	979	50	41	7.1	0.8	2.5	80
SVE	8/15/1990	973	30	1.2	0.0	0.0	0.0	2.2
SVE	3/5/1991	916	87	106	8.5	14	15	82
SVE	5/6/1991	907	99	105	10	8.0	20	151
SVE	8/19/1991	796	71	467	107	42	11	58
SVE	4/28/1992	601	115	115	4.7	6.2	11	98
SVE	1/21/1993	620	100	262	16	21	9.0	231
SVE	1/24/1993	616	100	262	16	21	9.0	231
SVE	1/28/1993	618	100	262	16	21	9.0	231
SVE	5/7/1993	616	108	123	1.2	16	10	73
SVE	5/10/1993	625	108	123	1.2	16	10	73
SVE	5/14/1993	623	108	123	1.2	16	10	73
SVE	5/28/1993	626	108	42	0.0	5.0	5.2	32
SVE	8/16/1993	652	87	0.5	0.0	0.0	0.1	0.5
SVE	4/12/1994	1020	47	6.9	0.0	0.0	0.3	9.5
SVE	6/14/1995	867	104	347	12	108	32	294
SVE	5/9/1996	840	25	0.6	0.0	0.0	0.0	0.5
SVE	7/9/1997	674	113	273	0.0	17	23	455
SVE	4/22/1998	596	98	76	0.0	8.4	7.2	93
SVE	6/9/1999	733	76	35	0.0	1.9	1.6	5.3
SVE	5/31/2000	850	23	2.8	0.0	0.0	0.1	1.4
SVE	6/14/2001	770	99	15	0.0	0.9	2.0	33
SVE	8/7/2002	760	105	116	0.0	2.1	11	111
SVE	5/28/2003	626	101	14	0.0	0.1	0.8	7.2

**Table A-1.** (cont.) Specific conductance and discharge rates, 1978–2003.

Site ID	Date	Specific conduc- tance ( $\mu\text{S}/\text{cm}$ )	Maximum 10-day discharge rates					Onion Creek ( $\text{ft}^3/\text{s}$ )
			Barton Springs ( $\text{ft}^3/\text{s}$ )	Barton Creek ( $\text{ft}^3/\text{s}$ )	Williamson Creek ( $\text{ft}^3/\text{s}$ )	Slaughter Creek ( $\text{ft}^3/\text{s}$ )	Bear Creek ( $\text{ft}^3/\text{s}$ )	
SVN	10/13/1978	500	24	0.4	0.0	0.3		
SVN	7/17/1979	480	100	17	0.9	2.1	2.5	16
SVN	8/19/1981	517	96	35	0.3	0.3	4.3	39
SVN	5/17/1982	506	72	1720	194	249	258	1960
SVN	6/20/1985	410	71		1.9	3.2	5.2	116
SVN	8/7/1985	496	65		0.0	0.2	1.0	16
SVN	1/15/1986	466	78		1.5	2.6	5.2	54
SVN	5/2/1986	389	62		59	3.2	6.4	38
SVN	6/24/1986	442	84		13	20	16	216
SVN	8/29/1986	514	64		0.0	0.0	0.4	5.8
SVN	2/10/1987	388	83		1.3	3.4	9.3	81
SVN	5/19/1987	480	100		12	2.6	2.8	38
SVN	5/31/1987	409	105		149	93	41	392
SVN	8/19/1987	630	110		0.0	0.0	1.6	33
SVN	2/24/1988	510	63		0.1	0.6	1.2	8.6
SVN	3/5/1991	560	87	106	8.5	14	15	82
SVN	5/6/1991	547	99	105	10	8.0	20	151
SVN	8/19/1991	480	71	467	107	42	11	58
SVN	4/29/1992	469	115	104	4.0	5.2	9.8	90
SVN	1/20/1993	453	98	262	16	21	9.0	231
SVN	1/23/1993	461	100	262	16	21	9.0	231
SVN	1/26/1993	455	100	262	16	21	9.0	231
SVN	5/6/1993	447	108	123	1.2	16	10	73
SVN	5/9/1993	471	108	123	1.2	16	10	73
SVN	5/12/1993	480	108	123	1.2	16	10	73
SVN	6/1/1993	464	108	42	0.0	5.0	5.2	32
SVN	8/16/1993	549	87	0.5	0.0	0.0	0.1	0.5
SVN	6/19/1995	460	102	281	12	108	32	172
SVN	7/9/1997	533	113	273	0.0	17	23	455
SVN	4/22/1998	507	98	76	0.0	8.4	7.2	93
SVN	6/9/1999	507	76	35	0.0	1.9	1.6	5.3
SVN	6/15/2001	710	98	14	0.0	0.9	2.0	33
SVN	8/7/2002	507	105	116	0.0	2.1	11	111
SVN	5/28/2003	603	101	14	0.0	0.1	0.8	7.2
SVS	8/8/1978	540	24	7.6	14	3.5		
SVS	7/17/1979	580	100	17	0.9	2.1	2.5	16
SVS	8/28/1980	620	41	0.0	0.0	0.0	0.1	1.1
SVS	8/10/1981	585	99	11	0.1	0.6	2.3	20
SVS	10/7/1981	600	84	854	12	3.2	19	1150
SVS	10/8/1981	588	86	854	12	3.2	19	1150
SVS	8/9/1982	584	50	1.1	0.0	0.1	0.4	1.1
SVS	7/19/1983	582	84		7.7	1.4	22	90

**Table A-1.** (cont.) Specific conductance and discharge rates, 1978–2003.

Site ID	Date	Specific conductance ( $\mu\text{S}/\text{cm}$ )	Maximum 10-day discharge rates					Onion Creek ( $\text{ft}^3/\text{s}$ )
			Barton Springs ( $\text{ft}^3/\text{s}$ )	Barton Creek ( $\text{ft}^3/\text{s}$ )	Williamson Creek ( $\text{ft}^3/\text{s}$ )	Slaughter Creek ( $\text{ft}^3/\text{s}$ )	Bear Creek ( $\text{ft}^3/\text{s}$ )	
SVS	6/19/1985	584	70		2.4	4.0	5.6	145
SVS	8/7/1985	592	65		0.0	0.2	1.0	16
SVS	1/13/1986	589	78		1.5	3.0	5.7	61
SVS	5/2/1986	606	62		59	3.2	6.4	38
SVS	6/23/1986	608	84		13	20	16	216
SVS	8/29/1986	596	64		0.0	0.0	0.4	5.8
SVS	2/9/1987	578	83		1.3	3.4	9.3	81
SVS	5/18/1987	616	100		1.0	0.5	2.3	38
SVS	6/1/1987	615	110		149	93	41	392
SVS	8/17/1987	603	110		0.0	0.0	1.6	34
SVS	2/22/1988	593	64		0.2	0.6	1.2	8.6
SVS	5/10/1988	609	50		0.0	0.1	0.7	4.7
SVS	7/14/1988	575	47		2.0	0.0	0.8	7.5
SVS	8/11/1988	607	43		1.1	0.0	0.0	11
SVS	2/21/1989	607	28	0.9	0.2	0.0	0.1	2.4
SVS	5/1/1989	586	36	19	0.3	0.0	3.7	7.3
SVS	7/21/1989	590	52	5.8	2.0	0.1	2.1	7.7
SVS	8/25/1989	595	34	0.5	0.0	0.0	0.0	3.5
SVS	1/30/1990	602	17	0.6	0.0	0.0	0.0	0.4
SVS	6/5/1990	590	50	41	7.1	1.0	2.5	80
SVS	8/14/1990	568	31	1.6	0.0	0.1	0.0	2.2
SVS	3/5/1991	560	87	106	8.5	14	15	82
SVS	5/13/1991	581	99	261	68	38	48	218
SVS	8/14/1991	608	75	4.1	12	5.9	1.7	6.5
SVS	5/1/1992	584	115	85	3.4	4.2	8.1	75
SVS	1/22/1993	603	100	262	16	21	9.0	231
SVS	1/25/1993	610	100	262	16	21	9.0	231
SVS	5/7/1993	614	108	123	1.2	16	10	73
SVS	5/10/1993	613	108	123	1.2	16	10	73
SVS	5/14/1993	614	108	123	1.2	16	10	73
SVS	5/28/1993	615	108	42	0.0	5.0	5.2	32
SVS	8/17/1993	618	87	0.5	0.0	0.0	0.1	0.5
SVS	4/8/1994	594	47	6.9	0.0	0.0	0.3	9.5
SVS	6/19/1995	611	102	281	12	108	32	172
SVS	5/2/1996	592	26	0.7	0.0	0.0	0.1	0.6
SVS	7/8/1997	585	113	322	0.9	21	26	510
SVS	4/22/1998	616	98	76	0.0	8.4	7.2	93
SVS	6/11/1999	599	73	21	0.0	1.4	1.4	4.9
SVS	6/1/2000	610	22	2.7	0.0	0.0	0.1	1.4
SVS	6/18/2001	613	97	13	0.0	0.9	1.9	31
SVS	6/6/2002	622	88	7.2	0.0	0.1	0.7	3.8
SVS	5/19/2003	620	102	13	0.0	0.3	1.3	13

**Table A-1.** (cont.) Specific conductance and discharge rates, 1978–2003.

Site ID	Date	Specific conduc- tance ( $\mu\text{S}/\text{cm}$ )	Maximum 10-day discharge rates					Onion Creek ( $\text{ft}^3/\text{s}$ )
			Barton Springs ( $\text{ft}^3/\text{s}$ )	Barton Creek ( $\text{ft}^3/\text{s}$ )	Williamson Creek ( $\text{ft}^3/\text{s}$ )	Slaughter Creek ( $\text{ft}^3/\text{s}$ )	Bear Creek ( $\text{ft}^3/\text{s}$ )	
SVW	6/27/1978	560	32	0.9	0.2	0.1		
SVW	7/12/1979	620	101	27	5.2	4.7	2.6	18
SVW	8/28/1980	592	41	0.0	0.0	0.0	0.1	1.1
SVW	8/10/1981	569	99	11	0.1	0.6	2.3	20
SVW	8/10/1982	597	49	1.1	0.0	0.1	0.4	1.2
SVW	7/19/1983	601	84		7.7	1.4	22	90
SVW	6/20/1985	611	71		1.9	3.2	5.2	116
SVW	8/9/1985	657	64		0.0	0.2	0.9	15
SVW	1/15/1986	622	78		1.5	2.6	5.2	54
SVW	5/2/1986	623	62		59	3.2	6.4	38
SVW	6/23/1986	638	84		13	20	16	216
SVW	8/29/1986	659	64		0.0	0.0	0.4	5.8
SVW	2/9/1987	591	83		1.3	3.4	9.3	81
SVW	5/18/1987	661	100		1.0	0.5	2.3	38
SVW	6/1/1987	603	110		149	93	41	392
SVW	8/17/1987	614	110		0.0	0.0	1.6	34
SVW	2/22/1988	637	64		0.2	0.6	1.2	8.6
SVW	5/9/1988	690	50		0.2	0.1	1.1	7.8
SVW	7/18/1988	569	45		2.0	0.0	0.8	7.5
SVW	8/11/1988	658	43		1.1	0.0	0.0	11
SVW	2/27/1989	630	27	1.0	0.3	0.0	0.1	2.4
SVW	5/1/1989	708	36	19	0.3	0.0	3.7	7.3
SVW	7/17/1989	650	55	8.9	2.0	0.2	2.9	12
SVW	8/29/1989	678	33	0.4	0.0	0.0	0.0	2.7
SVW	1/30/1990	688	17	0.6	0.0	0.0	0.0	0.4
SVW	6/8/1990	705	49	41	3.8	0.8	2.5	80
SVW	8/15/1990	694	30	1.2	0.0	0.0	0.0	2.2
SVW	3/11/1991	658	87	95	6.7	11	14	75
SVW	5/7/1991	646	99	105	10	8.0	20	151
SVW	8/14/1991	680	75	4.1	12	5.9	1.7	6.5
SVW	4/29/1992	639	115	104	4.0	5.2	9.8	90
SVW	1/22/1993	655	100	262	16	21	9.0	231
SVW	1/25/1993	621	100	262	16	21	9.0	231
SVW	1/28/1993	608	100	262	16	21	9.0	231
SVW	5/11/1993	611	108	123	1.2	16	10	73
SVW	5/15/1993	585	108	123	0.0	16	10	73
SVW	6/1/1993	630	108	42	0.0	5.0	5.2	32
SVW	8/20/1993	670	86	0.4	0.0	0.0	0.0	0.3
SVW	4/11/1994	645	47	6.9	0.0	0.0	0.3	9.5

**Table A-1.** (cont.) Specific conductance and discharge rates, 1978–2003.

Site ID	Date	Specific conduc- tance ( $\mu\text{S}/\text{cm}$ )	Maximum 10-day discharge rates					
			Barton Springs ( $\text{ft}^3/\text{s}$ )	Barton Creek ( $\text{ft}^3/\text{s}$ )	Williamson Creek ( $\text{ft}^3/\text{s}$ )	Slaughter Creek ( $\text{ft}^3/\text{s}$ )	Bear Creek ( $\text{ft}^3/\text{s}$ )	Onion Creek ( $\text{ft}^3/\text{s}$ )
SVW	<b>10/09/94 high resolution sampling, date format is DD HHMM</b>							
SVW	09 0700	570	35	476	73	99	33	30
SVW	09 1305	582	35	476	73	99	33	30
SVW	09 1855	592	35	476	73	99	33	30
SVW	10 0710	611	39	476	73	99	33	30
SVW	10 1300	620	39	476	73	99	33	30
SVW	10 1905	612	39	476	73	99	33	30
SVW	11 0705	624	39	476	73	99	33	30
SVW	11 1305	678	39	476	73	99	33	30
SVW	11 1900	634	39	476	73	99	33	30
SVW	12 0730	600	39	476	73	99	33	30
SVW	12 1900	598	39	476	73	99	33	30
SVW	13 0700	601	39	476	73	99	33	30
SVW	13 1930	619	39	476	73	99	33	30
SVW	14 0730	596	39	476	73	99	33	30
SVW	14 1800	594	39	476	73	99	33	30
SVW	15 1230	645	39	476	73	99	33	30
SVW	6/27/1995	647	98	99	0.0	18	12	96
SVW	5/2/1996	643	26	0.7	0.0	0.0	0.1	0.6
SVW	7/9/1997	580	113	273	0.0	17	23	455
SVW	4/21/1998	568	98	79	0.0	8.9	7.5	96
SVW	6/9/1999	644	76	35	0.0	1.9	1.6	5.3
SVW	6/1/2000	662	22	2.7	0.0	0.0	0.1	1.4
SVW	6/6/2001	659	103	36	0.0	1.4	2.9	64
SVW	6/3/2002	646	88	7.2	0.0	0.1	0.7	3.8
SVW	5/19/2003	644	102	13	0.0	0.3	1.3	13
TNR	7/17/1978	580	24		0.0	0.0		
TNR	7/9/1979	580	103	27	5.2	4.7	2.6	18
TNR	8/29/1980	592	40	0.0	0.0	0.0	0.1	1.0
TNR	8/18/1981	576	96	16	0.3	0.3	4.3	14
TNR	8/16/1982	584	46	1.1	0.0	0.0	0.2	1.9
TNR	7/21/1983	590	84		7.7	1.4	22	90
TNR	6/19/1985	588	70		2.4	4.0	5.6	145
TNR	8/9/1985	604	64		0.0	0.2	0.9	15
TNR	1/13/1986	576	78		1.5	3.0	5.7	61
TNR	5/3/1986	592	62		59	3.2	6.4	38
TNR	6/25/1986	646	84		13	20	16	216
TNR	9/2/1986	607	62		0.0	0.0	0.4	5.8
TNR	2/11/1987	597	80		1.3	3.2	8.9	76
TNR	5/19/1987	605	100		12	2.6	2.8	38
TNR	6/1/1987	595	110		149	93	41	392
TNR	8/18/1987	606	110		0.0	0.0	1.6	34

**Table A-1.** (cont.) Specific conductance and discharge rates, 1978–2003.

Site ID	Date	Specific conduc- tance ( $\mu\text{S}/\text{cm}$ )	Maximum 10-day discharge rates					Onion Creek ( $\text{ft}^3/\text{s}$ )
			Barton Springs ( $\text{ft}^3/\text{s}$ )	Barton Creek ( $\text{ft}^3/\text{s}$ )	Williamson Creek ( $\text{ft}^3/\text{s}$ )	Slaughter Creek ( $\text{ft}^3/\text{s}$ )	Bear Creek ( $\text{ft}^3/\text{s}$ )	
TNR	2/25/1988	597	63		0.1	0.6	1.2	8.6
TNR	5/9/1988	598	50		0.2	0.1	1.1	7.8
TNR	7/18/1988	599	45		2.0	0.0	0.8	7.5
TNR	8/9/1988	600	43		0.0	0.0	0.0	11
TNR	2/23/1989	579	28	0.9	0.3	0.0	0.1	1.4
TNR	5/2/1989	603	35	16	0.3	0.0	3.5	5.6
TNR	7/26/1989	592	48	2.5	0.3	0.0	1.6	5.5
TNR	8/30/1989	590	32	0.4	0.0	0.0	0.0	2.7
TNR	2/7/1990	558	22	4.3	8.6	0.0	0.1	1.5
TNR	4/30/1992	593	115	94	3.5	4.7	8.5	81
WBG	7/10/1978	700	26		0.0	0.0		
WBG	7/5/1979	799	105	13	0.8	2.9		14
WBG	8/28/1980	826	41	0.0	0.0	0.0	0.1	1.1
WBG	8/11/1981	788	99	11	0.0	0.5	2.2	19
WBG	8/10/1982	766	49	1.1	0.0	0.1	0.4	1.2
WBG	7/20/1983	767	84		7.7	1.4	22	90
WGF	6/28/1978	480	31	0.7	0.2	0.1		
WGF	7/17/1979	520	100	17	0.9	2.1	2.5	16
WGF	8/27/1980	500	41	0.1	0.0	0.0	0.1	1.1
WGF	8/10/1981	537	99	11	0.1	0.6	2.3	20
WGF	8/9/1982	505	50	1.1	0.0	0.1	0.4	1.1
WGF	7/19/1983	514	84		7.7	1.4	22	90

See Table 2-1 for information about site identifiers.

**Table A-2.** Results of non-parametric Spearman's rho rank correlation test between specific conductance and flow in five creeks and aquifer flow condition.

Site ID	Specific Conductance	Valid N <sup>1</sup>	Spearman	
	Compared To		Rank ( $\rho$ ) <sup>2</sup>	p-level <sup>3</sup>
BCK	Aquifer flow condition	6	-0.35	0.50
BCK	Barton Creek	5	-0.56	0.32
BCK	Bear Creek	5	-0.10	0.87
BCK	Onion Creek	5	-0.30	0.62
BCK	Slaughter Creek	6	-0.22	0.67
BCK	Williamson Creek	6	0.18	0.74
BDW	Aquifer flow condition	22	-0.20	0.38
BDW	Barton Creek	22	-0.39	0.07
BDW	Bear Creek	22	-0.47	0.03
BDW	Onion Creek	22	-0.38	0.08
BDW	Slaughter Creek	22	-0.37	0.09
BDW	Williamson Creek	22	-0.23	0.31
BPS	Aquifer flow condition	52	0.14	0.33
BPS	Barton Creek	31	0.10	0.61
BPS	Bear Creek	50	-0.07	0.64
BPS	Onion Creek	50	0.00	0.98
BPS	Slaughter Creek	52	-0.03	0.85
BPS	Williamson Creek	52	-0.07	0.62
CNE	Aquifer flow condition	6	0.14	0.78
CNE	Barton Creek	4	0.20	0.80
CNE	Bear Creek	5	0.56	0.32
CNE	Onion Creek	5	0.56	0.32
CNE	Slaughter Creek	6	0.75	0.08
CNE	Williamson Creek	6	0.79	0.06
FMW	Aquifer flow condition	31	-0.72	0.00
FMW	Barton Creek	18	-0.44	0.07
FMW	Bear Creek	31	-0.32	0.08
FMW	Onion Creek	31	-0.48	0.01
FMW	Slaughter Creek	31	-0.55	0.00
FMW	Williamson Creek	31	-0.15	0.41
FOW	Aquifer flow condition	42	0.32	0.04
FOW	Barton Creek	29	0.50	0.01
FOW	Bear Creek	41	0.14	0.40
FOW	Onion Creek	41	0.21	0.20
FOW	Slaughter Creek	42	0.28	0.07
FOW	Williamson Creek	42	0.19	0.24

**Table A-2.** (cont.) Spearman's rho rank correlation results.

Site ID	Specific Conductance Compared To	Spearman		
		Valid N <sup>1</sup>	Rank (rho) <sup>2</sup>	p-level <sup>3</sup>
GHW	<i>Aquifer flow condition</i>	24	0.41	0.05
GHW	<i>Barton Creek</i>	8	0.48	0.23
GHW	<i>Bear Creek</i>	23	0.40	0.06
GHW	<i>Onion Creek</i>	23	0.34	0.12
GHW	<i>Slaughter Creek</i>	24	0.25	0.25
GHW	<i>Williamson Creek</i>	24	0.33	0.11
HND	<i>Aquifer flow condition</i>	15	0.30	0.28
HND	<i>Barton Creek</i>	4	0.80	0.20
HND	<i>Bear Creek</i>	14	-0.32	0.27
HND	<i>Onion Creek</i>	14	-0.44	0.11
HND	<i>Slaughter Creek</i>	15	-0.14	0.63
HND	<i>Williamson Creek</i>	15	-0.34	0.22
HWD	<i>Aquifer flow condition</i>	6	-0.52	0.29
HWD	<i>Barton Creek</i>	5	-0.67	0.22
HWD	<i>Bear Creek</i>	5	-0.90	0.04
HWD	<i>Onion Creek</i>	5	-0.70	0.19
HWD	<i>Slaughter Creek</i>	6	-0.61	0.20
HWD	<i>Williamson Creek</i>	6	-0.76	0.08
ISD	<i>Aquifer flow condition</i>	6	-0.49	0.33
ISD	<i>Barton Creek</i>	4	-0.80	0.20
ISD	<i>Bear Creek</i>	5	-0.20	0.75
ISD	<i>Onion Creek</i>	5	-0.20	0.75
ISD	<i>Slaughter Creek</i>	6	-0.46	0.35
ISD	<i>Williamson Creek</i>	6	-0.27	0.60
JBS	<i>Aquifer flow condition</i>	13	0.16	0.60
JBS	<i>Barton Creek</i>	8	0.07	0.86
JBS	<i>Bear Creek</i>	12	0.20	0.53
JBS	<i>Onion Creek</i>	12	0.24	0.46
JBS	<i>Slaughter Creek</i>	13	0.32	0.29
JBS	<i>Williamson Creek</i>	13	0.27	0.37
KCH	<i>Aquifer flow condition</i>	60	-0.39	0.00
KCH	<i>Barton Creek</i>	45	0.01	0.96
KCH	<i>Bear Creek</i>	59	-0.20	0.14
KCH	<i>Onion Creek</i>	59	-0.47	0.00
KCH	<i>Slaughter Creek</i>	60	-0.26	0.05
KCH	<i>Williamson Creek</i>	60	-0.05	0.71

**Table A-2.** (cont.) Spearman's rho rank correlation results.

Site ID	Specific Conductance Compared To	Spearman		
		Valid N <sup>1</sup>	Rank (rho) <sup>2</sup>	p-level <sup>3</sup>
LWK	Aquifer flow condition	6	0.88	0.02
LWK	Barton Creek	5	0.56	0.32
LWK	Bear Creek	5	0.78	0.12
LWK	Onion Creek	5	0.78	0.12
LWK	Slaughter Creek	6	0.25	0.64
LWK	Williamson Creek	6	0.00	1.00
MCH	Aquifer flow condition	47	-0.12	0.43
MCH	Barton Creek	31	-0.46	0.01
MCH	Bear Creek	45	-0.44	0.00
MCH	Onion Creek	46	-0.42	0.00
MCH	Slaughter Creek	47	-0.43	0.00
MCH	Williamson Creek	47	-0.42	0.00
PLS	Aquifer flow condition	31	0.07	0.70
PLS	Barton Creek	27	0.02	0.93
PLS	Bear Creek	31	-0.02	0.93
PLS	Onion Creek	31	-0.09	0.64
PLS	Slaughter Creek	31	-0.09	0.65
PLS	Williamson Creek	31	-0.17	0.37
RAB	Aquifer flow condition	15	0.18	0.52
RAB	Barton Creek	15	0.10	0.72
RAB	Bear Creek	15	-0.01	0.98
RAB	Onion Creek	15	-0.20	0.46
RAB	Slaughter Creek	15	0.01	0.98
RAB	Williamson Creek	15	0.40	0.14
ROL	Aquifer flow condition	39	0.46	0.00
ROL	Barton Creek	24	0.53	0.01
ROL	Bear Creek	38	0.25	0.14
ROL	Onion Creek	38	0.30	0.07
ROL	Slaughter Creek	39	0.33	0.04
ROL	Williamson Creek	39	0.16	0.33
SLR	Aquifer flow condition	18	-0.63	0.01
SLR	Barton Creek	5	-0.80	0.10
SLR	Bear Creek	16	-0.63	0.01
SLR	Onion Creek	17	-0.41	0.10
SLR	Slaughter Creek	18	-0.44	0.07
SLR	Williamson Creek	18	-0.17	0.50

**Table A-2.** (cont.) Spearman's rho rank correlation results.

Site ID	Specific Conductance Compared To	Spearman		
		Valid N <sup>1</sup>	Rank (rho) <sup>2</sup>	p-level <sup>3</sup>
SNL	<i>Aquifer flow condition</i>	6	0.38	0.46
SNL	<i>Barton Creek</i>	5	0.10	0.87
SNL	<i>Bear Creek</i>	5	-0.30	0.62
SNL	<i>Onion Creek</i>	5	-0.21	0.74
SNL	<i>Slaughter Creek</i>	6	0.20	0.70
SNL	<i>Williamson Creek</i>	6	0.20	0.70
SVE	<i>Aquifer flow condition</i>	48	-0.69	0.00
SVE	<i>Barton Creek</i>	34	-0.50	0.00
SVE	<i>Bear Creek</i>	47	-0.39	0.01
SVE	<i>Onion Creek</i>	47	-0.40	0.01
SVE	<i>Slaughter Creek</i>	48	-0.44	0.00
SVE	<i>Williamson Creek</i>	48	-0.15	0.30
SVN	<i>Aquifer flow condition</i>	34	0.02	0.93
SVN	<i>Barton Creek</i>	23	-0.50	0.01
SVN	<i>Bear Creek</i>	33	-0.35	0.04
SVN	<i>Onion Creek</i>	33	-0.41	0.02
SVN	<i>Slaughter Creek</i>	34	-0.54	0.00
SVN	<i>Williamson Creek</i>	34	-0.63	0.00
SVS	<i>Aquifer flow condition</i>	50	0.29	0.04
SVS	<i>Barton Creek</i>	35	-0.07	0.67
SVS	<i>Bear Creek</i>	49	-0.10	0.49
SVS	<i>Onion Creek</i>	49	-0.10	0.49
SVS	<i>Slaughter Creek</i>	50	0.00	0.98
SVS	<i>Williamson Creek</i>	50	-0.23	0.11
SVW	<i>Aquifer flow condition</i>	64	-0.05	0.68
SVW	<i>Barton Creek</i>	49	-0.39	0.01
SVW	<i>Bear Creek</i>	63	-0.47	0.00
SVW	<i>Onion Creek</i>	63	-0.31	0.01
SVW	<i>Slaughter Creek</i>	64	-0.41	0.00
SVW	<i>Williamson Creek</i>	64	-0.28	0.03
TNR	<i>Aquifer flow condition</i>	26	0.25	0.22
TNR	<i>Barton Creek</i>	10	0.07	0.85
TNR	<i>Bear Creek</i>	25	0.06	0.77
TNR	<i>Onion Creek</i>	25	0.21	0.32
TNR	<i>Slaughter Creek</i>	26	0.00	0.98
TNR	<i>Williamson Creek</i>	26	-0.13	0.53

**Table A-2.** (cont.) Spearman's rho rank correlation results.

Site ID	Specific Conductance Compared To	Spearman		
		Valid N <sup>1</sup>	Rank (rho) <sup>2</sup>	p-level <sup>3</sup>
WBG	<i>Aquifer flow condition</i>	6	0.43	0.40
WBG	<i>Barton Creek</i>	4	-0.20	0.80
WBG	<i>Bear Creek</i>	4	-0.40	0.60
WBG	<i>Onion Creek</i>	5	-0.40	0.50
WBG	<i>Slaughter Creek</i>	6	0.09	0.87
WBG	<i>Williamson Creek</i>	6	0.21	0.69
WGF	<i>Aquifer flow condition</i>	6	0.94	0.00
WGF	<i>Barton Creek</i>	5	0.80	0.10
WGF	<i>Bear Creek</i>	5	0.60	0.28
WGF	<i>Onion Creek</i>	5	0.67	0.22
WGF	<i>Slaughter Creek</i>	6	0.72	0.10
WGF	<i>Williamson Creek</i>	6	0.29	0.58

<sup>1</sup> Number of values used to obtain statistical correlation values

<sup>2</sup> Number ranging from -1 to 1 showing nature and strength of correlation.

<sup>3</sup> Expression of statistical confidence. Values less than 0.05 are statistically significant.

See Table 2-1 for information about site identifiers.

**Table A-3.** Analytical results for dissolved major ions in Barton Springs segment, 1978–2003.

Site ID	Date	pH (standard units)	Specific conductance ( $\mu\text{S}/\text{cm}$ )	Ca (mg/L)	Mg (mg/L)	Na (mg/L)	K (mg/L)	HCO <sub>3</sub> (mg/L)	Cl (mg/L)	SO <sub>4</sub> (mg/L)	NO <sub>3</sub> -N (mg/L)
BCK	08/28/80	7.1	659	67	34	6	2.1	331	9	50	0.2
BCK	08/11/81	7.2	538	70	30	5	1.0	366	8	1	0.8
BCK	08/10/82	6.8	618	64	33	7	2.1	329	9	58	0.4
BDW	03/19/91	7.1	565	85	25	7	0.8	366	12	7	1.1
BDW	01/22/93	6.8	590	88	21	6	0.6	366	10	7	
BDW	01/25/93	6.8	589	88	21	6	0.6	366	10	7	
BDW	08/18/93	6.8	594	96	20	6	0.6	354	9	7	1.6
BDW	04/15/94	7.0	591	90	20	6	0.6	366	10	7	1.6
BDW	06/14/95	7.2	590	83	27	6	0.8	366	9	7	1.1
BDW	04/25/96	7.3	582	92	21	6	0.6	342	10	7	1.6
BDW	07/08/97	7.2	585	75	27	6	0.7	329	10	7	1.3
BDW	04/21/98	7.1	587	80	31	6	0.8	366	10	7	1.4
BDW	06/11/99	7.0	595	88	18	5	0.6	342	11	7	1.5
BDW	06/02/00	7.0	591	88	19	6	0.6	354	9	7	1.4
BDW	06/05/01	7.0	595	79	27	6	0.8	364	9	7	1.1
BDW	06/05/02	7.0	606	90	20	6	0.6	362	10	7	1.3
BDW	05/20/03	7.1	577	76	26	5	0.8	348	9	6	1.0
BPS	08/24/79	7.0	588	73	26	6	1.2	331	11	31	1.4
BPS	08/01/80	7.1	583	72	25	6	1.2	331	10	22	1.6
BPS	08/29/80	7.6	578	73	26	6	1.0	331	11	27	0.3
BPS	07/30/81	7.0	583	74	26	7	1.2	329	10	28	0.1
BPS	08/12/81	7.3	568	74	25	6	1.3	342	10	25	1.2
BPS	07/19/82	7.0	586	75	25	6	1.2	329	11	23	1.5
BPS	07/22/83	7.8	539	76	26	7	1.3	329	12	27	1.4
BPS	02/20/85	7.8	586	77	25	6	1.2	329	11	25	1.4
BPS	08/09/85	7.4	598	74	25	6	1.2	333	11	25	1.4
BPS	01/14/86	7.2	579	75	26	7	1.1	338	11	24	1.4
BPS	06/24/86	7.4	591	75	25	6	1.2	326	9	27	1.5
BPS	09/03/86	7.2	589	75	26	7	1.1	337	11	26	1.4
BPS	02/11/87	7.1	588	76	26	6	1.1	337	12	27	1.4
BPS	08/19/87	7.1	605	76	26	7	1.2	346	10	27	1.4
BPS	02/29/88	7.0	589	77	26	6	1.3	340	11	26	1.4
BPS	08/17/88	7.3	597	74	26	6	1.1	331	11	27	1.4
BPS	02/27/89	7.1	596	73	26	6	1.2	332	10	27	1.3
BPS	07/17/89	7.1	563	75	26	6	1.2	343	10	24	1.3

**Table A-3.** (cont.) Major ion analysis results, Barton Springs segment, 1978–2003.

Site ID	Date	pH (standard units)	Specific conductance ( $\mu\text{S}/\text{cm}$ )	Ca (mg/L)	Mg (mg/L)	Na (mg/L)	K (mg/L)	HCO <sub>3</sub> (mg/L)	Cl (mg/L)	SO <sub>4</sub> (mg/L)	NO <sub>3</sub> -N (mg/L)
BPS	08/29/89	7.0	581	78	26	7	1.1	338	10	25	1.3
BPS	01/29/90	6.9	585	72	25	6	1.2	328	10	26	1.3
BPS	08/14/90	7.1	566	76	26	6	1.1	342	13	25	1.2
BPS	03/22/91	7.2	586	76	24	6	1.3	329	10	27	1.2
BPS	04/30/92	6.9	589	81	24	6	1.2	342	13	28	1.3
BPS	08/28/92	7.2	584	77	24	6	1.3	342	14	27	1.4
BPS	08/19/93	7.4	539	76	25	6	1.1	342	10	26	1.3
BPS	08/20/93	7.0	579	79	25	7	1.2	329	10	26	1.4
BPS	04/14/94	7.1	578	74	24	6	1.2	317	10	25	1.3
BPS	06/14/95	7.2	585	78	25	6	1.2	329	11	23	1.3
BPS	05/09/96	7.2	576	76	26	6	1.1	317	11	25	0.8
BPS	07/08/97	7.2	575	72	24	6	1.2	317	11	24	1.3
BPS	04/22/98	7.1	565	80	23	6	1.1	329	10	24	1.4
BPS	06/11/99	7.0	591	74	24	6	1.1	329	12	25	1.3
BPS	06/02/00	7.1	592	74	24	6	1.1	329	11	25	1.1
BPS	06/12/01	7.1	593	77	24	7	1.3	333	10	25	1.3
BPS	06/06/02	7.1	596	75	24	6	1.1	343	11	25	1.3
CNE	07/24/78	7.3	1040	65	41	93	7.8	290	96	160	0.0
CNE	09/04/80	7.5	1030	61	39	99	7.9	293	98	170	0.0
CNE	08/12/81	7.8	996	59	38	92	8.2	281	92	170	0.0
CNE	08/11/82	7.7	1020	59	39	98	7.3	281	91	180	0.1
CNE	07/21/83	7.6	1060	59	38	97	7.4	281	93	170	0.1
FMW	08/11/81	7.2	531	82	19	5	0.8	342	8	1	1.5
FMW	08/04/82	6.9	566	80	22	6	0.6	342	12	7	1.7
FMW	07/19/83	7.0	568	83	23	6	0.7	342	10	8	1.5
FMW	08/08/85	7.1	567	82	22	6	0.6	350	10	6	1.7
FMW	01/15/86	7.1	545	81	22	5	0.5	346	12	6	1.7
FMW	09/03/86	7.2	568	83	21	6	0.6	353	10	6	1.7
FMW	02/09/87	7.4	552	84	19	4	0.8	348	8	6	1.7
FMW	08/18/87	7.5	564	84	19	5	0.8	350	7	7	1.6
FMW	02/25/88	7.1	573	84	23	6	0.6	354	11	7	1.7
FMW	02/23/89	6.9	560	82	23	6	0.6	340	10	7	1.6
FMW	08/21/89	7.3	587	83	23	6	0.6	356	10	6	1.5
FMW	03/05/91	7.1	571	79	21	6	0.6	354	11	5	1.6
FMW	04/28/92	7.2	545	81	18	5	0.7	329	11	7	1.3
FMW	01/21/93	6.9	536	81	18	4	0.8	342	7	8	
FMW	01/24/93	7.0	537	82	19	5	0.8	342	7	7	

**Table A-3.** (cont.) Major ion analysis results, Barton Springs segment, 1978–2003.

Site ID	Date	pH (standard units)	Specific conductance ( $\mu\text{S}/\text{cm}$ )	Ca (mg/L)	Mg (mg/L)	Na (mg/L)	K (mg/L)	HCO <sub>3</sub> (mg/L)	Cl (mg/L)	SO <sub>4</sub> (mg/L)	NO <sub>3</sub> -N (mg/L)
FMW	01/28/93	6.8	537	86	19	5	0.8	342	7	7	
FMW	05/08/93	7.3	535	86	19	5	0.8	342	7	7	1.4
FMW	08/16/93	7.0	537	87	19	4	0.8	329	7	7	1.5
FMW	04/08/94	7.1	563	79	22	6	0.6	342	10	7	1.7
FOW	06/28/78	7.2	620	73	35	7	1.5	360	15	48	0.7
FOW	07/10/79	6.6	620	77	35	8	1.2	350	15	36	1.1
FOW	08/28/80	7.2	686	78	35	8	1.2	360	15	53	0.1
FOW	08/11/81	7.2	595	75	31	8	0.8	366	16	9	0.9
FOW	08/10/82	7.0	595	72	30	8	0.7	354	16	8	1.1
FOW	07/19/83	7.1	597	75	31	8	0.8	366	16	7	1.1
FOW	08/08/85	7.0	641	80	37	8	1.9	354	15	52	0.7
FOW	01/14/86	7.1	624	75	33	8	0.7	370	20	16	1.0
FOW	09/03/86	7.2	610	75	31	9	0.8	354	17	8	1.1
FOW	02/10/87	7.5	625	76	32	8	0.9	368	12	21	1.0
FOW	08/26/87	7.3	687	75	37	8	1.8	356	14	58	0.8
FOW	08/17/88	7.2	705	76	38	8	1.9	350	14	61	0.6
FOW	02/27/89	6.9	660	77	34	9	1.1	368	15	28	1.0
FOW	02/09/90	7.0	658	77	37	9	1.8	359	14	56	0.8
FOW	05/01/92	6.9	771	84	45	7	4.0	342	14	150	0.2
FOW	01/21/93	6.9	863	80	54	8	5.8	342	10	190	
FOW	01/24/93	7.0	895	85	56	9	4.7	342	12	200	
FOW	05/07/93	7.3	775	75	48	6	4.5	329	9	150	0.1
FOW	04/18/94	6.9	645	78	33	9	1.0	366	18	30	1.1
FOW	06/19/95	7.1	760	78	42	8	3.2	342	13	110	0.5
FOW	05/07/96	7.2	635	81	34	10	1.0	354	18	31	1.0
FOW	07/09/97	7.0	616	71	30	9	0.8	329	18	12	1.1
FOW	04/23/98	7.1	652	89	35	9	0.8	354	18	34	4.6
FOW	06/11/99	7.0	654	75	31	9	0.9	329	19	31	1.2
FOW	06/19/01	7.0	742	77	33	10	0.9	359	18	33	1.1
FOW	06/05/02	6.9	660	75	31	10	0.8	357	18	17	1.2
FOW	05/21/03	6.9	747	87	40	11	1.7	367	19	77	1.2
GHW	07/09/79	7.2	670	80	37	6	1.6	410	13	19	1.0
GHW	08/29/80	7.9	666	78	36	6	1.3	410	12	14	0.0
GHW	08/12/81	7.2	650	78	37	7	1.7	415	16	1	0.7
GHW	08/16/82	6.9	666	80	36	7	1.3	415	12	17	0.9
GHW	07/21/83	7.2	667	88	35	7	1.3	415	14	16	1.1

**Table A-3.** (cont.) Major ion analysis results, Barton Springs segment, 1978–2003.

Site ID	Date	pH (standard units)	Specific conductance ( $\mu\text{S}/\text{cm}$ )	Ca (mg/L)	Mg (mg/L)	Na (mg/L)	K (mg/L)	HCO <sub>3</sub> (mg/L)	Cl (mg/L)	SO <sub>4</sub> (mg/L)	NO <sub>3</sub> -N (mg/L)
GHW	08/09/85	7.1	648	75	35	7	1.5	394	10	19	0.9
GHW	01/13/86	7.0	644	76	38	7	1.4	416	13	15	0.8
GHW	09/02/86	7.3	671	81	36	7	1.3	416	12	16	0.9
GHW	02/11/87	7.2	672	80	37	7	1.5	420	13	16	0.8
GHW	08/19/87	7.1	683	81	37	7	1.5	403	11	17	0.8
GHW	02/24/88	6.9	655	82	38	7	1.6	422	12	17	0.9
GHW	08/10/88	7.1	635	77	37	7	1.4	410	11	15	0.8
GHW	02/23/89	7.1	640	82	37	7	1.4	404	10	16	0.9
GHW	08/30/89	7.1	640	80	36	7	1.4	412	11	14	0.8
HND	07/11/79	6.6	580	88	21	8	1.1	320	15	22	2.1
HND	09/08/80	7.1	559	72	28	6	1.1	340	11	20	0.9
HND	08/11/81	7.2	589	88	20	8	1.1	342	17	13	1.8
HND	08/10/82	7.1	575	72	28	7	1.1	342	12	19	0.9
HND	07/20/83	7.4	475	69	17	7	1.2	268	10	18	0.6
HND	08/08/85	7.1	580	89	21	8	1.1	351	13	22	1.6
HND	01/13/86	7.0	575	83	22	8	1.3	340	14	17	1.5
HND	09/03/86	7.2	600	84	23	8	1.2	338	14	20	2.1
HND	02/11/87	7.2	607	89	19	8	1.3	348	12	20	2.0
HWD	07/09/79	7.1	560	77	22	6	0.9	331	12	17	1.5
HWD	08/28/80	7.1	575	79	21	6	0.9	331	10	13	1.7
HWD	08/18/81	7.2	551	79	23	7	1.1	342	18	1	1.6
HWD	08/04/82	7.1	563	79	24	7	0.9	329	11	12	1.5
HWD	07/22/83	7.5	553	85	23	7	0.9	342	13	12	1.6
ISD	07/11/79	6.9	480	48	25	5	1.2	220	8	21	0.4
ISD	09/04/80	7.3	487	56	27	5	1.0	300	10	15	0.6
ISD	08/12/81	7.3	482	55	27	6	1.1	293	9	15	0.4
ISD	08/11/82	7.0	495	53	27	6	1.0	293	9	17	0.5
ISD	07/22/83	7.8	489	56	28	6	1.2	293	9	16	0.5
JBS	07/16/79	6.7	580	90	20	8	1.2	320	14	32	1.7
JBS	08/27/80	7.4	587	86	20	8	1.1	320	13	26	0.6
JBS	08/04/81	7.3	570	86	21	9	1.1	317	12	30	3.0
JBS	08/09/82	6.9	592	84	20	9	1.1	317	14	31	1.6
JBS	07/18/83	7.4	586	85	21	9	1.2	317	16	28	1.7

**Table A-3.** (cont.) Major ion analysis results, Barton Springs segment, 1978–2003.

Site ID	Date	pH (standard units)	Specific conductance ( $\mu\text{S}/\text{cm}$ )	Ca (mg/L)	Mg (mg/L)	Na (mg/L)	K (mg/L)	HCO <sub>3</sub> (mg/L)	Cl (mg/L)	SO <sub>4</sub> (mg/L)	NO <sub>3</sub> -N (mg/L)
KCH	07/10/79	6.6	620	82	26	13	1.0	320	18	40	6.4
KCH	08/28/80	7.2	660	87	25	16	1.0	310	21	48	4.7
KCH	08/11/81	7.2	621	82	25	16	0.9	329	19	42	4.0
KCH	08/10/82	7.0	652	83	24	16	0.9	317	23	45	4.8
KCH	07/19/83	7.0	670	88	25	17	1.0	329	23	45	4.7
KCH	08/07/85	7.2	635	86	24	14	0.9	322	19	35	4.4
KCH	08/29/86	7.3	674	89	25	15	0.8	328	19	42	4.5
KCH	02/09/87	7.3	641	83	25	14	0.9	325	18	35	7.1
KCH	08/19/87	7.4	675	83	25	14	0.9	322	18	35	8.6
KCH	03/09/88	7.2	655	90	26	18	1.0	316	22	60	4.9
KCH	08/11/88	7.1	691	85	26	18	0.8	318	22	52	4.7
KCH	02/27/89	6.9	690	90	25	18	0.9	325	20	44	4.7
KCH	08/29/89	7.2	668	89	24	18	0.9	326	27	45	4.6
KCH	02/07/90	7.0	622	88	25	15	1.0	325	20	31	4.7
KCH	03/11/91	7.1	642	90	25	14	1.0	342	20	29	4.2
KCH	04/29/92	6.5	623	77	24	12	0.9	329	23	33	3.8
KCH	01/20/93	7.0	652	82	25	16	0.8	317	20	44	
KCH	01/23/93	6.9	650	83	25	15	0.9	317	21	44	
KCH	01/26/93	7.2	652	83	25	16	0.9	317	20	47	
KCH	05/06/93	7.2	641	88	26	15	0.9	317	18	43	4.6
KCH	08/18/93	6.9	664	92	25	15	0.9	317	19	51	4.8
KCH	04/12/94	7.0	652	91	24	15	0.9	317	23	45	5.6
KCH	10/10/94	6.7	652	85	23	15	1.1	317	22	38	5.0
KCH	06/19/95	7.1	641	84	24	15	0.9	305	19	34	5.1
KCH	05/06/96	7.2	648	89	23	16	0.8	305	22	39	5.1
KCH	07/08/97	7.5	568	66	26	9	0.9	293	14	17	3.9
KCH	04/21/98	7.1	628	89	25	15	0.9	305	21	37	5.9
LWK	07/11/79	6.9	499	60	23	6	1.3	270	12	24	1.6
LWK	08/29/80	7.6	496	59	22	6	1.3	270	8	18	0.4
LWK	08/18/81	7.3	499	62	23	7	1.3	293	11	9	1.6
LWK	08/17/82	6.9	493	59	23	7	1.3	268	11	22	1.5
LWK	07/21/83	7.4	499	60	23	7	1.4	281	12	19	1.6
MCH	07/05/79	7.0	540	85	17	8	1.0	320	11	18	1.1
MCH	08/28/80	7.1	570	79	19	6	0.9	320	11	12	1.3
MCH	08/11/81	7.1	537	82	18	7	0.8	329	11	10	0.9
MCH	08/11/82	7.6	528	77	20	7	1.0	329	10	14	1.1
MCH	07/20/83	7.5	476	71	17	7	1.2	268	11	16	0.5
MCH	08/09/85	7.1	540	80	18	7	1.0	305	12	15	0.8

**Table A-3.** (cont.) Major ion analysis results, Barton Springs segment, 1978–2003.

Site ID	Date	pH (standard units)	Specific conduc- tance ( $\mu\text{S}/\text{cm}$ )	Ca (mg/L)	Mg (mg/L)	Na (mg/L)	K (mg/L)	HCO <sub>3</sub> (mg/L)	Cl (mg/L)	SO <sub>4</sub> (mg/L)	NO <sub>3</sub> -N (mg/L)
MCH	01/13/86	7.1	537	79	18	7	0.9	327	12	14	0.9
MCH	09/02/86	7.2	550	85	21	7	3.3	338	12	15	1.1
MCH	02/10/87	7.1	554	87	18	7	0.9	331	12	16	0.9
MCH	08/17/87	7.2	560	84	20	7	1.0	342	11	16	1.0
MCH	02/22/88	7.1	519	81	20	7	1.0	312	12	22	0.8
MCH	08/10/88	7.1	552	78	21	7	0.9	328	11	15	1.0
MCH	02/21/89	7.2	584	83	23	7	1.1	334	11	21	0.9
MCH	08/29/89	7.1	547	81	20	7	1.0	326	13	15	0.9
MCH	01/31/90	6.9	587	81	23	6	0.9	346	10	13	1.2
MCH	03/13/91	7.3	518	81	17	8	1.1	293	14	24	0.6
MCH	04/30/92	6.9	564	94	17	6	0.9	329	15	19	0.8
MCH	01/22/93	6.9	504	75	16	7	1.0	293	11	18	
MCH	01/25/93	6.9	503	75	16	6	0.9	293	10	19	
MCH	05/08/93	7.3	521	81	17	7	1.0	305	11	19	0.5
MCH	08/18/93	6.8	550	83	19	6	1.3	317	10	15	0.9
MCH	04/15/94	7.0	506	71	18	7	1.0	268	12	26	0.5
MCH	06/14/95	7.1	550	89	16	6	0.9	317	10	13	0.5
MCH	05/07/96	7.6	555	80	22	7	0.9	317	10	14	0.9
MCH	07/08/97	7.2	555	87	15	6	0.9	293	10	13	0.7
MCH	04/22/98	7.0	534	83	18	7	0.9	293	11	19	4.0
MCH	06/06/99	7.0	545	83	20	7	0.9	305	12	18	0.8
MCH	06/29/00	7.0	538	79	18	7	1.3	305	11	18	0.7
MCH	06/20/01	6.8	554	80	18	7	1.0	311	12	18	0.6
MCH	06/04/02	7.3	558	73	20	10	1.0	293	14	17	1.0
MCH	05/20/03	7.1	565	85	18	7	1.0	312	12	19	0.7
PLS	02/26/88	7.1	568	74	24	7	1.2	332	12	17	1.5
PLS	08/11/88	7.2	564	73	25	7	1.1	320	11	16	1.4
PLS	02/28/89	7.1	548	75	25	8	1.2	328	11	18	1.4
PLS	08/30/89	7.0	542	76	24	7	1.1	328	11	17	1.4
PLS	02/07/90	7.0	550	76	24	7	1.3	328	10	17	1.5
PLS	03/18/91	7.2	533	76	24	7	1.0	317	12	18	1.5
PLS	05/01/92	7.0	543	79	24	7	1.1	317	15	20	1.4
PLS	01/21/93	6.8	560	72	24	7	1.1	329	12	17	
PLS	01/24/93	7.0	559	73	24	7	1.1	329	12	17	
PLS	01/28/93	6.8	559	77	25	8	1.1	329	12	17	
PLS	08/17/93	6.9	560	78	24	7	1.1	317	11	17	1.4
PLS	04/12/94	7.0	546	78	24	7	1.1	329	12	17	1.6
PLS	06/19/95	7.2	561	75	23	7	1.1	317	12	16	1.5
PLS	04/25/96	6.9	544	76	25	7	1.1	305	11	16	1.5

**Table A-3.** (cont.) Major ion analysis results, Barton Springs segment, 1978–2003.

Site ID	Date	pH (standard units)	Specific conductance ( $\mu\text{S}/\text{cm}$ )	Ca (mg/L)	Mg (mg/L)	Na (mg/L)	K (mg/L)	HCO <sub>3</sub> (mg/L)	Cl (mg/L)	SO <sub>4</sub> (mg/L)	NO <sub>3</sub> -N (mg/L)
PLS	07/08/97	7.3	550	72	24	7	1.1	317	12	16	1.5
PLS	04/21/98	7.1	528	81	25	7	1.1	329	12	17	1.4
PLS	06/01/00	7.1	573	75	24	7	1.0	329	12	17	1.4
PLS	06/08/01	7.0	590	77	24	7	1.1	299	13	19	1.4
PLS	05/23/02	7.1	570	78	24	7	1.1	296	13	18	1.5
PLS	05/21/03	7.0	576	77	24	7	1.2	315	13	17	1.3
RAB	05/06/93	7.3	596	77	25	12	1.6	256	16	81	0.6
RAB	04/15/94	7.3	522	67	21	9	1.2	268	15	37	0.8
RAB	06/27/95	7.4	507	66	19	9	1.2	244	16	31	0.7
RAB	05/06/96	7.3	504	67	21	10	1.2	244	16	37	0.6
RAB	07/09/97	7.2	542	67	22	11	1.4	232	18	49	0.6
RAB	04/21/98	7.3	525	66	20	11	1.3	281	18	33	0.6
RAB	06/08/99	7.2	755	75	23	13	1.5	244	21	70	0.6
RAB	05/31/00	7.2	555	71	21	11	1.3	256	19	51	0.6
RAB	06/07/01	7.2	532	67	21	12	1.3	250	20	41	0.6
RAB	06/03/02	7.3	617	70	21	12	1.5	239	22	48	0.6
RAB	05/30/03	7.0	1190	140	49	27	3.5	271	37	287	0.4
ROL	07/10/79	6.7	521	72	20	7	1.0	290	13	23	1.1
ROL	08/27/80	7.3	559	74	21	7	1.2	320	12	17	0.3
ROL	08/04/81	7.5	528	76	22	8	1.0	305	12	19	1.1
ROL	08/09/82	7.0	532	72	20	8	1.1	293	13	25	1.0
ROL	07/18/83	7.1	546	77	22	8	1.1	293	15	24	1.1
ROL	08/07/85	7.4	586	86	22	9	1.1	320	18	30	1.2
ROL	01/15/86	7.1	610	84	23	9	1.0	310	22	32	1.3
ROL	09/03/86	7.4	586	83	22	9	1.1	312	17	31	1.2
ROL	02/09/87	7.2	624	88	22	10	1.1	316	21	35	1.6
ROL	08/17/87	7.2	642	91	22	10	1.2	321	19	40	1.5
ROL	02/22/88	7.0	587	89	23	10	1.2	326	19	34	1.3
ROL	08/16/88	7.0	596	85	23	9	1.0	314	18	33	1.3
ROL	02/27/89	7.3	583	81	22	9	1.1	309	16	30	1.0
ROL	08/25/89	7.2	607	86	22	10	1.1	318	19	32	1.2
ROL	01/30/90	6.9	572	78	21	9	1.2	300	17	29	1.0
ROL	03/13/91	7.2	612	89	22	11	1.2	317	28	35	1.5
ROL	04/29/92	6.9	694	94	21	14	1.1	317	41	45	2.0
ROL	01/20/93	7.2	654	86	21	12	1.1	317	25	40	
ROL	01/23/93	6.9	630	88	22	12	1.1	317	26	42	
ROL	01/26/93	6.8	625	86	21	12	1.1	317	24	41	

**Table A-3.** (cont.) Major ion analysis results, Barton Springs segment, 1978–2003.

Site ID	Date	pH (standard units)	Specific conductance ( $\mu\text{S}/\text{cm}$ )	Ca (mg/L)	Mg (mg/L)	Na (mg/L)	K (mg/L)	HCO <sub>3</sub> (mg/L)	Cl (mg/L)	SO <sub>4</sub> (mg/L)	NO <sub>3</sub> -N (mg/L)
ROL	05/06/93	7.9	635	93	22	12	1.1	317	26	41	1.4
ROL	08/13/93	6.9	660	98	23	12	1.1	329	25	43	1.5
ROL	04/12/94	7.1	597	88	22	10	1.1	305	22	38	1.2
SLR	07/05/79	6.9	630	100	19	6	0.5	400	9	7	0.3
SLR	09/04/80	7.1	680	100	20	6	0.6	400	9	35	0.5
SLR	08/18/81	7.1	583	97	19	6	0.6	378	9	1	0.5
SLR	08/17/82	7.0	625	98	21	6	0.6	390	9	9	1.2
SLR	07/20/83	7.3	600	98	19	5	0.6	378	9	10	0.7
SLR	09/02/86	7.1	655	110	21	6	0.6	414	10	11	1.1
SLR	02/10/87	7.0	624	110	20	5	0.5	440	10	13	0.7
SLR	08/18/87	7.1	636	100	18	5	0.5	403	9	10	0.4
SLR	02/22/88	7.1	575	100	22	6	0.5	399	9	12	1.1
SLR	08/09/88	7.1	727	110	25	6	0.6	416	9	56	0.1
SLR	02/21/89	7.0	736	105	27	6	0.9	409	8	60	0.1
SNL	06/26/78	7.2	460	67	19	7	1.0	281	15	22	0.4
SNL	07/10/79	6.8	525	70	20	8	1.0	260	15	33	0.5
SNL	08/27/80	7.4	503	65	18	9	1.0	260	14	24	0.1
SNL	08/04/81	7.6	462	65	19	8	1.0	281	11	23	0.4
SNL	08/09/82	7.0	468	62	18	8	1.0	244	14	25	0.3
SNL	07/18/83	7.8	494	67	19	9	1.1	256	14	26	0.1
SVE	07/18/79	6.8	445	58	18	11	2.9	220	14	42	1.0
SVE	08/19/81	7.3	638	74	29	11	2.2	329	12	42	1.3
SVE	08/30/82	7.4	1530	140	80	100	11.0	317	46	570	1.6
SVE	08/12/85	7.2	936	97	38	44	3.8	336	46	160	1.6
SVE	01/15/86	7.1	913	92	37	48	3.2	334	46	160	1.4
SVE	08/29/86	7.1	874	92	35	44	3.0	318	45	130	1.4
SVE	02/10/87	7.4	610	73	30	9	1.7	346	16	38	1.3
SVE	08/19/87	7.5	603	67	28	10	1.8	303	15	26	1.2
SVE	02/24/88	7.1	704	90	34	14	2.7	326	20	96	0.9
SVE	08/09/88	7.0	917	96	40	39	3.7	332	31	170	1.7
SVE	02/21/89	6.9	857	90	37	34	3.5	334	27	150	1.8
SVE	08/25/89	6.9	949	100	39	40	4.0	326	34	180	1.7
SVE	01/30/90	6.9	942	98	41	41	4.3	332	31	190	1.8
SVE	03/05/91	7.3	916	100	38	40	4.2	342	32	180	1.6
SVE	04/28/92	7.1	601	71	29	11	2.0	305	22	48	1.3
SVE	01/21/93	6.9	620	74	29	10	1.5	329	16	43	
SVE	01/24/93	7.0	616	75	29	11	2.3	329	17	50	

**Table A-3.** (cont.) Major ion analysis results, Barton Springs segment, 1978–2003.

Site ID	Date	pH (standard units)	Specific conduc- tance ( $\mu$ S/cm)	Ca (mg/L)	Mg (mg/L)	Na (mg/L)	K (mg/L)	HCO <sub>3</sub> (mg/L)	Cl (mg/L)	SO <sub>4</sub> (mg/L)	NO <sub>3</sub> -N (mg/L)
SVE	01/28/93	6.9	618	76	29	10	1.5	342	16	37	
SVE	05/07/93	7.3	616	80	29	10	1.5	329	17	38	1.6
SVE	08/16/93	7.1	652	85	30	11	2.8	256	15	110	0.4
SVE	04/12/94	7.0	1020	110	46	51	5.7	329	35	250	2.0
SVE	06/14/95	7.1	867	92	32	29	2.3	317	37	97	1.4
SVE	05/09/96	7.4	840	97	36	34	3.4	390	32	140	1.3
SVE	07/09/97	7.2	674	77	29	19	1.9	293	28	57	1.4
SVE	04/22/98	7.2	596	75	30	10	1.5	305	17	36	1.4
SVE	05/31/00	7.2	850	95	34	31	3.1	317	30	134	0.1
SVE	06/14/01	7.1	770	90	31	33	0.1	334	40	93	1.6
SVE	08/07/02	7.0	760	89	30	28	2.0	322	36	79	1.6
SVE	05/28/03	7.1	626	81	28	10	1.5	345	17	32	1.5
SVN	07/17/79	6.8	480	70	18	7	1.4	260	11	25	0.3
SVN	08/19/81	7.2	517	70	20	8	1.3	293	14	16	0.3
SVN	08/07/85	6.9	496	69	18	7	1.3	283	14	22	0.4
SVN	01/15/86	7.4	466	66	19	8	1.0	259	17	21	0.3
SVN	08/29/86	6.8	514	72	19	8	1.2	281	12	24	0.4
SVN	02/10/87	7.3	388	58	5	5	13.0	212	5	15	0.2
SVN	08/19/87	7.4	630	77	17	8	3.2	288	12	32	0.8
SVN	02/24/88	7.2	510	72	21	8	1.3	281	14	32	0.3
SVN	03/05/91	7.5	560	75	19	15	1.5	256	30	44	0.2
SVN	01/20/93	6.9	453	59	15	11	1.4	220	16	32	
SVN	01/23/93	6.8	461	60	15	11	1.4	232	16	31	
SVN	01/26/93	6.8	455	65	16	12	1.6	232	15	32	
SVN	05/06/93	7.5	447	60	16	11	1.2	220	16	29	0.1
SVN	08/16/93	7.1	549	77	20	11	1.5	281	17	34	0.5
SVN	06/19/95	7.1	460	62	16	12	2.0	232	17	25	0.2
SVN	07/09/97	7.2	533	67	18	12	1.6	244	21	30	0.1
SVN	04/22/98	7.4	507	67	18	14	1.2	244	22	42	0.6
SVN	06/15/01	6.8	710	97	21	20	1.3	338	38	50	0.3
SVN	08/07/02	7.2	507	64	17	15	1.6	231	26	33	0.1
SVN	05/28/03	7.2	603	84	20	17	1.4	272	30	45	0.3
SVS	08/08/78	7.0	540	69	30	8	1.3	360	12	6	2.3
SVS	07/17/79	6.8	580	71	25	9	1.2	331	11	17	4.0
SVS	08/28/80	7.0	620	70	28	9	1.2	350	13	5	1.1
SVS	08/10/81	7.3	585	77	27	10	1.2	342	14	7	3.5
SVS	08/09/82	6.7	584	68	29	9	1.3	342	12	7	2.7
SVS	07/19/83	6.9	582	70	30	9	1.3	342	13	9	2.6

**Table A-3.** (cont.) Major ion analysis results, Barton Springs segment, 1978–2003.

Site ID	Date	pH (standard units)	Specific conductance ( $\mu\text{S}/\text{cm}$ )	Ca (mg/L)	Mg (mg/L)	Na (mg/L)	K (mg/L)	HCO <sub>3</sub> (mg/L)	Cl (mg/L)	SO <sub>4</sub> (mg/L)	NO <sub>3</sub> -N (mg/L)
SVS	08/07/85	7.1	592	73	29	9	1.3	360	12	6	2.7
SVS	01/13/86	7.0	589	73	29	9	1.0	356	14	9	3.0
SVS	08/29/86	7.2	596	75	29	10	1.2	356	13	8	3.1
SVS	02/09/87	7.1	578	77	26	10	1.3	350	14	10	3.8
SVS	08/17/87	7.3	603	79	24	10	1.2	350	12	16	3.9
SVS	02/22/88	7.1	593	82	28	10	1.2	362	13	16	4.3
SVS	08/11/88	7.2	607	72	31	10	1.1	353	11	8	2.7
SVS	02/21/89	7.1	607	71	31	9	1.3	348	11	8	2.5
SVS	08/25/89	7.0	595	71	29	10	1.2	356	12	8	2.6
SVS	01/30/90	6.9	602	71	29	9	1.2	356	11	8	2.7
SVS	03/05/91	7.1	560	73	30	9	1.3	354	13	7	2.3
SVS	05/01/92	7.1	584	82	25	9	1.1	342	19	20	3.5
SVS	01/22/93	6.7	603	77	27	9	1.1	366	12	10	
SVS	01/25/93	7.0	610	79	27	9	1.1	366	12	10	
SVS	05/07/93	7.1	614	78	26	9	1.1	366	12	10	3.7
SVS	08/17/93	7.0	618	83	27	9	1.1	366	12	9	3.9
SVS	04/08/94	7.0	594	71	29	9	1.2	354	12	8	3.1
SVS	06/19/95	7.1	611	79	27	10	1.1	342	12	9	3.7
SVS	05/02/96	7.7	592	73	30	10	1.2	329	12	8	3.0
SVS	07/08/97	7.2	585	74	27	9	1.1	342	13	9	3.5
SVS	04/22/98	7.0	616	78	28	10	1.1	354	13	12	3.6
SVS	06/11/99	7.0	599	79	27	9	1.1	342	13	7	3.1
SVS	06/01/00	7.0	610	72	28	9	1.1	354	12	8	2.8
SVS	06/06/02	7.0	622	83	27	9	1.0	359	13	10	3.1
SVS	05/19/03	6.9	620	87	26	9	1.3	333	14	15	2.7
SVW	06/27/78	6.6	560	78	24	10	1.0	331	18	15	1.9
SVW	07/12/79	6.9	620	73	24	21	1.0	340	32	14	1.7
SVW	08/28/80	7.0	592	79	24	9	0.9	342	14	7	1.8
SVW	08/10/81	7.2	569	77	23	9	0.9	329	19	7	1.4
SVW	08/10/82	6.8	597	80	24	10	1.0	329	21	20	1.7
SVW	07/19/83	6.9	601	79	23	12	1.2	317	22	23	1.2
SVW	08/09/85	7.1	657	89	24	14	1.1	348	31	23	1.8
SVW	01/15/86	7.0	622	85	25	13	0.8	331	32	20	1.6
SVW	08/29/86	7.0	659	91	24	12	1.0	359	22	22	2.0
SVW	02/09/87	7.4	591	79	24	11	0.9	331	17	21	1.4
SVW	08/17/87	7.3	614	82	23	12	0.9	337	21	18	1.9
SVW	02/22/88	7.1	637	93	25	14	1.1	354	24	35	1.5
SVW	08/11/88	7.1	658	89	25	12	1.0	353	21	23	2.1
SVW	02/27/89	7.1	630	81	25	12	1.0	337	23	23	1.9

**Table A-3.** (cont.) Major ion analysis results, Barton Springs segment, 1978–2003.

Site ID	Date	pH (standard units)	Specific conduc- tance ( $\mu\text{S}/\text{cm}$ )	Ca (mg/L)	Mg (mg/L)	Na (mg/L)	K (mg/L)	HCO <sub>3</sub> (mg/L)	Cl (mg/L)	SO <sub>4</sub> (mg/L)	NO <sub>3</sub> -N (mg/L)
SVW	08/29/89	7.1	678	93	24	13	1.0	360	28	23	2.1
SVW	01/30/90	6.8	688	93	25	14	1.2	368	26	27	2.3
SVW	03/11/91	7.2	658	90	25	15	0.9	317	37	41	1.5
SVW	04/29/92	7.0	639	82	23	13	1.0	329	29	32	1.6
SVW	01/22/93	6.8	655	86	23	15	1.0	329	31	31	
SVW	01/25/93	6.8	621	82	24	13	1.0	329	25	27	
SVW	01/28/93	6.9	608	79	24	12	0.9	329	24	23	
SVW	08/20/93	6.9	670	98	25	13	0.9	354	23	24	2.1
SVW	04/11/94	7.0	645	94	25	12	1.0	342	27	21	2.8
SVW	<b>10/09/94 high resolution sampling, date format is DD HHMM</b>										
SVW	09 0700	6.3	570	85	18	10	1.5	293	16	23	1.5
SVW	09 1305	6.3	582	86	18	9	1.3	305	17	25	1.5
SVW	09 1855	6.4	592	87	19	9	1.3	317	17	26	1.5
SVW	10 0710	6.3	611	88	19	10	1.2	329	18	27	1.6
SVW	10 1300	6.4	620	89	20	10	1.2	342	18	27	1.6
SVW	10 1905	6.4	612	91	20	10	1.3	329	18	27	1.7
SVW	11 0705	6.8	624	93	21	11	1.1	342	19	27	1.7
SVW	11 1305	7.2	678	97	21	13	1.2	342	26	28	2.2
SVW	11 1900	6.8	634	90	22	12	1.0	317	26	22	2.2
SVW	12 0730	6.8	600	86	23	11	1.2	317	22	18	1.9
SVW	12 1900	7.0	598	80	22	10	1.2	317	23	16	2.0
SVW	13 0700	6.9	601	84	24	11	1.1	317	23	16	2.0
SVW	13 1930	6.9	619	88	24	10	1.2	329	20	22	1.8
SVW	14 0730	7.2	596	79	23	11	1.0	305	23	15	2.1
SVW	15 1230	6.9	645	96	25	12	1.1	342	24	25	2.0
SVW	06/27/95	7.0	647	87	23	13	0.9	329	24	30	1.4
SVW	05/02/96	7.1	643	90	25	13	1.0	354	29	19	2.6
SVW	07/09/97	7.1	580	73	23	9	0.9	281	22	13	2.2
SVW	04/21/98	7.2	568	80	24	9	0.8	305	24	12	2.3
SVW	06/01/00	6.9	662	91	23	10	0.9	354	23	20	2.2
SVW	06/06/01	6.8	659	95	26	13	1.0	348	27	29	1.9
SVW	06/03/02	7.0	646	92	25	12	1.0	331	25	24	2.0
SVW	05/19/03	6.9	644	93	25	13	1.1	364	26	29	1.9
TNR	07/09/79	6.9	580	78	27	6	0.9	360	11	12	1.3
TNR	08/29/80	7.7	592	89	19	12	0.6	360	13	3	1.3
TNR	08/18/81	7.1	576	79	26	7	0.8	366	14	1	1.2
TNR	08/16/82	6.9	584	91	20	7	0.6	366	11	7	1.7
TNR	07/21/83	7.4	590	81	27	7	0.8	366	14	7	1.2
TNR	08/09/85	7.1	604	82	27	7	0.8	366	14	20	1.2

**Table A-3.** (cont.) Major ion analysis results, Barton Springs segment, 1978–2003.

Site ID	Date	pH (standard units)	Specific conductance ( $\mu\text{S}/\text{cm}$ )	Ca (mg/L)	Mg (mg/L)	Na (mg/L)	K (mg/L)	HCO <sub>3</sub> (mg/L)	Cl (mg/L)	SO <sub>4</sub> (mg/L)	NO <sub>3</sub> -N (mg/L)
TNR	01/13/86	7.0	576	73	29	8	0.8	370	13	9	1.1
TNR	09/02/86	7.2	607	89	23	7	0.8	368	13	7	1.4
TNR	02/11/87	7.1	597	79	28	7	0.7	370	11	21	1.1
TNR	08/18/87	7.2	606	84	25	6	0.8	368	12	7	1.4
TNR	02/25/88	7.1	597	93	21	7	0.7	372	12	8	1.7
TNR	08/09/88	7.1	600	92	21	6	0.7	368	10	7	1.7
TNR	02/23/89	6.9	579	92	21	7	0.6	362	10	7	1.6
TNR	08/30/89	7.0	590	93	20	7	0.5	368	10	7	1.6
TNR	02/07/90	6.9	558	94	20	7	0.7	362	9	7	1.7
WBG	07/10/78	6.2	700	62	34	32	3.0	281	28	110	0.0
WBG	07/05/79	7.4	799	63	34	44	3.8	260	23	140	0.1
WBG	08/28/80	7.5	826	64	35	50	4.2	281	38	140	0.0
WBG	08/10/82	6.9	766	62	34	43	3.3	281	32	130	0.1
WBG	07/20/83	7.5	767	61	33	38	2.9	281	29	130	0.1
WGF	06/28/78	6.7	480	62	23	6	1.3	290	15	12	1.1
WGF	07/17/79	6.9	520	73	20	8	1.4	300	11	15	1.5
WGF	08/27/80	7.4	500	64	22	7	1.2	290	11	7	0.6
WGF	08/10/81	7.4	537	74	22	10	1.4	317	18	6	1.6
WGF	08/09/82	7.0	505	62	22	7	1.2	293	15	12	1.3
WGF	07/19/83	7.1	514	66	23	8	1.4	293	16	13	1.7

Samples with > 5% charge balance error were excluded.

See Table 2-1 for information about site identifiers.

## **APPENDIX B. Analytical results for Chapter 3**

This appendix contains the site information and analytical results for Chapter 3. The site information includes site descriptions and cross references with state well numbers and USGS site identifiers (Table B-1). Analytical results for major ion analyses and strontium, oxygen, and hydrogen isotope analyses are also provided (Table B-2).

**Table B-1.** Site information for sites sampled in Chapter 3.

Site ID	Site Type	State well number <sup>1</sup>	USGS site identifier <sup>2</sup>	Comments
MSP	Spring	--	08155500	Main Barton Spring; near diving board
ESP	Spring	--	08155501	Eliza Spring; behind concession stand
OSP	Spring	--	08155503	Old Mill Spring; southeast of pool
USP	Spring	--	08155395	Upper Barton Spring; upstream in creekbed
ALB	Well	LR-58-50-840	300747097475401	Saline zone well referred to in text
BDW	Well	LR-58-57-311	300646097533202	
BPS	Well	LR-58-58-403	300453097503301	
FON	Well	YD-58-50-417	301142097504701	
FOW	Well	YD-58-50-408	301031097515801	Mixes with trinity aquifer water (Chapter 2)
MCH	Well	YD-58-50-704	300813097512101	
PLS	Well	YD-58-50-520	301226097480701	
RAB	Well	YD-58-42-915	301526097463201	
SVE	Well	YD-58-50-216	301356097473301	Sometimes mixes with saline zone (Chapter 2)
SVN	Well	YD-58-50-217	301432097480001	
SVS	Well	YD-58-50-215	301339097483701	
SVW	Well	YD-58-50-211	301423097495901	

<sup>1</sup> For locating wells in Texas Water Development Board databases, among others (e.g., <[http://www.twdb.state.tx.us/GwRD/waterwell/well\\_info.asp](http://www.twdb.state.tx.us/GwRD/waterwell/well_info.asp)>).

<sup>2</sup> For locating wells in United States Geological Survey databases (e.g., <<http://waterdata.usgs.gov/>>).

**Table B-2.** Analytical results for water quality sampling of the Barton Springs segment, 2003–2005.

Site ID	Date	pH (std. units)	Specific conductance (µS/cm)	Ca (mg/L)	Mg (mg/L)	Na (mg/L)	K (mg/L)	HCO <sub>3</sub> (mg/L)	Cl (mg/L)	SO <sub>4</sub> (mg/L)	NO <sub>3</sub> -N (mg/L)	Sr (mg/L)	<sup>87</sup> Sr/ <sup>86</sup> Sr	δ <sup>18</sup> O (‰)	δ <sup>2</sup> H (‰)
MSP	08/06/03	6.9	636	85	18	15	1.3	334	26	28	1.5	0.81	0.70795		-27
MSP	08/20/03	7.1	643	89	22	14	1.3	340	25	27	1.5	0.96			
MSP	09/03/03	7.1	649	84	22	14	1.2	336	26	28	1.5	1.09	0.70795	-4.1	-25
MSP	09/16/03	7.1	637	91	22	16	1.5	323	27	26	1.4	1.22			
MSP	09/25/03	7.2	663	94	24	19	1.4	327	31	29		1.36	0.70795	-4.1	-26
MSP	09/30/03	7.2	656	91	24	17	1.4	350	28	29	1.5	1.38	0.70796		-27
MSP	12/23/03	7.1	678										0.70793		
MSP	06/21/04	7.0	622	91	20	15	1.4	312	26	34	1.1	0.70			
MSP	07/07/04	6.9	643	96	19	14	1.3	340	24	34	1.0	0.56			
MSP	07/21/04	6.8	632	91	20	14	1.3	282	25	33	1.0	0.67	0.70797		
MSP	08/04/04	6.9	622	85	21	14	1.2	317	24	30	1.1	0.74			
MSP	08/25/04	6.9	586	89	22	14	1.2	327	23	28	1.2	0.83	0.70796	-3.9	-25
MSP	09/15/04	6.8	597	88	22	13	1.4	322	23	27	1.3	0.88			
MSP	10/04/04	7.1	638	91	23	14	1.4	317	24	26	1.3	1.00			
MSP	10/23/04	7.0	565	89	23	13	1.3	322	22	26	1.4	1.13			
MSP	11/24/04	7.0	587	95	12	11	1.7	305	16	27	1.7	0.42			
MSP	12/14/04	7.0	650	100	20	13	1.3	343	21	30	1.2	0.63	0.70797		
MSP	01/03/05	7.0	650	95	21	14	1.2	325	22	30	1.2	0.69			
MSP	01/26/05	7.1	645	97	22	14	1.3	316	22	29	1.2	0.74	0.70795	-28	
MSP	02/16/05	7.0	665	96	21	14	1.2	332	24	33	1.2	0.69	0.70796		
MSP	03/09/05	7.0	677	104	20	16	1.3	311	25	35	1.1	0.61	0.70797		
MSP	03/30/05	6.9	655	100	21	16	1.2	328	25	33	1.2	0.68			
MSP	04/20/05	6.8	649	100	21	15	1.3	321	24	29	1.2	0.70			
MSP	05/11/05	6.8	634	95	22	14	1.2	332	23	28	1.2	0.69	0.70796		-26
MSP	06/09/05	6.9	638	88	22	13	1.3	332	22	28	1.3	0.71	0.70795		



**Table B-2. (cont.) Analytical results for water quality sampling of the Barton Springs segment, 2003–2005.**

Site ID	Date	pH (std. units)	Specific conductance (µS/cm)	Ca (mg/L)	Mg (mg/L)	Na (mg/L)	K (mg/L)	HCO <sub>3</sub> (mg/L)	Cl (mg/L)	SO <sub>4</sub> (mg/L)	NO <sub>3</sub> -N (mg/L)	Sr (mg/L)	<sup>87</sup> Sr/ <sup>86</sup> Sr	δ <sup>18</sup> O (‰)	δ <sup>2</sup> H (‰)
OSP	08/06/03	6.8	725	88	21	29	1.7	333	46	42	1.4	0.94	0.70802		-28
OSP	08/20/03	7.1	729	93	25	29	1.5	329	48	42	1.5	1.15			
OSP	09/03/03	7.1	732	88	25	27	1.6	326	47	42	1.5	1.18	0.70800	-4.1	
OSP	09/16/03	7.1	727	91	24	29	1.8	326	45	40	1.5	1.28			
OSP	09/25/03	7.2	744	94	26	32	1.7	323	50	45		1.26	0.70803	-4.1	-28
OSP	09/30/03	7.2	748	91	25	30	1.7	333	48	43	1.5	1.35	0.70800		
OSP	12/23/03	7.1	848												
OSP	06/21/04	7.0	671	89	21	25	1.6	298	41	46	1.0	0.82			
OSP	07/07/04	7.0	698	91	21	26	1.5	289	42	47	0.9	0.71			
OSP	07/21/04	6.9	688	91	22	25	1.6	265	42	46	0.9	0.80			
OSP	08/04/04	7.1	699	85	23	27	1.6	262	44	45	1.0	0.87			
OSP	08/25/04	6.9	677	93	24	30	1.7	318	47	44	1.1	1.00	0.70802	-3.8	-24
OSP	09/15/04	6.7	695								1.2				
OSP	10/04/04	7.1	735								1.3				
OSP	10/23/04	7.1	636	91	24	29	1.7	310	46	43	1.3	1.29			
OSP	11/24/04	7.0	686	96	17	26	1.9	300	40	42	1.5	0.66			
OSP	12/14/04	7.0	716	97	22	26	1.7	353	40	44	1.1	0.79			
OSP	01/03/05	7.0	724	89	23	27	1.5	314	43	45	1.2	0.81			
OSP	01/26/05	7.1	717	92	24	26	1.6	318	41	44	1.2	0.84	0.70802		-21
OSP	02/16/05	7.0	738	95	23	26	1.5	322	43	46	1.2	0.84			
OSP	03/09/05	7.0	737	107	21	15	1.3	312	42	46	1.2	0.64			
OSP	03/30/05	7.0	725	97	24	27	1.5	325	43	45	1.2	0.82			
OSP	04/20/05	7.0	719	103	24	28	1.7	327	42	42	1.3	0.88			
OSP	05/11/05	6.9	723	96	25	28	1.6	331	43	42	1.3	0.87	0.70803		-27
OSP	06/09/05	7.0	731	90	25	28	1.7	331	44	43	1.3	0.88			

**Table B-2. (cont.) Analytical results for water quality sampling of the Barton Springs segment, 2003–2005.**

Site ID	Date	pH (std. units)	Specific conductance (µS/cm)	Ca (mg/L)	Mg (mg/L)	Na (mg/L)	K (mg/L)	HCO <sub>3</sub> (mg/L)	Cl (mg/L)	SO <sub>4</sub> (mg/L)	NO <sub>3</sub> -N (mg/L)	Sr (mg/L)	<sup>87</sup> Sr/ <sup>86</sup> Sr	δ <sup>18</sup> O (‰)	δ <sup>2</sup> H (‰)
ESP	08/06/03	6.8	638	85	19	15	1.3	336	27	28	1.4	0.87	0.70796		-26
ESP	08/20/03	7.1	623	93	22	16	1.3	336	27	26	1.4	1.05			
ESP	09/03/03	7.1	630	87	23	15	1.3	333	27	27	1.4	1.20	0.70795	-4.1	
ESP	09/16/03	7.1	645	90	22	17	1.5	326	27	27	1.4	1.30			
ESP	09/25/03	7.2	675	92	24	21	1.5	331	35	32		1.37	0.70796	-4.0	-23
ESP	09/30/03	7.1	631	90	23	18	1.4	331	29	29	1.5	1.47	0.70795		
ESP	12/23/03	7.1	684												
ESP	06/21/04	7.0	623	92	19	15	1.4	316	26	34	1.0	0.75			
ESP	07/07/04	6.9	647	98	19	14	1.3	311	25	35	0.9	0.61			
ESP	07/21/04	6.8	632	93	20	14	1.3	285	25	33	0.9	0.72			
ESP	08/04/04	7.0	623	83	20	13	1.3	277	25	30	1.0	0.75			
ESP	08/25/04	6.9	586	91	22	15	1.4	326	24	27	1.1	0.89	0.70794	-3.8	-26
ESP	09/15/04	6.8	596								1.2				
ESP	10/04/04	7.1	641								1.3				
ESP	10/23/04	7.1	550	89	23	14	1.3	315	23	27	1.3	1.28			
ESP	11/24/04	6.9	600	100	13	12	1.7	308	17	28	1.6	0.48			
ESP	12/14/04	7.0	651	102	20	13	1.3	328	21	30	1.1	0.67			
ESP	01/03/05	7.0	652	93	20	14	1.2	326	23	30	1.2	0.70			
ESP	01/26/05	7.0	647	96	22	14	1.3	321	23	29	1.2	0.76	0.70795	-26	
ESP	02/16/05	7.0	667	102	22	15	1.2	331	24	33	1.1	0.77			
ESP	03/09/05	7.0	681	103	20	16	1.3	317	25	36	1.1	0.66			
ESP	03/30/05	7.0	658	100	21	16	1.3	322	25	32	1.1	0.71			
ESP	04/20/05	7.0	650	102	21	15	1.3	337	25	29	1.2	0.74			
ESP	05/11/05	7.0	636	92	21	14	1.2	325	23	29	1.2	0.70	0.70796		-23
ESP	06/09/05	7.0	638	89	22	14	1.3	344	23	28	1.2	0.76			

**Table B-2. (cont.) Analytical results for water quality sampling of the Barton Springs segment, 2003–2005.**

Site ID	Date	pH (std. units)	Specific conductance (µS/cm)	Ca (mg/L)	Mg (mg/L)	Na (mg/L)	K (mg/L)	HCO <sub>3</sub> (mg/L)	Cl (mg/L)	SO <sub>4</sub> (mg/L)	NO <sub>3</sub> -N (mg/L)	Sr (mg/L)	<sup>87</sup> Sr/ <sup>86</sup> Sr	δ <sup>18</sup> O (‰)	δ <sup>2</sup> H (‰)
ALB	09/29/03	7.2	2600	125	76	323	13	264	447	534		21.80	0.70806	-4.0	-24
CSC	09/29/03	7.4	522	67	25	8	1.3	292	13	31		7.86		-3.9	
HBG	09/29/03	7.3	516	60	33	6	2.4	311	9	32		15.00		-4.1	
BDW	07/13/04	7.1	609	91	23	6	0.8	354	11	8	1.1	0.15			
BPS	07/16/04	7.2	607	78	25	7	1.2	342	72	37	1.2	10.30			
FON	07/08/04	7.2	445	46	26	6	1.4	233	8	11	0.1	3.67			
FOW	07/09/04	7.1	718	81	34	11	0.9	370	19	32	1.3	0.55			
MCH	07/12/04	6.9	554	86	17	7	1.1	315	13	20	0.5	0.23			
PLS	07/21/04	7.1	580	80	25	7	1.1	305	13	19	1.4	2.50			
RAB	07/07/04	7.3	556	70	20	13	1.2	251	24	38	0.7	0.31			
SVE	07/15/04	7.1	780	89	30	29	2.1	340	38	78	1.7	1.90			
SVN	07/15/04	7.3	580	74	20	19	1.6	248	31	45	0.2	0.25			
SVS	07/16/04	7.1	619	80	26	9	1.1	357	12	9	3.0	0.46			
SVW	07/08/04	6.9	601	77	24	10	0.9	314	22	13	2.0	0.18			
BDW	05/24/05	7.0	606	86	27	6	0.8	363	9	7	1.2	0.23	0.70788	-26	
BPS	05/24/05	7.0	616	81	28	7	1.1	337	11	26	1.2	9.59	0.70789	-23	
FON	05/26/05	7.3	509	56	27	8	1.3	270	15	9	2.7	2.82	0.70827	-26	
FOW	05/26/05	7.1	714	82	38	11	1.1	366	18	41	1.0	5.57	0.70763	-27	
MCH	05/25/05	7.1	561	86	20	8	1.0	314	12	20	0.7	0.26	0.70798	-27	
PLS	05/27/05	7.0	580	80	27	8	1.3	323	13	19	1.4	2.68	0.70788	-25	
RAB	05/23/05	7.4	571	73	24	14	1.3	250	23	46	0.7	0.35	0.70799	-28	
SVE	06/15/05	7.0	717	91	32	21	1.8	332	30	64	1.5	1.54	0.70801	-21	
SVN	06/14/05	7.1	619									0.00	0.70819	-29	
SVS	05/24/05	7.1	624	87	29	10	1.3	354	13	13	3.0	0.45	0.70832	-25	
SVW	05/23/05	7.0	700	99	28	14	1.1	357	26	31	1.8	0.31	0.70816	-21	

Major ion samples analyzed by U.S. Geological Survey. Hydrogen isotope samples analyzed at Southern Methodist University.

## **APPENDIX C. Analytical results for Chapter 4**

This appendix contains the analytical results discussed in Chapter 4.

Analytical results for Main Barton Spring are presented (Table C-1). Results for Eliza Spring, Old Mill Spring, and Upper Barton Spring are also presented (Table C-2).

Omitted from this appendix are the approximately 300 results of hourly monitoring of Main Barton Spring, as well as measurements of stream discharge on the five creeks in the study area. Including these results would have added considerably to the bulk of this thesis. Furthermore, data of this type are not especially useful in hard-copy format. For access to this data, the reader is directed to the URL <http://waterdata.usgs.gov/>. The following USGS site identifiers are useful for obtaining the data: (1) Main Barton Spring, 08155500; (2) Eliza Spring, 08155395; (3) Old Mill Spring, 08155503; (4) Upper Barton Spring, 08155395; (5) Barton Creek, 08155240; (6) Williamson Creek, 08158920; (7) Slaughter Creek, 08158840; (8) Bear Creek, 08158810; and (9) Onion Creek, 08158700.

**Table C-1.** Results of oxygen and hydrogen isotope ratio analyses, with accompanying real-time physical and geochemical data for Main Barton Spring. Composite samples from creeks (not shown here) had values of -5.0‰ SMOW for both Bear Creek and Onion Creek.

<b>Date and Time</b>	<b>Barton Springs discharge (ft<sup>3</sup>/s)</b>	<b>Specific conductance (μS/cm)</b>	<b>Dissolved oxygen (mg/L)</b>	<b>Turbidity (NTU)</b>	<b>δ<sup>18</sup>O (‰)</b>	<b>δ<sup>2</sup>H (‰)</b>
08/25/2004 0800	60	658	6.19	< 0.1 <sup>1</sup>	-3.9	-25
10/23/2004 1400	68	636	6.47	13	-3.9	-
10/24/2004 1000	71	597	6.65	5.4	-4.3	-
10/24/2004 2100	71	573	6.45	3.5	-4.4	-
10/25/2004 1030	71	579	6.28	2.2	-4.5	-29
10/26/2004 0900	70	579	5.95	1.5	-4.5	-
10/27/2004 1100	70	591	5.90	0.4	-4.4	-
10/28/2004 0900	70	596	5.92	0.3	-4.3	-
10/30/2004 1000	73	602	5.93	0.1	-	-29
11/05/2004 1030	73	618	6.09	0.8	-4.1	-

<sup>1</sup> Measured value was less than instrument detection limit.

**Table C-2.** Results of oxygen and hydrogen isotope ratio analyses for Upper Barton, Old Mill, and Eliza Springs.

Date and Time	Upper Barton Spring		Old Mill Spring		Eliza Spring	
	$\delta^{18}\text{O}$ (‰)	$\delta^2\text{H}$ (‰)	$\delta^{18}\text{O}$ (‰)	$\delta^2\text{H}$ (‰)	$\delta^{18}\text{O}$ (‰)	$\delta^2\text{H}$ (‰)
08/25/2004 0800	-3.8	-16	-3.8	-	-3.8	-
10/23/2004 1400	-4.6	-	-3.9	-	-3.9	-
10/24/2004 1000	-	-	-4.0	-	-	-
10/24/2004 2100	-5.2	-38	-4.2	-	-	-
10/25/2004 1030	-	-	-4.2	-	-4.4	-
10/26/2004 0900	-4.6	-	-4.4	-	-	-
10/27/2004 1100	-	-	-4.3	-	-	-
10/28/2004 0900	-4.2	-	-4.2	-	-4.3	-
10/30/2004 1000	-	-	-	-	-	-
11/05/2004 1030	-4.2	-	-4.0	-	-4.1	-

## **APPENDIX D. Quality assurance data**

This appendix presents an analysis of quality assurance and quality control data (QA/QC) associated with this thesis. QA/QC data is used as evidence that methodologies are valid, results are reproducible, and establish the uncertainty in the results reported. This is accomplished using (a) blanks to establish background levels; (b) replicates to ensure reproducibility; and (c) lab standards to determine the efficiency of laboratory analytical methods.

### **D.1. HISTORICAL GROUND-WATER DATA, 1978–2003 (CHAPTER 2)**

#### **D.1.1. Specific conductance data quality assurance**

The quality of specific conductance data was monitored through the National Field Quality Assurance (NFQA) program, which began in 1979. For a summary of results from 1979 through 1997, see Stanley et al. (1998). Because quality control is maintained across the years and across different instruments, long-term measurement uncertainty is estimated at  $\pm 5$  percent, although measurements made after 1999 should have uncertainties of  $\pm 3$  percent (Wagner et al., 2000).

### **D.1.2. Major ion data quality assurance**

Overall, the major ion dataset analyzed in Chapter 2 had poor quality assurance and quality control. Replicates and blanks for major ion and nitrate analyses were infrequently collected until year 2001 (M.E. Dorsey, U.S. Geological Survey, personal communication, 2005). However, the historic dataset contained instances where multiple water samples were collected within several days of each other, with no intervening change in hydrologic condition. These samples from well BPS in 1980, 1981, 1989, and 1993 can be thought of as sequential replicates. Results from these samples indicate that field and analytical techniques were carried out appropriately, with replicate results being within 5 percent of one another. Despite the minimal amount of QA/QC, the analysis of Chapter 2 was performed with the assumption that methods were carried out appropriately.

From year 2001 onward, results of quality-control samples suggest that field techniques were carried out appropriately (Table D-1). The only detection in a blank is calcium at 10  $\mu\text{g/L}$ , which is over three orders of magnitude less than the smallest environmental sample concentration. A replicate sample as well PLS showed essentially identical concentrations.

Throughout the study period, the National Water Quality Laboratory performed ongoing internal quality control, including the use of standard reference materials, laboratory replicates, data review, blind samples, and performance

evaluation studies (Pritt and Raese, 1995). The results of internal NWQL quality control are not part of the published USGS data record.

### **D.1.3. Data screening**

Two additional criteria were used to screen some analytical results from the large historical record used in Chapter 2. First, water analyses with a charge balance error greater than  $\pm 5$  percent were excluded. Second, wells with fewer than six specific conductance measurements were excluded, as they did not provide a sufficient record for statistical analysis.

## **D.2. MAJOR IONS, 2003–2005 (CHAPTER 3)**

Two years of major ion data were analyzed by the USGS and were used in Chapter 3. The USGS National Water Quality Lab (NWQL) in Denver, Colorado maintains a strict internal QA/QC program, including the use of standard reference materials, laboratory replicates, data review, blind samples, and performance evaluation studies (Pritt and Raese, 1995). An external lab QA/QC program was also developed for this major ion analysis, based upon protocols outlined in Wilde et al. (1999). Overall, 10 percent of all collected samples were designated for QA/QC purposes.

Major cation ( $\text{Ca}^{+2}$ ,  $\text{Mg}^{2+}$ ,  $\text{Na}^+$ ,  $\text{K}^+$ ,  $\text{Sr}^{2+}$ ) concentrations, and non-carbonate anion ( $\text{Cl}^-$ ,  $\text{SO}_4^{2-}$ ,  $\text{NO}_3^-$ ) concentrations were analyzed by the NWQL. Carbonate ion ( $\text{HCO}_3^-$ ,  $\text{CO}_3^{2-}$ ) were analyzed by the USGS Austin Water Quality laboratory.

#### **D.2.1. Cations and non-carbonate anions**

Inorganic grade blank water was sampled and processed identically to standard environmental samples. These blank samples are known as field blanks because the blank analysis traces the full analytical procedure, from sample collection to final analysis. The reported level can be thought of as a background concentration level introduced by the cumulative effects of the entire procedure.

Replicate samples were also collected. The style of replicate employed is known as a sequential replicate, wherein samples of water are taken from the same site within minutes of each other. Assuming no very short-term variability in the site (including incompletely mixed waters), this method effectively tests the collection, processing, and analysis chain of analysis.

#### **D.2.2. Carbonate anions**

Carbonate ions ( $\text{HCO}_3^-$  and  $\text{CO}_3^{2-}$ ) were measured using titrimetric methods with sulfuric acid, and carbonate speciation was calculated using the inflection point

method. Quality was assured using field replicates that were sequentially collected and sequentially analyzed.

The USGS National Field Quality Assurance program (e.g., Stanley et al., 1998) is implemented to ensure that carbonate ion measurements from individual USGS water quality laboratories are comparable to one another on a nationwide basis. During the period of study, this program sent sets of unknown samples to USGS offices nationwide. These studies were carried out in May 2004 and May 2005.

### **D.2.3. Summary**

Analysis of this full set of QA/QC data by USGS data evaluators indicated that laboratory techniques were carried out appropriately (B.J. Mahler, U.S. Geological Survey, personal comm., 2005). The USGS does not generally publish results of their QA/QC unless specifically requested by a cooperating agency. These data, however, are of public record and are available on request from the USGS.

## **D.3. STRONTIUM ISOTOPES (CHAPTER 3)**

### **D.3.1. NBS 987 standard**

Analyses of NBS 987 standards (Table D-2) resulted in a mean value of 0.710265 (n=10,  $2\sigma=0.000015$ ). The measured values for the NBS 987 standard may have decreased slightly between December 2003 and July 2005 (Figure D-1).

However, the post-July 2005 measurements remained within the analytical uncertainty of the pre-July 2005 measurements, so a correction was not applied to any analytical results.

### **D.3.2. Laboratory blanks**

Laboratory blanks are a way of measuring the background level, or amount of contamination, introduced by the ambient laboratory environment and the analysis procedure. A laboratory blank is prepared for analysis identically to a normal (i.e., environmental) sample, except that a solution of strontium spike of known molarity and isotopic composition is dispensed instead of sample water. In the same way that an environmental sample is processed, a laboratory blank is dried down, passed through Sr spec resin columns, dried down again, and dispensed onto a tantalum filament (see Appendix E). Blank samples were analyzed by isotope dilution.

Laboratory and analysis procedures added an insignificant amount of strontium to sample analyses. A laboratory blank analysis in July 2004 contained 4 picograms (pg) of strontium, and a laboratory blank in August 2005 contained 7 pg of strontium. For all environmental sample analyses, a minimum of 2  $\mu\text{g}$  (2,000,000 pg) of strontium was dispensed onto a tantalum filament. Thus, the sample-to-blank

ratio is over 200,000:1, which is over 2 orders of magnitude above the generally-accepted minimum 1,000:1 sample-to-blank ratio.

### **D.3.3. Field blank**

A field blank measures the total amount of strontium added by the process of sample collection, processing, and analysis. For a field blank, nanopure water is taken to a sampling site and dispensed into a sampling container. This blank sample is then treated identically to a normal sample, except that a spike solution is added during laboratory work to permit analysis by isotope dilution.

Combined sample collection, processing, and analysis methods added an insignificant amount of strontium to sample analyses. A field blank collected in June 2005 and analyzed in August 2005 contained 150 pg of strontium. Because the analysis procedure involved drying down 5 mL of this sample, this suggests that the entire sampling procedure adds approximately 30 pg/mL of strontium. The smallest dissolved Sr concentration analyzed in this thesis was 200  $\mu\text{g/L}$ , or 200,000 pg/mL. Thus, the sample-to-blank ratio is over 6,000:1—well above the generally-accepted minimum 1,000:1 sample-to-blank ratio.

#### **D.3.4. Replicate Sample**

A replicate analysis was performed in July 2004. Two full separate analyses were performed on water from two separate sample bottles that were collected sequentially from Old Mill Spring (OSP) on September 30, 2003.  $^{87}\text{Sr}/^{86}\text{Sr}$  values from these two analyses were 0.708009 and 0.707996, which are within the 0.000015 external precision used for reported values in this thesis. These data indicate that sample collection, processing, and analysis methods were reproducible.

#### **D.4. OXYGEN ISOTOPES (CHAPTERS 3 AND 4)**

During analysis, approximately 1 primary laboratory standard sample ("Berkeley Tap Water") was analyzed for every 10 environmental samples (Table D-3). All analyses were equal to the accepted standard values, within the standard 0.1‰ external precision. A secondary laboratory standard sample ("BEVO") was also analyzed alongside environmental samples, approximately one standard analyzed for every two environmental samples. The secondary standard measurements were corrected to the accepted standard value, thus correcting for evaporation that may have occurred during sample dispensing and processing.

Two sample bottles were sequentially filled from well YD-58-50-231 on September 30, 2003. Each sample bottle was then analyzed independently in January 2005. The two measured values were  $-3.85\text{‰}$  and  $-3.87\text{‰}$ , which are within the

0.1‰ external precision used for reported values in this thesis. These data indicate that sample collection and analysis methods were reproducible.

#### **D.5. HYDROGEN ISOTOPES (CHAPTERS 3 AND 4)**

Hydrogen analyses were performed by the Stable Isotope Laboratory at Southern Methodist University. This laboratory maintained an internal quality assurance program, summarized as follows: “At least one in-house laboratory standard is analyzed with each set of unknown samples. Isotopic values are determined versus working gas standards that have been calibrated against international standards. International standards are run periodically as a check on the isotopic composition of the working gas standards.” (K. Ferguson, Southern Methodist University, written comm., 2005).

In addition to internal lab quality assurance, 11 replicates were analyzed. Unlike strontium and oxygen replicates, these replicates were “splits” taken from a single sample container by the laboratory. As such, these split replicates do not test for temporal variability in water at the site, or variability in sample collection and processing techniques. However, other sequential replicate analyses described in this appendix suggest that these effects were not of concern for the sites and methods in this thesis.

Results of split replicates (Table D-4) suggest that the standard external precision of 1‰ for  $\delta^2\text{H}$  values may not be large enough to encompass the analytical uncertainty seen in these samples, as nearly 50 percent of the replicates analyses had a difference greater than 1‰. However, these uncertainties did not affect the conclusions reached in this study, as all samples plotted near the global meteoric water line (Figures 3-10 and 4-5).

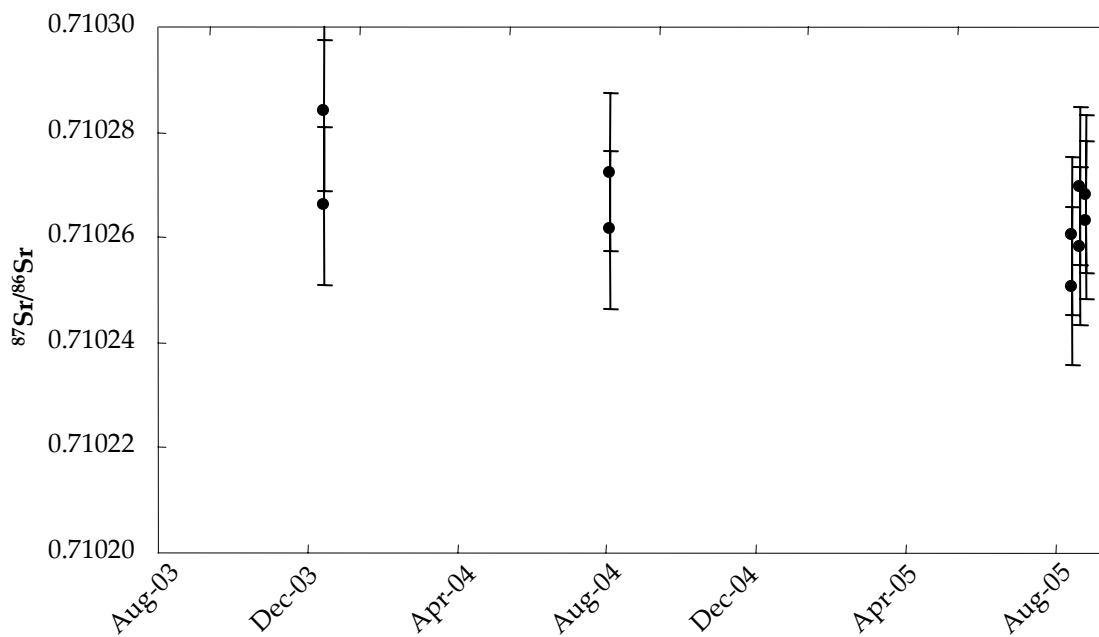


**Figure D-1.** Measurements of the SRM NBS 987 standard as a function of time, using the University of Texas at Austin's Finnigan MAT 261 thermal ionization mass spectrometer. There may be a slight decreasing trend, but any such trend is within the external  $2\sigma$  precision of  $\pm 0.000015$  noted on the diagram.

**Table D-1.** Quality assurance data for the major ion dataset used in Chapter 2.

Site ID	Date	Specific conductance ( $\mu\text{S}/\text{cm}$ )	Ca (mg/L)	Mg (mg/L)	Na (mg/L)	K (mg/L)	HCO <sub>3</sub> (mg/L)	Cl (mg/L)	SO <sub>4</sub> (mg/L)	NO <sub>3</sub> -N (mg/L)
<b>SEQUENTIAL REPLICATES</b>										
BPS	8/1/1980	583	72	25	6	1.2	331	10	22	1.6
BPS	8/29/1980	578	73	26	6	1.0	331	11	27	0.3
BPS	7/30/1981	583	74	26	7	1.2	329	10	28	0.1
BPS	8/12/1981	568	74	25	6	1.3	342	10	25	1.2
BPS	7/17/1989	563	75	26	6	1.2	343	10	24	1.3
BPS	8/29/1989	581	78	26	7	1.1	338	10	25	1.3
BPS	8/19/1993	539	76	25	6	1.1	342	10	26	1.3
BPS	8/20/1993	579	79	25	7	1.2	329	10	26	1.4
<b>BLANK SAMPLES</b>										
SVE	6/14/2001	< 3 <sup>1</sup>	0.02	< .008	< .06	< .09		< .08	< .1	< .05
SVE	8/8/2002	< 3	E 0.01 <sup>2</sup>	< .008	< .09	< .1		< .3	< .1	< .05
<b>REPLICATE SAMPLE</b>										
PLS	5/23/2002	570	78	24	7	1.1	296	13	18	1.5
PLS	5/23/2002	572	78	24	7	1.1		13	18	1.4

<sup>1</sup> Concentration was below detection limit

<sup>2</sup> Concentration was below method reporting level, concentration estimate

**Table D-2.** Analytical results for the SRM NBS 987 standard.

<b>Analysis Date</b>	<b><math>^{87}\text{Sr}/^{86}\text{Sr}</math></b>	<b>Internal precision (<math>2\sigma</math>)</b>
<i>01/05/04</i>	<i>0.710266</i>	<i><math>\pm 0.000007</math></i>
<i>01/05/04</i>	<i>0.710284</i>	<i><math>\pm 0.000008</math></i>
<i>08/17/04</i>	<i>0.710272</i>	<i><math>\pm 0.000008</math></i>
<i>08/17/04</i>	<i>0.710262</i>	<i><math>\pm 0.000008</math></i>
<i>08/07/05</i>	<i>0.710251</i>	<i><math>\pm 0.000008</math></i>
<i>08/07/05</i>	<i>0.710260</i>	<i><math>\pm 0.000008</math></i>
<i>08/14/05</i>	<i>0.710270</i>	<i><math>\pm 0.000008</math></i>
<i>08/14/05</i>	<i>0.710258</i>	<i><math>\pm 0.000007</math></i>
<i>08/17/05</i>	<i>0.710268</i>	<i><math>\pm 0.000007</math></i>
<i>08/17/05</i>	<i>0.710263</i>	<i><math>\pm 0.000007</math></i>
<b>Mean:</b>	<i>0.710265</i>	<i><math>\pm 0.000015</math></i> <b>(external precision)</b>

**Table D-3.** Standards analyzed during  $\delta^{18}\text{O}$  analysis at the University of Texas. The primary standard's accepted value was  $-12.7\text{‰}$  and the secondary standard's accepted value was  $-2.6\text{‰}$ . The secondary standard measurements were corrected to the accepted values, to account for fractionation during analysis.

Analysis date	$\delta^{18}\text{O}$ (‰)	Internal precision ( $2\sigma$ ‰)
<b>"Berkeley Tap Water" primary lab standard</b>		
10/29/03	-12.90	$\pm 0.006$
10/29/03	-12.82	$\pm 0.009$
11/6/03	-12.85	$\pm 0.015$
11/6/03	-12.84	$\pm 0.011$
1/23/05	-12.70	$\pm 0.014$
1/23/05	-12.69	$\pm 0.011$
1/26/05	-12.71	$\pm 0.004$
1/26/05	-12.69	$\pm 0.007$
<b>"BEVO" secondary lab standard</b>		
10/29/03	-2.64	$\pm 0.011$
10/29/03	-2.67	$\pm 0.008$
10/29/03	-2.61	$\pm 0.007$
10/29/03	-2.57	$\pm 0.016$
1/23/05	-2.66	$\pm 0.008$
1/23/05	-2.66	$\pm 0.006$
1/23/05	-2.64	$\pm 0.008$
1/23/05	-2.62	$\pm 0.009$
1/23/05	-2.64	$\pm 0.009$
1/23/05	-2.63	$\pm 0.006$
1/23/05	-2.61	$\pm 0.005$
1/23/05	-2.63	$\pm 0.007$
1/23/05	-2.66	$\pm 0.007$
1/26/05	-2.65	$\pm 0.011$
1/26/05	-2.64	$\pm 0.006$
1/26/05	-2.67	$\pm 0.007$
1/26/05	-2.62	$\pm 0.006$
1/26/05	-2.65	$\pm 0.007$
1/26/05	-2.69	$\pm 0.01$
1/26/05	-2.66	$\pm 0.008$
1/26/05	-2.62	$\pm 0.009$
1/26/05	-2.62	$\pm 0.008$

**Table D-4.** Replicate analysis results for hydrogen isotope samples, analyzed at Southern Methodist University.

Site ID	Sample date	Sample time	$\delta^2\text{H}$ (‰)	$\delta^2\text{H}$ Repeat (‰)	Difference (‰)
<i>MSP</i>	9/3/2003	8:00	-25.2	-26.5	1.3
<i>ESP</i>	9/25/2003	9:30	-22.9	-22.7	0.2
<i>ALB</i>	9/29/2003	9:30	-24.2	-22.5	1.7
<i>ESP</i>	8/25/2004	10:30	-26.1	-26.1	0.1
<i>BPS</i>	5/24/2005	11:30	-23.0	-24.3	1.3
<i>SVW</i>	5/23/2005	12:00	-20.6	-19.7	0.9
<i>FOW</i>	5/26/2005	11:30	-27.4	-25.8	1.6
<i>SVN</i>	6/14/2005	10:00	-21.4	-21.6	0.2
<i>SVE</i>	6/15/2005	12:00	-28.7	-27.3	1.3
<i>USP</i>	5/11/2005	7:30	-22.7	-22.3	0.4
<i>MSP</i>	10/25/2004 <sup>1</sup>	10:30	-29.6	-29.6 <sup>1</sup>	0.0

<sup>1</sup> The first repeat analysis of this sample measured -27.8‰. A third repeat analysis resulted in the reported value.

## **APPENDIX E. Methods for isotopic analysis**

### **E.1. ISOTOPE SAMPLING EQUIPMENT CLEANING**

Prior to collecting a sample, some the following cleaning procedures were carried out on plastic sample bottles:

- 1) 24 hour soak in distilled water + soap solution (“Micro”)
- 2) Thorough rise of each bottle, 5 times
- 3) 24 hour soak in distilled water
- 4) Brief rinse of each bottle
- 5) 48 hour soak in 20 percent nitric acid solution
- 6) Thorough rinse of each bottle, 3 times
- 7) 24 hour soak in deionized (not distilled) water
- 8) Drying in laminar flow vent hood

For glass sample containers (oxygen and hydrogen isotopes), these procedures are the same, except for the omission of steps involving acid rinsing (steps 5 and 6).

### **E.2. SAMPLE COLLECTION**

To collect a sample from a springs, the following steps were performed: (1) rinse the bottle once with water from the collection site; (2) immerse the bottle into

the sample source, filling completely with water; (3) cap and remove the bottle from the sample source; (4) wrap bottle cap with ParaFilm; (5) store in dark, refrigerated conditions.

### **E.3. SAMPLE STORAGE AND DATA MANAGEMENT**

I was responsible for collecting water samples for isotopic analysis (i.e., Chapters 3 and 4). While these samples were collected concurrently with USGS water quality samples, they were not tracked by the USGS National Water Information System (NWIS). At the outset of my graduate education, I issued this challenge to myself: “Never lose track of a sample bottle, and never ambiguously identify a sample bottle or its analytical results.”

Traditionally, scientists use spreadsheets to track water samples and results, but spreadsheets present data management problems. The potential for human error, plus subtle errors arising from manually “copying and pasting” data in spreadsheets can lead to lost and misidentified samples. Also, spreadsheets have limited data summarizing and manipulation abilities.

To keep track of these samples and their analysis results, I designed a relational database. Broadly speaking, the database consisted of four tables: Site, Sample, Result, and Parameter. Additional tables were added to track batches of samples as they were analyzed in the laboratory. For a thorough introduction to the

subject of relational databases, consider an introductory level database textbook such as Silberschatz et al. (2002).

Despite having a digital database with all sample information, sample bottles had self-explanatory labels that contained all of the information needed to positively identify a sample, in the event of catastrophic digital data loss. The sample label contained (1) site name; (2) sampling date and time; (3) typical analysis for this container; (4) whether the sample was filtered and acidified; (5) whether the sample has been analyzed or not; (6) whether the sample has been placed into archival storage; and (7) a unique numeric sample identifier that cross-referenced to the relational database.

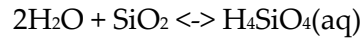
#### **E.4. HOLDING TIME CONSIDERATIONS**

Some isotope samples were stored for up to 23 months before being analyzed. When water is removed from its original environment and placed in a sample container, it can undergo alterations to its chemical and isotopic composition. Therefore, it is important to consider whether isotopic ratio being measured could have changed in the sample bottle during this time.

Strontium isotope ratios for samples in this thesis were unlikely to change measurably while the water was stored in its sample container. Decay of  $^{87}\text{Rb}$  to  $^{87}\text{Sr}$  is very slow ( $t_{1/2} = 48.8 \text{ Ga}$ ), and ratios will not change measurably during our

lifetime (McNutt, 2000). There are natural processes that can fractionate Sr isotopes (thus altering the  $^{87}\text{Sr}/^{86}\text{Sr}$  ratio), but the effects are negligible (Banner and Kaufman, 1994). Thus, Sr isotope analyses of water samples are not measurably affected by processes such as evaporation, biological activity, and mineral precipitation. However, Sr isotopic ratios of waters can be significantly (i.e., measurably) affected by mineral dissolution, ion exchange with clays, and leaching from sample containers. Mineral dissolution and ion exchange are not significant post-collection processes for this thesis' samples, as the sample waters either had low turbidity (< 2 NTU) or were filtered to remove particulates. Leaching from the sample container was minimized by pre-cleaning the containers with a strong, trace element grade  $\text{HNO}_3$  nitric acid solution.

Oxygen and hydrogen isotope ratios are unlikely to measurably change while water is held in a sample container. Evaporation is the most significant concern for fractionation in these samples, and was prevented by using glass containers wrapped with ParaFilm and ensuring there was zero headspace (no air) in the container after sampling. Oxygen and hydrogen also can be modified by exchange with solid minerals including silicate clays, carbonate minerals, and even the glass walls of a sample container. This is because of the hydrolysis reaction



where there is an exchange of oxygen atoms between water molecules and quartz. However, the amount of oxygen in water (56 mol/L) which is much larger than the typical molarity of all dissolved ions in most natural waters (say, 0.001 to 0.010 mol/L). Furthermore, the kinetics of isotope exchange between quartz and water are very slow; a study by Longinelli et al. (2004) found that glass from a sunken ship had only developed a 900 nanometer zone of alteration after 1800 years of exposure to an infinite reservoir of seawater.

#### **E.5. SAMPLE ANALYSIS**

Strontium isotope samples were analyzed at The University of Texas at Austin. Each sample was evaporated and then redissolved in 3N HNO<sub>3</sub>. This solution was passed through a Sr-spec resin column to selectively sequester dissolved Sr<sup>2+</sup>. Sr<sup>2+</sup> was eluted from the column using 0.1N HNO<sub>3</sub>. The eluted solution was evaporated, redissolved in 0.01N phosphoric acid, and dispensed onto a tantalum filament. The filament was placed into a Finnigan MAT 261 thermal ionization mass spectrometer. The heated, ionized sample was analyzed in dynamic collection mode. To correct for strontium fractionation during ionization, the measured <sup>84</sup>Sr/<sup>88</sup>Sr ratio was corrected to a value of 0.1194, and the other ratios (namely, <sup>87</sup>Sr/<sup>86</sup>Sr) were corrected using an exponential fractionation law (Banner and

Kaufman, 1994). Standard samples, blank water samples, and a replicate sample were analyzed in order to ensure precision and accuracy (see Appendix D).

Oxygen isotope samples were analyzed at The University of Texas at Austin. Samples were dispensed into glass vials filled with carbon dioxide gas, and were allowed to equilibrate with this gas for 8 hours at 40°C. The carbon dioxide gas was fed into a light isotope mass spectrometer alternately with a reference gas of known isotopic composition (Epstein and Mayeda, 1953). Approximately one third of analyzed samples were internal lab standards, and external precision was estimated to be  $\pm 0.1\text{‰}$  or better (see Appendix D).

Hydrogen isotope samples were analyzed at Southern Methodist University. Samples were passed over depleted uranium metal at 800°C (Bigeleisen et al., 1952), which reduced the hydrogen in the water molecule to H<sub>2</sub> gas. The H<sub>2</sub> gas was collected onto activated carbon, and then analyzed by mass spectrometer. Internal laboratory standards were analyzed frequently, but not reported by the lab. The lab reports that results from standard and duplicate analyses define an analytical precision of  $\pm 1.2 \text{‰}$  or better (see Appendix D)

## E.6. RESULTS REPORTING

Strontium isotope ratios are reported as the ratio of  $^{87}\text{Sr}$  to  $^{86}\text{Sr}$  ( $^{87}\text{Sr}/^{86}\text{Sr}$ ).

Oxygen and hydrogen isotopes are reported using delta notation (Gonfiantini, 1981; Coplen, 1994), and are referenced to standard mean ocean water (SMOW).



**Figure E-1.** Samples that required filtration were pumped through a 0.45  $\mu\text{m}$  cellulose filter that was placed in a polycarbonate housing. Tygon tubing and a peristaltic pump was used to pump water, typically from a 3 liter Teflon bottle or a 1 liter polypropylene bottle.

## REFERENCES

- Abbott, P.L. (1975) On the hydrology of the Edwards Limestone, south-central Texas: *Journal of Hydrology*, v. 24, p. 251-269.
- Andrews, F.L., Schertz, T.L., Slade, R.M., Jr., and Rawson, J. (1984) Effects of storm-water runoff on water quality of the Edwards aquifer near Austin, Texas: U.S. Geological Survey Water-Resources Investigations Report 84-4124, 50 p.
- Ashton, K. (1966) The analysis of flow data from karst drainage systems: *Transactions of the Cave Research Group*, v. 7, p. 167-203.
- Asquith, W.H., and Gary, M.O. (2005) Acoustic doppler velocity monitoring within Main Spring, Barton Springs, Austin, Texas, April–September 2004—Enhancing the accuracy of springflow data: U.S. Geological Survey Fact Sheet 2005-3044, 4 p.
- Atkinson, T.C. (1977) Diffuse flow and conduit flow in limestone terrain in the Mendip Hills, Somerset (Great Britain): *Journal of Hydrology*, v. 35, p. 93-110.
- Austin American-Statesman, 2003, Toxic chemicals taint Barton waters: Austin, Texas, p. A1.
- Back, W. (1961) Techniques for mapping of hydrochemical facies: U.S. Geological Survey Professional Paper, p. 380-382.
- Banner, J.L. (2004) Radiogenic isotopes—Systematics and applications to earth surface processes and chemical stratigraphy: *Earth-Science Reviews*, v. 65, p. 141-194.
- Banner, J.L., Guilfoyle, A., Musgrove, M., and James, E.W. (2004) Seasonal variations in modern speleothem calcite growth: Abstracts With Programs—Geological Society of America, v. 36, p. 305.
- Banner, J.L., and Hanson, G.N. (1990) Calculation of simultaneous isotopic and trace element variations during water-rock interaction with applications to carbonate diagenesis: *Geochimica et Cosmochimica Acta*, v. 54, p. 3123-3127.

- Banner, J.L., and Kaufman, J. (1994) The isotopic record of ocean chemistry and diagenesis preserved in non-luminescent brachiopods from Mississippian carbonate rocks, Illinois and Missouri: *Geological Society of America Bulletin*, v. 106, p. 1074-1082.
- Banner, J.L., Musgrove, M., Asmerom, Y., Edwards, R.L., and Hoff, J.A. (1996) High-resolution temporal record of Holocene ground-water chemistry—Tracing links between climate and hydrology: *Geology*, v. 24, p. 1049-1053.
- Banner, J.L., Musgrove, M., and Capo, R.C. (1994) Tracing ground-water evolution in a limestone aquifer using Sr isotopes—Effects of multiple sources of dissolved ions and mineral-solution reactions: *Geology*, v. 22, p. 687-690.
- Banner, J.L., Wasserburg, G.J., Dobson, P.F., Carpenter, A.B., and Moore, C.H. (1989) Isotopic and trace element constraints on the origin and evolution of saline groundwaters from central Missouri: *Geochimica et Cosmochimica Acta*, v. 53, p. 383-398.
- Barrett, M.E. (1996) A parsimonious model for simulation of flow and transport in a karst aquifer, unpublished PhD dissertation, University of Texas, Austin, Texas, 180 p.
- Barrett, M.E., and Charbeneau, R.J. (1997) A parsimonious model for simulating flow in a karst aquifer: *Journal of Hydrology*, v. 196, p. 47-65.
- Bigeleisen, J., Perlman, M.L., and Prosser, H.C. (1952) Conversion of hydrogenic materials for isotopic analysis: *Analytical Chemistry*, v. 24, p. 1356.
- Bishop, P.K., and Lloyd, J.W. (1990) Chemical and isotopic evidence for hydrogeochemical processes occurring in the Lincolnshire Limestone: *Journal of Hydrology*, v. 121, p. 293-320.
- Buchanan, T.J., and Somers, W.P. (1969) Discharge measurements at gaging stations: U.S. Geological Survey Techniques of Water-Resources Investigations book 3, chap. A8, 65 p.
- Burke, W.H., Denison, R.E., Hetherington, E.A., Koepnick, R.B., Nelson, H.F., and Otto, J.B. (1982) Variation of seawater  $^{87}\text{Sr}/^{86}\text{Sr}$  throughout Phanerozoic time: *Geology*, v. 10, p. 516-519.

- Buttle, J.M. (1994) Isotope hydrograph separations and rapid delivery of pre-event water from drainage basins: *Progress in Physical Geography*, v. 18, p. 16-41.
- Cane, G., and Clark, I.D. (1999) Tracing ground water recharge in an agricultural watershed with isotopes: *Ground Water*, v. 37, p. 133-139.
- Capo, R.C., and DePaolo, D.J. (1992) Homogeneity of Sr isotopes in the oceans: *Transactions—American Geophysical Union*, v. 73, p. 272.
- Christian, L.N. (in preparation) Geochemical constraints of Austin-area streamwater evolution—An investigation of urbanization using Strontium isotopes, unpublished M.S. thesis, University of Texas, Austin, Texas.
- Ciais, P., and Jouzel, J. (1994) Deuterium and oxygen 18 in precipitation—Isotopic model, including mixed cloud processes: *Journal of Geophysical Research*, v. 99, p. 16793-16803.
- City of Austin (1997) *The Barton Creek Report: Water Quality Report Series*, 460 p.
- Clark, I.D., and Fritz, P. (1997) *Environmental isotopes in hydrogeology*, Lewis Publishers, Boca Raton, Florida, 328 p.
- Clement, T.J. (1989) Hydrochemical facies in the badwater zone of the Edwards aquifer, central Texas, unpublished M.A. thesis, University of Texas, Austin, Texas, 168 p.
- Cooke, M.J. (2005) Soil formation and erosion in central Texas—Insights from relict soils and cave deposits, unpublished PhD dissertation, University of Texas, Austin, Texas, 219 p.
- Cooke, M.J., Stern, L.A., Banner, J.L., Mack, L.E., Stafford, T.W., Jr., and Toomey, R.S. (2003) Precise timing and rate of massive late Quaternary soil denudation: *Geology*, v. 31, p. 853-856.
- Coplen, T.B. (1994) Reporting of stable hydrogen, carbon, and oxygen isotopic abundances: *Pure and Applied Chemistry*, v. 66, p. 273-276.
- Craig, H. (1961) Isotopic variations in meteoric waters: *Science*, v. 133, p. 1702-1703.
- Darling, W.G., and Bath, A.H. (1988) A stable isotope study of recharge processes in the English Chalk: *Journal of Hydrology*, v. 101, p. 31-46.

- Deike, R.G. (1987) Comparative petrology of cores from two test wells in the eastern part of the Edwards aquifer, south-central Texas: U.S. Geological Survey Water-Resources Investigations Report 87-4266, 142 p.
- Desmarais, K., and Rojstaczer, S. (2002) Inferring source waters from measurements of carbonate spring responses to storms: *Journal of Hydrology*, v. 260, p. 118-134.
- Dreiss, S.J. (1989) Regional scale transport in a karst aquifer—1. Component separation of spring flow hydrographs: *Water Resources Research*, v. 25, p. 117-125.
- Droste, R.L. (1997) *Theory and practice of water and wastewater treatment*, John Wiley and Sons, New York, New York, 800 p.
- Eagleson, P.S. (1991) Hydrologic science—A distinct geoscience: *Reviews of Geophysics*, v. 29, p. 237-248.
- Edmunds, W.M., and Walton, N.G.R. (1983) The Lincolnshire Limestone—Hydrochemical evolution over a ten year period: *Journal of Hydrology*, v. 61, p. 201-211.
- Edwards Aquifer Authority (2004) Edwards Aquifer Authority hydrologic data report for 2004: accessed 4 Dec. 2005  
<[http://edwardsaquifer.org/pdfs/Hydro%20Reports/Hydro\\_Rept04.pdf](http://edwardsaquifer.org/pdfs/Hydro%20Reports/Hydro_Rept04.pdf)>.
- Epstein, S., and Mayeda, T.K. (1953) Variations of the  $^{18}\text{O}/^{16}\text{O}$  ratio in natural water: *Geochimica et Cosmochimica Acta*, v. 4, p. 213-224.
- Fahlquist, L., and Ardis, A.F. (2004) Quality of water in the Trinity and Edwards aquifers, south-central Texas, 1996-98: U.S. Geological Survey Scientific Investigation Report 2004-5201, 17 p.
- Faure, G. (1986) *Principles of isotope geology*, John Wiley and Sons, New York, New York, 589 p.
- Fishman, M.J. (1993) Methods of analysis by the U.S. Geological Survey National Water Quality Laboratory—Determination of inorganic and organic constituents in water and fluvial sediments: U.S. Geological Survey Open-File Report 93-125, 217 p.

- Fishman, M.J., and Friedman, L.C. (1989) Methods for the determination of inorganic substances in water and fluvial sediments: U.S. Geological Survey Techniques of Water-Resources Investigations book 6, chap. A1, 545 p.
- Folk, R.L. (1974) *Petrology of sedimentary rocks*, Hemphill Publishers, Austin, Texas, 182 p.
- Ford, D.C., and Williams, P.W. (1989) *Karst geomorphology and hydrology*, Chapman and Hall, London, England, 601 p.
- Freeze, R.A., and Cherry, J.A. (1979) *Groundwater*, Prentice Hall, Englewood Cliffs, New Jersey, 604 p.
- Fritz, P., Cherry, J.A., Weyer, K.U., and Sklash, M.G. (1976) Storm runoff analyses using environmental isotopes and major ions, *in* Interpretation of environmental isotope and hydrochemical data in groundwater hydrology—Proceedings of an advisory group meeting 1975: International Atomic Energy Agency, Vienna, Austria, p. 111-130.
- Frost, C.D., and Toner, R.N. (2004) Strontium isotopic identification of water-rock interaction and ground water mixing: *Ground Water*, v. 42, p. 418-432.
- Gale, S.J. (1984) The hydraulics of conduit flow in carbonate aquifers: *Journal of Hydrology*, v. 70, p. 309-327.
- Garcia-Fresca Grocin, B. (2004) Urban effects on groundwater recharge in Austin, Texas, unpublished M.S. thesis, University of Texas, Austin, Texas, 175 p.
- Garner, B.D., Mahler, B.J., and Sunvison, M.W. (in press) An investigation of the relation between surface-water flow, aquifer flow conditions, and karst ground-water geochemistry from 1978-2003, in the Barton Springs segment of the Edwards aquifer, Austin, Texas: U.S. Geological Survey Scientific Investigation Report.
- Gat, J.R. (1981) Groundwater, *in* Gat, J.R., and Gonfiantini, R., eds., Stable Isotope hydrology—Deuterium and Oxygen-18 in the water cycle: International Atomic Energy Agency, Vienna, Austria, p. 223-240.
- Gonfiantini, R. (1981) The d-notation and the mass-spectrometric measurement techniques, *in* Gat, J.R., and Gonfiantini, R., eds., Stable isotope hydrology—Deuterium and Oxygen-18 in the water cycle, Vienna, Austria, p. 35-84.

- Good, H.R. (2000) Cold Springs—Hydrogeology, groundwater quality and research recommendations, unpublished undergraduate Honors thesis, University of Texas, Austin, Texas, 52 p.
- Greene, E.A. (1997) Tracing recharge from sinking streams over spatial dimensions of kilometers in a karst aquifer: *Ground Water*, v. 35, p. 898-904.
- Groisman, P.Y., and Legates, D.R. (1994) The accuracy of United States precipitation data: *Bulletin of the American Meteorological Society*, v. 75, p. 215-227.
- Groschen, G.E. (1994) Analysis of data from test-well sites along the downdip limit of freshwater in the Edwards aquifer, San Antonio, Texas, 1985-87: U.S. Geological Survey Water-Resources Investigations Report 93-4100, 92 p.
- Guyton, W.F., and Associates (1958) Recharge to the Edwards reservoir between Kyle and Austin: report prepared for the City Water Board of San Antonio, 9 p.
- Halihan, T., Sharp, J.M., Jr., and Mace, R.E. (2000) Flow in the San Antonio segment of the Edwards aquifer—Matrix, fractures, or conduits?, *in* Sasowsky, I.D., and Wicks, C.M., eds., *Groundwater flow and contaminant transport in carbonate aquifers*: A.A. Balkema Publishers, Rotterdam, The Netherlands, p. 129-146.
- Halihan, T., and Wicks, C.M. (1998) Modeling of storm responses in conduit flow aquifers with reservoirs: *Journal of Hydrology*, v. 208, p. 82-91.
- Halihan, T., Wicks, C.M., and Engeln, J.F. (1998) Physical response of a karst drainage basin to flood pulses; example of the Devil's Icebox cave system (Missouri, USA): *Journal of Hydrology*, v. 204, p. 24-36.
- Han, G., and Liu, C. (2004) Water geochemistry controlled by carbonate dissolution—a study of the river waters draining karst-dominated terrain, Guizhou Province, China: *Chemical Geology*, v. 204, p. 1-21.
- Hauwert, N.N., Johns, D.A., Hunt, B., Beery, J., Smith, B., and Sharp, J.M., Jr. (2005) Flow systems of the Edwards aquifer Barton Springs segment interpreted from tracing and associated field studies: *Proceedings of Edwards water resources in Central Texas*, South Texas Geological Society and Austin Geological Society, 18 p.

- Hauwert, N.N., and Vickers, S. (1994) Barton Springs Edwards aquifer hydrogeology and groundwater quality: Barton Springs/Edwards Aquifer Conservation District Contract 93483-346 Report to Texas Water Development Board, 92 p.
- Helsel, D.R., and Hirsch, R.M. (1995) *Statistical methods in water resources*, Elsevier Science Publishers, Amsterdam, The Netherlands, 529 p.
- Hem, J.D. (1982) Conductance—A collective measure of dissolved ions, *in* Minear, R.A., and Keith, L.H., eds., *Water Analysis: Volume 1*: Academic Press, New York, New York, p. 137-161.
- Hem, J.D. (1985) Study and interpretation of the chemical characteristics of natural water: US Geological Survey Water Supply Paper 2254, 264 p.
- Herczeg, A., Leaney, F.W., Stadter, M.F., Allan, G.L., and Fifield, L.K. (1997) Chemical and isotopic indicators of point-source recharge to a karst aquifer, South Australia: *Journal of Hydrology*, v. 192, p. 271-299.
- Herczeg, A.L., and Edmunds, W.M. (2000) Inorganic ions as tracers, *in* Cook, P.G., and Herczeg, A.L., eds., *Environmental tracers in subsurface hydrology*: Kluwer Academic Publishing, Dordrecht, The Netherlands, p. 31-77.
- Hess, J.W., and White, W.B. (1988) Storm response of the karstic carbonate aquifer of south-central Kentucky: *Journal of Hydrology*, v. 99, p. 235-252.
- Horowitz, A.J., and Sandstrom, M.W. (1998) Cleaning of equipment for water sampling: U.S. Geological Survey Techniques of Water-Resources Investigations book 9, chap. A3, 83 p.
- International Atomic Energy Agency (2005) Global network for isotopes in precipitation: International Atomic Energy Agency, accessed 29 Sept. 2005 <<http://isohis.iaea.org>>.
- Jacobson, A.D., and Wasserburg, G.J. (2005) Anhydrite and the Sr isotope evolution of groundwater in a carbonate aquifer: *Chemical Geology*, v. 214, p. 331-350.
- James, N.P., and Choquette, P.W. (1984) Diagenesis 9—Limestones—The meteoric diagenetic environment: *Geoscience Canada*, v. 11, p. 161-194.
- Jones, I.C., and Banner, J.L. (2000) Estimating recharge in a tropical karst aquifer: *Water Resources Research*, v. 36, p. 1289-1299.

- Kattan, Z. (1997) Environmental isotope study of the major karst springs in Damascus limestone aquifer systems; case of the Fiegh and Barada springs: *Journal of Hydrology*, v. 193, p. 161-182.
- Katz, B.G., Catches, J.S., Bullen, T.D., and Michel, R.L. (1998) Changes in the isotopic and chemical composition of ground water resulting from a recharge pulse from a sinking stream: *Journal of Hydrology*, v. 211, p. 178-207.
- Katz, B.G., Coplen, T.B., and Bullen, T.D. (1997) Use of chemical and isotopic tracers and geochemical modeling to characterize the interactions between ground water and surface water in mantled karst: *Ground Water*, v. 35, p. 1014-1028.
- Kehew, A.E. (2001) *Applied chemical hydrogeology*, Prentice Hall, Upper Saddle River, New Jersey, 368 p.
- Kendall, C., Sklash, M.G., and Bullen, T.D. (1995) Isotope tracers of water and solute sources in catchments, *in* Trudgill, S.T., ed., *Solute modelling in catchment systems*: John Wiley and Sons, Somerset, New Jersey, p. 261-303.
- Koterba, M.T., Wilde, F.D., and Lapham, W.W. (1995) Ground-water data-collection protocols and procedures for the National Water-Quality Assessment Program—Collection and documentation of water-quality samples and related data: U.S. Geological Survey Open-File Report 95-399, 113 p.
- Lakey, B., and Krothe, N.C. (1996) Stable isotopic variation of storm discharge from a perennial karst spring: *Water Resources Research*, v. 32, p. 721-731.
- Land, L.S., and Prezbindowski, D.R. (1981) The origin and evolution of saline formation water, Lower Cretaceous carbonates, south-central Texas, U.S.A.: *Journal of Hydrology*, v. 54, p. 51-74.
- Lee, E.S., and Krothe, N.C. (2001) A four-component mixing model for water in a karst terrain in south-central Indiana, USA. Using solute concentration and stable isotopes as tracers: *Chemical Geology*, v. 179, p. 129-143.
- Lindgren, R.J., Dutton, A.R., Havorka, S.D., Worthington, S.R.H., and Painter, S. (2005) Conceptualization and simulation of the Edwards aquifer, San Antonio region, Texas: U.S. Geological Survey Scientific Investigation Report 2004-5277, 154 p.

- Liu, Z., Groves, C., Yuan, D., and Meiman, J. (2004) South China karst aquifer storm-scale hydrochemistry: *Ground Water*, v. 42, p. 491-499.
- Long, A.J., and Putnam, L.D. (2004) Linear model describing three components of flow in karst aquifers using  $^{18}\text{O}$  data: *Journal of Hydrology*, v. 296, p. 254-270.
- Longinelli, A., Silvestri, A., Molin, G., and Salviulo, G. (2004) 1.8 ka old glass from the Roman ship *Julia Felix*—Glass-water oxygen isotope exchange: *Chemical Geology*, v. 211, p. 335-342.
- Lynch, F.L., Mahler, B.J., and Hauwert, N.N. (2004) Provenance of suspended sediment discharged from a karst aquifer determined by clay mineralogy, *in* Sasowsky, I.D., and Mylroie, J., eds., *Studies of cave sediments—Physical and chemical records of paleoclimate*: Kluwer Academic—Plenum Publishers, New York, New York.
- Maclay, R.W. (1995) *Geology and hydrology of the Edwards aquifer in the San Antonio Area, Texas*: U.S. Geological Survey Water-Resources Investigations Report 95-4186.
- Maclay, R.W., and Land, L.F. (1988) Simulation of flow in the Edwards aquifer, San Antonio area, Texas, and refinement of storage and flow concepts: U.S. Geological Survey Water-Supply Paper 2336-A, 48 p.
- Maclay, R.W., and Small, T.A. (1983) Hydrostratigraphic subdivisions and fault barriers of the Edwards aquifer, south-central Texas, U.S.A.: *Journal of Hydrology*, v. 61, p. 127-146.
- Mahler, B.J. (1997) *Mobile sediments in a karst aquifer*, unpublished PhD dissertation, University of Texas, Austin, Texas, 171 p.
- Mahler, B.J. (2003) Quality of sediment discharging from the Barton Springs system, Austin, Texas, 2000-2002: U.S. Geological Survey Fact Sheet 089-03, 6 p.
- Mahler, B.J., and Lynch, F.L. (1999) Muddy waters—Temporal variation in sediment discharging from a karst spring: *Journal of Hydrology*, v. 214, p. 165-178.
- Mahler, B.J., Lynch, F.L., and Bennett, P.C. (1999) Mobile Sediment in an urbanizing karst aquifer; implications for contaminant transport: *Environmental Geology*, v. 39, p. 25-38.

- Mahler, B.J., and VanMetre, P.C. (2000) Occurrence of soluble pesticides in Barton Springs, Austin, Texas, in response to a rain event: U.S. Geological Survey, accessed 29 Sept 2005 <<http://tx.usgs.gov/reports/dist/dist-2000-02/>>.
- Malard, F., and Chapuis, R. (1995) Temperature logging to describe the movement of sewage-polluted surface water infiltrating into a fractured rock aquifer: *Journal of Hydrology*, v. 173, p. 191-217.
- Maloszewski, P., Stichler, W., Zuber, A., and Rank, D. (2002) Identifying the flow systems in a karstic-fissured-porous aquifer, the Schneealpe, Austria, by modeling of environmental  $^{18}\text{O}$  and  $^3\text{H}$  isotopes: *Journal of Hydrology*, v. 256, p. 48-59.
- Massei, N., Wang, H.Q., Dupont, J.P., Rodet, J., and Laignel, B. (2003) Assessment of direct transfer and resuspension of particles during turbid floods at a karstic spring: *Journal of Hydrology*, v. 275, p. 109-121.
- McCrea, J.M. (1950) The isotopic chemistry of carbonates and a paleotemperature scale: *Journal of Chemical Physics*, v. 18, p. 857-859.
- McNutt, R.H. (2000) Strontium Isotopes, in Cook, P., and Herczeg, A., eds., *Environmental tracers in subsurface hydrology*: Kluwer Academic Publishing, Dordrecht, The Netherlands, p. 233-260.
- Moore, C.H. (1989) *Carbonate diagenesis and porosity*, Elsevier Science Publishers, Amsterdam, The Netherlands, 338 p.
- Mueller, D.K., and Helsel, D.R. (1996) Nutrients in the Nation's waters—Too much of a good thing?: U.S. Geological Survey Circular 1136, 24 p.
- Musgrove, M. (2000) Temporal links between climate and hydrology—Insights from central Texas cave deposits and groundwater, unpublished PhD dissertation, University of Texas, Austin, Texas, 432 p.
- Musgrove, M., and Banner, J.L. (1993) Regional ground-water mixing and the origin of saline fluids—Midcontinent, United States: *Science*, v. 259, p. 1877-1882.
- Musgrove, M., and Banner, J.L. (2004) Controls on the spatial and temporal variability of vadose dripwater geochemistry—Edwards aquifer, central Texas: *Geochimica et Cosmochimica Acta*, v. 68, p. 1007-1020.

- Oetting, G.C. (1995) Evolution of fresh and saline groundwaters in the Edwards aquifer, Central Texas—Geochemical and isotopic constraints on processes of fluid-rock interaction and fluid mixing, unpublished M.A. thesis, University of Texas, Austin, Texas, 204 p.
- Oetting, G.C., Banner, J.L., and Sharp, J.M., Jr. (1996) Regional controls on the geochemical evolution of saline groundwaters in the Edwards aquifer, central Texas: *Journal of Hydrology*, v. 181, p. 251-283.
- Palmer, A.N. (1991) Origin and morphology of limestone caves: *Geological Society of America Bulletin*, v. 103, p. 1-12.
- Panno, S.V., Hackley, K.C., Hwang, H.H., and Kelly, W.R. (2001) Determination of the sources of nitrate contamination in karst springs using isotopic and chemical indicators: *Chemical Geology*, v. 179, p. 113-128.
- Panno, S.V., Krapac, I.G., Weibel, C.P., and Bade, J.D. (1996) Groundwater contamination in karst terrain of southwestern Illinois: *Illinois State Geological Survey Environmental Geology Series EG 151*, 43 p.
- Parkhurst, D.L., and Appelo, C.A.J. (1999) User's guide to PHREEQC (Version 2)—A computer program for speciation, batch-reaction, one-dimensional transport, and inverse geochemical calculations: *U.S. Geological Survey Water-Resources Investigations Report 99-4259*, 312 p.
- Peterson, E.W., and Wicks, C.M. (2003) Characterization of the physical and hydraulic properties of the sediment in karst aquifers of the Springfield Plateau, Central Missouri, USA: *Hydrogeology Journal*, v. 11, p. 357-367.
- Pinder, G.F., and Jones, J.F. (1969) Determination of the groundwater component of peak discharge from the chemistry of total runoff: *Water Resources Research*, v. 5, p. 435-445.
- Piper, A.M. (1944) A graphic procedure in the geochemical interpretation of water analyses: *Transactions—American Geophysical Union*, v. 25, p. 914-923.
- Prezbindowski, D.R. (1981) Carbonate rock-water diagenesis, lower Cretaceous, Stuart City trend, South Texas, unpublished PhD dissertation, University of Texas, Austin, Texas, 252 p.

- Pritt, J.W., and Raese, J.W. (1995) Quality assurance/quality control manual— National Water Quality Laboratory: U.S. Geological Survey Open-File Report 95-443, 35 p.
- Quinlan, J.F. (1989) *Ground-water monitoring in karst terrains—Recommended protocols and implicit assumptions*, U.S. Environmental Protection Agency, 79 p.
- Quinlan, J.F., Ray, J.A., and Schindel, G.M. (1995) Intrinsic limitations of standard criteria and methods for delineation of groundwater-source protection areas (springhead and wellhead protection areas) in carbonate terranes, *in* Beck, B.F., and Pearson, F.M., eds., *Karst geohazards—Engineering and environmental problems in karst terrane*: A.A. Balkema Publishers, Rotterdam, The Netherlands, p. 525-537.
- Radtke, D.B., Davis, J.V., and Wilde, F.D. (1998a) Specific electrical conductance: U.S. Geological Survey Techniques of Water-Resources Investigations book 9, chap. A6, section 3, 22 p.
- Radtke, D.B., Wilde, F.D., Davis, J.V., and Popowski, T.J. (1998b) Alkalinity and acid neutralizing capability: U.S. Geological Survey Techniques of Water-Resources Investigations book 9, chap A6, section 6.
- Rose, P.R. (1972) Edwards Group, surface and subsurface, central Texas: Bureau of Economic Geology Report of Investigations 74, 198 p.
- Ryan, M., and Meiman, J. (1996) An examination of short-term variations in water quality at a karst spring in Kentucky: *Ground Water*, v. 34, p. 23-30.
- Scanlon, B.R. (2000) Uncertainties in estimating water fluxes and residence times using environmental tracers in an arid unsaturated zone: *Water Resources Research*, v. 36, p. 395-409.
- Scanlon, B.R., Mace, R.E., Barrett, M.E., and Smith, B.A. (2003) Can we simulate groundwater flow in a karst system using equivalent porous media models? Case study, Barton Springs Edwards aquifer, USA: *Journal of Hydrology*, v. 276, p. 137-158.
- Senger, R.E. (1983) Hydrogeology of Barton Springs, Austin, Texas, unpublished M.A. thesis, University of Texas, Austin, Texas, 120 p.

- Senger, R.E., and Kreitler, C.W. (1984) Hydrogeology of the Edwards aquifer, Austin area, central Texas: Texas Bureau of Economic Geology Report of Investigations 141, 35 p.
- Sharp, J.M., Jr. (1993) Fractured aquifers/reservoirs—Approaches, problems, and opportunities, *in* Banks, D., and Banks, S., eds., Hydrogeology of Hard Rocks, Memoires of the 24th Congress, International Association of Hydrogeologists: Volume 24, Oslo, Norway, p. 23-38.
- Sharp, J.M., Jr., and Banner, J.L. (1997) The Edwards aquifer—A resource in conflict: *GSA Today*, v. 7, p. 1-9.
- Sharp, J.M., Jr., and Clement, T.J. (1988) Hydrochemical facies as hydraulic boundaries in karstic aquifers—the Edwards aquifer, U.S.A., *in* Daoxian, Y., ed., Proceedings of the 21st IAH Congress, karst hydrogeology and karst environment protection: Geological Publishing House, Beijing, China, p. 841-845.
- Shuster, E.T., and White, W.B. (1971) Seasonal fluctuations in the chemistry of limestone springs—A possible means for characterizing carbonate aquifers: *Journal of Hydrology*, v. 14, p. 93-128.
- Siegenthaler, U., and Schotterer (1984) Isotopic and chemical investigations of springs from different karst zones in the Swiss Jura, *in* Isotope hydrology 1983—Proceedings of an international symposium on isotope hydrology in water resources development: International Atomic Energy Agency, Vienna, Austria, p. 153-172.
- Silberschatz, A., Korth, H.F., and Sudarshan, S. (2002) *Database System Concepts*, McGraw-Hill, Boston, Massachusetts, 1064 p.
- Slade, R.M., Jr., Dorsey, M.E., Gordon, J.D., Mitchell, R.N., and Gaylord, J.L. (1981) Hydrologic data for urban studies in the Austin, Texas, metropolitan area, 1979: US Geological Survey Open-File Report 81-628, 281 p.
- Slade, R.M., Jr., Dorsey, M.E., and Stewart, S.L. (1986) Hydrology and water quality of the Edwards aquifer associated with Barton Springs in the Austin area, Texas: U.S. Geological Survey Water-Resources Investigations Report 86-4036, 117 p.

- Slade, R.M., Jr., Gordon, J.D., and Mitchell, R.N. (1979) Hydrologic data for urban studies in the Austin, Texas, metropolitan area, 1977: US Geological Survey Open-File Report 79-271, 192 p.
- Slade, R.M., Jr., Ruiz, L.M., and Slagle, D.L. (1985) Simulation of the flow system of Barton Springs and associated Edwards aquifer in the Austin area, Texas: U.S. Geological Survey Water-Resources Investigations Report 85-4299, 49 p.
- Slagle, D.L., Ardis, A.F., and Slade, R.M., Jr. (1986) Recharge zone of the Edwards aquifer hydrologically associated with Barton springs in the Austin area, Texas: U.S. Geological Survey Water-Resources Investigations Report 86-4062, 1 p.
- Small, T.A., Hanson, J.A., and Hauwert, N.N. (1996) Geologic framework and hydrogeologic characteristics of the Edwards aquifer outcrop (Barton Springs segment), northeastern Hays and southwestern Travis counties, Texas: U.S. Geological Survey Water-Resources Investigations Report 96-4306, 15 p.
- Smith, B.A., and Hunt, B.B. (2004) Evaluation of sustainable yield of the Barton Springs segment of the Edwards aquifer, Hays and Travis counties, central Texas: Barton Springs Edwards Aquifer Conservation District Report 55 p.
- St. Clair, A.E. (1979) Quality of water in the Edwards aquifer, central Travis county, Texas, unpublished M.A. thesis, University of Texas at Austin, Austin, Texas.
- Stanley, D.L., Boozer, T.M., and Schroder, L.J. (1998) Summary of the U.S. Geological Survey National Field Quality Assurance Program from 1979 through 1997: U.S. Geological Survey Open-File Report 98-392, 11 p.
- Stueber, A.M., Pushkar, P., and Hetherington, E.A. (1984) A strontium isotopic study of formation waters from the Illinois basin: *Geochimica et Cosmochimica Acta*, v. 48, p. 1637-1649.
- Stumm, W., and Morgan, J.J. (1995) *Aquatic chemistry—Chemical equilibria and rates in natural waters*, John Wiley and Sons, New York, New York, 1022 p.
- Swarzenski, P.W., Reich, C.D., Spechler, R.M., Kindinger, J.L., and Moore, W.S. (2001) Using multiple geochemical tracers to characterize the hydrogeology of the submarine spring off Crescent Beach, Florida: *Chemical Geology*, v. 179, p. 187-202.

- Turner, M. (2000) Update of Barton Springs water quality data analysis-Austin, Texas: City of Austin Water Quality Report Series COA-ERM/2000, 21 p.
- Uliana, M.M., and Sharp, J.M., Jr. (2001) Tracing regional flow paths to major springs in Trans-Pecos Texas using historical geochemical data: *Chemical Geology*, v. 179, p. 53-72.
- United States Environmental Protection Agency (2005) Current drinking-water standards: Office of Ground Water and Drinking Water, accessed 29 Sept. 2005 <<http://www.epa.gov/safewater/mcl.html>>.
- United States Geological Survey (1980) Hydrologic data for urban studies in the Austin, Texas, metropolitan area, 1978: U.S. Geological Survey Open-File Report 80-728, 229 p.
- United States Geological Survey (1984) Chemical and physical quality of water and sediment, *in* National handbook of recommended methods for water-data acquisition: Office of Water Data Coordination, p. 5-1 to 5-194.
- Vallejos, A., Pulido-Bosch, A., Martin-Rosales, W., and Calvache, M.L. (1997) Contribution of environmental isotopes to the understanding of complex hydrologic systems—A case study—Sierra de Gador, SE Spain: *Earth Surface Processes and Landforms*, v. 22, p. 1157-1168.
- Vineyard, J. (1960) The reservoir theory of spring flow: *Bulletin of the National Speleological Society*, v. 20, p. 46-50.
- Wagner, R.J., Mattraw, H.C., Ritz, G.F., and Smith, B.A. (2000) Guidelines and standard procedures for continuous water-quality monitors—Site selection, field operation, calibration, record computation, and reporting: U.S. Geological Survey Water-Resources Investigations Report 00-4252, 53 p.
- White, W.B. (1988) *Geomorphology and hydrology of karst terrains*, Oxford University Press, New York, New York, 464 p.
- Wilde, F.D., Radtke, D.B., Gibs, J., and Iwatsubo, R.T. (1999) Collection of water samples: U.S. Geological Survey Techniques of Water-Resources Investigations book 9, chap. A4, 158 p.

- Wisconsin Department of Natural Resources (2003) Nitrate in drinking water: Environmental Health Division of the Wisconsin State Laboratory of Hygiene, accessed 29 Sept. 2005  
<<http://www.slh.wisc.edu/ehd/pamphlets/nitrate.php>>.
- Woodruff, C.M., and Abbott, P.L. (1979) Drainage-basin evolution and aquifer development in karstic limestone terrain, south-central Texas, U.S.A.: *Earth Surface Processes*, v. 4, p. 319-334.
- Worthington, S.R.H., Smart, C.C., and Ruland, W.W. (2002) Assessment of groundwater velocities to the municipal wells at Walkerton, *in* Stolle, D., Piggott, A.R., and Crowder, J.J., eds., *Proceedings of the 55th Canadian Geotechnical and 3rd Joint IAH-CNC and CGS Groundwater Specialty Conferences*, October 20-23, 2002: Canadian Geotechnical Society, Niagara Falls, Ontario, p. 1081-1086.
- Yurtsever, Y., and Gat, J.R. (1981) Atmospheric waters, *in* Gat, J.R., and Gonfiantini, R., eds., *Stable isotope hydrology – Deuterium and Oxygen-18 in the water cycle*: International Atomic Energy Agency, Vienna, Austria, p. 103-142.

## VITA

Brad Garner was born on February 28, 1977 in Irving, Texas, the first child of Steve and Ann Garner. He graduated from Arlington High School in May 1995. Beginning in August 1995, he attended the University of Texas at Austin. Despite majoring in computer science, he spent his carefree collegiate summers as a seasonal park ranger at Great Sand Dunes National Park. In August 1999, he received his Bachelor of Science. After spending three and a half years as a professional software engineer in Austin, he discovered that software engineering was neither suited to him nor sustainable as a career path. He survived this quarter-life crisis, began working part-time at the United States Geological Survey, and enrolled in the University of Texas Jackson School of Geosciences in August 2003.

Permanent Address: 209 Mill Creek Drive

Arlington, TX 76010

This thesis was typed by the author.